University of Southampton

Faculty of ENVIRONMENTAL AND LIFE SCIENCES

SCHOOL OF GEOGRAPHY AND ENVIRONMENTAL SCIENCE

ESTIMATION OF RICE CROP YIELD IN THAILAND USING SATELLITE DATA

DOI 10.1117/12.2513281

by

JATUPORN NONTASIRI

Thesis for the degree of DOCTOR OF PHILOSOPHY

March 2023

UNIVERSITY OF SOUTHAMPTON

ABSTRACT

FACULTY OF ENVIRONMENTAL AND LIFE SCIENCES
School Of Geography and Environmental Science

Doctor of Philosophy

ESTIMATON OF RICE CROP YIELD IN THAILAND USING SATELLITE DATA

by
Jatuporn Nontasiri

Occupying over 12% of the global cropland area, rice is the predominant crop in many regions of the world. Southeast Asia alone accounts for 31% of the world's rice harvesting area, making this region vital for the food security of the growing global population. Current literature in the field indicates that there are several factors impacting rice productivity, however there are gaps pertaining to country-specific studies, namely the impact of climate change and challenges regarding effective monitoring. Therefore, this study focuses on four research questions, they are: *(1)* the climate parameters influencing rice productivity in Thailand; *(2)* the correlation between rice biophysical variables and growth rate as a determinant to overall rice yield; *(3)* the potential of satellite sensors for rice yield; and *(4)* the development of a regression model for rice yield estimations.

For the first question, climate data (measured by two rainfall parameters and six crucial temperature parameters) and rice yield data, which were collected at the provincial level between the years 1981-2015, are used to determine the impacts of the climate on rice productivity in Thailand. The result indicates a significance increasing/decreasing trend in the mean minimum temperature, mean maximum temperature, and cumulative rainfall. The study further investigates the importance of geographical variation by adopting spatial autocorrelation (Moran's *I* index). The result reveals that in 1992 there was a significant shift in cumulative rainfall and the average temperature.

Furthermore, field experiments were conducted on rice crops in Thailand during the wet season of 2017 to explore the correlation between rice biophysical variables and growth rate. The temporality of rice biophysical variables is demonstrated by separating rice variety and irrigation system. The leaf area index (LAI) peaks in the flowering stage and LAI development can be slightly different depending on the rice variety and irrigation system. The correlation between yield and other rice biophysical elements on a specific variety (RD41) is highly correlated to rice age, stem density, height, chlorophyll contents, and wet and dry biomass. The correlation between yield, and wet and dry biomass during the harvesting stage was the strongest.

To develop a rice yield prediction model, data collected from the time series of two different satellite sensors: Sentinel-2 (optical) and Sentinel-1 (Synthetic Aperture Radar, or SAR) were utilised. The vegetation indices (NDVI and EVI) and backscatter coefficient (sigma nought; σ^0) usefully tracked rice phenology. The study furthers develop a linear regression model for rice yield estimations based on different sensors and yields from in-situ measurements via Crop Cutting Experiments (CCEs). The accuracy of the results is compared to official rice yields.

The correlation between vegetation indices, backscatter coefficient, and rice yield variables is investigated in different growth stages and irrigation systems. Based on the simple regression model for the optical sensors, the developed yield estimation model is correlated with NDVI in the panicle stage ($r = 0.37$ and SEE = 0.70 tonnes/ha). While SAR (σ^0) is significant in the ascending VV/VH ratio during the harvesting stage ($r = 0.54$ and SEE = 0.68 tonnes/ha). The findings suggest remotely sensed data can be a good predictor for rice yield during the booting and mature stages.

Table of Contents

Table of Tables

Table of Tables

Table of Figures

Table of Figures

Table of Figures

List of Accompanying Materials

Proceedings Volume 10783, Remote Sensing for Agriculture, Ecosystems, and Hydrology XX; 107832K (2019) http://doi.org/10.1117/12.2513281

Event: SPIE Remote Sensing, 2018, Berlin, Germany.

Research Thesis: Declaration of Authorship

Print name: JATUPORN NONTASIRI

Title of thesis: Estimation of Rice Crop Yield in Thailand Using Satellite Data

I declare that this thesis and the work presented in it are my own and have been generated by me as the result of my own original research.

I confirm that:

1. This work was done wholly or mainly while in candidature for a research degree at this University;
2. Where any part of this thesis has previously been submitted for a degree or any other qualification at this University or any other institution, this has been clearly stated;
3. Where I have consulted the published work of others, this is always clearly attributed;
4. Where I have quoted from the work of others, the source is always given. With the exception of such quotations, this thesis is entirely my own work;
5. I have acknowledged all main sources of help;
6. Where the thesis is based on work done by myself jointly with others, I have made clear exactly what was done by others and what I have contributed myself;
7. Parts of this work have been published as:-

Proceeding Volume 10783, Remote Sensing for Agriculture, Ecosystems, and Hydrology XX; 107832K (2018) https://doi.org/10.1117/12.2513281

Signature: ..... Date: ……27 March 2023.....

Acknowledgements

After an intensive period of studying, today is an important day to thank everyone involved in my PhD study. I would like to take this opportunity to thank those who have supported me throughout this period.

First, I would like to express my sincere gratitude to my supervisory team, Prof. Jadu Dash and Dr Gareth Roberts, for all their Geo-informatics knowledge, academic support and suggestions, field survey design, motivation, and patience with my studies and the writing of this thesis. Without their guidance, this PhD would not have been possible.

Besides my supervisors, I would like to thank my internal and external examiners: Dr Jim Wright and Dr Booker Ogutu, for their comments to fill my research gaps during my PhD upgrade examination and Dr Paul Aplin and Dr Booker Ogutu, for the viva examination. I would like to thank the Geography and Environmental Science laboratory staff for providing field equipment.

My sincere thanks to the Office of Agricultural Economics, Ministry of Agricultural and Cooperatives, Thailand, for providing greatest opportunity to this PhD study and regional office for ground experiments during the 2017 growing season. I am pleased to thank the Rice Research Centre in Suphan Buri for providing equipment, and would like to acknowledge the Thai Meteorological Department, Ministry of Digital Economy and Society, for weather data support.

In particular, I gratefully acknowledge the funding received from the Office of the Civil Service Commission and Royal Thai government, for financial support and suggestions during my study. Without their support, this research would not have been completed.

Last but not the least, I would like to thank my mom and family, who continue to support me spiritually, encourage my PhD study, and even joined in my field survey.

Definitions and Abbreviations

σ^0 ..... Normalised backscatter coefficients

σ_{VV} ..... Backscatter coefficient for VV polarisation

σ_{VH} ..... Backscatter coefficient for VH polarisation

$\sigma_{VV/VH}$ ..... Ratio of backscatter coefficient for VV and VH polarisation

CCE ..... Crop cutting experiment

CI ..... Change index

DEM ..... Digital elevation model

DOS ..... Day of sowing

DOY ..... Day of year

EO ..... Earth observation

EOS ..... End of season

ESA ..... European space agency

ET ..... Evapotranspiration

EVI ..... Enhanced vegetation index

FAPAR ..... Fraction absorbed photosynthetically active radiation

GDB ..... Grain dry biomass

GDP ..... Gross domestic product

GEOGLAM ..... Group on earth observations global agricultural monitoring initiative

GHGs ..... Greenhouse gases

GIS ..... Geographic information system

GMSL ..... Global mean sea level

GWB ..... Grain wet biomass

HH ..... Horizontal emitted, horizontal received polarisation

HNT ..... High night-time temperature

HV ..... Horizontal emitted, vertical received polarisation

HYVs ..... High-yielding rice varieties

IPCC..... Intergovernmental panel on climate change

IRRI..... International rice research institute

IW..... Interferometric wide swath

LAD..... Leaf angle distribution

LAI ..... Leaf area index

MSI..... Multi-spectral instrument

NASA ..... National aeronautics and space administration

NDVI..... Normalised difference vegetation index

PAR..... Photosynthetically active radiation

PDF..... Possibility distribution function

POS..... Peak of season

RCSM..... Rice canopy scattering model

RIICE ..... Remote sensing-based information and insurance for crops in emerging economies

RUE ..... Radiation use efficiency

RVI..... Radar vegetation index

SAR..... Synthetic aperture radar

SLC ..... Single look complex

SDB..... Stem dry biomass

SOA ..... Start of season

SRI ..... System of rice intensification

SRTM..... Shuttle radar terrain mission

SWB..... Stem wet biomass

TOPSAR ..... Terrain observation with progressive scanning

TRMM ..... Tropical rainfall measuring mission

TDB..... Total dry biomass

TWB ..... Total wet biomass

UTM ..... Universal transverse mercator

VV.....Vertical emitted, vertical received polarisation

VH.....Vertical emitted, horizontal received polarisation

WGS.....World geodetic system

Chapter 1 Introduction

Globally, climate change and extreme weather events, which are linked to increasing concentrations of greenhouse gases (GHGs), are becoming more widespread, occurring more frequently and having significant environmental and societal impact (Enríquez-de-Salamanca et al., 2017; Halsnas & Trarup, 2009; Malhi et al., 2020; Reser & Swim, 2011). Extreme weather events include intense heatwaves, heavy rainfalls, long-spell droughts, and wildfires, which directly and indirectly impacts the environment, economy, biodiversity, agricultural production, and human health. The consequences of climate change are a major problem in most countries and threaten food production. In order to develop strategies to mitigate the impacts of climate change, evaluating its impact on regional and country levels is necessary. For example, some countries employ national surveys to understand public perceptions and attitudes, as well as the impact of climate change, and based on the results governments can implement efficiency strategies for climate change adaptation (Laukkonen et al., 2009; Lawler, 2009; Masud et al., 2017; Morecroft et al., 2019). Climate change-induced weather events have a significant impact on the agricultural sector and food security - including an increase in pests, weeds, disease, and water stress- which serves to reduce crop yield and increase food insecurity. Therefore, improved understanding of the influence of climate on crop production is necessary if improvements in food security are to be made through climate mitigation adaptations.

Cereal grains (e.g. barley, wheat, rice, sorghum, and maize) are the world's dominant agricultural crops and have seen an increase in demand due to growing population. Rice is the world's major staple food crop, with paddies accounting for over 12% of global cropland; nearly 90% of the world's rice is produced and consumed in Asia (FAOSTAT, 2010). There, rice is grown in two seasons (i.e. the wet and dry season) with the wet season coinciding with the monsoon rainfall (between May and October). The dry season lasts from November to April and rice planting depends on irrigation schemes. Rice cultivation is dependent on the availability of sufficient water, so most farmers plant their crop in the wet season, while those with access to irrigation may cultivate throughout the year. Increasing demand from the growing population has resulted in rice production continuously increasing in Asia, achieved through the expansion of areas under cultivation, increasing cropping intensity, use of high-yielding rice varieties (HYVs), and the adoption of mechanised practices after the Green Revolution during the 1930s and 1960s. The Green Revolution played an important role in developing countries through the growth of high yield varieties (Evenson & Gollin, 2003), use of fertiliser (Murgai, Ali, & Byerlee, 2001; Tilman, 1998), water supply improvements (e.g. irrigation systems), and implementation of improved cultivation methods (e.g. system of rice intensification; SRI) (Satyanarayana, Thiyagarajan, &

Uphoff, 2007). These developments have increased the potential of rice yield and reduced agricultural production costs.

In Thailand, the main agricultural commodities are rice, cassava, sugarcane, maize, para rubber, and oil palm, which serve both consumption within the country and export to foreign markets. Rice production in Thailand has increased from 6.74 to 24.93 million tonnes between 1960 and 2020, and the export of rice and related products now accounts for 10.69% of the export value of major agricultural product (OAE, 2020b). Rice cultivation is largely located in the Chao Phraya River Delta, which covers area of 15,986 km^2 containing ten rice varieties with an average annual yield 3.79 ton/ha. The Chao Phraya River delta largely consists of lowland irrigated rice areas covering ~6 million rai (0.96 million hectares), of which 70% of the cultivated area is irrigated. The prevalence of irrigation systems in this region enables farmers to increase rice production through double-rice and triple-rice cropping. However, this is not the case in all areas of Thailand, where rice production methods vary according to the local climate (e.g. precipitation), topography, availability of irrigation systems, farming practices, and government policies. Water availability influences rice development, particularly the structure of plants and yield (Belder et al., 2004; Monaco et al., 2016; Pourgholam-Amiji et al., 2021); therefore, regions with limited water availability plant rice varieties resilient to lower rainfall conditions.

Agriculture- including crops, livestock, and fisheries- is the largest economic sector in Thailand, providing gross revenue of approximately 1,343.5 million Baht ($41.98 million) per year. Agricultural monitoring and yield prediction and estimation are vital to ensure food security and agricultural trade, and to provide early warnings of issues concerning production. A key concern is the growing demand from a rapidly increasing global population, which is estimated to increase to 9.8 billion by 2050 (United Nations, 2017). To meet this demand, increased agricultural production in the order of 60-110% is needed (Ray, Mueller, West, & Foley, 2013). The government, agricultural policy planners, and agricultural associations require accurate and timely agricultural statistics for decision making. In Thailand, agricultural information is collected concerning the cultivated area, harvested area, yield, production, and timing of harvested production, which is used to balance the production capability and demand-supply of crops in domestic and foreign markets. At present, the cultivated area in Thailand is estimated using a list frame survey (or list of farm holdings) as the main sampling frame via stratified two-stage sampling and using remotely-sensed images to measure the cultivated and harvested area (Gallego et al., 2014; Pradhan, 2001; Tsiligirides, 1998). Yield estimations have traditionally been derived using crop cutting experiments (CCE) at designated ground sample plots during harvesting. The CCE method involves harvesting the crop in each sampling plot and measuring the yield, which is then extrapolated to a larger spatial extent to estimate the final yield of a region.

However, the CCE approach is expensive, time-consuming, covers a limited spatial extent, and only provides yield estimates at the end of the growing season, which can result in outdated information with respect to predictions and to developing any interventions. On the other hand, remotely-sensed data have the ability to provide information on the crop aerial extent at a particular stage of the growing season over large regions, and therefore have potential to lead to improved crop monitoring and yield estimation. Numerous methods exist for monitoring rice production using either optical or microwave data and for deriving estimates of vegetation biophysical variables such as leaf area index (LAI). Yield estimation can be derived using remotely-sensed data, either via the development of the empirical models that relate remotely-sensed measurement or biophysical variable estimates (e.g. LAI) to yield (Erten et al., 2016; Li et al., 2016; Yuzugullu et al., 2017) or through crop growth models, which are parameterised using remotely sensed biophysical variable estimates (Curnel et al., 2011; Launay & Guerif, 2005; Setiyono et al., 2019). In the optical domain, time-series of vegetation indices, which are sensitive to vegetation health and vigour, are often used to monitor crop production and estimate crop yield (Feizolahpour et al., 2019; Panda et al., 2010; Wiegand et al., 1991). A limitation of optical measurements is their inability to see through clouds, which is a major challenge to providing coverage in many parts of Asia, particularly during the monsoon season. Longer wavelength microwave backscatter observations are able to penetrate cloud cover and have been successfully used to monitor rice cultivation and to estimate rice yield (Aschbacher et al., 1995; Setiyono et al., 2019; Wiseman, McNairn, Homayoun, & Shang, 2014). Improved and timely estimates of the area under rice cultivation and rice yield using remotely-sensed data will provide a more cost-effective method for gathering agricultural statistics and would lead to improved food security.

1.1 Research problems

1.1.1 Why is research needed on the impact of climate change on rice production?

This section highlights the important role of climate change in rice production. Climate change is an adverse effect caused by long-term changes in temperature due to increasing concentrations of greenhouse gases (GHGs) in the atmosphere by natural and anthropogenic activities. One consequence of climate change has been an increase in global mean sea level (GMSL) of around 8-9 inches since 1880 due to meltwater from glaciers and ice sheets (Vermeer & Rahmstorf, 2009; Wigley & Raper, 1987).

Climate change has the potential of positively or negatively influencing crop production at local, national, and regional levels. For example, Kukal and Irmak (2018) found climate-induced temperature trends in the United States (U.S.) Great Plains to be beneficial to some crops but

detrimental to others, whilst precipitation increases were found to be beneficial to all crops. However, short-term weather extremes (e.g. drought and flooding) due to climate change typically have negative impacts on agricultural production, and these events are forecast to occur with increasing frequency (Liu et al., 2018; Zhao et al., 2020). Precipitation and temperature both influence rice production with the former influencing the planting date, crop development, and yield (Dharmarathna et al., 2014; Huang et al., 2017; Laux, Jäckel, Tingem, & Kunstmann, 2010; Mahmood et al., 2012) whilst temperature influences grain quality (size and completeness of grain) (Cooper et al., 2006; Lanning et al., 2011). In recent years, the impact of climate change on rice production in Southeast Asia has been investigated through different climate change scenarios. For example, Felkner, Tazhibayeva, & Townsend (2009) found that both high and low future global anthropogenic pollution emission scenarios led to increased daily temperature, with the high emission scenario resulting in 40% higher temperatures. The impact on precipitation was to increase throughout the year in the low emission scenario, but to reduce in the second half of the year in the high emission scenarios, which coincides with the month of critical rainfall (June) for the rice growing season. This could be interpreted as low emission scenarios being positive for rice production, whilst high emission scenarios, with increased temperature and decreased rainfall, being negative. Previous studies (Amien et al., 1999; Roy et al., 2012; Zhang & Tao, 2013) analysed the impacts of climate change on rice yield by applying various climate scenarios to crop growth models (e.g. dry matter, planting date, rainfall, temperature, production, and amount of CO_2). Kang, Khan, & Ma (2009) investigated the relationship between crop production (e.g. rice, wheat, and maize) and climatic variables in regional and global food production such as impacts on crop water productivity and soil water balance. The results found were either increased or decreased crop yields, depending on latitude and irrigation applications.

Natural disasters, such as drought and flooding, also severely impact crop production, and these are forecast to increase with the changing climate. For example, drought stress has a crucial influence on water deficit and strains (e.g. leaf heating) and biomass (Loo, Billa, & Singh, 2015). However, to date, there have been few detailed assessments of climatic trends and their impact on agriculture across Thailand. One study investigated the impact of low and high emission scenarios on rice yield estimation using the Decision Support System for Agro-technology Transfer (DSSAT) model. This showed reductions in rice yield by 3.53% and 13.79% for the high and low emission scenarios, respectively (Felkner, Tazhibayeva, & Townsend, 2009). Further to this, Polthanee and Promkhambut (2014) investigated the impact of climate change on rice and evaluated farmers' adaptation strategies in northeast Thailand. They found an increase in mean minimum and maximum temperature, which is extreme in the winter season, whilst the rainfall increased in intensity and changed their beginning of rainy season from previous. The limited

number of studies on climate impact on rice production in Thailand with regard to precipitation and temperature highlights the research gaps; identifying the impacts would enable development of methods to mitigate the effects. It is important that the agricultural sector is resilient and able to adapt to changes in climate, where the main pattern of adaptation has been through shifting of planting period, crop rotation, introducing tolerant varieties, water management, and improved farming practices.

1.1.2 Understanding the influence of irrigation on rice cultivation

Variations in rice biophysical variables may occur for several reasons, including changes in precipitation. Investigating the influence of irrigation on rice production provides a means to indirectly assess the role of climate (precipitation) on rice production. The implementation of irrigation systems guarantees sufficient water resources throughout the growing season. It is important to have sufficient water at the start of the planting season during the vegetative phase. In beginning of the growing season, flooded paddy fields are essential for the decay of organic matter and increasing the mineral absorptivity of the crop. In more arid regions or those without irrigation, the paddy field is bare soil, in which case rice is seeded in a nursery and transplanted to the paddy when water is available. This influences the variety of rice planted, and potentially the yield, where the majority of long duration rice is planted in irrigated areas whilst medium and short duration rice varieties are planted in both irrigated and non-irrigated areas. This highlights the role that water availability and irrigation system provision play in rice cultivation and in rice variety, biophysical variables, and yield (Belder et al., 2004; Dangi et al., 2017; Kropff & Cassman, 1994; Ohe et al., 2010). This research aims to investigate the different patterns of rice biophysical variables in irrigated areas and non-irrigated areas, as this can influence yield and therefore needs to be considered. This study will investigate the variation of a number of rice biophysical variables (e.g. plant height, leaf area index [LAI], biomass, and yield) with irrigation systems. Later chapters will explore the estimation of rice yield using remotely-sensed estimates of some of these biophysical variables.

1.1.3 Remote sensing for yield estimation

Yield information, which describes the production per unit area, is essential for agricultural planning and is normally used to calculate rice production by multiplying rice yield by cultivated area. In general, the yield data are derived from Crop Cutting Experiments (CCE), which involve cutting and measuring the rice grain in representative sample plots. However, these yield estimates are derived close to the harvesting period, which hinders forward planning for exporting rice and ensuring sufficient availability for the population. Therefore, developing

methods to estimate yield earlier in the season would be advantageous in supporting the decision-making process with respect to agricultural markets.

One technique, which has been widely adopted for crop monitoring and yield estimation, is via remotely-sensed measurements (Awad, 2019; Doraiswamy et al., 2003; Holzman et al., 2018). Conceptually, remote sensing involves using spectral measurements in wavebands that are sensitive to vegetation biophysical characteristics, such as visible and near-infrared (NIR) wavelengths, to monitor crop growth and estimate vegetation biophysical variables. Over the last ten years, remote sensing has been increasingly applied to monitor agricultural rice production due to the availability of moderate and high spatial resolution imagery. Owing to their moderate spatial resolution (< 30 m), Landsat Thematic Mapper (TM) and SPOT High Resolution Visible (HRV) satellite sensors have been applied to map the surface area under rice production due to the typically small size of paddy fields (Frolking et al., 2002; Nguyen et al., 2012; Shiu & Chuang, 2019; Torbick et al., 2011). Despite its low (250 m) spatial resolution, the Moderate Resolution Imaging Spectroradiometer (MODIS) is widely applied to map rice production and offers the advantage of daily temporal resolution, which improves the probability of cloud-free acquisitions (Boschetti, Stroppiana, Brivio, & Bocchi, 2009; Nuarsa, Si, & Nuarsa, 2011; Son et al., 2013). High-temporal resolution also enables monitoring of crop phenology (Boschetti et al., 2017; Hmimina et al., 2013; Pan et al., 2012; Sakamoto et al., 2005; Zhang et al., 2003) and cropping intensity (e.g. single-crop, double-crop, or triple-crop) (Boschetti et al., 2017; Nguyen et al., 2012; Pan et al., 2012). Integrating the Earth Observation (EO)-derived information, such as vegetation indices, with in-situ measurements (empirical approach) or crop growth models enables estimation of the importance of rice biophysical variables (e.g. rice height, LAI, and biomass). A key aspect of this approach is to understand the relationship between rice biophysical variables and remote sensing data at different growth phases to facilitate predictions of yield prior to harvest. Wang et al. (2019) selected three main rice growth stages- the vegetative, reproductive pre-heading, and reproductive post-harvesting stages- to estimate LAI using machine learning methods. The results revealed the random forest was preferable in LAI estimation during the vegetative stage.

Rice yield can be estimated by using econometric models and crop growth models. Econometric models simulate crop yield by inputting previous agricultural areas, fuel costs, price, and weather data (Allen & Fildes, 2001). Crop growth models are more widely applied and can be either empirically based and driven by climatic variables, or physically based, where plant physiological development is simulated throughout the growing season based on a range of soil, meteorological, and vegetation inputs (Singh et al., 2014). A number of these models exist, such as estimate Environmental Policy Integrated Climate Model (EPIC) (Williams, Jones, Kiniry, & Spanel, 1989), Crop-Environment Resource Synthesis (CERES) (Jones et al., 2003), and ORYZA 2000

(Li et al., 2017). These models require parameterisation using meteorological information, soil characteristics, land management practices, and plant biophysical variables. Earth Observation (EO) sensors play a key role in the provision of crop biophysical variables used to parameterise crop simulation models and can do so throughout the growing season. A number of studies have demonstrated such benefits. For example, LAI and biomass of wheat were assimilated from remote sensing data (e.g. ASAR (Advanced SAR) and MERIS (Medium Resolution Imaging Spectrometer) data) and CERES-Wheat model; the simulated LAI and biomass data were then validated with ground and remote sensing data to seek the optimal set of input parameters (Dente, Satalino, Mattia, & Rinaldi, 2008). To improve parameterising crop growth models using remote sensing data, data assimilation methods, such as Ensemble Kalman Filter (EnKF), have been used to improve LAI monitoring and crop yield estimation. Using the CERES-wheat model, He et al. (2017) employed an EnKF to assimilated LAI estimates to predict yield, and found strong correlations with in-situ measurements. Data assimilation has been applied to LAI and canopy nitrogen accumulation from hyperspectral data using the DSSAT-CERES model with an excellent prediction accuracy (Li et al., 2015).

As a result of the benefits brought by EO sensors, satellite observations have been employed to monitor rice production at regional and global scales. For example, the Group on Earth Observation (GEO) Global Agricultural Monitoring Initiative (GEOGLAM) project utilises daily satellite and meteorological data to monitor global rice production and current crop conditions for four main crops (maize, soybeans, rice, and wheat) to generate Agricultural Market Information System (AMIS) of member organisations (CEOS, 2013). The main obstacle of remote sensing for rice monitoring using optical data is cloud cover, particularly during the wet season, which can be mitigated by the use of microwave observations through Synthetic Aperture Radar (SAR) sensors. SAR data have been successfully applied to map areas under rice cultivation and has been carried out in Kanchanaburi province with a classification accuracy of 89% (Aschbacher et al., 1995). A pilot project in Lao People's Democratic Republic, the Philippines, Thailand, and Viet Nam explored the potential of PALSAR-2 satellite images to estimate paddy rice cultivation area and production via developed INAHOR-AD (an advanced version of INternational Asian Harvest mOnitoring system for Rice) software based on remote sensed data (Rotairo et al., 2019).

Estimates of vegetation biophysical variables have been widely derived using optical measurements and spectral vegetation indices. However, cloud cover limits observations during key stages of the phenological cycle, and it is therefore important to assess the potential of both optical and microwave methods for estimating vegetation biophysical variables. In this research, the utility of vegetation indices (VIs; Normalised Difference Vegetation Index, NDVI; and Enhanced Vegetation Index, EVI) and backscatter (sigma nought) to estimate rice biophysical variables (e.g.

rice height, density, leaf area index, chlorophyll content, and biomass) will be investigated. The field experiments were conducted in the main cultivation area, an irrigated lowland rice area in the middle region.

1.2 Research questions

The research questions listed below are based on analysis of the scientific literature.

Research question 1: What is the role of changes in rainfall and temperature on rice yield and rice production, and how does this vary with the irrigation system in Thailand?

Research question 2: How does the irrigation system influence rice plant growth and development of biophysical variables during the growing season, and which rice biophysical variable is the best predictor of rice yield?

Research question 3: What is the potential of optical and SAR data for estimating rice biophysical variables in Thailand, and how does this vary between rice growth phases?

Research question 4: What is the potential of remote sensing estimates of biophysical variables to estimate rice yield?

This thesis sets out to contribute to our understanding of the importance of rice monitoring, rice farming systems, and the potential of remote sensing for rice yield prediction. A description of the thesis structure that highlights the content of each chapter is provided below; limitations and suggestions for future research build upon these new analyses.

1.3 Thesis scope and structure

The literature review (Chapter 2) found that precipitation and temperature are crucial factors in crop yield and production. This thesis aims to investigate the role of climatic parameters (temperature and rainfall) on annual rice yield and rice production in Thailand over 35 years (1981-2015) at the provincial level (Chapter 3). To provide a better understanding of the influence of climate on rice production, the analysis is stratified according to the percentage of cultivated rice area under irrigation.

Current methods for predicting rice yield are based on crop cutting experiments, which are time consuming and carried out close to crop harvesting. A field campaign was carried out during the growing season wherein a number of rice biophysical variables were measured during difference rice growth stages (Chapter 4). This allowed assessment of how rice development varied

throughout the growing season, under irrigated/non-irrigated conditions, and with rice variety. An analysis (Chapter 5) of the relationship between remote sensing observations and the in-situ measurements was carried out to investigate the potential of remote sensing to estimate rice biophysical variables at different stages of the growing season. The rice yield estimation approach developed in Chapter 5, based on the development of linear regression models using satellite observations and in-situ crop biophysical variables, aims to provide a timely and spatially dense approach for estimating yield than that currently provided by crop cutting experiments.

Chapter 2 Literature review

The purpose of this chapter is to critically review existing research on the relationship between climatic variables and rice production, with a specific focus on Thailand. Central to this is assessing state-of-the-art research on the potential to estimate rice biophysical variables using earth observation (EO) data and methods for estimating rice yield, specifically focusing on the Chao Phraya River delta. The structure of this chapter is as follows: Section 2.1 defines the rice ecosystem and the specifically categorised rice land ecosystem across the agro-ecological zones (AEZs) of the world. Section 2.2 sets out rice crop phenology and associated rice crop productivity stages, while Section 2.3 discusses the rice farming system in Thailand with respect to the timing of rice farming practices (e.g. planting/transplanting and weeding) and how these rice systems are linked. Section 2.4 investigates the factors that influence rice production and focuses on the role of meteorology and the impact of climate change on agriculture. Section 2.5 describes current methods for estimating rice productivity through surveying and, finally, Section 2.6 assesses the remote sensing techniques used for rice crop monitoring and yield estimation.

2.1 Rice ecosystem

There are 111 countries growing rice across the world, including most Asian countries, most countries of West and North Africa, some countries in Central and East Africa, most South and Central American countries, Australia, and some states in the U.S. Rice production occurs in wet, tropical and temperate climates due to appropriate temperatures and adequate rainfall. Rice is usually grown between 25° North and 25° South and from sea level to 2,500 m. The largest, and highest proportion of rice growing areas are located in South and Southeast Asia, where rice is cultivated in lowland areas and where monsoons ensure sufficient water.

Moormann and Breemen (1978) classify rice areas based on rice physiography and hydrology, with the latter separated into irrigated and non-irrigated areas. By determining physiographic and hydrology, the non-irrigated rice area is classified as pluvial (well drained and typically located in upland areas), phreatic (naturally slope or flat), and fluvial (lower or flat areas and most flooding).

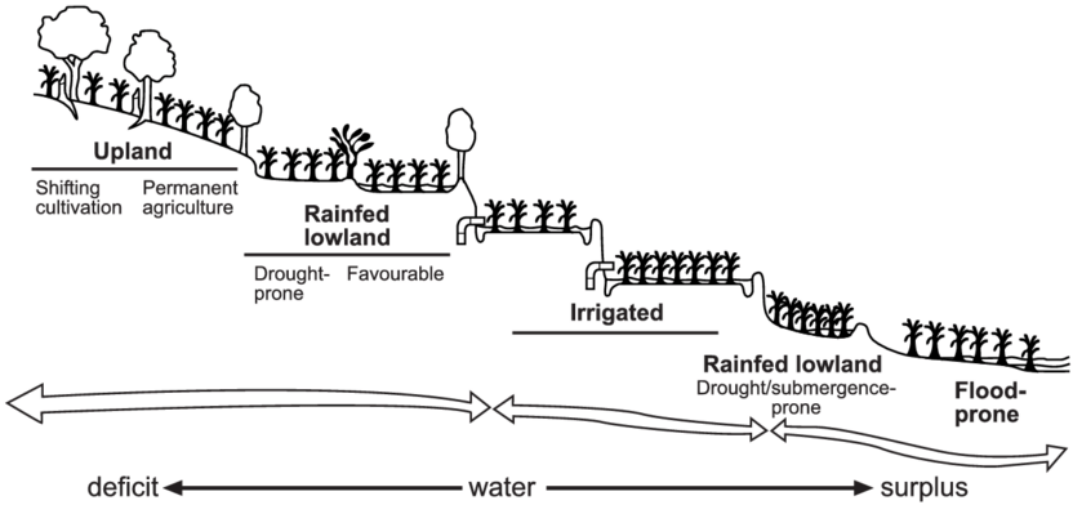

Upland	Rainfed lowland	Irrigated	Flood-prone
Level to steeply sloping fields; rarely flooded, aerobic soil; rice direct seeded on plowed dry soil or dibbled in wet, non-puddled soil	Level to slightly sloping, bunded fields; non-continuous flooding of variable depth and duration; submergence not exceeding 50 cm for more than 10 consecutive days; rice transplanted in puddle soil or direct seeded on puddle or plowed dry soil; alternating aerobic to anaerobic soil of variable frequency and duration	Leveled, bunded fields with water control; rice transplanted or direct seeded in puddle soil; shallow flooded with anaerobic soil during crop growth	Level to slightly sloping or depressed fields; more than 10 consecutive days of medium to very deep flooding (50 to more than 300 cm) during crop growth; rice transplanted in puddle soil or direct seeded on plowed dry soil; aerobic or anaerobic soil; soil salinity or toxicity in tidal areas

Figure 2.1 Four main types of rice-based cropping system during growing season (Halwart & Gupta, 2004).

Figure 2.1 illustrates the characteristics of rice-based cropping systems based on water availability and topography: upland, rainfed lowland, irrigated, and flood-prone. Irrigated rice areas mean rice is grown with adequate water supply and is flooded throughout the growing season. Under these conditions, rice is transplanted or direct seeded in the puddle soil. The rainfed rice areas or non-irrigated areas mean rice growth is reliant on rainfall, with non-continuous flooding and duration of the rice fields. Paddies are normally bundled to store water in the field not exceeding 50 cm depth for a maximum of 10 consecutive days. In upland areas, rice is grown on level to steeply-sloped fields and typically depends on rainfall. Finally, in flood-prone areas, rice is grown on level to slightly-sloping or depressed fields and is located near rivers where water depth exceeds 100 cm between >10 days to several months. Barker and Herdt (1979) classified rice cultivated areas in South and Southeast Asia into four main groups: irrigated, shallow rainfed, deep-water, and upland rice growing areas. In these regions, rice cropping is divided into two main seasons, wet and dry. The wet season is when the main proportion of rice is cultivated globally, as rainfall is the main restriction for rice cultivation in non-irrigated environments. The main limitation in the dry season is rainfall, and therefore there are fewer rice cultivated areas in the dry season. The proportion of rice cultivation in shallow rainfed, double cropping irrigated, and medium deep rainfed and deep-water is 34%, 19%, and 15%, respectively. With respect to

rice production in each of the groups, shallow rainfed, double crop irrigated, and single crop irrigated account for 33%, 31%, and 19%, respectively. These figures reveal that rice yield in irrigated areas is typically higher than non-irrigated areas.

In principle, rice is grown under different conditions, from waterlogged and poorly drained soils to well drained soils. The soil's physical properties are an important factor in rice-based cropping systems. In a rice growing environment, rice cultivated area is categorised into lowland (wetland preparation on rice fields) and upland (dryland preparation on rice fields) based on water supply and water management practices. Rice lands have been classified according to water regimes into upland (with standing water), lowland (with 5-50 cm of standing water), and deep water (with more than 51 cm to 5 m of standing water). Within this, rice cultivation is divided, based on the rice variety planted, into three main groups: lowland rice (with plants of semi-dwarf variety of medium to tall structure (100 cm to 2 m height)), upland rice with plants of medium to tall structure (130-150 cm height), deep water rice (with plants of medium to tall structure in different standing water (120-150 cm without standing water and 2-3 m height with rising water level)), and floating rice, with tall structures above 150 cm without standing water and 5-6 m with rising flood water.

In lowland rice areas, the paddy field is prepared either in wet or dry conditions; however, water is held and stored by bunds. In the pre-germination process, rice seeds are soaked in water for 24 hours and then incubated for 48 hours before being placed in the seedbed. This process assures a quick start in the seedbed. Most countries adopt the wet bed pattern for growing seedlings, in which pre-germinated rice seeds and are sown in puddled soil where the seedlings are ready for transplanting ~20-25 days after being sown. The current establishment techniques differ between non-irrigated and irrigated lowland rice. In non-irrigated lowland rice, the current establishes technique classified into transplanted in puddle soil, direct-seeded on puddled soil, and direct-seeded on dry soil. While irrigated lowland rice, the farmer directly seedling rice sprouts onto puddle soil, drill seeding into dry soil, broadcast seedling onto dry or moist soils, and water-seeded rice.

Each rice ecosystem utilises different methods of land preparation, which is relevant to the planting method and water availability and is influenced by precipitation availability and irrigation systems. Land and water management systems and tillage practices vary with the rice system, with the latter varying according to water availability, soil texture, topography, resources available to farmers, and farmers' preference for cropping pattern (Badshah et al., 2014; Chakraborty et al., 2017; Dou et al., 2016; Ye et al., 2013). The timeliness and quality of land preparation are important factors controlling rice growth and yield which result in differences in yield of up to 56.85% (Nwite et al., 2016).

2.2 Rice phenology

Rice is an annual grass with round, jointed culms, flat leaves, and panicles. The organism consists of the root, clump, and leaves. Tillers or panicles grow from the main clump and the primary tiller grows from the lowermost nodes, rising to secondary and tertiary tillers. Rice leaves, which grow at each node, consist of a blade, leaf sheath, flag leaf, auricles, and ligule. The panicle is enlarged beyond the flag leaf sheath. The spikelet is a unit of the panicle and continues to develop rice grains in a ripened ovary. Rice is a caryopsis in which a single rice seed is fused with a wall to form rice grain. A caryopsis is covered by two main leaves, the palea and lemma. There are three layers which cover the caryopsis coat: the pericarp, seed coat, and nucellus.

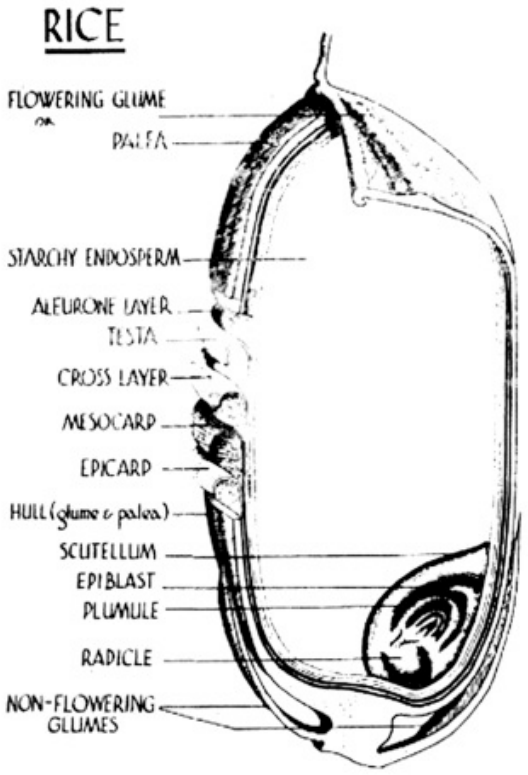

Figure 2.2 Cross-section of rice grain (Rosentrater & Evers, 2017).

The length of the phenological cycle of rice varies depending on environmental conditions, the rice variety, and management practice. Understanding rice phenology is essential for evaluating crop productivity and management practice. Changes in phenological period and length of growing season can lead to crop intensification and irrigated area. Normally, the duration from seeding to harvesting is 3-6 months, and is characterised by three physiologically distinct stages: vegetative, reproductive, and ripening. Rice variety controls the length of growing season and these are usually are defined as short-duration and long-duration rice varieties (Chen et al., 2020). Research found the shorter length of growing on short-duration rice to be 11-12 days and similar grain yield to long-duration rice. Other factors (e.g. spikelet filling rates, high harvest index,

biomass accumulation, crop growth rate, and radiation use efficiency (RUE)) are higher in short-duration rice than long-duration rice. Further studies found the delay of flowering on long-duration rice corresponds with photoperiods (Vergara & Chang, 1985).

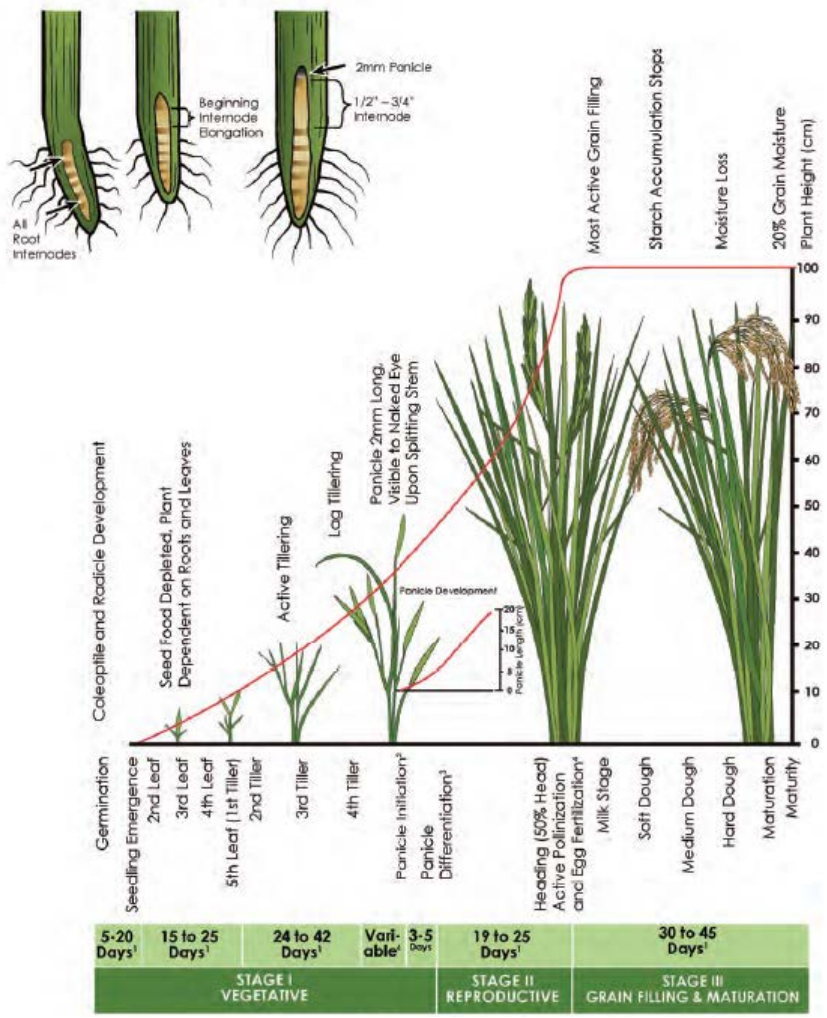

Figure 2.3 Rice development stages. The top left image illustrates the development of root internodes elongation and panicle and the large image illustrates the development of rice growth stage in vegetative, reproductive, and grain filling & maturation stages (Hardke, 2013).

Figure 2.3 represents the rice development stages, with different structures over the growing season. In the vegetative stage, rice is normally in the germination process and develops leaves and tillers. The vegetative stage ends with the development of the panicle initiation and differentiation. This is followed by the reproductive stage; rice in this stage is developing heading and active pollination. In the ripening stage, the rice grains develop, such as milk, dough, and mature grains. These stages are discussed in more detail below.

2.2.1 Vegetative phase

The vegetative phase occurs from germination to panicle initiation. Rice seeds are germinated and the radicle through the coleorhiza; young leaves then emerge under suitable warm and moist conditions. Tropical rice varieties have periods of dormancy, and some rice varieties protect rice lodging (when plant stems weaken and are unable support grain weight) during the ripening stage. When the rice grain is germinated, two or more seminal roots emerge from the rice seed. In the seeding phase, the rice emerges from soil and seeding develops seminal roots. After ten days, two or more rice leaves will have developed, and leaves continue to develop every 3-4 days in the early stages; with adequate water and temperature, five leaves will typically develop by the end of vegetative stage.

The tillering stage follows the seeding stage and begins with the appearance of the first tiller from the axillary bud and the development of secondary and tertiary tillers. The development of tertiary tillers is classified into two sub-stages: the maximum tillering stage and stem elongation stage. After the maximum tillering stage, some tillers gradually die, the number of tillers decreases, and vertical growth ceases. The stem elongation stage starts before panicle initiation; however, the stem elongation and panicle initiation stages occur simultaneously in short rice varieties. In this stage, the rice root system consists of two major categories: crown roots and nodal roots. The crown root develops from nodes below the soil surface and nodal roots which develop above soil surface (De Datta, 1981).

2.2.2 Reproductive phase

De Datta (1981) clarified that the reproductive stage begins after the maximum tillering stage and depends on the rice variety and environmental conditions. Panicle initiation is noticeable when the rice is a differentiated of primordium. Then, the panicle occurs in the main clump, followed by other clumps with no exact pattern.

In the panicle initiation stage, the rice stem ceases vertical growth to develop rice grains following the growth phase and panicle initiation occurs simultaneously. The significant structures that develop during the panicle stage are the base, axis, primary and secondary branches, pedicel, rudimentary glumes, and spikelet. Rice plants have a fully developed flower per spikelet approximately 52 days after sowing in the panicle stage. During the panicle stage, the spikelet develops inside a flag leaf sheath and continues to develop the panicle slowly. There are three sub-phases within the reproductive stage: booting, heading, and flowering. The booting stage begins when the flag leaf sheath is a well-developed and other below leaf is senescence. The heading stage occurs with the emergence of the panicle on the flag leaf sheath, and the flowering stage

occurs when the rice begins anthesis and panicles occur at the top, middle, and lower portion of the rice structure. However, the period of the flowering stage is dependent on the rice variety and environment.

2.2.3 Ripening phase

The ripening phase is the growth phase that occurs between the flowering and maturity stages and usually lasts ~30 days (De Datta, 1981). Several factors influence the duration of ripening, such as the number of rainy days, temperature, fertiliser use, and rice variety (Okamura et al., 2018; Rathnayaka, Iqbal, & Rifnas, 2018; Sabaruddin et al., 2002; Vergara et al., 1966) with the latter varying the ripening period by between 35-50 days (Moldenhauer & Slaton, 2001). High temperature during the grain filling and ripening stages produces imperfect or empty grain, especially in the upper and lower part of grain. There are three sub-phases which are relevant to grain colour: the milk grain stage, dough grain stage, and mature grain stage. In the milk grain stage, the caryopses are watery and develop a milky substance on grains; during the dough grain stage the grains turn into soft and hard dough. During the mature stage, between 90-100% of the filled spikelet, rice turn into yellow and harder grains, and the senescence of the upper leaves is apparent; however, the clumps and upper rice leaves remain healthy with green colour while the grain is fully ripened.

The growth phase of rice is distinguished by the number of leaves and varies between short and long duration rice. The length of the vegetative and reproductive period varies depending on rice varieties; however, the ripening stage is equal among rice varieties, about 30 days. In principle, the order of rice leaves is positioned as the first, second, and third leaf, and so on in the order they emerge. The physiological growth stage is determined when rice have fully developed their leaves on the main culm.

2.3 Rice farming system in Thailand

In Southeast Asia, most rice cultivation occurs in lowland rice systems found in both humid and moist sub-humid agro-ecological zones, where farmers are typically small holders. Rice cultivation accounts for 71 million ha, and approximately 45% of irrigated areas are found in Indonesia, Vietnam, the Philippines, and Thailand. In Thailand, the lowland rice area, irrigated and non-irrigated area, is 2,075 ha and 6,792 ha, respectively (Redfern, Azzu, & Binamira, 2012). This section discusses the rice farming systems in Thailand in terms of the timing of planting/transplanting, weeding, cropping patterns, and rice farm business.

2.3.1 Timing of planting and transplanting

The rice growing season is defined as being either wet or dry, with more rice grown during the wet season. Planting dates in wet season are usually based on the start of monsoon season, especially in transplanted non-irrigated rice areas. In tropical and sub-tropical climatic zones, the day length for photoperiod-insensitive rice varieties is suitable all year, allowing farmers to plant rice in all periods in irrigated areas. By definition, rice cropping in Thailand is divided into rainy season, which occurs between May and October in most areas, except the southern part of Thailand, where rice grows between June and February. Dry season occurs between November to April in most areas, except the southern part of Thailand (OAE, 2014b).

The growing period of rice in the wet season begins when monsoons hit, at which time farmers prepare their paddies for planting by ploughing the soil and releasing the standing water. The traditional rice cropping pattern in Thailand involves farmers soaking and incubating the rice seed in water and then seeding the rice directly into the fields, defined as wet or dry seeding. In wet seeding, the most common method, rice seeds are sown into flooded fields, whilst dry seeding involves sowing rice seeds into dry bare soil and waiting for rainfall to germinate the rice.

2.3.2 Rice cropping patterns

As mentioned above, the methods of rice planting in Thailand depend on several factors. The rice cropping pattern influences the timing of the sowing and harvesting periods, and the land preparation varies according to the rice cropping pattern. The latter is classified into three main types – transplanting-flooded rice, dry direct seeding, and wet direct seeding.

2.3.2.1 Transplanting-flooded rice

Transplanting flooded rice is the method used when young rice sprouts from the nursery are transplanted into paddy fields in a row pattern. Transplanting is either carried out manually (using a random or straight-row method) or by machine, with the former being labour-intensive whilst the latter increases the farmers' costs. At present, the "system of rice intensification" (SRI, Upboff, 2008) has been adopted, which allows a farmer to plant rice seeds in a small pot and sow the rice stems directly into the field, potentially increasing yield (Latif, Islam, Ali, & Saleque, 2005; Sinha & Talati, 2007), reducing labour inputs (Sinha & Talati, 2007), and saving water usage. Rice yield is dependent on farm management practices as when best management practices are implemented. The best management practice experiment was conducted on irrigated and non-irrigated lowland rice in Bangladesh between System of Rice Intensification (SRI) and Best Management Practices (BMPs) by evaluating varied practices (e.g. seeding age, plant spacing,

application of organic manure, seeding density, duration of planting, planting shape, and time of planting). The result proved no useful impact on yield with SRI, because there were individual crop management techniques (Latif et al., 2009).

2.3.2.2 Dry direct seeding

Direct seeding is a method wherein dry seeds are sown directly into paddies, suitable in non-irrigated drought-prone areas (Pandey, 2002). Typically, this cropping pattern requires rainfall after seeding for germination. After seeding, the farmer ploughs the topsoil in their field and rice seed is rather deep and uses moisture in the soil to penetrate the root system. Another technique involves the farmer direct seeding after rainfall has flooded the paddy. Research comparing parameters such as LAI, yield, and water productivity between dry direct seeded rice (DDSR) and traditional transplanted rice (TPR) found DDSR had a higher yield (13.18%) and reduced total water input (8-12%) in comparison with TPR (Ishfaq et al., 2020). Conversely, other research proved the rice yield of direct-seeded rice (DSR) was 12% lower than conventional transplanted rice (TPR) and yield loss of DSR and TPR depended on management practices, soil type, and climate conditions (Xu et al., 2019). In addition, there were differences in the panicle number among dry direct-seeded and transplanted-flooded rice across rice varieties (Liu et al., 2014).

2.3.2.3 Wet direct seeding

Wet direct seeding involves seeding rice for germination in soil with 2-3 cm of standing water in the fields. Farmers in irrigated areas utilise this technique to increase their chances of achieving improved rice production; it also has the advantage of screening sub-optimal rice seeds and eliminating weeds before planting. The paddy needs to be flooded at least two weeks prior to planting to ensure the decay of organic soil matter.

2.3.3 Post-harvest rice processing in Thailand

After harvesting, farmers transport rice grains to rice mills. Rice mills in Thailand are divided into three classes based on production capability: small (1-12 tonnes/24 hours), medium (30-60 tonnes/24 hours), and large (more than 60 tonnes/24 hours). Normally, medium and large rice mills are located in essential rice growing areas in the central region, while most rice farmers in the north and northeast regions bring their produce to small rice mills, with most of the grains consumed within the household. In local areas, there are commission merchants who buy rice grains directly from farmers for quality approval. Rice grain markets include farmers, merchants, and the owners of rice mills, and farmer and rice mill owner join the negotiation for an acceptable price. Finally, rice production transport to the rice markets for domestic and export markets. The

Office of Agricultural Economics (OAE) analyses rice prices and publishes the information on a daily, weekly, and monthly basis for crops.

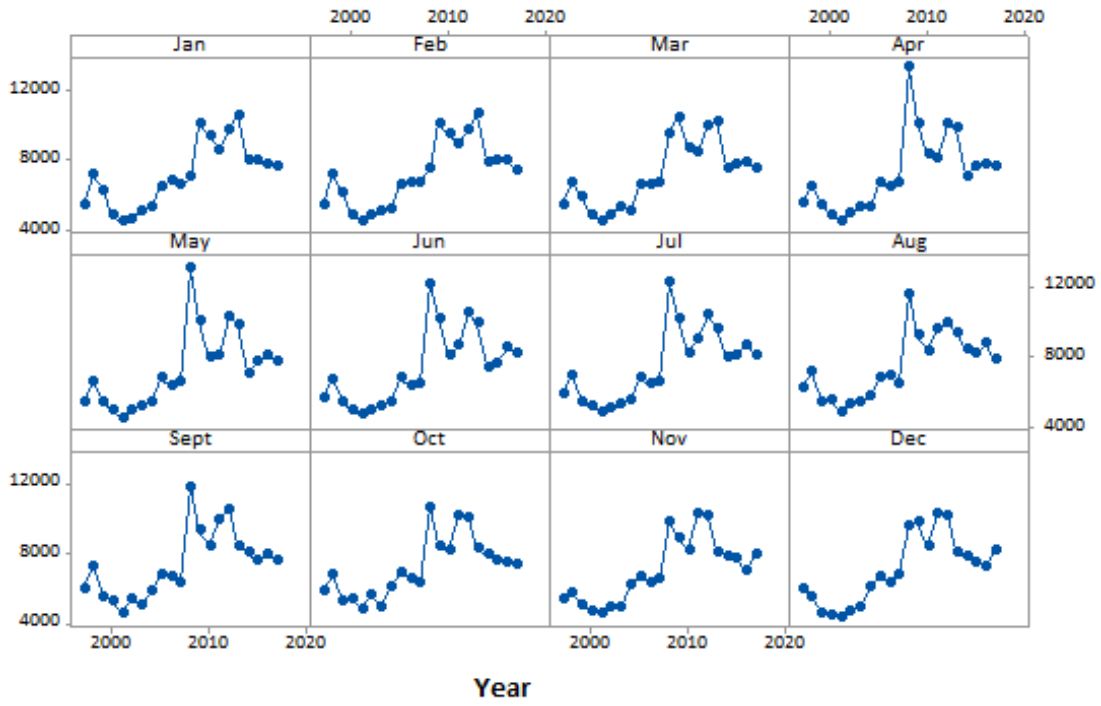

Figure 2.4 Rice price at farm gate- directed purchase from farmer (at 15% humidity) between 1997-2017.

Figure 2.4 illustrates the fluctuation of the farm gate price of rice grains at 15% humidity between 1997-2017. The minimum, maximum, and average farm gate price were 7,040 THB/ton (November), 7,421 THB/ton (August), and 7,201 THB/ton, respectively. This figure reveals two price peaks after the adoption of the rice mortgage policy (March 2011) and a period of flooding (October 2011). The rice mortgage policy guaranteed a rice price of 15,000 THB/ton, which is nearly double the price in earlier years. Also, government policy influenced the rice price between 2008-2009 and price range from 8,460 THB/ton (October 2009) to 13,259 THB/ton (April 2008). In addition, Thailand was severely affected by flooding in Chao Phraya River delta in 2011 (Komori et al., 2012) which severely impacted rice production (Son et al., 2013) and caused high prices the following year. Prices ranged between 9,641 THB/ton in January and 10,584 THB/ton in September, which is dependent on the export situation and rice stocks.

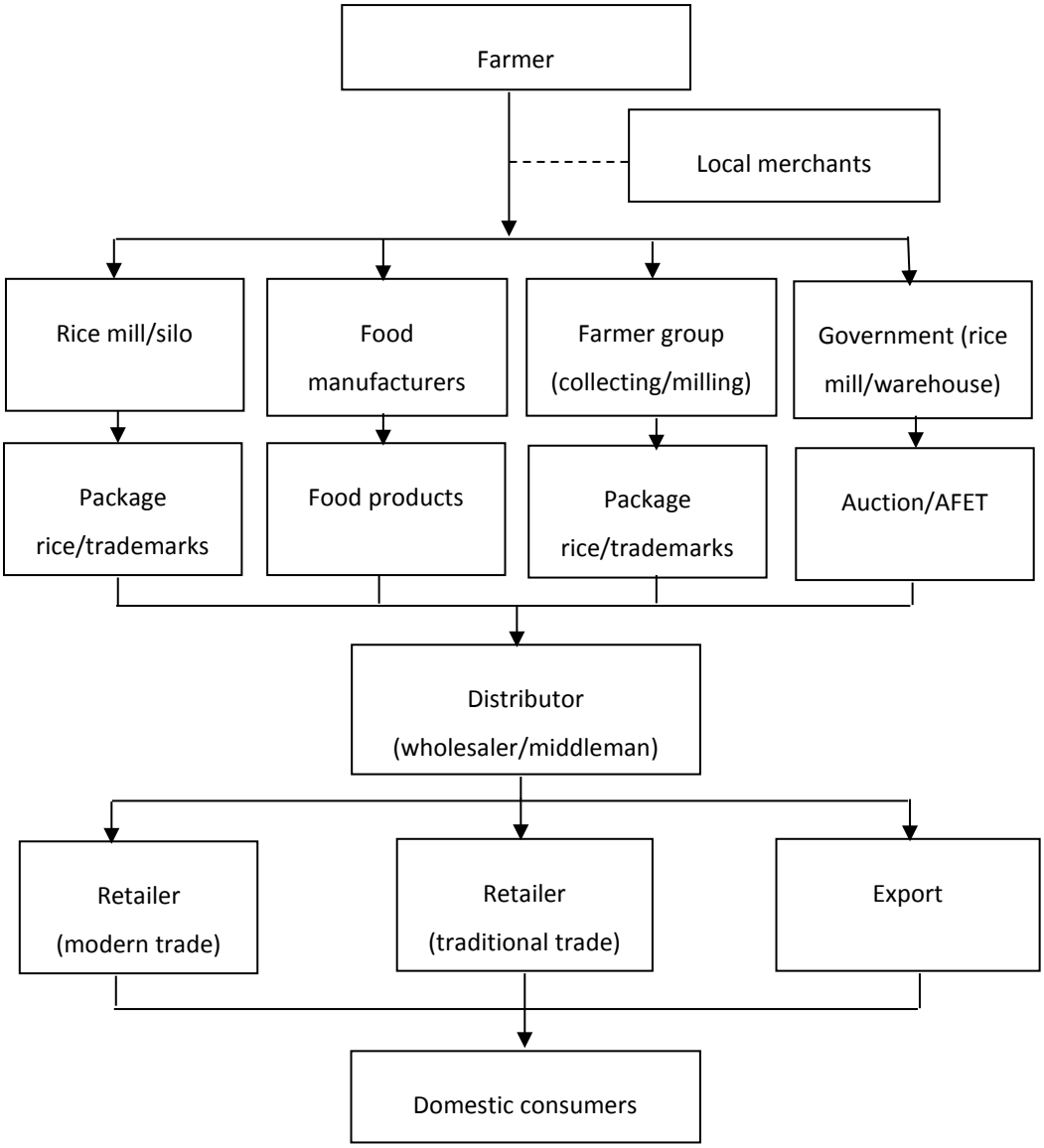

Figure 2.5 Flowchart illustrating the rice supply chain in Thailand (Titapiwatanakun, 2012).

Figure 2.5 shows the intermediaries involved in the rice farming and supply system in Thailand (Titapiwatanakun, 2012). At the local level, intermediaries are local buyers, local commission agents, cooperatives, farmer groups, local assembling markets, and millers. After harvesting, farmers sell their product directly to small rice mills or silos in the local area, although due to transportation issues some sell to local merchants who then negotiate the price with mill owners. Most local assemblers are shopkeepers who provide credit to farmers or production inputs (ADB, 2012). In the main rice cultivation areas, government agencies and business sectors establish rice mills and warehouses for use by local farmers, local assemblers, and merchants. Central paddy markets also provide labour, moisture gauges, drying lawns, warehouses, and loan systems. After processing the rice packaging, the rice is distributed to wholesalers or middlemen who sell the rice to modern trade markets or traditional markets. On a national scale, the rice remaining after

consumption is exported to foreign markets, typically 44.61% of the total rice produced (OAE, 2018a). In 2018, annual rice production was 34.5 million tonnes (22.8 million tonnes; milled basis) (FAO, 2018).

2.4 Factors affecting rice production

Rice production is influenced by both natural and agricultural practices. Farmers maximise crop growth and grain yield using fertiliser and pesticide for increasing incomes on their agricultural product. However, weather, soil characteristics, biotic conditions, and agricultural practices all impact rice production. This section discusses the role of weather, geography, water availability, disease and pests, rice variety, and government policy on annual rice production.

2.4.1 Weather and climate

Rainfall is essential for rice cultivation, and in areas with suboptimal rainfall, irrigation is necessary to ensure sufficient water is available throughout the growing season. Dams and irrigation canals are constructed by government to meet this requirement, and in Thailand 25.68% of the rice cultivated area relies on irrigation (OAE, 2018c). In tropical regions such as Thailand, rice areas are divided into two climatic types based on rainfall distribution: tropical rainy and tropical wet-dry. The former has sufficient rainfall throughout the growing season and is not considered drought-prone, while the latter receives adequate rainfall but the variability in rainfall distribution is the main restriction of rice planting. Most rice grown in the tropics depends on the monsoon rains and planting dates coincide with the onset of the rainy season. Variability in the amount and distribution of rainfall is a major factor influencing yield. Excessive rainfall is the main cause of flooding, which reduces yield and severely damages the crop when the rice develops milk or dough grains (see **Section 2.2.3**).

Several studies have investigated the impact of rainfall on crop yield and agricultural production. A study simulating hydrological conditions in the Lower Mekong Basin found evaporation-transpiration increased in the baseline between 1985-2000 and the climate change scenario in 2010-2050 and 90% cumulative probability value raising the irrigation demand. Larger variation in annual rainfall causes water shortages at the crucial time of rice planting, thus delaying the transplanting date in non-irrigated rice areas, and longer dry spells during the wet season raise drought risks in the same. These factors impact reducing rice yield and production in terms of delaying rice transplanting and increasing drought risks, which depend on photoperiod lengths (Yamauchi, 2014). This study highlighted how sensitive the planting dates are to the onset of rainfall; they can be shifted earlier or delayed to avoid crop damage. Mainuddin et al. (2012)

simulated the AquaCrop models by shifting planting dates plus or minus two weeks in Cambodia and Vietnam; their results indicated that shifting the planting dates increased crop yield per unit of actual evapotranspiration (WP_{ET}; kg m^{-3}), but also greatly increased WP_{ET} and had an impact on spikelet sterility. Water scarcity can lead to delaying of anthesis, resulting in a reduction of the number of spikelets per panicle by up to 60% and decreasing grain yield to 20% (Boonjung & Fukai, 1996). These studies highlight the value of irrigation systems in areas with less stable rainfall patterns, which typically result in higher rice productivity (Laux, Jäckel, Tingem, & Kunstmann, 2010; Rockström et al., 2010; Sharma et al., 2010). Bouman and Tuong (2001) analysed a method for water-saving irrigation in India and the Philippines by suggesting a reduction of pond water depth and alternating cropping patterns into wetting/drying.

Solar radiation is the radiant spectral energy directly emitted from the sun, which varies according to geographic location, time, and local topographic and weather conditions. Solar radiation in the visible wavelength (380-720 nm) is essential for crop photosynthesis; thus, the intensity of solar radiation is closely related to crop growth. There are slightly differences in solar radiation between tropical and temperate regions and the beginning of planting determines the suitable crop ripening period (Wang et al., 2016). Chen, Baethgen, and Robertson (2013) examined the impact of inter-annual variability and temperature/solar radiation/precipitation trends of wheat and maize yield in the double cropping systems from 1961-2003 developed 129 climate scenarios, and simulated crop yield with Agricultural Production Systems Simulator (APSIM). The result proved the reduction of simulated yield on both wheat and maize and led to the reduction of potential yield for both crops. Islam and Morison (1992) examined the impact of total incident solar radiation (irradiance) and temperature on irrigated rice grain yield in Bangladesh by developing the linear relationship between grain yield and irradiance in the reproductive and ripening stages. The photo thermal quotient, which was calculated from the ratio between mean daily irradiance and mean temperature above base temperature, was related to rice yield. The result illustrated the varied relationship due to rice variety influenced the number of spikelets, grain weight, and percentage of sterile spikelets. Other important research investigated the influences of low solar radiation (10 days before and 25 days after the flowering stage); then, a reduction in amount and weight of spikelets occurred and led to a reduction in the final yield. Because this stage requires high solar radiation for photo assimilation, the result suggested rice variety improvement and shifting of planting date for the properly amount of solar radiation in the reproductive and grain filling stages (Santos et al., 2017).

Temperature is a crucial factor for crop growth, affecting the degradation of pollen viability, spikelet and filling grain quality, and decreasing grain yield (Yang et al., 2017). Analysis of the impact of daytime and night-time temperatures on crop growth have found reductions in grain

yield by 10% for each 1°Celsius increase in minimum temperature in the dry season, but little impact was found when the maximum temperature increased (Laza, Peng, Akita, & Saka, 2004). Night-time post-anthesis warming influenced rice productivity and grain quality. Using two rice cultivars in east China, an increase in temperature by 3°Celsius led to greater night-time respiration rates and decreased photosynthesis rates, resulting in a decrease in aboveground biomass accumulation of 22% on average and reduced rates of seed setting and grain filling (Dong et al., 2014). High maximum daytime temperatures affect rice yield via spikelet sterility and grain quality (Rang et al., 2011), while night-time temperatures decrease grain yield by 10% for each 1°Celsius increase in minimum temperature due to physiological effects (Peng et al., 2004).

Droughts often occur with high temperatures and reduced precipitation, and drought observations between 1980-2008 identified several regions worldwide as being a high agricultural drought hazard for various crops (Geng et al., 2016). International agencies have programmes to monitor and forecast trends in global temperature. The National Oceanic and Atmospheric Administration (NOAA) analysed global temperatures in several regions, revealing Asia observed its warmest year in 2015. The Asia-Pacific region has increasingly endured heat waves, tropical cyclones, prolonged dry spells, intense rainfall, tornadoes, snow avalanches, thunderstorms, and severe dust storms (IFAD, 2016). Figure 2.6 illustrates the change in temperature witnessed since 1880, wherein the positive values indicate an increase in temperature while negative values indicate a lower temperature. Climate models have forecast temperature increases in the Asia-Pacific area of approximately 0.5-2°Celsius by 2030 and 1-7°Celsius by 2070 (Preston, Suppiah, Macadam, & Bathols, 2006). Studies investigating the potential impact of future temperature increases on rice production have found temperature increase and reduced soil moisture impacts driven by El Niño–Southern Oscillation (ENSO). By 10% variance in anomalous rice production linked soil moisture variability. The rice production proved strong negative correlated with El Niño

3.4 index and production in non-irrigated upland rice production was high responded than irrigated rice production (Stuecker et al., 2018).

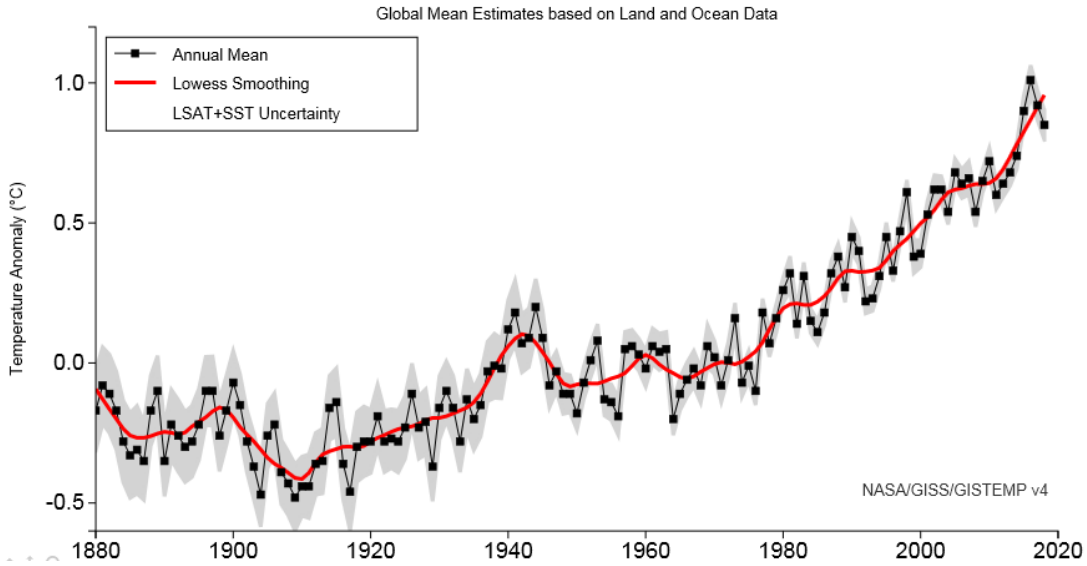

Figure 2.6 Global mean estimates based on land and ocean data between 1880-2020. Black line is the global annual mean, the red line is the five-year running average, and the grey boundary is the total (LSAT and SST) annual uncertainty at a 95% confidence interval (NASA, 2019).

It is widely recognised that climate change has had negative consequences on water resources, with seasonal decreases in global rainfall and runoff particularly apparent in south and southeast Asia (Gistemp Team., 2020). Arnell, Lindberg, and Grimmond (1999) simulated numerous climate change scenarios using Hadley Centre climate simulations and found an increase in annual runoff in high latitudes, equatorial Africa and Asia, and southeast Asia, with a decrease in annual runoff in mid-latitudes and sub-tropical regions. A number of studies (Loo et al., 2015; Singh & Qin, 2020) have also found seasonal decreases in rainfall and runoff in south and southeast Asia have directly affected water resources and freshwater availability. The impact of water viability on crops is noticeable on different scales. Here, it has been revealed that there have been negative impacts of climate change, especially yield reduction (e.g. wheat, rice, and maize) in the tropical and temperature regions for every 2°Celsius increase. Whilst some areas are benefits from climate change in the medium confidence (IPCC, 2014).

Climate change- induced changes in agricultural production can impact the price of commodities. For example, the price of agricultural product is forecast to increase by approximately 32-37% with rice yield losses of between 10-15% by 2050 (IFPRI, 2017). Regarding, reduction in crop yield, farmers will inevitably have to adapt their practices for traditional rice varieties or begin breeding new rice varieties tolerant to higher temperatures, use of irrigation systems, shifting planting dates, utilising fertiliser, and applying management practices (Chun et al., 2016; Redfern, Azzu, &

Binamira, 2012). The Asian Development Bank (ADB) predicted that without instigating climate change policies in Indonesia and Thailand, these countries' Gross Domestic Product (GDP) would reduce by around 6.7% by 2010 (Weiss, 2009). Therefore, it is essential to mitigate and adapt agricultural practices for changes in climate.

Lobell, Schlenker, and Costa-Roberts (2011) studied trends in climate and global crop production on a national scale between 1980 – 2008 for four crops. The study demonstrated that the impact of climate varied spatially for wheat and maize, whereby reduction on production 3.8% and 5.5% of global net losses. With respect to rice, high latitude areas benefitted from global warming, whereas there were no significant impacts found on rice productivity in Asia. Ye et al. (2019) investigated the phenological date of median length of nursery, vegetative, and reproductive stages with changing date to -1.9%, 2.7 and 0 day/decade. Ye et al. (2015) evaluated the effects of climate change on rice areas, cropping systems, and crop water requirements by exploring the ratio of Potential Growing Season Length (PGSL) and ideal growing season length (IGSL). This study indicated that both the growing season length and paddy water consumption would increase with rising temperatures. Other studies have found that differences in the maximum and minimum temperature can reduce rice growth in different cropping system. The night-time warming was shortening in the pre-flowering and prolonged in the post-flowering. The increase of temperature was increment grain yield 16.2%, 12.7%, and 12% in the late rice in the rice-rice cropping system, wheat in the rice-wheat cropping system, and rice in single rice cropping system; then, there were decreasing on grain yield 4.5% and 6.5% in the early rice in the rice-rice cropping system and rice in rice-wheat cropping system (Chen et al., 2017). Fang et al. (2015) proved the increase in global temperature increases aboveground biomass, grain yield, plant height, and panicle number while decreasing harvest index (HI).

2.4.2 Geographic and soil characteristics

Local geographic conditions, such as altitude and soil characteristics, can play an important role in crop production. Most rice is grown in tropical wetland areas, which results in higher yields than other zones. Altitude also affects rice grain yield with the yield 1.7 times higher in the mid-altitude than in high and low altitude, which few upland rice cultivated areas due to difficulties concerning planting and management. The flowering duration fluctuates at different altitudes, with averages in low altitude, mid-altitude, and high altitude areas of 12 days, 16 days, and 24 days, respectively (Shrestha et al., 2012). Soil characteristics influence the capacity of rice and maize to absorb water and nutrients and therefore impact crop development (Egamberdiyeva, 2007; Yang, Yang, Yang, & Ouyang, 2004). Soil characteristics such as texture, density, organic matter, salinity, and acidity also influence crop development, with enriched soils typically having 24% increased yields than

those are sub-optimal (Oladele, Adeyemo, & Awodun, 2019). 'Soil horizon' refers to a layer of soil parallel to the surface, and there are several horizons, such as O (organic), A (surface or topsoil), E (eluviation), B (subsoil), C (sub-stratum), and R (bedrock). The A horizon is a suitable environment for crop root growth due to water and nutrient absorption. The mineral or organic matter transmits to other soil horizons throughout water and wind erosions. Rice has a shallow root structure (below 20 cm), so its roots spread across the A and B horizons.

2.4.3 Diseases and pests

Disease- mainly caused by bacteria, viruses, or fungi- and pests- such as golden snails, birds, and nematodes- serve to reduce yield. Pesticides and insecticides are used but are often only applied once damage is visible, which may be too late. It is estimated that pests and disease reduce rice yield by 37% annually (IRRI, 2017). To mitigate this, some farmers adopt hybrid rice more resistant to pests, which reduces the cost for insecticides and rice variety can be more productive (Huang et al., 2005).

The overuse of fertiliser, especially nitrogen, can lead to an increase in pests and disease and a decrease in grain yield, while also reducing the biodiversity of the rice ecosystem (Peng et al., 2009). The misuse of pesticide has inequitable ecological consequences; therefore, agricultural practices and post-harvest management need to be implemented to address physical spoilage and grain contamination.

2.4.4 Weeding

Weeds in paddy fields can reduce rice productivity, increase costs, and reduce grain quality by competing with rice plants for nutrients, soil, and solar radiation. Typically, direct seeding has a higher proportion of weeds than transplanting rice, as the latter involves greater input in land preparation. There are different methods to control weeds, such as ploughing the topsoil and abandoning land for seed germination, after which farmers plough the soil to bury the weeds and harrow remaining weeds from the fields. This improves soil characteristics and levels the fields. Weeds also affect soil moisture, and so farmers must release water into their fields approximately seven days prior to planting to prevent weed development.

2.4.5 Rice variety

The variety of rice has an impact on its yield, characteristics, and resistance to damage from stressful conditions. Some countries have developed new rice varieties to be more tolerant of extreme conditions such as drought, cold, heat, salt, and flooding (Ahuja, de Vos, Bones, & Hall,

2010). There are two main species of rice: Oryza Sativa (*O.Sativa*, Asian rice) and Oryza Glaberimma (*O. Glaberimma*, African rice). *O. Sativa* is the most common, containing and more than 100 rice varieties (Wei & Huang, 2019). Rice varieties are classified into two main categories: sensitive and non-sensitive. The difference between these categories comes down to genotypic variation and influences on length of panicle emergence and panicle initiation (Collinson, Ellis, Summerfield, & Roberts, 1992). Sensitive rice varieties have nearby flowering dates despite differences in planting dates, and as their photoperiod is shorter, almost all are planted in the wet season. Sensitive rice varieties flower when the daytime is shorter than 12 hours, with less sensitive varieties having a photoperiod of 11 hours 40 minutes and more sensitive varieties having a photoperiod of 11 hours 10-20 minutes. These sensitive rice varieties are planted once a year and are the most common rice variety. Non-sensitive varieties can be planted in all conditions where there is adequate water for planting. The main difference between photoperiod-sensitive and photoperiod-insensitive rice is panicle emergence (Collinson, Ellis, Summerfield, & Roberts, 1992) depending on day length and temperature (Vergara & Chang, 1985)

2.4.6 Government policies, economic conditions and market factors

Government policy and economic conditions influence agricultural areas and, consequently, yield. Government policy is influenced by agricultural production demand, both internal and external; for example, low rice production can raise consumption demand, requiring the government to implement policies to motivate farmers to increase their planting area or frequency of planting (i.e. double or triple cropping). Such government policies include price incentives, tax reductions, provision of seeds, technology, and expert knowledge to support farmers.

Thailand is continuously establishing agricultural policies to balance production and guarantee good performance by farmers. The “farmer aid committee” has existed since 1965 to support farmers (e.g. increasing rice yield, supporting rice prices, and agricultural credits); in 1966, the Bank for Agriculture and Agricultural Cooperatives (BAAC) was established to provide farm credits. Between 1974-83, the Thai government intervened in rice markets through the Marketing Organization of Farmers (MOF) and indirectly through buffer stocks of the Public Warehouse Organization (PWO). In 1985, a minimum farm price was introduced and provided rice millers with low-interest rate loans to motivate buying paddies at minimal cost. In 1984, the Warehousing and Pledging policy was implemented to provide high prices with low-interest rates for farmers. In 1986, premiums, export quotas, and export stocks were cancelled (Wiboonpongse & Chaovanapoonphol, 2001).

Recently, Thailand has adopted agricultural policies (Figure 2.7) which mainly impact rice production, such as rice mortgage (regulation in 2008), agricultural zoning (regulation in 2009 - 2012), crop insurance (2016), and reduction of rice cultivated areas in the dry season (2017). Rice mortgage policies have resulted in rice prices higher than the average (15,000 THB/ton), motivating farmers to plant rice instead other crops and thus increasing the rice cultivated area. In 2013, rice harvested area, production, and yield increased by 57.50 million rai (9.2 million ha), 23.43 million milled tonnes, 436 kilogram/rai (69.76 kilogram/ha) increased 1.6%, 3.53%, and 1.83%, respectively. Other significant policies include a new project that links farmers in important rice areas to local markets, with the aim reducing cost (20%) and increasing rice production (20%) (2018).

At present, government policies aim to reduce rice cultivated areas by promoting rezoning of agricultural areas to encourage farmers to plant other suitable crops, aiming to reduce rice cultivated area reduce by 6 million rai (0.96 million hectares) between 2017-36 by using several Geographic Information System (GIS) layers (e.g. natural resources, soil characteristic, existing crop areas, production, demand and supply). To reduce unsuitable rice area, government motivated farmers changing to plant the other crops; then, government provides infrastructure, subsidy, low rate of interest charged, and facilitates knowledge on agricultural and markets.

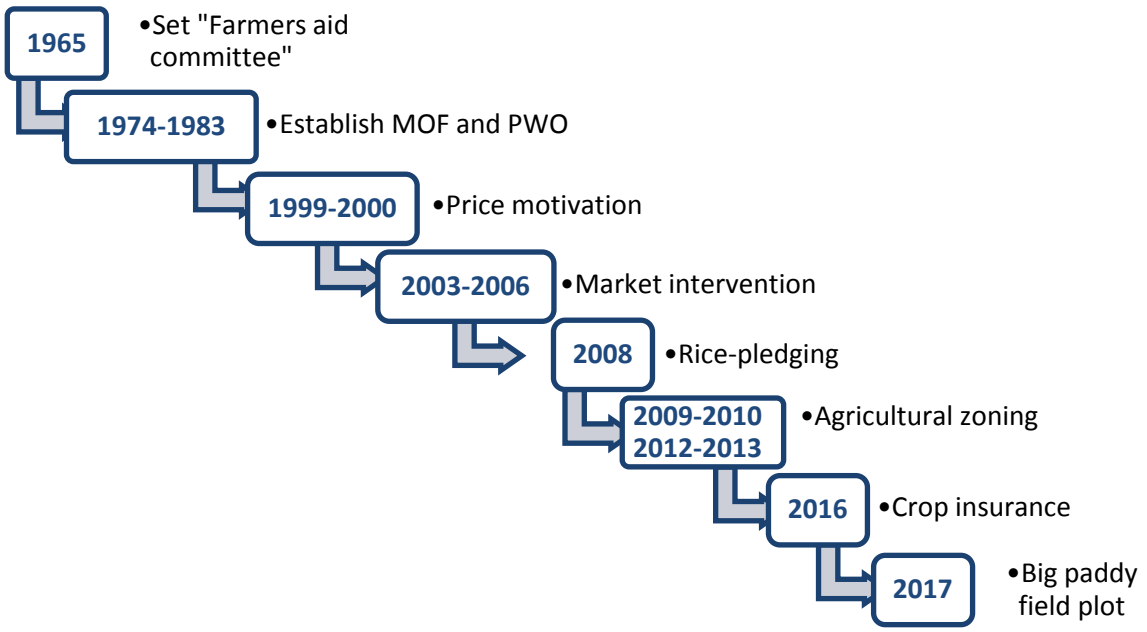

Figure 2.7 Development of agricultural policies in Thailand between 1981-2015.

Figure 2.7 enumerates several agricultural policies from 1965-2017; the rice-pledging and agricultural zonings have had a significant effect on rice cultivated area and production in

Thailand. Rice-pledging is guaranteeing the high selling price; thus, there are increasing in rice cultivated area. While the agricultural zoning controls farmer to plant rice in suitable area.

2.5 Agricultural data collection in Thailand

The Office of Agricultural Economics (OAE) is the government department responsible for providing agricultural information, collecting information on rice, upland crops, and tree perennials using stratified two-stage random sampling at a village level for selected crops. A first step is a random village. The second step is a random household who plant specific crop by using simple random sampling without replacement. Several techniques for obtaining agricultural information, such as lists of cropping villages or areas, are used for defining the sampling frame. The survey data collected include the cultivated agricultural area, harvested area, total production, fertiliser application, amount of crop seeds usage, and plant and harvest date (OAE, 2014). Two approaches are used to collect agricultural information: using lists of villages, and crop cutting experiments.

2.5.1 Using lists of villages

A survey based on lists of villages, referred to as a 'list frame survey', is developed using stratified sampling of villages who plant particular crops obtained from production reports at sub-district and district level. The list samples independently select crop commodities by listing of units (e.g. farm, household, and population census). The time-surveyed for each crop is different throughout the year. The advantage of the list frame survey is that it lists the interested farm/household and is properly representative of the population (stratum). In addition, the list frame survey reduces survey costs; thus, it is the most common method of obtaining agricultural information. However, this method may lead to errors in the sample frame selection. The questionnaire should be testing for reduction on ambiguous/unclear inquiry. Figure 2.8 illustrates the agricultural sampling procedure applied to calculate the agricultural statistics. Farmers register their land area under cultivation, and the central office sends a list of samples to the regional office listing all farmers who plant particular crops. Further, the household sampling is adopting by random without replacement. The surveyed data is summarised into cultivated agricultural areas, production, and yield at the district level. To account for variations in population density, the survey areas are grouped into small, middle, and large agricultural areas and villages are selected that are representative of each group ('first stratified random sampling'); from this the random household stratification is applied.

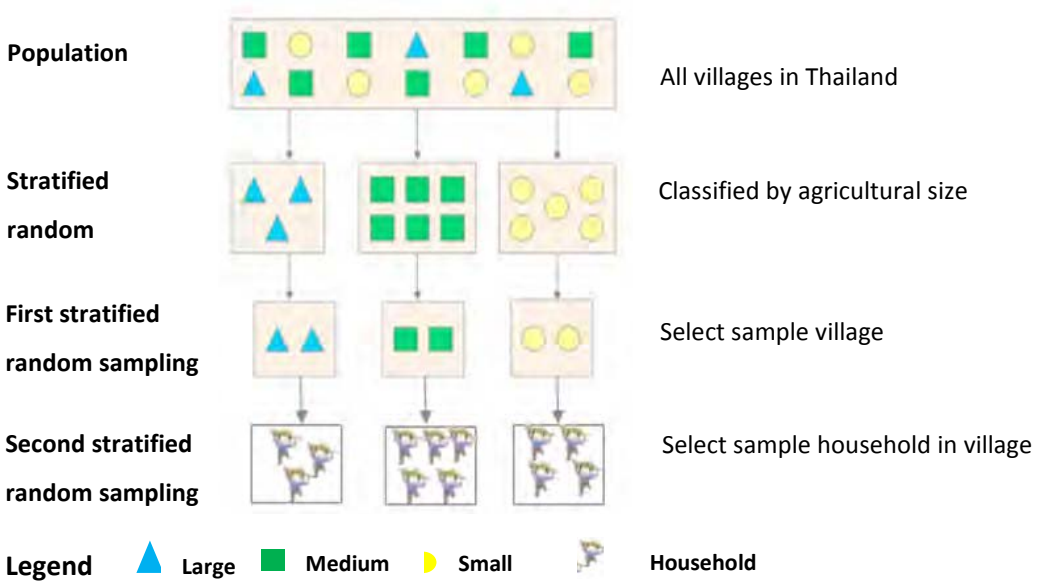

Figure 2.8 Two-stratified random sampling (OAE, 2014a).

2.5.2 Crop cutting experiment

Yield surveys are conducted using crop cutting experiment (CCE) (FAO, 1982; Fermont & Benson, 2011), a survey method to estimate approximate crop yield in specific areas using sampling plots in fields. The CCE is widely used and conducting on field crops. The advantage of CCE is to derive the average yield in the district or state level before the end of growing season; a limitation is partial or complete crop damage sample unit by winds, animal, etc. There are several steps in the CCE technique to determine yield: selection (village and field), identification of sample plot location, measurement, harvesting from the sample plot, threshing crops, cleaning, and weighting (Ahmad, Sahoo, Singh, & Biswas, 2021). The sample plot size is defined as 1 m x 1 m for rice and soybean yield, while the sample size of cassava, sugarcane, and maize is bigger with sample plot size as 3 m x 3 m. At each sample plot, the crop is harvested, and yield is measured by removing and weighting all grains. The yield per unit area estimates is then extrapolated to estimate yields at sub-district, district, and provincial levels based on the area of land under rice cultivation. This is derived from interviews with farmers and spatial mapping using satellite observations (**Section 2.6.2**). Several researchers have applied the CCE technique to gain crop yield information and estimate crop yield using satellite data (Bhutada, Kohirepatli, & Chavan, 2016; Ranjan & Parida, 2021).

2.6 Remote sensing within rice crop mapping and rice yield estimation

2.6.1 Introduction to remote sensing

Remote sensing is a technique for gaining information on the Earth's environment using measurements of spectral reflected and emitted radiance and, in the context of terrestrial remote sensing, has been widely applied in areas such as forestry, natural resources, agriculture, and urban planning. The Sun is the main source of electromagnetic radiation but all materials above absolute zero emit radiation which can be measured. The electromagnetic spectrum, part of which is shown in Figure 2.9, ranges from very short, high intensity Gamma wavelengths through to longer, low intensity radio wavelengths. Remote sensing instruments are either passive or active, with the former measuring reflected or emitted radiation. Most passive remote sensing instruments collect measurements in the visible, near-infrared (NIR), and longwave parts of the spectrum, which include parts of the spectrum most sensitive to characterising vegetation properties (Richards, 2013). The optical wavelengths occur between 0.4-2.5 µm with the reflectance profiles of a number of different land surface types shown in Figure 2.9. Remote sensing exploits the differing optical properties of surface objects to differentiate them and characterise their crop status.

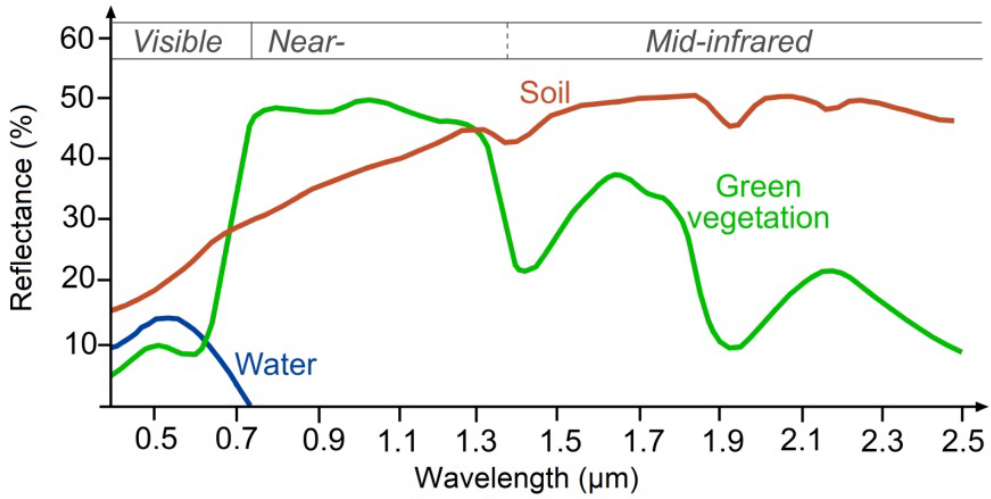

Figure 2.9 Spectral response of soil, vegetation, and water in the visible and infrared wavelength range (Remote Sensing Applications Consultants Ltd (RSAC) (2021)).

Figure 2.9 depicts the reflectance profiles of three of Earth's surface materials in visible and infrared spectrum. Water has low reflectance (< 10%) in visible wavelengths, which varies according to the concentrations of sediment, organic matter and water depth; while energy in the NIR is absorbed, soil reflectance typically increases with wavelength, and water absorption features at 1.4 µm, 1.9 µm, and 2.7 µm. Finally, vegetation reflectance in the visible spectrum is controlled by its

composition of pigments such as chlorophyll, which absorb energy in the red and blue wavelengths for use in photosynthesis (Liu & Iersel, 2021). When vegetation senescence, the pigment concentration reduces, and this results in greater red reflectance, turning the leaves shades of orange and red. In the NIR (0.7 - 1.2 μm), leaf structure and morphology influence the transmission and reflectance properties of vegetation, whilst in shortwave infrared, vegetation moisture content defines the magnitude of reflectance. The variation of reflectance at different wavelengths enables the inference of the materials being measured and their properties, which in the case of vegetation may relate to its health and vigour. The boundary between the red and NIR wavelengths is referred to as the 'red-edge' and the position of the inflection points has been found to be sensitive to chlorophyll concentration in the leaves (Curran, Dungan, Macler, & Plummer, 1991; Li et al., 2015) and this has led to the development of sensors that contain wavebands in this region, such as the Multispectral Instrument (MSI) on Sentinel-2.

2.6.2 Spectral vegetation indices

While individual spectral wavebands provide useful information for monitoring the environment, combining two or more spectral wavebands can improve the available information. These are referred to as spectral indices, which utilise waveband combinations to facilitate the characterisation of surface types such as water bodies or geological features. Vegetation indices (VI) are spectral transformations of remotely-sensed images using arithmetic operations among pixel brightness, such as subtraction or division of brightness, for two or more spectral bands (Schowengerdt, 2007; Xue & Su, 2017). The ratio of different spectral bands relates to the influence of 'noise', such as view and illumination angles, whilst enhancing the detectability of the feature of interest. A number of vegetation indices have been developed over time, including the simple ratio (SR; Chen (1996)), normalised difference vegetation index (NDVI; Rouse, Haas, Schell, & Deering (1974)), soil adjusted vegetation index (SAVI; Huete (1988)) and enhanced vegetation index (EVI; Huete, Liu, Batchily, & Leeuwen (1997)). Two of the most commonly applied vegetation indices are the NDVI and EVI. The NDVI, proposed by Rouse and Tucker (Rouse et al., 1974; Tucker, 1979), utilises red and NIR wavebands and has been applied to estimate vegetation cover (Ding, Zhao, Zheng, & Jiang, 2014; Jafari, Lewis, & Ostendorf, 2007; Zhu et al., 2008) and land use changes (Chen et al., 2006; Shalaby & Tateishi, 2007), to assess the impact of droughts (Peters et al., 2002; Singh et al., 2003; Yagci et al., 2011), and to estimate biomass (Bao et al., 2019; van der Meer et al., 2000). The EVI was developed to exploit MODIS spectral bands, to minimise the influence of vegetation canopy background variations, and to maintain sensitivity over dense vegetation canopies (Huete et al., 2002).

Currently, there is a wide range of vegetation indices that utilise combinations of different spectral bands to enhance specific characteristics of vegetation. As noted previously, VIs is often used to estimate vegetation biophysical variables using empirical models. Nguy-Robertson et al. (2014) assessed the potential of estimating LAI using ten vegetation indices, including the simple ratio, green NDVI (GNDVI), red edge NDVI, red edge chlorophyll index ($CL_{red\ edge}$), and MERIS Terrestrial Chlorophyll Index (MTCI). The results revealed a strong relationship between vegetation indices and green LAI over four crop canopies (potato, wheat, soybean, and maize) with $R^2 > 0.8$. However, the drawback of some VIs tends to saturated at high LAIs by using the Scattering of Arbitrarily Inclined Leaves (SAIL) model. Baret and Guyot (1991) investigated the sensitivity of different spectral indices to vegetation canopy characteristics and found, for example, the soil-adjusted vegetation index (SAVI) and transformed soil-adjusted vegetation index (TSAVI) were less effected by soil background reflectance and thereby offered benefits in low vegetation cover environments compared to other indices.

One of the main applications of vegetation indices is monitoring crop phenology (Figure 2.10), which is associated with time detection of biological events of plant growth by exploiting the frequency (e.g. daily, weekly) of satellite overpasses (Weng, 2011). These measurements provide information on the start, peak, end, and length of the growing season, which can be used to, for example, identify changes in planting patterns (Gim et al., 2020). Vegetation index measurements during the growing season have been used to classify crops by exploiting their different seasonal cycles (Gumma, Nelson, & Yamano, 2019) and to identify areas under different cropping intensities (Kotsuki & Tanaka, 2015; Li et al., 2014; Pan et al., 2021; Yan et al., 2019).

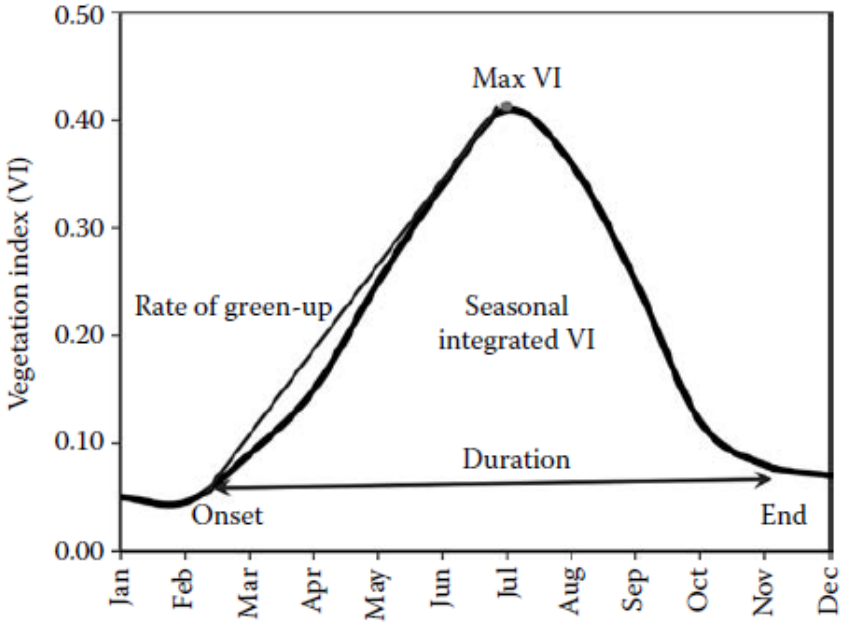

Figure 2.10 Phenology metrics derived from VI measurements showing the key phenological stages (Weng, 2011).

The dynamics of rice growth have three main periods: 1) flooding and transplanting period, 2) growing including the vegetative, reproductive, and ripening stages, and 3) fallow after harvesting. Despite its low spatial resolution (250-500 m), the daily temporal resolution of MODIS has seen it widely applied to monitoring the phenological cycle using vegetation indices in order to detect areas under rice cultivation by detecting the different growth stages (Son et al., 2013; Son et al., 2012; Tingting & Chuang, 2010; Xiao et al., 2006). These researchers created a time-series of MODIS data vital to processing the noise filtering. Then, there were adopt Empirical Mode Decomposition (EMD) and developed the vegetation indices (e.g. NDVI, EVI, LSWI, and NDSI) to monitor rice crop and classify land use/land cover. The Artificial Neural Networks (ANNs) technique, which is nonlinear mapping structure based on the human brain (Lek, 2008), was applied for land use/land cover classification. There were temporal characteristics of rice cropping pattern through year. The phenology-based classification approach based on MODIS data was compared with ground reference data and national census data, which allowed researchers to assess the accuracy via overall accuracy, Kappa coefficient, or relative error.

Medium spatial resolution optical imagery (Landsat 7, Landsat 8, SPOT, and HJ 1A/B) is also used to study crop phenology, which has the advantage of more reliably mapping individual fields but is constrained by fewer temporal observations (Dao & Liou, 2015). Using an NDVI time-series, reconstructed using a Fast Fourier Transformation (FFT), Zhao et al. (2016) developed a classification to map the key transitions of rice cultivation areas: 1) double-season early stage rice cultivation where paddy fields were inundated with water; 2) a single-season middle rice-transplanting stage; and 3) double-season late rice wherein the field still contains standing water but some fields show existence other aquatic plant. The study then compared relative error in different cities located in the Dongting Lake basin in Hunan and Yanjiang and found the relative error in three growth phases in Hunan were -10.99%, 1.46%, and -5.87%, respectively, whilst in Yanjiang these errors were 12.1%, 16.7%, and 0.8%, respectively. The transplanting and heading is preferable for time-series analysis. Similar research has been carried out by Zhang et al. (2015), who developed an algorithm that utilised pixel and phenological information to classify rice areas into three phases: 1) flooding and rice transplanting; 2) rapid plant growth and canopy closure after transplanting; and 3) fallow after harvesting. An area of 39,239 km^2 in northeast China was mapped as being under rice cultivation with an overall accuracy of 97%, producer accuracy 92%, and user accuracy 96%, with omission and commission of errors of 8% and 4%, respectively.

In addition to mapping the location of areas under rice cultivation, remote sensing phenological data also enable mapping of the intensity of farming in terms of single, double, or triple cropping. A study investigated the relationship between phenology-based classification and remotely-sensed data by developing time-series of EVI from MODIS data during 2001-2012. The Empirical

Mode Decomposition (EMD) was then related with EVI in the paddy fields to determine the temporal characteristics of the rice. The rice cultivated areas in single-cropped rainfed rice, double-cropped irrigated rice, and double-cropped rainfed rice decreased -5%, -19.2%, and -0.74%, respectively (Son et al., 2013). Minh et al. (2019) studied the rice cropping system in the An Giang province of the Vietnamese Mekong Delta (VMD) from March 2017 to March 2018 based on dual-polarisation Sentinel-1 and considered backscatter coefficients. The VH backscatter coefficients were associated with all growth phases, especially the reproductive phase, because there was less influence from soil moisture and water in paddies. The Support Vector Machine (SVM) classified the rice cultivated area with 80.7% overall accuracy and 0.78 Kappa coefficient.

2.6.3 Estimation of vegetation biophysical variables

Plants intercept direct and diffuse sunlight, with the upper leaves receiving higher amounts of radiation compared to lower leaves, which influences the morphology of leaves of different crop species, particularly leaf area and colour (Burgess et al., 2017; Chang et al., 2019). Canopy biophysical variables relevant to vegetation characteristics include vegetation fraction (F_v), leaf area index (LAI), fraction of absorbed photosynthetically active radiation (fAPAR), chlorophyll content, and water content. The spectral profile of healthy green vegetation is influenced by the level of pigment concentration (visible), cell structure (NIR) and moisture content (SWIR), and changes to plant health can be identified by changes in the reflectance characteristics in these spectral regions. Such measurements also enable estimates of vegetation biophysical variables to be made, which in turn can be used in forecasting yield. The vegetation fraction (F_v) defines ground surface covered with vegetation and considers the distribution and properties in a horizontal perspective of crop canopy, and is therefore useful for evapotranspiration (Et), rainfall interception, and energy transfer assessment (Olioso et al., 2019). The leaf area index (LAI) or green leaf area index (GLAI) are defined as the one-sided green leaf area per unit of ground surface (Chen & Black, 1992). In principle, the LAI is an excellent indicator of crop development and is widely used as an input parameter in crop growth models (Saseendran et al., 1998; Setiyono et al., 2018; Raoufi et al., 2018; Tang et al., 2009). LAI is one of the crop biophysical variables routinely retrieved using remote sensing observations, with operational products produced by using coarse MODIS (Knyazikhin et al., 1999; Yan et al., 2016) and Sentinel-3/PROBA data (Fuster et al., 2020). Higher spatial resolution LAI retrievals can also be derived using Sentinel-1 and Sentinel-2 data. Campos-Taberner et al. (2017) derived LAI estimates over rice canopies in Italy, Spain, and Greece using Sentinel-2A and Sentinel-1A; SAR data from Sentinel-1A were used to map rice cultivated areas due to the strong separability of backscatter in water inundated paddy fields, while reflectance observations from Landsat and Sentinel-2 were used to invert the PROSAIL

(Baret, Jacquemoud, Guyot, & Leprieur, 1992) model, which is a combination of the PROSPECT and SAIL models for shifting red-edge region analysis. When compared to in-situ ground LAI measurements, the LAI retrievals had an overall RMSE 0.69 m^2 m^{-2}, with the time-series of LAI reaching a maximum of 5.3 m^2 m^{-2} using Sentinel-2 data and 4.3 m^2 m^{-2} using Landsat data.

The boundary between red and NIR wavelengths, referred to as the 'red-edge' (0.7-0.74 μm), changes position as the chlorophyll content of the leaves changes due to the influence of chlorophyll absorption in red wavelengths. The chlorophyll content at leaf and canopy level is an indicator of the health of plant communities, which can change in response to stress imposed by climate extremes or disease. The launch of the Medium Resolution Imaging Spectrometer (MERIS), and more recently the MSI on Sentinel-2, provided instruments with wavebands located in the red-edge, which have been exploited to derive chlorophyll estimates using VIs such as the MERIS Terrestrial Chlorophyll Index (MTCI; Dash & Curran (2004)). Croft, Chen, and Zhang (2014) investigated chlorophyll content on needle leaf and broadleaf in Ontario, Canada in 2004 by adopting 47 vegetation indices by using MERIS. High correlation was found between chlorophyll content and the Double Difference (DD)-index (R^2 = 0.78 and RMSE = 3.56 μg cm^{-2}), although poorer relationships were found in needle leaf canopies (D_{red} R^2 = 0.71 and RMSE = 2.32 μg cm^{-2}). Numerous studies have utilised spectral vegetation indices to identify stressed crops by detecting the shift of the red-edge toward shorter wavelengths, referred to as the "blue shift". This study then simulated the PROSPECT model with canopy reflectance and MNDVI8 (Modified NDVI) revealed a strong relationship between dynamics of chlorophyll and leaf structure. The vegetation indices were stable when LAI > 4 m^2 m^{-2}. The spectral regions, especially red and near-infrared, estimated chlorophyll content; high chlorophyll content reflected red saturation. The estimation chlorophyll contents conducted during growing season of 2001, 2002, and 2003 at University of Nebraska-Lincoln research facility in maize and soybean and the result proved chlorophyll content ((R_{NIR}/R_{red} edge)-1) with RMSE less than 61 mg m^{-2}) (Gitelson et al., 2005). Xu et al. (2011) investigated five vegetation indices (e.g. Normalised Difference Vegetation Index (NDVI), Modified Simple Ratio Index (MSR), Modified Chlorophyll Absorption Ratio Index (MCARI), Transformed Chlorophyll Absorption Ratio Index (TCARI), and Optimized Soil-Adjusted Vegetation Index (OSAVI)) on rice in Qianjin and Youyi farm, Heilongjiang Nongken, China in 2009. All five were closely related with chlorophyll content: the study then estimated with Weight Optimization Combination (WOC) method and there was improved performance in OSAVI and MSR.

The fraction of Photosynthetically Active Radiation Absorbed (fAPAR) is related to primary productivity as a function of the light-use efficiency (LUE) coefficient, which defines the amount of carbon fixed per unit radiation intercepted (Landsberg et al., 1997). Approximately 50% of incident photosynthetically active radiation (PAR) is absorbed for photosynthesis. Ehammer,

Fritsch, Conrad, Lamers, and Dech (2010) estimated the fraction of photosynthetic active radiation (fPAR) and LAI for cotton and rice canopies in Amu Darya Delta, Uzbekistan using RapidEye imagery, findings that increased plant height coincided with increased fPAR and LAI, whilst on the field scale, strong correlations (R^2 = 0.95 and R^2 = 0.92) were found using a linear regression between VIs and fPAR and LAI, respectively. Similar results were found by Gitelson, Vina, Ciganda, Rundquist, and Arkebauer (2005) when assessing the relationship between NDVI and fAPAR on maize and soybean by using MODIS and MERIS.

Biomass is an essential variable to estimate crop production in terms of wet and dry biomass. Several studies have investigated the relationship between biomass, LAI, and production using linear and non-linear regression to describe the relationship between two or more variables. Marshall and Thenkabail (2015) estimated above-water biomass (AWB) using multiple regressions between non-remotely sensed variables (e.g. aboveground biomass, visible canopy, background RGB light intensity, height, and above-below canopy irradiance) and remotely-sensed variables and in-situ measurements. The hyperspectral narrowband (HNBs), between 350-2,500 nm, were combined (height and HNBs in the NIR region, height, F_{APAR}, and HNBs in NIR region, height and HNBs in visible and NIR region, and Fraction of Vegetation Cover (FVC) in the visible). The results indicated that the correlation coefficient (R^2) of rice, maize, cotton, and alfalfa yield were 0.84, 0.59, 0.91, and 0.86, respectively. Compared with using HNBs alone, there was improved the aboveground wet biomass variance of rice, maize, cotton, and alfalfa: 12%, 29%, 14%, and 6%, respectively.

2.6.4 Crop yield estimation using optical data

There are a range of approaches that can be utilised to relate the crop canopy with remotely-sensed data. A commonly applied approach to estimate crop yield is through the development of regression models between remotely-sensed metrics and in-situ measurements. Often these have involved relating vegetation index values to vegetation biophysical variables. Bolton and Friedl (2013) developed maize and soybean yield models based on linear regressions between three VIs (NDVI, two-band Enhanced Vegetation Index (EVI2), and NDWI) and yield, using a time-series of MODIS data. The results revealed the EVI2 predicted yield for maize in non-semi-arid countries with R^2 = 0.67 (cross-validated calculating 2004-2006 versus 2007-2009, R^2 = 0.59) whilst the NDWI had better agreement in semi-arid countries (R^2 = 0.69, cross-validated calculating, R^2 = 0.62). The relationship between the NDVI and EVI2 and soybean yield was also good and the same as cross-validated (R^2 = 0.69 and 0.7). The phenological measurements using vegetation indices have also proved their utility in estimating crop yield. Zheng et al. (2016) derived the red-edge chlorophyll index ($CI_{red\ edge}$) and NDVI in the National Engineering and Technology Centre for

Information Agriculture in 2013 from two different handheld spectrometer measurements throughout the growing season to characterise the phenology of a rice canopy. These data detected the main phenological in the tillering, middle heading, and maturity, at which point the temporal of indices and phonological date was adopted. The performance of $CI_{red\ edge}$ with RMSE 2.3-4.6 days proved excellent in indica rice than japonica rice cultivar for middle booting date and dough grain date estimation; thus, the result assumed rice cultivars influenced their relation.

Dash and Curran (2007) estimated crop yield in South Dakota, U.S. in 2003 by using a time-series of two spectral vegetation indices: the MERIS Global Vegetation Index (MGVI) and MTCI. Key metrics extracted from the VI time-series are the maximum VI value and the area under curve: the relationship correlation between yield and area under the curve to peak VI value were 0.61 and 0.69 for the MGVI and MTCI, respectively. The correlation between yield and area under the whole VI time-series was stronger, at 0.83 and 0.85 for the MGVI and MTCI, respectively. Mechanistic models simulate the time-series of crop state variables (e.g. LAI, dimension and biomass of various organs, and crop development), energy, carbon, water, and nutrient fluxes on crop, soil, and atmosphere. One of the key parameters used in these models is LAI, which is influenced for the absorption of solar radiation, evapotranspiration, and carbon assimilation. In terms of remote sensing, the spectral bands are useful for analysis crop canopy structure and photosynthesis activity, thermal infrared on water status, and microwave on water contents, soil moisture, and canopy structure (Moulin, Bondeau, & Delecolle, 1998). Crop growth models (e.g. ORYZA2000, DSSAT, EPIC, and WOFOST model) (Jin et al., 2018; Kasampalis et al., 2018; Launay & Guerif, 2005) and volume scattering model (Wang et al., 2009; Zhang, Yang, Liu, & Wang, 2016) are widely used to simulate daily crop growth in terms of crop photosynthesis, respiration, transpiration, and morphogenesis growth. Crop growth models, parameterised using remotely-sensed LAI estimates, have been applied to estimate yield for winter wheat using the WOFOST model (Huang et al., 2015) and maize using the Agricultural Production Systems SIMulator (APSIM; Machwitz et al. (2014)) with good results. Similar methods have also been applied to estimate rice yield in Terai districts of Nepal between 2016-2018 using the multi-temporal of Sentinel-2 data and 3D Convolutionmal Neural Network (CNN) under several conditions (e.g. using satellite data, combining with climate or soil data, or combining satellite with climate and soil data) in four experiments and the CNN-3D is better results than CNN-2D (Fernandez-Beltran et al., 2021). The remote sensed data are develop vegetation index. Nuarsa, Nishio, and Hongo (2011) study the NDVI development based on Landsat Enhanced Thematic Mapper Plus (ETM+) image with field observation data by using the exponential equation on model development based on NDVI. The result compared with reference data in the linear relationship and proved strong agreement between NDVI and reference data. Jing-feng et al. (2002) applied the crop simulation model to

describe the relationship between physiological processes and environmental growing conditions. The Rice-SRS based on ORYZA model was developed and combined with 3 sources of NDVI - NOAA AVHRR (LAC) NDVI, NOAA AVHRR (GAC) NDVI, and radiometric measurement NDVI (measured in the tillering, booting, heading, and milk stages). The result proved a reduction in estimating error by 1.03%, 0.79%, and -0.79% for early, single, and late rice season. The NOAA AVHRR (GAC) NDVI was an excellent input, with an average error of -7.43%.

2.6.5 Application of active remote sensing for vegetation monitoring and crop yield estimation

Active remote sensing involves transmitting a pulse of energy from an instrument and measuring the return signal, often focused on NIR or radio wavelength, termed LiDAR and radar respectively. Radar sensors measure the strength of the signal scattered back from the surface, which is influenced by the surface structure (e.g. canopy geometry and topography) and surface moisture content (Martinez-Agirre, Álvarez-Mozos, & Lievens, 2017; Martinez-Agirre & Álvarez-Mozos, 2017) and the angle by which the surface is viewed, also influence the backscatter signal. The advantages of microwave sensors include their longer wavelengths, which can penetrate cloud cover and light rain, thereby enabling imagery to be acquired in all weather conditions and at night. This attribute has led to radar sensors being widely applied in tropical environments. Volume scattering from crop canopies is comparatively low, with the backscatter coefficient largely influenced by the surface underneath the canopy (Choudhury & Chakraborty, 2006; Liu et al., 2019; Phan, 2018). Moisture content influences electrical properties of the surface, and this called “complex permittivity”. The scattering mechanism combines four reflections: specular, diffuse, corner reflector, and volume scatter. The specular reflection occurs on smooth and flat surfaces, while diffuse reflection occurs over rough surfaces which scatter the signal in all directions. These scattering effects reflect the different signals that occur during growing season, since they are influenced by the rice canopy structure composed of stem, stalk, and grain (Inoue et al., 2014; Yuzugullu et al., 2016). The polarisation of a radar sensor is configured to transmit either horizontal (H) or vertical (V) signals and receive these data either horizontal or vertical polarisation. In principle, the polarimetric radar measures scattering of transmitting and receiving polarisation combinations, which include is HH, VV, HV, and VH combinations. These combinations of different polarisations influence the scattering coefficient and the ratio between scattered and transmitted fields in each polarisation.

The scattering of microwave wavelengths from crop canopies is influenced by three components: 1) direct backscatter from an object; 2) multiple volume scattering from canopy; and 3) double-bounce effects, when the edge of a reflection on rice to water surface and off-rice to water

surface (Pichierri, Hajnsek, Zwieback, & Rabus, 2018; Zhao & Cui, 2013). The maximum backscatter depends on the dielectric constant of materials, distribution size and orientation of scattering elements in the canopy, and surface roughness (Marghany, 2020). Rice is a semi-aquatic plant whose temporal dynamics of backscatter will differ from other crops, and this has often been exploited by using radar data to map areas under rice production (Boschetti et al., 2014). In the seeding stage, paddy fields are highly reflected with water surface and quasi-vertical/quasi-horizontal structures in tillers and leaves, and the backscatter demonstrates an incoherent sum of interactions. As the rice develops in height and density, the backscatter coefficients increase due to greater volume scattering within the canopy and increased multiple scattering between stems (include tillers) until a reduction in moisture content during the ripening phase.

Several studies have been successful in using SAR data to map areas under rice cultivation. Hoang, Bernier, Duchesne, and Tran (2013) classified rice fields in Vietnam between 2009-2010 by using RADARSAT-2 C-band data with a Support Vector Machine (SVM) approach that exploited the narrow dynamic range of radar backscatter found over residential and forested areas, which contrasted with the large dynamic range found over paddy fields. Corresponding classification accuracy of 71% and 80% was achieved for HH and quad-polarised imagery, respectively. Clauss et al. (2018), using Sentinel-1 Interferometric Wide (IW) mode and Ground Range Detected (GRD) in VV and VH polarisation, mapped areas of rice cultivation using super-pixel segmentation and phenology-based decision tree and a random forest model. High correlation was found between area measurements at the district level ($R^2 = 0.93$) for winter-spring rice and for autumn-winter rice ($R^2 = 0.87$). Numerous studies that utilise SAR imagery with different polarisations illustrate the importance of canopy structure on the success of the rice classification. Bouvet, Le Toan, and Dao (2014) investigated the influence of polarisation for mapping rice cultivation and estimating biophysical variables in Vietnam. The HH and VV polarisation increased at the beginning of the season and decreased in the tillering stage, whereas the VV backscatter decreased due to the vertical structure of the rice stem and increased when the panicle emerged approximately 60 days after sowing. Changes in the backscatter due to changes in the structure of the rice canopy enabled mapping the sowing date based on the ratio of HH/VV backscatter. The ratio of polarised signals was also exploited by Zheng et al. (2016b) who classified the winter-spring and summer-autumn cropping season in Vietnam using the ratio of VH/VV polarisation. This study developed a normalised difference between the sowing dates (SD) and heading dates (HD) index (NDSH) (NDSH = HD-SD/HD+SD) for use in classification and achieved an overall accuracy and Kappa coefficient of 86.2% and 0.72, respectively.

There are three types of radar signal: gamma nought, beta nought, and sigma nought. Sigma nought (σ^0) refers to the scattering coefficient and illustrates the amount of average backscattered power compared to power of incident field. Several factors influence the magnitude of σ^0 including the physical and electrical properties of target, wavelength, polarisation, and incidence angles (Lusch, 1999). The strong influence of canopy structure on radar signals has led to radar being used to estimate several structural biophysical vegetation variables. Many studies have focused on forest canopies, although several have applied radar data from crop canopies to estimate crop biophysical variables, such as height, water content, LAI, and biomass (Inoue et al., 2014; Inoue & Sakaiya, 2013; Kim et al., 2012; Li et al., 2016; Zhang et al., 2009; Zhang et al., 2014). One of the key biophysical variables is LAI, as this is a factor in many crops growth models, and retrieving estimates of LAI is often carried out using empirical methods or canopy scattering models, which simulate the radiative transfer.

Hosseini, McNairn, Merzouki, and Pacheco (2015) adopted multi-polarisation of different frequency SAR sensors such as C-band (RADARSAT-2) and L-band (Uninhabited Aerial Vehicle Synthetic Aperture Radar; UAVSAR) to estimate LAI of soybeans and corn in the Red River Watershed of Winnipeg, Canada using radar canopy reflectance models. The correlation between LAI and RADARSAT-2 over corn canopies was moderate at 0.40 (HH), 0.46 (VV), and 0.82 (HV), respectively. Similar results were found when estimating LAI using RADARSAT-2 for soybean - 0.45 (HH), 0.47 (VV), and 0.80 (HV), respectively. Previous research has revealed that C-band backscatter is significantly associated between LAI and leaf biomass and σ^0 in all rice growth stages (Inoue, Sakiya, & Wang, 2014a), whilst other studies have found better correlation between LAI and σ^0 for VV/HH polarisation when LAI < 3.5 m^2 m^{-2} (Chen, Lin, Huang, & Fang, 2009). Hirooka, Homma, Maki, and Sekiguchi (2015) examined backscatter coefficients of X-band from COSMO-SkyMed and found a reasonable correlation (r = 0.58) between backscatter with LAI (r = 0.58).

Some rice biophysical variables (e.g. row spacing) remain stable throughout the growing season, while others, such as water content, height, and leaf length, change considerably. To understand their effect on radar backscatter, Shao et al. (2001) measured a number of rice variables (e.g. leaf length and canopy height) throughout growing season. Rice height increased from 20 to 100 cm, peaking during the heading stage, before decreasing by 5 cm prior to harvesting. The length of leaves varied, with upper leaves increasing consistently with lower leaves gradually increasing and reaching the maximum of ear differentiation stage. Vegetation moisture content was highest in the seeding (80%) and ear differentiation (85%) stages before decreasing during the mature stage (55%). These changes impacted the backscatter, which was 9 dB higher for late mature rice than medium mature rice. RADARSAT backscatter coefficients were then used to estimate yield by using

an empirical backscatter model. The total rice productions in late mature rice, medium-late mature rice, early mature rice were 208,548 tonnes, 174,636 tonnes, and 17,978 tonnes, respectively. This classification in average accuracy and overall accuracy were 90.1% and 91.49%, respectively. Developing regression models between in-situ measurements and remote sensing metrics is a widely applied approach to estimate yield. Nguyen, Phung, Huth, and Phung (2012) analysed the correlation between backscatter coefficients ($\sigma°$) of multi-date images with in-situ yield by using multiple linear regression. Rice yield estimation requires a minimum of three rice growth stages and at least two first stages, or two final stages, and band combinations between images. The coefficient determination and standard error estimation were 0.795, 0.781 and 0.18, 0.16 ton/ha, respectively. The rice yield estimates were 0.5-10 ton/ha which compared favourably with in-situ measurements. Li et al. (2016) studied the temporal RADARSAT-2, which is C-band frequency, covering critical growth stages in southwest China, and observed the rice biophysical variables (e.g. LAI, Fraction of Photosynthetically Active Radiation (FPAR), height, biomass, and canopy water contents (WC)). The backscatter coefficients in HH, VV, VH and ratio between VV and VH were then developed and related with rice biophysical variables. The VV and VH ratio was significant when determining the Pearson correlation in each growth stage. The regression model with exponential curve was applied to rice biophysical variables and found no significant correlation with water content in their ratio $\sigma^0_{VV}/\sigma^0_{VH}$. Guo et al. (2018) investigated the capability of the compact-polarimetric (CP) SAR in the inversion of rice biophysical variables by adopting the various models (e.g. Water Cloud Model (WCM), Modified Water Cloud Model (MWCM), and Genetic Algorithm (GA)). The result found MWCM were highly correlated with rice height (R^2 = 0.92 and RMSE = 5.81 cm), volumetric water content of rice canopy (R^2 = 0.95 and RMSE = 0.31 kg m^{-3}), m-χdecomposition with ear biomass (R^2 = 0.89 and RMSE = 0.17 kg m^{-2}), and LAI with RH (right circular transmit and horizontal linear receive) (R^2 = 0.79 and RMSE = 0.33).

In addition to estimating yield using empirical models, a number of studies have integrated backscatter data with crop models. Pazhanivelan et al. (2015) combined the multi-temporal of SAR data with ORYZA2000 in India; SAR data were used to estimate the seasonal rice area, start of season (SoS) and rice growth rate, whilst the ORYZA2000 model was parameterised with daily weather data, soil properties, rice variety, water availability, and management practices. Model-derived yield estimations compared well with those from CCE, with accuracy of 99%, 88%, and 86.7%, in Cuddalore, Sivaganga, and Thanjavur, respectively. A similar approach was taken by Setiyono et al. (2017), who developed a rice yield interface for southeast Asia using Sentinel-1A data and the ORYZA Crop Growth Simulation Model (CGSM). The LAI estimates used to parameterise CGSM were derived using a water cloud vegetation model and the resulting yield estimation was accurate to 81-93% when compared with the official yield. Using the same

approach, Quicho et al. (2015) utilised of Sentinel-1 LAI and start of season (SoS) estimates to parameterise the ORYZA crop growth model. The maximum LAI was 10-12 m^2 m^{-2}, which occurred at the flowering stage for hybrid rice varieties, but which was lower (6-7 m^2 m^{-2}) for typical rice varieties. The accuracy in yield estimates in the Red River Delta was 89%, with RMSE of 630 kg/ha whilst in Cambodia, the accuracy was 84% with RMSE of 560 kg/ha. Overall, yield estimation was 81- 94% and RMSE was 340-1,110 kg/ha.

2.6.6 Integrating SAR and optical imagery for rice mapping and yield estimation

The previous sections have discussed the applications of either optical or radar backscatter data in monitoring rice production. Many studies have integrated both optical and SAR imagery to monitor rice production to reap the benefits provided by observations in different spectral regions. Sentinel-1 and Landsat 8 data have been applied to maps in Poyang Lake Plain, China using VH polarisation and NDVI measurements at three stages of the growing season (Tian, Wu, Wang, & Niu, 2018). The adjusted multi-season rice planting area, adjusted middle rice planting area, and adjusted late rice planting area were 1,630.84 ($\pm$ 58.21) km^2, 556.21 ($\pm$24.7) km^2, 3,138.37 ($\pm$77.62) km^2, respectively. The overall accuracy was 98.10% and Kappa coefficient was 0.94. The unbiased error for early, middle, and early rice were 0.18, 0.07, and 0.35, respectively, while standard error of the estimated area was 0.003, 0.001, and 0.004, respectively. The advantage of using both SAR and optical data is increased satellite imagery for analysis, as there was uncertainty of optical remotely-sensed data from clouds or cloud shadow, and led to the insufficient cloud-free images, whilst the SAR data were less affected by cloud coverage.

A similar study was carried out by Yang et al. (2017), who integrated NDVI from the HJ-1A/B and backscatter coefficients from RADARSAT-2 to classify eight phenological stages of rice growth. The benefit of using data from both instruments is that the NDVI and backscatter measurements behave differently at different stages of growth, which improves the ability to distinguish them. For example, in the heading to flowering stage (canopy height 50-69 cm), the NDVI was very high due to the green rice canopy and canopy density; the SAR signature σ_{HV} was also high but the σ_{VV} was low due to the significant attenuation from the dense canopy. Therefore, the increased information content provided by the measurements allowed greater differentiation of growth stages. This is supported by the work of Gebhardt et al. (2012), who analysed the relationship between TerraSAR-X quad-polarised (Quadpol) backscatter and RapidEye derived multispectral vegetation indices (without ground truth data and setting these vegetation indices as reference) and found weak agreement between the optical metrics and different polarisation combinations. However, the modified chlorophyll absorption ration index (MCARI)/second modified triangular vegetation index (MTVI2) and transformed chlorophyll absorption in reflectance index

(TCARI)/optimized soil-adjusted vegetation index (OSAVI) proved correlation with VV, HV and VH backscatter model ($R^2 > 0.6$) and HH/VV ratio model ($R^2 = 0.5$). This result concluded the canopy architecture parameters potentially from SAR images.

2.7 Conclusion

Rice is particularly important in Southeast Asia, with the largest producing countries being China, India, Indonesia, Bangladesh, Vietnam and Thailand (ASEAN Information Center, 2021). Thailand is an agriculture-based country, and its main source of income is from agricultural exports; rice is the major crop, and rice ecosystems are dominated by non-irrigated and irrigated lowland areas, with a small proportion of rice in upland and deep-water areas. The rice season depends on the monsoon rains; thus, the planting date coincides with the onset of the rainy season. The rice growing season is classified into two seasons: wet (May-October) and dry (November-April). Precise and timely rice production data is vital to the food security and economy of the country. Rice agricultural areas and production data are derived from several methods, including remote sensing, which provides an essential technology to monitor rice cultivated area and yield estimation due to its scientific accuracy, speed, and large coverage capabilities.

This chapter presented an overview of the literature on how remote sensing contributes to the rice yield estimation. Numerous studies have implemented for individual satellite sensors, while others have integrated several together. However, the potential of optical and SAR sensors has not been fully investigated in the relationship between rice biophysical characteristics and yield estimation in Thailand. Further, a basic study on the regression model for yield forecasting is still lacking. All sections from the literature review address the factors' impact on rice productivity, in particular weather factors; thus, it is important to investigate the relationship between weather and rice variables. Further, the importance of remote sensing on rice yield estimation is vital for investigation, as it can contribute to precise rice yield and the assessment of dynamics of rice growth; however, the analyses of growth stages, satellite sensors, spectral vegetation index (optical), and differences in orbital direction and polarisation (SAR) require further investigation.

Chapter 3 Analysis of the impact of rainfall and temperature on rice production in Thailand

As discussed in the literature review, climate change affects agriculture and food production systems. To ensure global food security, it is essential to monitor the impact of climatic variables (e.g. temperature, precipitation, relative humidity, and solar radiation) on crop production. In addition, the global population is projected to reach 9.8 billion in 2050 (Roberts, 2011) and the total agricultural food production needs to be significantly increased to ensure adequate food supplies to meet the demands from the rapidly growing population.

Over the past 40 years, the global average temperature has increased by 0.2°Celsius per decade, with the most enormous changes occurring in the Western Equatorial Pacific (WEP) than in the Eastern Equatorial Pacific (EEP) (Hansen et al., 2006). Increasing temperatures have been found to have a detrimental effect on crop development and production, with a decrease in productivity between 11 and 14% for every 1°Celsius increase (Yuliawan & Handoko, 2016). Meanwhile, precipitation influences the availability of adequate water supply for agricultural activities in many parts of the world. Changes in global precipitation patterns in terms of precipitation intensity and frequency have also impacted agricultural production worldwide. In particular, water availability is a crucial requirement for planting rice. For example, in some areas relying on monsoon rainfall, a delay in the monsoon onset (Naylor et al., 2007) can cause severe water shortage required during the plantation. Especially some regions in Thailand have altered their planting dates to accommodate changes in precipitation seasonality which shifted up to 54 days (Ding et al., 2020). Over the past 40 years, the frequency of extreme precipitation events has increased (Myhre et al., 2019), and these can have a negative impact on crop production through flooding (Banerjee, 2010; Khan et al., 2012) and soil erosion (Bauer & Quinton, 2019; Mullan et al., 2019). An example is the flooding disaster in Thailand in 2011, which was caused by a strong summer Southeast Asia monsoon, which resulted in 143% higher than average rainfall during the rainy season. These flooding events affected 9,700,000 hectares of cropland in the lower Chao Phraya River delta and caused approximately 30 million dollars of damage to rice crops (Gale & Saunders, 2013; Jular, 2017). Severe flooding is significant abiotic stress and can also encourage farmers to harvest production earlier where possible to avoid complete damage, it adversely impacts crop structure which can reduce yield by as much as 2.66-2.71% (Lang, Yang, Wang, & Zhu, 2012). This can significantly impact whole grain (head rice) milling yield and eventually, a reduction in the market's price (Salassi et al., 2013).

Extreme weather events frequently occur and seriously impact rice production (Dong et al., 2018; Wu et al., 2020). As a result of the risks, there is increasing awareness for planning adaptation measures to cope with these climatic events. Numerous studies have attempted to quantify the appropriate adaptation strategies under different climate change scenarios, i.e. shifting earlier or lately sowing/planting date, supplementary irrigation system, nutrients management, other inputs (fertiliser, tillage methods, grain drying, and field operations), and adopting new breeding rice cultivars. However, the success of these adaptation measures depends on farmers experiences and knowledge of the impact at the local scale and their view on climate change (Niles et al., 2015).

Limited research has been conducted to investigate the impact of climate change on crop production in Thailand. This chapter seeks to fill that gap by investigating how climatic variables such as rainfall and temperature impact rice production in Thailand. It further analyses the role of irrigation as an adaptation strategy in controlling the relationship between rice production and climatic variables. This chapter aims to investigate the variation in rice productivity over the past four decades concerning climate factors (i.e. precipitation and temperature) and cultivation methods (i.e. irrigated vs non-irrigated).

This chapter first provides a description of the climate and rice production in Thailand, followed by a description of the climatic and rice production data, the pre-processing steps carried out, and the methodology applied in assessing the relationship between weather (temperature and precipitation) and rice production data. This study was conducted at a provincial level, of which there are 77 in Thailand, using annual data from 1981-2015.

3.1 Background of the study area region

Thailand is located in the tropical region in Southeast Asia between latitude 5°37’ North and 20°27’ North and longitude 97°22’ East and 105°37’ East, covering an area of 500,000 square kilometres (Table 3.1). Thailand has 77 provinces, which are the primary local government units, that vary in size from <500 km^2 (Samut Songkhram) to >20,000 km^2 (Nakhon Ratchasima) and which are then further divided into amphoe (sub-district).

According to the Thai Department of Provincial Administration (DOPA), Thailand is broadly divided into four geographic regions (north, northeast, central, and south region), with different topographic characteristics. The north region is mountainous, comprising natural forests, hill ridges, and alluvial valleys and has 18 provinces. The northeast region consisting of 19 provinces is mainly arid, and the Phu Phan ridge separates the region into two basins: the northern Sakhon Nakhon basin and the southern Khorat basin. The central region is a low-level fertile valley located around the Chao

Phraya River delta, containing 26 provinces. Finally, the south region comprises 14 provinces of mountainous areas with thick forests. The south region is a peninsula along two seas: the west side is the Andaman Sea, and the east side is the Thai Gulf; thus, the south region separates into the south east coast and west east coast.

3.1.1 Climatic conditions in Thailand

Thailand has a tropical climate influenced by two monsoons, whose direction across Thailand is shown in Figure 3.1, along with the passage of tropical cyclones, all of which influence temperature and precipitation (Appendix A) across Thailand. The southwest monsoon (mid-May to mid-October) and the northeast monsoon (mid-October to mid-February) have different origins and wind directions. The southwest monsoon, which occurs between mid-May and mid-October, usually originates over the Indian Ocean and brings cloudy conditions and rainfall to the mainland. The northeast monsoon, which occurs from mid-October to mid-February, begins after the fading influences of the southwest monsoon and brings cooler temperatures and generally causes low rainfall. Therefore, the seasons are categorised into the summer, rainy, and winter seasons, and the monsoon influences each. The summer season runs from mid-February to mid-May and is influenced by the north-eastern and south-western monsoon. Typically, the weather is dry, with cold air masses from China affecting northern Thailand. The rainy season, in which rainfall varies between 680 and 1,400 mm, occurs between mid-May to mid-October and results from the influence of the south-western monsoon. These phenomena cause widespread rains across Thailand. Finally, winter spans from mid-October to mid-February. The north-eastern monsoon passes Thailand around mid-October for 1-2 weeks and leads to cold air within the country or storm rains in some areas especially in the lower central and eastern regions. The monsoon direction and passage of tropical cyclones influence Thailand, as demonstrated in Figure 3.1.

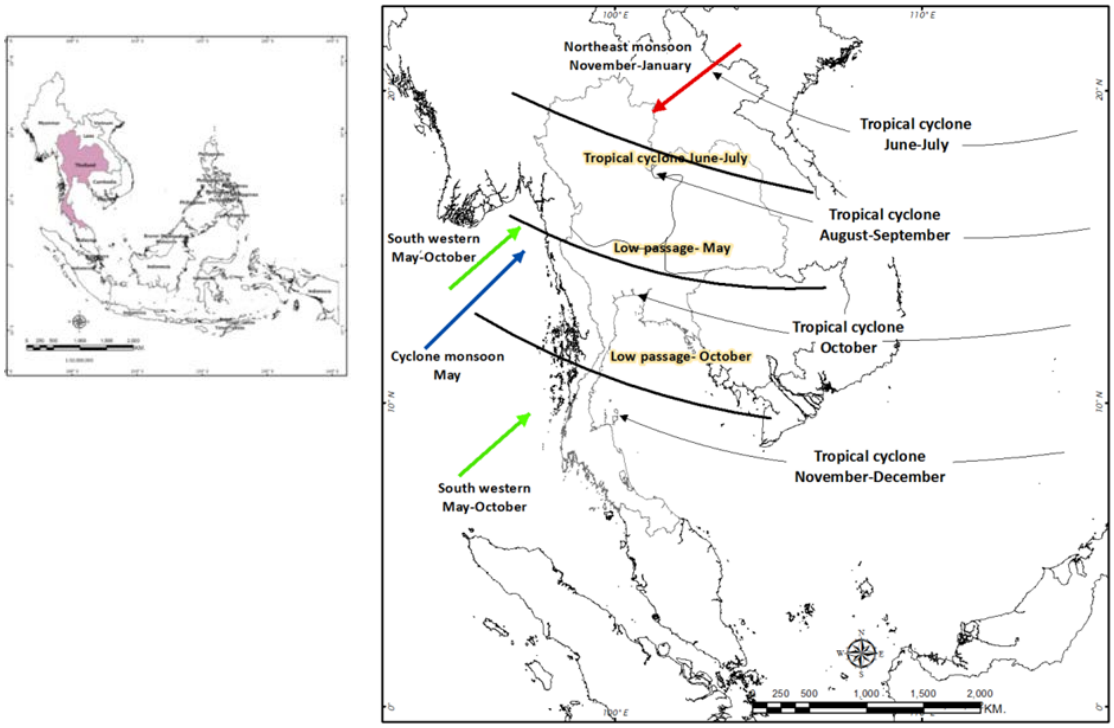

Figure 3.1 Map showing the area Thailand (left) and the direction of the passage of the monsoons (right) (TMD, 2015).

Most regions experience the highest temperatures in the summer season, although the highest average minimum temperature occurs in the rainy season. Large differences in the amount of rainfall are evident between the winter or summer season and the rainy season, which vary by up to ~ a factor of 10. However, it is evident that most regions have similar amounts of seasonal precipitation.

3.1.2 Rice cultivation system in Thailand

In Thailand, most rice cultivation occurs in lowland areas in the tropical zone with varying soil characteristics, environment, and topography. For example, soils in the Central plain are Tropaquepts and comprise ~ 50% acid sulphate soil, whereas, in the northeast Plateau, Paleaqults and Plinthagults soils dominate the landscape (Piyapakorn, n.d.). Therefore, land preparation is an important process to accommodate different soil types and typically varies for rice growing, such as soil management, tillage practices, and land levelling. As a result, soil management practices are one critical management practice and vary management in rice-cultivated areas to achieve high crop productivity. For example, dry-seeded rice should be prepared wet ploughed at 30-50 days after emergence and land levelled in the non-irrigated area in the Eastern India (Siopongco, Ingram, Pablico, & Moody, 1994). Another essential soil management practice is puddling by destroying the topsoil structure in wetland rice (Sanchez, 2019). Another potential agricultural

practice is direct-seeded rice (DSR) which involves sowing pre-germinated seed into the puddled soil surface, water seeding and dry seeding because of their low inputs (Farooq et al., 2011; Kakumanu et al., 2019).

In Thailand, rice cropping can be irrigated or non-irrigated depending on whether there is sufficient rainfall for cultivation and whether the environment is suitable for the irrigation infrastructure required for water storage and water delivery (e.g. main and lateral canals). The majority (80%) of the cultivated rice area in Thailand is non-irrigated (Suwanmontri et al., 2020). It relies on precipitation, which is generally supported by the construction of dykes or small ponds to store water. Water availability is vital in the seeding stage of rice, where rice seeds are sowed into a flooded paddy field or, if the area is experiencing low precipitation, growing in a nursery and then transplanting the sprouts into paddies. Irrigated rice constitutes around 25% of the area and is concentrated mainly around the Chao Phraya River delta (Figure 4.1); with sufficient precipitation for planting rice, this region also has the potential for double or triple rice crops. One of the benefits of using irrigation systems is that they reduce the sensitivity to planting date to the arrival of monsoon onset and the respective length of growing season is also important in rice production and yield (Uzzaman et al., 2015). The length of the growing season depends on environmental constraints and is broadly categorised into three groups: short-duration (100-120 days), medium-duration (120-140 days), and long-duration (140-160 days). The most common varieties grown in Thailand are short-duration and medium-duration, which facilitates double cropping systems and broadly adapt in drought and flood-prone areas (Bera & Kelley, 1990), which occur in 25% of the cultivated rice area.

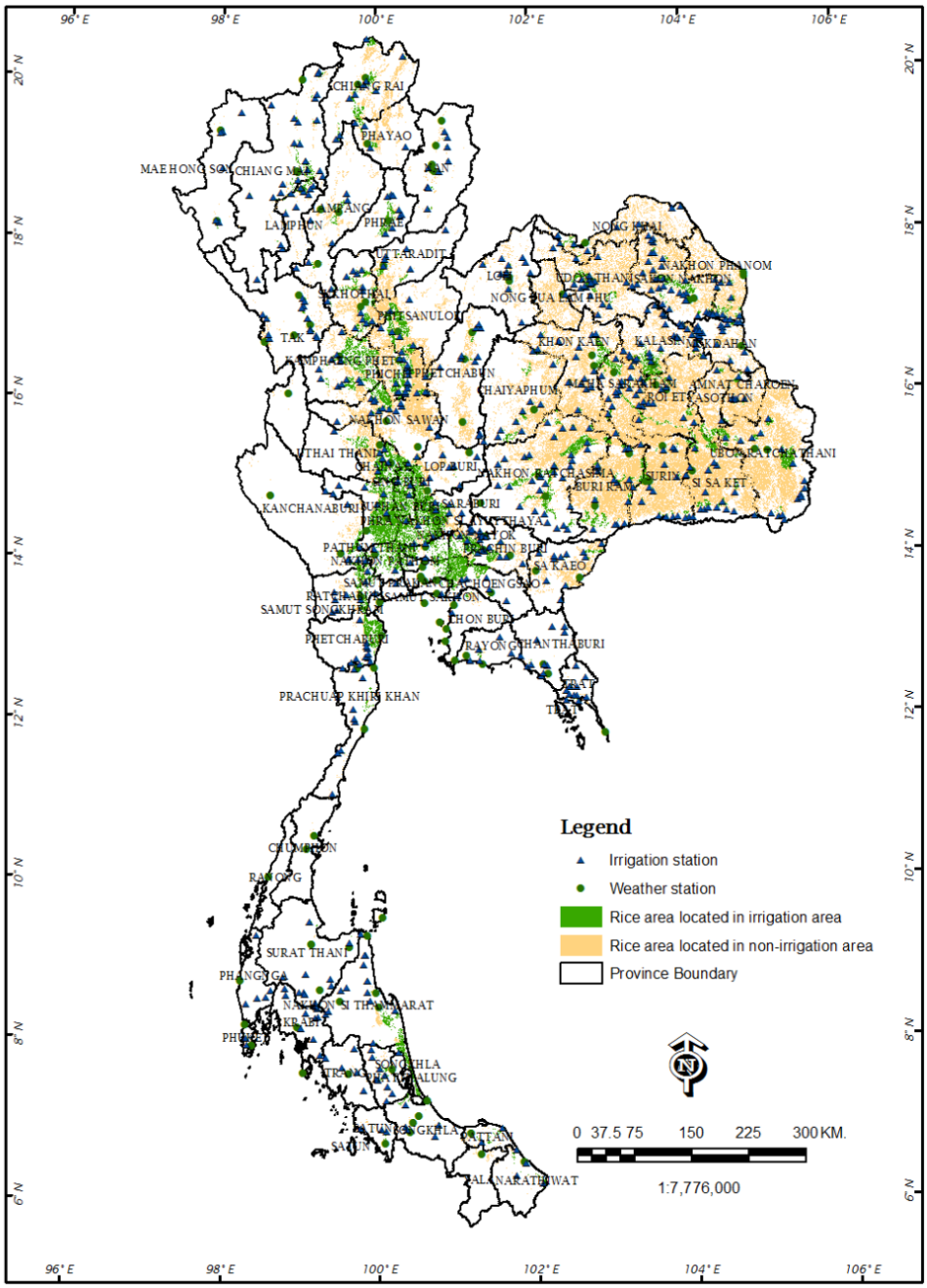

Figure 3.2 Rice productions across Thailand, showing areas that rely on precipitation (yellow) or irrigation (green areas in blue are irrigated areas not under rice cultivation).

The figure 3.2 shows the cultivated rice area across Thailand and the different irrigation systems (i.e. irrigated and non-irrigated areas) used. Irrigation stations, which focus on irrigation facilities on a large scale (>100 million m^3 water storage volume) and medium scale (<100 million m^3 water storage volume) and provide water resources, are distributed throughout Thailand. Nevertheless, the majority (25%) of rice cultivated area does not use these irrigation methods. This is particularly the case in north-eastern Thailand, where only 75% of the area under rice cultivation does not use irrigation methods and is dependent on rainfall (OAE, 2018a). This region also has lower levels of double or triple cropping systems (Suwanmontri, Kamoshita, & Fukai, 2021) and

rice productivity is lower than that found elsewhere in Thailand (Figure 3.4). Also shown in Figure 3.2 is the spatial distribution of the 129 weather stations across Thailand, which provide the precipitation and temperature data, used in the analysis in this chapter.

3.2 Methodology

3.2.1 Data

To understand the relationship between rice productivity with climate data at the provincial level, the agricultural productivity, and climatic data for the period 1981-2015 have been acquired from government agencies on the provincial level. These data are discussed in detail below.

3.2.1.1 Agricultural data

The agricultural data consisted of seasonal yield and production estimates at the provincial level between 1981 and 2015 and was obtained from the Office of Agricultural Economics (OAE), Ministry of Agriculture and Cooperatives, Thailand. The primary agricultural data collection provides information on the seed's rate usage, rice cultivated area, harvested area, production, yield (i.e. the weight of grain per unit of land area using standard moisture content), percentage of cultivated area (monthly), and the cultivated area stratified by irrigation system. The agricultural data are based on statistical analysis wherein each agricultural area adopts a stratified two-stage sampling approach to select sample fields for the yield survey (Crop Cutting Experiments, CCE). The number of sample fields depends on the agricultural area at the amphoe (sub-district) level. In this analysis, we utilise information on rice production and rice yield between 1981 and 2015 at the provincial level, of which there are 77 in Thailand.

To achieve the pattern of rice productivity during the study period, the present study prepares the historical data on agricultural data. It demonstrates the time-series pattern as in Figure 3.3.

a) Annual time-series on rice production

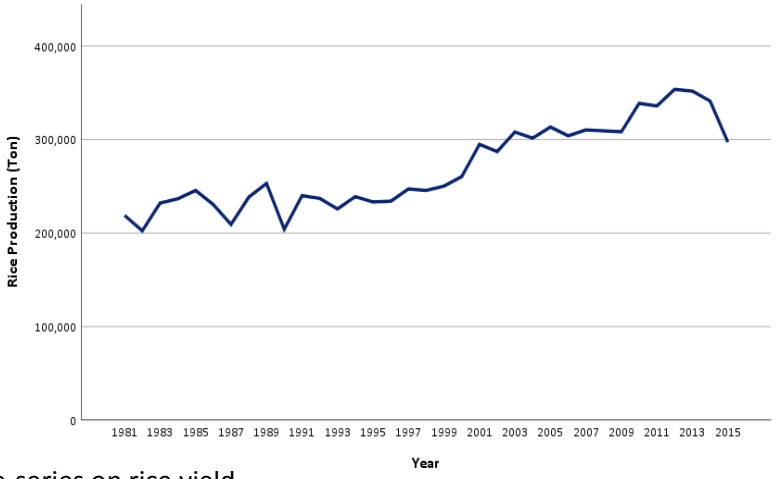

b) Annual time-series on rice yield

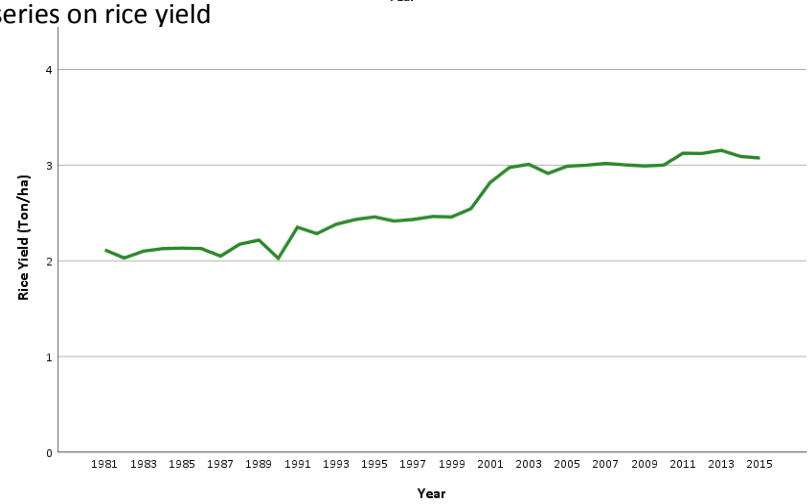

Figure 3.3 Annual time-series on rice productivity.

The annual time series is a summation of rice production and yield in Thailand from 1981 to 2015. Figure 3.3 demonstrates the fluctuation of rice yield and production during 1981-2000; then, rice productivity increasing trends until 2015. The changes in rice yield/production are associated with improved rice variety, higher crop intensity, control of rice weeds, and changes in the rice farming system from subsistence farming to commercial farming (Titapiwatanakun, 2012).

As an example, Figure 3.4 shows rice plantation area (a), yield (b), and production (c) across Thailand in 2015, where the rice cultivated and harvested area comprised 8,913,576 ha and 8,414,975 ha, respectively, with 22,893,719 tonnes of rice produced, providing an average yield of 3.1 tonnes/ha. In the northeast region, provinces with the largest cultivated area include Ubon Ratchathani (617,744 ha), Nakhon Ratchasima (617,744 ha), Roi Et (523,024 ha), and Surin (786,611 ha). Farmers in this area typically plant photoperiod-sensitive rice varieties with less input and low yield potential. The provinces with the highest rice yield per unit area are located in the central region. The average yield was ~ 4.5-5 tonnes/ha, and most cultivated areas utilise

irrigation for sufficient water. However, not all high-yield areas utilise irrigation, suggesting that proper agricultural practices and the rice variety may also play an important role. However, information on rice variety and agricultural practices are not collected by government agencies, and therefore their influence cannot be accounted for in the production and yield statistics.

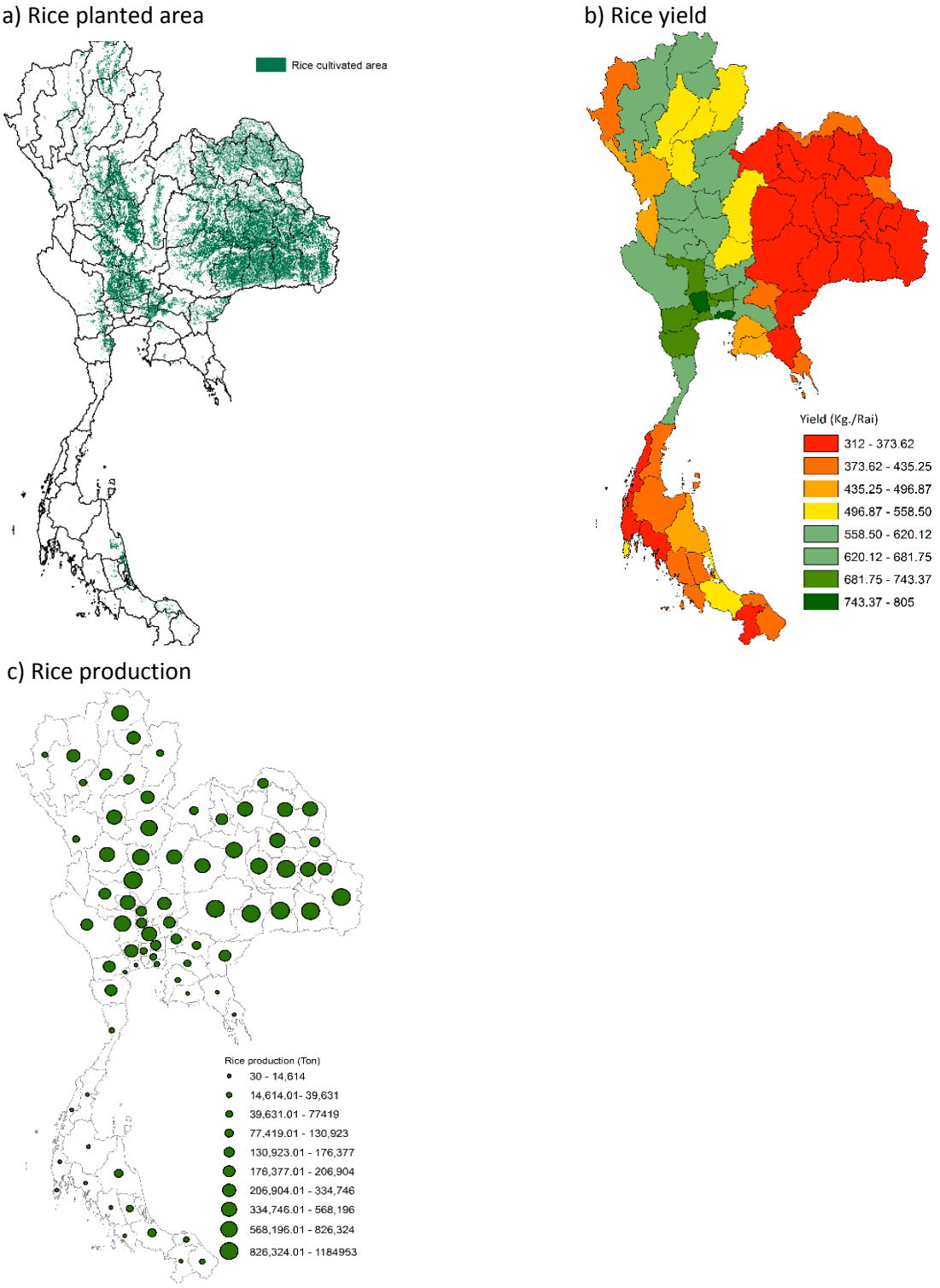

Figure 3.4 Rice productivity for 2015. a) Rice planted area (ha), b) Rice yield (kg/rai), and c) Rice production (tonnes).

3.2.1.2 Weather data

Weather data at the provincial level covering the study period was obtained from the Thai Meteorological Department (TMD), Ministry of Digital Economy and Society, Thailand. Weather data were used to assess the role of climate on rice production and yield between 1981 and 2015. The dataset is derived from 129 weather stations across the country, which provides measurements of precipitation and temperature, amongst other variables. The weather data used here are daily measurements of total precipitation (mm), the number of rainy days (day), and daily maximum and minimum temperature. The present study then calculated additional temperature variables on a monthly basis, e.g. monthly mean temperature (°Celsius), monthly mean maximum temperature (°Celsius), monthly mean minimum temperature (°Celsius), and differences between maximum and minimum temperature (°Celsius). There are no weather stations in 11 provinces in the middle and north-eastern regions of Thailand; therefore, these provinces were not used in the analysis.

3.2.1.3 Irrigation data

The irrigation dataset was derived from the Royal Irrigation Department (RID), Ministry of Agriculture and Cooperatives, Thailand, and contains information on the irrigation stations and the boundaries of serviced irrigated areas. Irrigated area is defined as the area that water can be delivered for agricultural activities within the irrigation project which is classified in several levels i.e. large scale (water storage dam, irrigation dam, pumping, water supply/drainage system, and irrigation in paddy in the function water storage $\geq$100 million m^3 or supporting irrigation area $\geq$12,800 ha), medium scale (water storage dam, irrigation dam, pumping, water supply/drainage system, and irrigation in paddy in the capacity function water storage <100 million m^3 or supporting irrigation area <12,800 ha), and small scale irrigation (development on small water body on resilient water consumption and agricultural activities (Royal Irrigation Department, 2007). The irrigation data allows calculation of the cultivated rice area reliant on irrigation for water supply and directly influences irrigated rice and production. In this study, we focused on cultivated agricultural areas located in large and medium irrigation systems. It provides a means to assess the impact of the irrigation system on the relationship between precipitation and rice yield.

3.2.2 Data preparation

Prior to any analysis, the time-series data were pre-processed to improve data quality. The daily weather data were first averaged into monthly and then organised three seasonal periods – summer (mid-February to mid-May), rainy (mid-May to mid-October), and winter (mid-October to mid-February). Here, we focused on the rainy season as this period has the most significant impact on rice production (FAO, 2000) due to the majority of rice planting in Thailand coinciding with this season.

As there is often more than one weather station present in each province, the average rainfall and temperature at the provincial level are calculated using all weather station data in the province:

$$Mean = \frac{station1 + station2 + \ldots + station\ n}{n} \qquad \text{Equation 3.1}$$

Where *Mean* is the average precipitation or temperature at the provincial level, the station is the weather station located within the province, and n is the number of weather stations in the province. At the beginning of the year (January to May) for two specific years, i.e. 1983 and 1999, several months of data were missing and therefore these years were excluded from further analysis. Using the monthly averages for precipitation and temperature, each variable's cumulative and annual average value was calculated during the rainy season only. In the case of precipitation, the number of rainy days was also determined for our study because there is a strong relationship when integrating with total precipitation (Fishman, 2016).

Further, spatial autocorrelation statistics have also been investigated at the province level for obtaining the spatial clustering association.

3.2.2.1 Detrending rice yield and rice production

Determining trends and detrending the data are essential for comprehensive statistical analysis. There are two classes of trends: deterministic trends (which show consistent increases and decreases) and stochastic trends (which show increases and decreases without consistency). Rice yield and production are defined as deterministic trends since agricultural production is inconsistent over the study period for many reasons, such as government policy instability (Abdulwaheed et al., 2017; Longtau, 2003), agricultural technology improvements (e.g. seeds and machinery development), and rice farm diversification. For example, the Thai government reformed the structure of agricultural production on the area-based approach by introducing effectiveness of large-scale rice production or big paddy field plot policy during 2017- 2021. This policy assists farmers in gathering agricultural groups/enterprises and collaborates with their management by guaranteeing agricultural markets and helps Thai farmers reduce agricultural

costs to enhance the quality standard of agricultural products. Due to changes in rice yield and production, detrending the yield and production data mitigates agricultural fluctuations not caused by climatic variations. Detrending is an approach that involves eliminating trends from time-series data, referred to as change or distortion of mean values. The detrending technique is a reliable method using the multifractal scaling behaviour of time-series data and is frequently applied in data analysis to remove systematic changes. A wide variety of techniques exists for detrending data, including the application of filters such as the low-pass Kolmogorov-Zurbenko filter (Botlaguduru & Kommalapati, 2020), regression analysis (Ye et al., 2015) and Detrended Fluctuation Analysis (DFA) (Horvatic et al., 2011). Thus, the approach is necessary to formulate rice yield and production (Chung et al., 2015; Ye et al., 2015). To reduce the influences of agricultural development, the study creates more variables on rice yield and rice production based on detrending approaches. Two standard methods of detrended analysis: detrended by differencing and detrended by model fitting. Firstly, the detrended by differencing creates a new dataset where each value is based on differences between the original and previous observations. The disadvantage of differencing is that the process loses one observation in each time difference. Secondly, detrended by model fitting calculates by fitting with linear regression model; then, calculates the differences between the observed values and predicted values or applies more advanced models (e.g. Empirical Mode Decomposition (EMD) and Detrended Window Autocorrelation (DWA) (Lemoine & Delignieres, 2009)). Several researchers investigated climate change impacts using crop yield data (Lobell & Field, 2007; Lu et al., 2017).

The detrended by differencing between yield and production in the current time step and the previous time step applies under the present study. The objective of weather detrended is removing non-weather effects such as technology improvement, agronomics practices, and rice cultivars changes. The approach applied to detrend the data follows that of Mills (2011) and detrends the data by differencing on an annual basis:

$$\Delta\ rice\ yield\ and\ rice\ production = rice\ yield\ production_{x} - \ rice\ yield\ production_{x-1} \qquad \text{Equation 3.2}$$

Where x is the present year and $x - 1$ is the previous year for the variable of interest a particular province. First, an evaluation of the detrended data will be carried out through an analysis of the correlation between rice yield/production and rice detrended yield/production. Figure 3.5 provides an example of a time series of rice yield and detrended rice yield over two representative provinces in the different irrigation systems. Then, the detrended rice productivity (rice yield/production adjusted for trend) is regressed with weather variables.

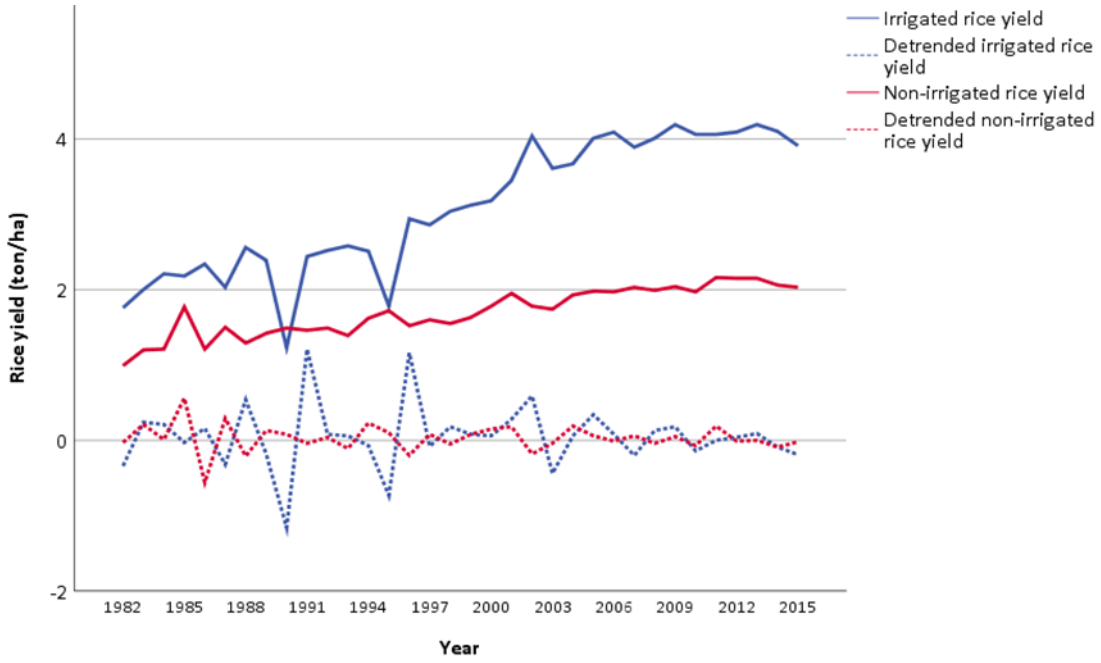

Figure 3.5 Illustration of the rice detrending in different irrigation systems.

3.2.2.2 Calculation the other important weather variables

The differences between the maximum (day-time) and minimum (night-time) temperature have also been shown to impact on rice production through changes in evapotranspiration (ET_o; the sum of evaporation from the soil and transpiration from crop), and in some cases it was found to be associated with 6% declined in yield (Saseendran et al., 2000). Two additional temperature parameters, which are based on maximum and minimum temperature, are also calculated: 1) differences between extra-maximum temperature (highest temperature during the month) and extra-minimum temperature (lowest temperature during the month) and 2) differences in mean monthly maximum and mean monthly minimum temperature in the provincial level.

3.2.2.3 Setting thresholds of rice cultivated area and grouping provinces by percentage of rice cultivated area and irrigation system

To consider irrigation systems' impact on rice yield, it was crucial to identify those provinces located in different irrigated areas by overlaying irrigation and existing rice cultivated boundaries. The underlying assumption is that using irrigation systems ensures sufficient water throughout the growing season and is therefore beneficial for rice productivity. In contrast, rice cultivated in non-irrigation areas is more susceptible to changes in precipitation which may impact crop production. Based on this, a threshold of $\geq$40% rice cultivated area was used to identify provinces for further analysis, which were subsequently grouped into provinces containing large and medium irrigation projects.

To account for different irrigation systems in this analysis, the provinces were categorised into four groups considering only >40% rice cultivated area: rice cultivated area >40% and located in the irrigated area (8 provinces) and rice cultivated area >40% and located in the non-irrigated area (27 provinces). Here, we focus on the 35 provinces that met this requirement with >40% planted rice area per province in both irrigated and non-irrigated areas, which are primarily located in the Chao Phraya River delta.

3.2.2.4 Calculation changes on rice production

To perceive the temporal changes in weather data over the past 35 years, the data are grouped into those provinces with a >10% reduction in rice cultivation, those with +/-10% differences in rice cultivation and those that experience a >10% increase in rice cultivation during 1981-2015.

3.2.2.5 Defining variables of the impact of weather on rice production

Table 3.1 List of weather variables and the basis for analysis considering between May and October

Variable	Purpose
Rainfall	To study if increasing rainfall leads to rice production increase
Rainy day	To study if an increasing number of rainy days increases rice production
Extra-maximum temperature	Assess whether greater maximum increase temperatures result in a decrease in rice production
Extra-minimum temperature	Assess if minimum temperature increase reduces rice production
Difference in extra-maximum and extra-minimum temperature	To study if greater extreme of temperature increase leads to rice production decrease and influence photosynthesis's rate of crop (Sheehy & Mitchell, 2015)
Mean temperature	Analyse whether greater average temperatures reduce rice productivity
Mean maximum temperature	Assess if the increases in the average maximum temperature reduce rice productivity
Mean minimum temperature	To study if average minimum temperature increase leads to rice production decrease in terms of total biomass production
Difference in mean maximum and mean minimum temperature	Investigate whether differences in temperature leads to rice production decreases

3.2.2.6 Correlation analysis

Having detrended the data, a correlation analysis was conducted between the weather and rice parameters which have been carried out previously for various crops (Choudhury et al., 2015; Gurung et al., 2017; Ye et al., 2019) With regards to rainfall, positive correlations are assumed to

indicate that increases in rainfall have increased rice yield. However, it is known that high rainfall prior to harvesting can have a negative effect on rice production, which is not accounted for (Asada, Matsumoto, & Rahman, 2009). With respect to temperature, a positive correlation indicates that higher temperatures result in an increase in rice yield. The analysis uses the parametric bivariate Pearson Correlation to characterise the strength and direction of the relationship and a P-value of 0.05 for the two-tailed significance.

3.2.2.7 Analysis spatial autocorrelation with Global Moran's I index

Spatial autocorrelation refers to the systematic spatial variation of a variable and enables the assessment of whether features with similar values are clustered, random, or dispersed (Du, Wang, Zhuang, & Jiang, 2017; Mathur, 2015). The aim of this analysis is to assess the spatial variation on a provincial level of the relationship among weather parameters on a provincial level based on feature location and their weather attribute values. To do so, the adjacent provinces are given a weight of 1, whilst all non-adjacent provinces are given a weight of 0. To measure the relationship between selected weather variables and the surrounding value, Moran's I statistic is used, which identifies local measures for analysing the clustering multivariate on spatial data (Scrucca, 2005).

For n observations on a variable x at locations i, j, the Global Moran's I calculated as follows (Anselin, 1995):

$$I = \frac{n}{S_0} \frac{\sum_{i=1}^{n} \sum_{j=1}^{n} W_{i,j} Z_i Z_j}{\sum_{i=1}^{n} Z_i^2} \qquad \text{Equation 3.3}$$

$$S_0 = \sum_i^n \sum_j^n wij \qquad \text{Equation 3.4}$$

Where Z_i is the deviation of an attribute for feature i from its mean, $w_{i,j}$ is the spatial weight between feature i and j, n is equal to the total number of features (total of administrative units), and S_0 is the aggregate of all spatial weights. The observed value of I compared to its distribution under the null hypothesis of no spatial autocorrelation.

The spatial pattern analysis tool in ArcGIS Pro was used to calculate Moran's I Index, expected index, and scale of significance level (i.e. Z-score and P-value) and optionally generate reports. An explanation of Moran's Index value is near 1.0 indicates clustering, whilst a value near -1.0 indicates the variable is dispersed, and a value around 0 indicates a random distribution. The present study sets the null hypothesis and states that there is no spatial clustering in the location. The Moran's I value is computed on an annual basis. The critical value (i.e. Z-score) and P-value are determined for inferential spatial pattern analysis techniques. The null hypothesis is that weather influences in neighbouring provinces. Some spatial analysis methods require the

specification of a distance threshold to characterise the sphere of influence, which in this instance is unknown. To mitigate this, the contiguity edge only or Rooks case is used to characterise the conceptualization of spatial autocorrelation between polygons that share an edge with the target polygon or overlap will influence on computation for neighbouring polygon features that share the boundary of the administrative polygon. The spatial autocorrelation is important for the present study because the result presents the level of relationship between one object with the neighbouring objects by assuming the nearby objects have high correlation than the distance objects. Besides, the positive and negative correlation able to prove the random or cluster on the map. Thus, the study investigated the influences of weather parameters on the neighboring in terms of adjacent polygon of administrative boundary. The main purpose of spatial autocorrelation is determined the importance of geographical variation both sign and strength of their relationship.

3.2.2.8 Analysis and summary of the study

The following sections provide an analysis of the relationship between the climate parameters and rice production across Thailand with reference to the research questions identified in Chapter 1.

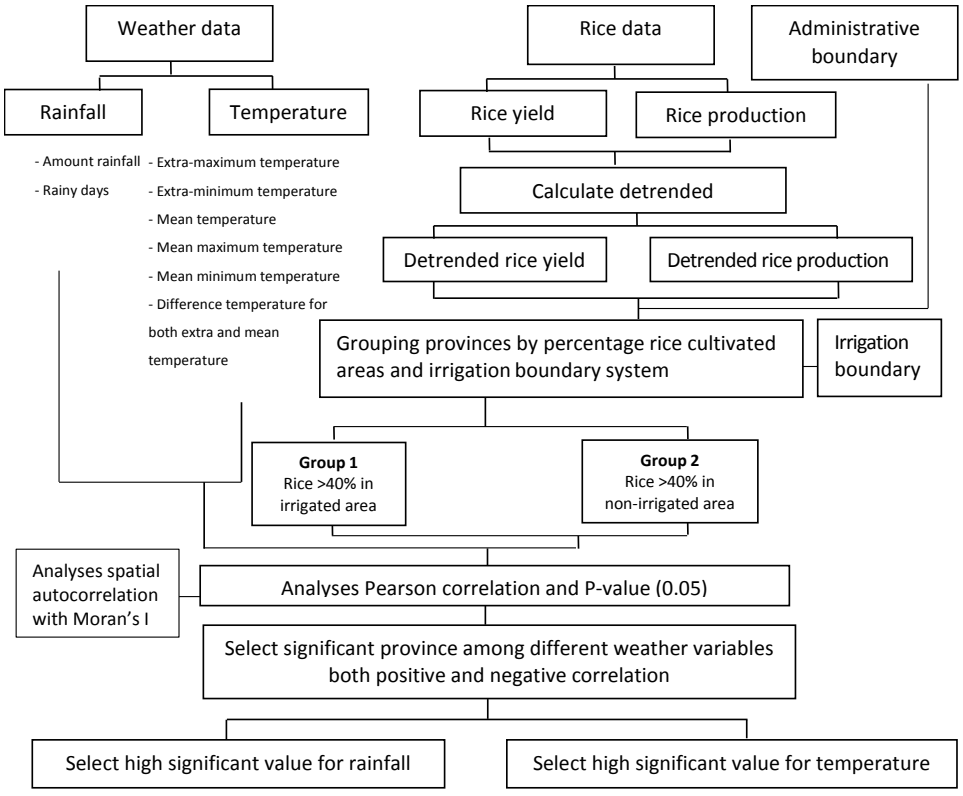

Figure 3.6 Flowchart showing the methodology of identifying provinces for analysis of the relationship between rice production and weather parameters.

3.3 Results

The number of provinces where the correlation analysis was carried out varies according to the availability of data on rice yield and rice production (77 provinces), rainfall (65 provinces), and temperature (63 provinces). Consequently, the analysis was carried out in the 63 provinces where data was available for all parameters. To understand the climate trend at the regional level, the study is specific to rainfall and temperature variations over the study period. Therefore, the statistical analysis is split into two sections, detailing the trend analysis and the correlation analysis (both in statistical correlation and spatial autocorrelation).

3.3.1 Trend analysis

This section analyses the temporal trends in rice productivity and weather during the study period using the data described in **Sections 3.2.1.1** and **3.2.1.2**.

3.3.1.1 Rice trends

The cultivated rice area is predominantly found in the central and north-eastern regions of Thailand. As shown in Figure 3.4, illustrates the low rice yield found in the north-eastern region, where the average rice yield is ~ 1.9 tonnes/ha whilst higher rice yields (3.6 – 3.9 tonnes/ha) are found in provinces located in close proximity to irrigation systems. Figure 3.7 shows the provinces that utilise irrigation (green; 14 provinces) and non-irrigation agricultural methods (yellow), where rice yield is typically higher in the former, as these areas may double or triple plant due to the availability of sufficient water throughout the year (Suwanmontri, Kamoshita, & Fukai, 2021). The remaining 63 provinces that do not utilise full irrigation typically have lower yields, resulting in a yield gap of 1.5-2 tonnes/ha.

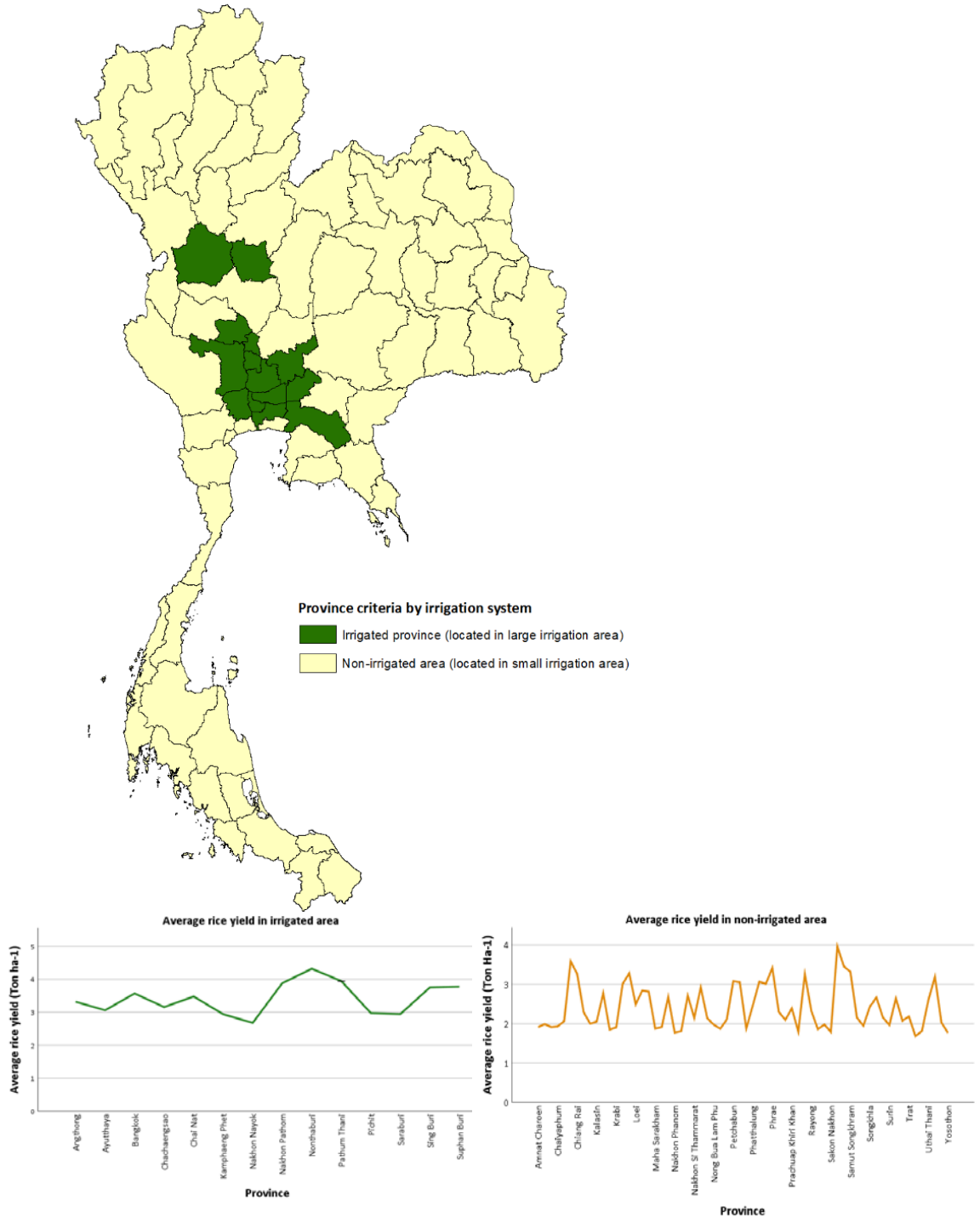

Figure 3.7 Average rice yield (ton/ha) at the provincial level between 1981 and 2015. Provinces in green are those that use large and medium irrigation; those in yellow are non-irrigated provinces (small irrigation).

An analysis of the difference between rice cultivated area and production between 1981 and 2015 was carried out to determine which provinces show the greatest differences, which may be indicative of improved agricultural practices and differences in the variety of rice grown. The

result, shown in Figure 3.7, reveals that the east, northernmost part of the north-east, and southern regions had the greatest changes in cultivated rice area. Overall, most provinces (42) have seen a >10% reduction in cultivated rice area; 15 have seen increases and decreases of +/- 10%, and 20 have seen rice cultivated area increase by >10%. A number of provinces, such as Chiang Mai, Lop Buri, Prachin Buri, Chachoengsao, Surat Thani, and Phatthalung, showed the largest decreases in cultivated rice area due to a combination of urban expansion (Jiang et al., 2013; Shi & Jiang, 2016), farmers' decision-making (Beretta et al., 2013; Johnson et al., 2019), and governmental policies (Ahuja, de Vos, Bones, & Hall, 2010; Lencucha et al., 2020). The latter include, for example, the Thai government encouraging farmers to cease rice cultivation in the dry season and alter to plant less water consuming crops (e.g. beans, chili, watermelon, and sweet corn) for drought adaptation, especially in the drought-prone non-irrigated area (Chaowiwat, 2016).

An analysis of the difference between rice cultivated area and production between 1981 and 2015 was carried out to determine which provinces show the greatest difference, which may be indicative of improved agricultural practices and differences in the variety of rice grown. The result, shown in Figure 3.8, reveals that the east, northernmost part of the north-east, and southern regions had the greatest changes in cultivated rice area. Overall, most provinces (42) have seen a >10% reduction in cultivated rice area; 15 have seen increases and decreases of +/- 10%, and 20 have seen rice cultivated area increase by >10%. A number of provinces, such as Chiang Mai, Lop Buri, Prachin Buri, Chachoengsao, Surat Thai, and Phatthalung, showed the largest decreases in cultivated rice area due to a combination of urban expansions (Jiang et al., 2013; Shi & Jiang, 2016), farmers' decision-making (Beretta et al., 2013; Johnson et al., 2019), and governmental policies (Ahuja, de Vos, Bones, & Hall, 2010; Lencucha et al., 2020).

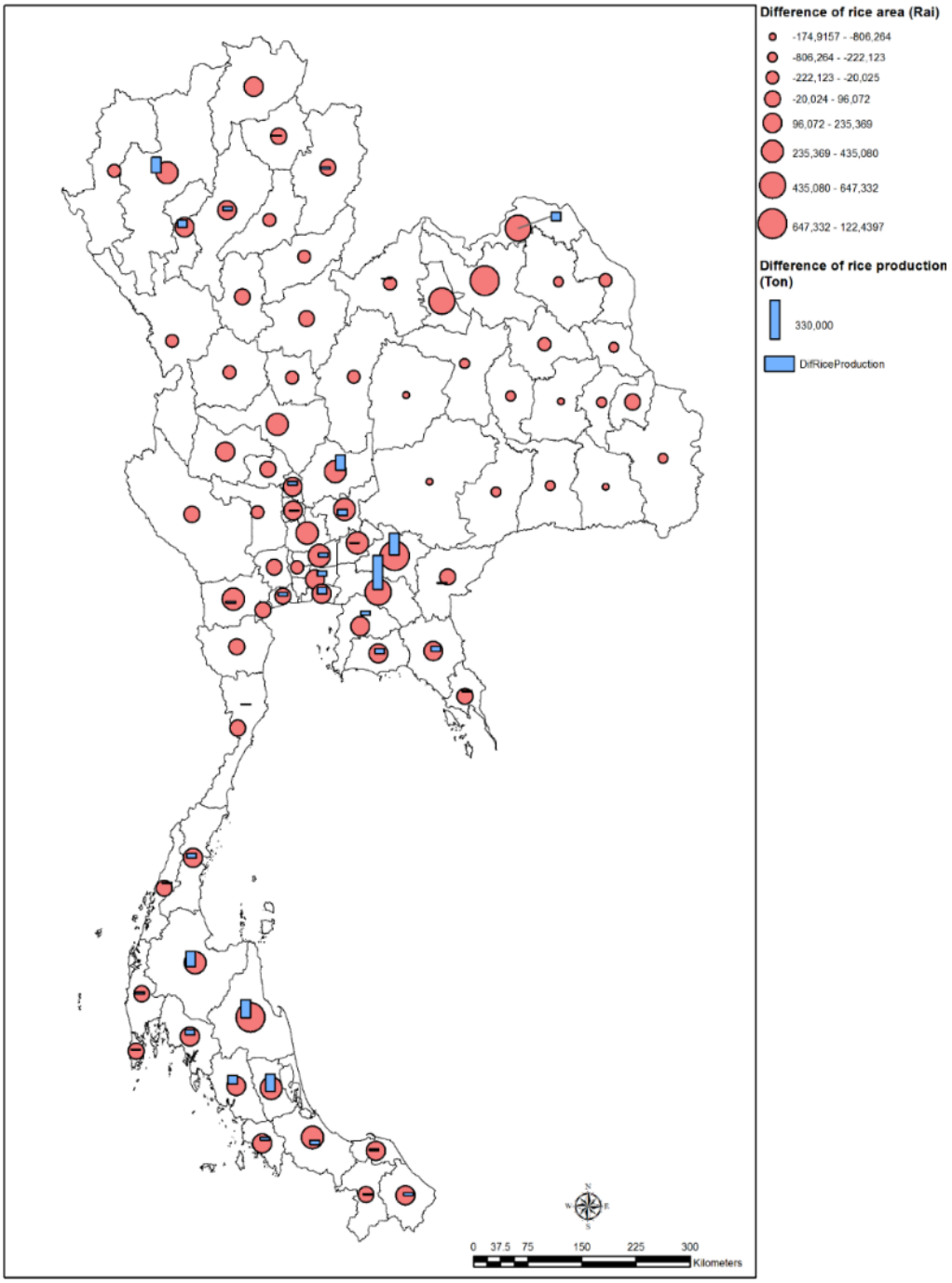

Figure 3.8 Differences in rice cultivated area and rice production between 1981 and 2015. Red circles represent differences of rice cultivated area and blue bars represent differences on rice production.

3.3.1.2 Weather trends

The annual monthly variation in rainfall and temperature was assessed by averaging the time series on a monthly basis. Figure 3.9 and Figure 3.10 show the monthly average and accumulative precipitation in terms of monthly rainy days data over the full 35-year period (red line) with one

standard deviation (S.D.) error, which measures variance or dispersion of data around the mean value.

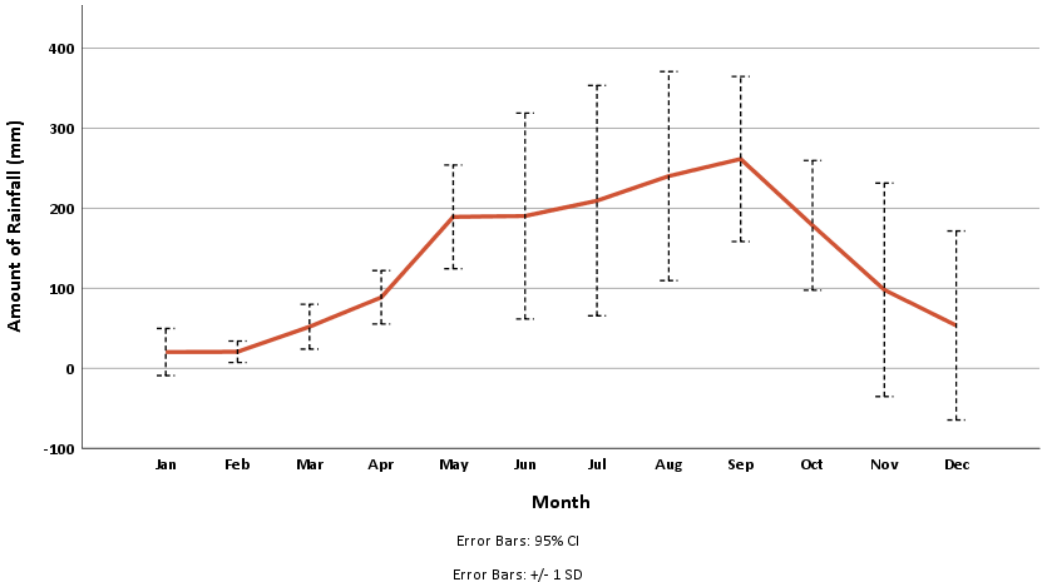

Figure 3.9 Mean monthly amount of rainfall in Thailand (1981-2015).

The figure 3.9 reveals that the lowest monthly rainfall (<20 mm) is found at the beginning of the year, with a steady increase to the maximum in September at 260 mm before decreasing through to December. The steady increase in precipitation in May coincides with the start of the wet season of rice production in Thailand, with the growing season typically ending in October. The error bars indicate greater variability in precipitation during the rainy season (June and August), which coincides with the main growing season, although significant variation is also evident in November and December which occur in the dry season. Change in rainfall pattern or rainfall distribution in terms of annual and seasonal rainfall impact rice production. Sujariya et al.(2020) proved to delay in rainfall patterns on the start growing period (SGP) and end growing period (EGP) and a slightly shortened length of growing period (LGP) in the wet season in transplanting system lowland rice area in the northeast Thailand by using rainfall data derived via weather station and using simulation model from 2000 to 2015. The results revealed the increasing potential yield because the planting avoided drought stress at the end of the growing season by shifting planting time closer to the optimum after changes in rainfall pattern. Similarly, this study examined rainfall variability changes in seasonal rainfall patterns and affected on duration and grain yield. Whilst the shifting of planting period closely to the optimum maximum yield for the KDML105 variety. The other factor is extreme precipitation or uneven precipitation affecting rice yield (Fishman, 2016; Huang et al., 2017).

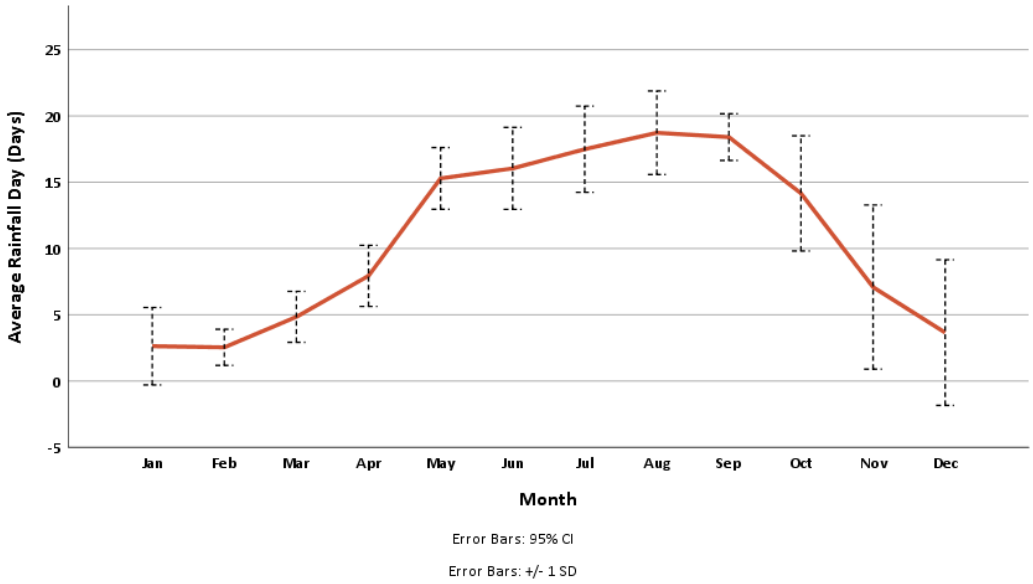

Figure 3.10 Mean monthly rainy days in Thailand (1981-2015).

The number of rainy days influences the availability of water for crop growth and development; thus, there are essential parameters to observe rainfall variability. The number of rainy days per month follows a similar pattern to mean precipitation, with few rainy days between January and March before steadily increasing until August with 18 rainy days. The seasonal distribution of rainfall, rainy days and temperature metrics are vital for rice phenology. Also, climate change shifts the potential of rice planting in single and double-cropping rice systems (Saud et al., 2022).

a) Mean minimum temperature

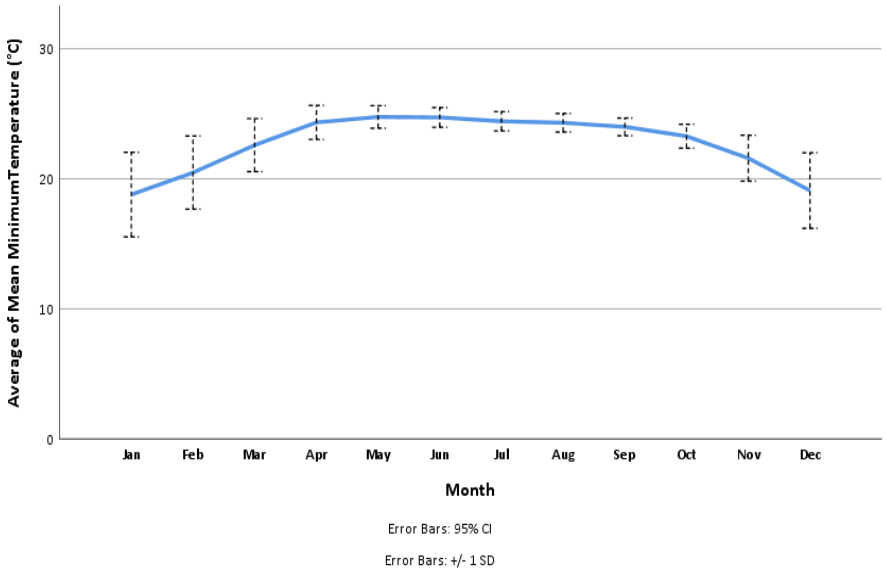

b) Mean maximum temperature

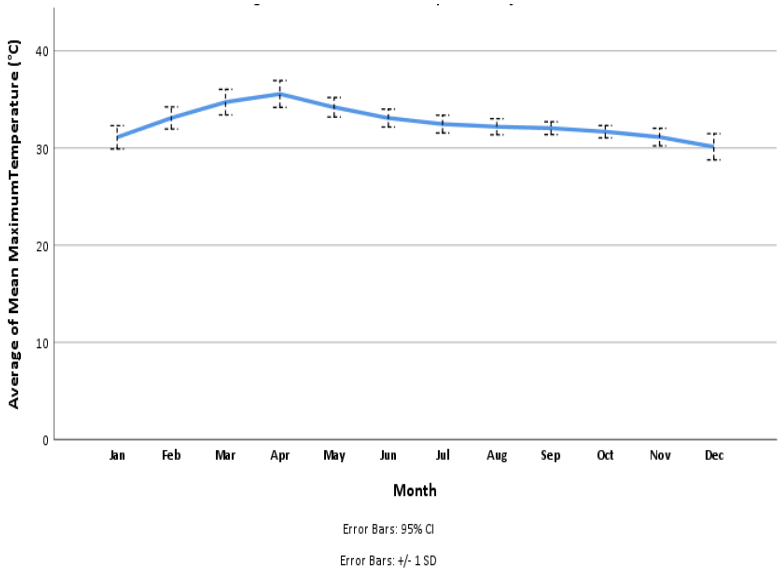

c) Difference mean maximum and minimum temperature

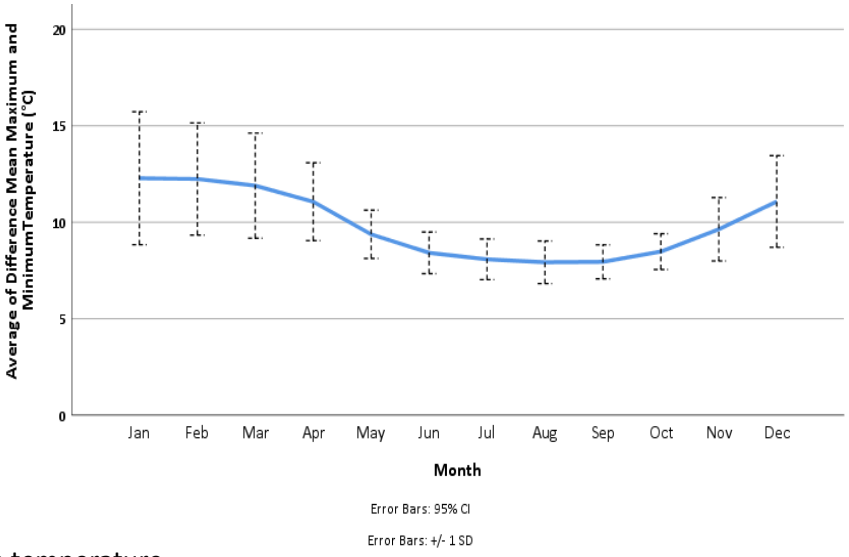

d) Mean temperature

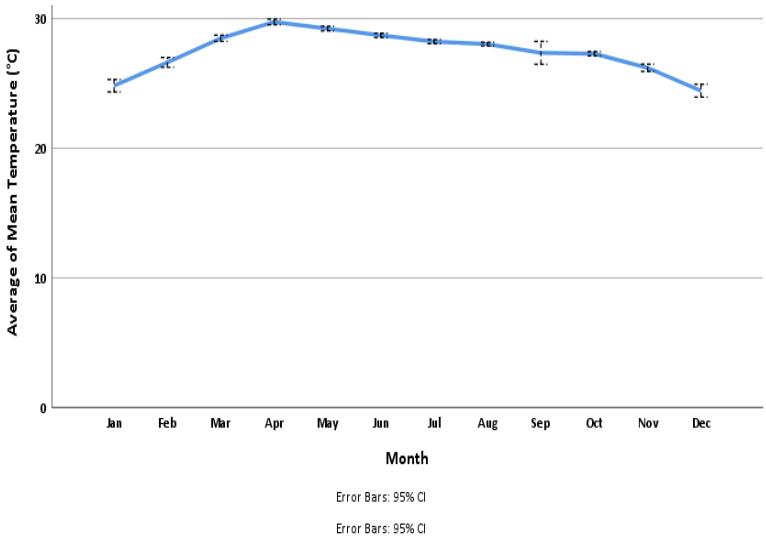

e) Extra-minimum temperature

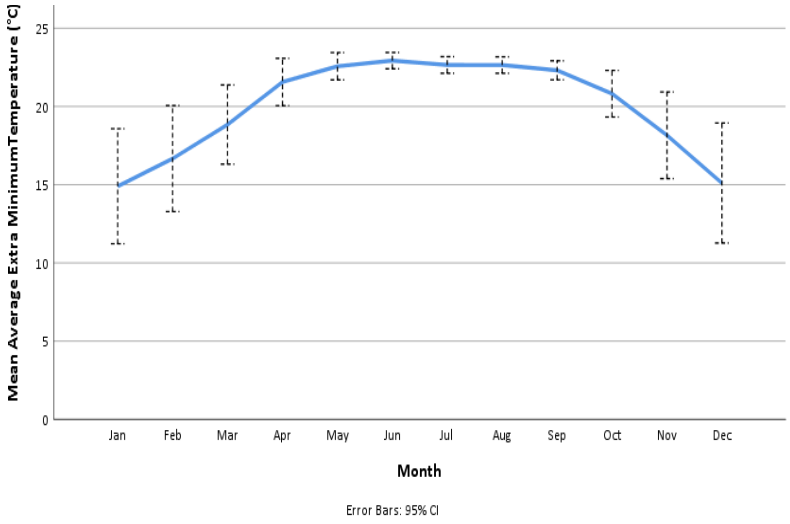

f) Extra-maximum temperature

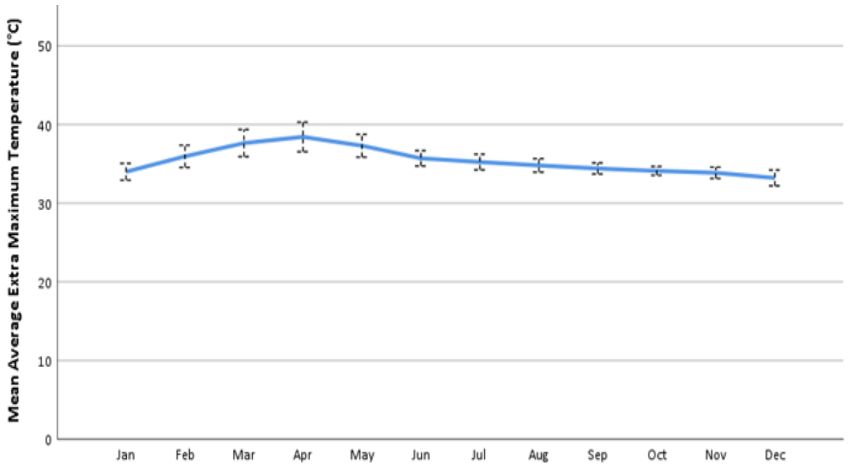

g) Difference in extra-maximum and extra-minimum temperature

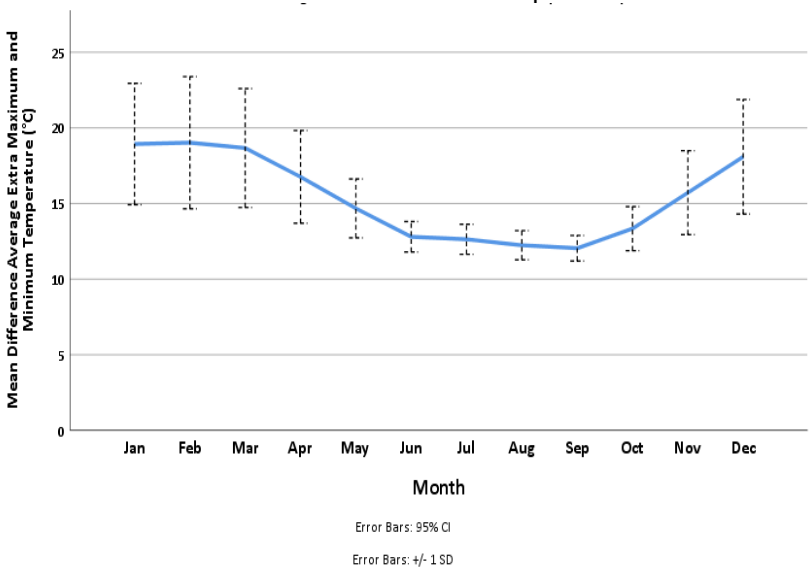

Figure 3.11 Temperature and mean monthly average temperature in Thailand (1981 to 2015). a) Mean minimum temperature, b) Mean maximum temperature, c) Difference in mean maximum and mean minimum temperature, d) Mean temperature, e) Extra-minimum

temperature, f) Extra-maximum temperature, and g) Difference in extra-maximum and extra-minimum temperature.

The temperature datasets (Figure 3.11) show averages in the same manner as the precipitation data. Figure 3.11a, b and c show the mean of the average daily maximum and minimum temperature and their difference which shows that the temperature increases through to April before decreasing through the year in the case of the maximum temperature or plateauing to some extent in the case of the minimum temperature. The difference is greatest in the dry season (November to April of the following year) and least during the growing season (May to October). Overall, the variation through the year is 3.32 and 6.91°Celsius for the maximum and minimum temperatures, respectively, and by 26.96 and 4.03°Celsius during the growing season. Research proved the essential optimum temperature for rice growth and rice production with 25°-35°Celsius in temperate regions. Temperature below or higher than the optimal temperature is negatively affected by crop growth. However, the seasonal dynamics of temperature during the study period do not exceed the optimum rice yield. Likewise, other temperature parameters (Figure 3.11 c-g) show similar temporal dynamics.

It is clear from the analysis of the seasonality of the precipitation and temperature that they are relevant to optimum growing conditions. However, there are few provinces that exceed the optimum temperature range during the study period.

3.3.2 Correlation between rice production and weather parameters

Table 3.2 presents a summary of the number of provinces where a significant relationship was found between weather parameters and rice production. The mean minimum temperature and mean maximum temperature shows the highest correlation among the temperature parameters. However, rainfall proved to be less significant as compared to temperature. The summary of Pearson's correlation and the number of significant values in the overall and specific irrigation groups is shown in Table 3.2.

Table 3.2 Amount of significant provinces in focus group (>40% cultivated rice) with Pearson's correlation and P-value between temperature metrics and weather parameter.

Weather parameter	Number of significant provinces (province) (Number of provinces in positive, negative correlation)							
	Yield		Detrended yield		Production		Detrended production	
	irrigated rice	non-irrigated rice	irrigated rice	non-irrigated rice	irrigated rice	non-irrigated rice	irrigated rice	non-irrigated rice
Amount rainfall (average)	0	3 (3,0)	0	1 (1,0)	1 (1,0)	3 (3,0)	0	2 (0,2)
Amount rainfall (cumulative)	0	3 (3,0)	0	1 (1,0)	1 (1,0)	3 (3,0)	0	2 (0,2)
Rainy day (average)	0	3 (2,1)	0	1 (1,0)	0	4 (4,0)	1 (1,0)	1 (1,0)
Rainy day (cumulative)	0	2 (2,0)	1 (1,0)	1 (1,0)	0	4 (4,0)	1 (1,0)	2 (1,1)
Extra-maximum temperature (average)	2 (2,0)	10 (10,0)	1 (0,1)	2 (0,2)	2 (2,0)	9 (9,0)	2 (1,1)	3 (1,2)
Extra-minimum temperature (average)	3 (3,0)	13 (13,0)	0	3 (0,3)	1 (1,0)	13 (12,1)	0	4 (1,3)
Mean temperature (average)	2 (1,1)	3 (1,2)	1 (0,1)	1 (1,0)	0	4 (0,4)	1 (0,1)	3 (3,0)
Mean maximum temperature (average)	3 (3,0)	11 (11,0)	1 (0,1)	6 (0,6)	2 (2,0)	10 (9,1)	2 (1,1)	3 (1,2)
Mean minimum temperature (average)	3 (3,0)	15 (15,0)	1 (0,1)	3 (0,3)	0	16 (15,1)	1 (0,1)	3 (2,1)
Difference in extra-maximum/minimum temperature (average)	0	2 (1,1)	1 (0,1)	2 (0,2)	2 (2,0)	3 (1,2)	0	2 (1,1)
Difference in mean monthly maximum/minimum temperature (average)	0	5 (3,2)	1 (0,1)	4 (1,3)	3 (3,0)	2 (0,2)	0	7 (1,6)

Table 3.2 summarises the correlation and individual significant provinces by considering both positive and negative correlations within the cultivated rice area over 40% in the different irrigation systems. The amount of significance is separated into irrigated rice and non-irrigated rice groups. With regards to accumulative amounts of rainfall, rice yield and rice production had the highest correlation, with a range of 0.33 - 0.60. Conversely, the correlation between the detrended rice yield and rice production data resulted in fewer provinces with significant relationships. The correlation between the average number of rainy days and the cumulative number of rainy days results in an equal number of significant provinces, but the significance is higher with the relationship between rice production and the average number of rainy days. In terms of temperature, the highest correlation between rice production and yield was found in the mean minimum temperature and mean maximum temperature. Overall, 18 and 16 provinces had

a significant relationship between average mean minimum temperature and rice yield and rice production, respectively. However, the number of provinces with a significance correlation with the average of mean maximum temperature data was slightly lower, with 14 and 12 provinces having significant relationships with rice production and yield, respectively. The correlation between the detrended rice data and mean minimum temperature (average) was less significant. The average temperatures in terms of minimum and maximum temperature increased the correlation among these parameters. Finally, the temperature difference (average), between the mean maximum and mean minimum temperature was significantly correlated in 5 and 5 provinces with rice production and yield, respectively. The results indicate only 2 and 5 provinces recorded a significant correlation between the difference between extra-maximum and extra-minimum temperature with rice production and rice yield in the non-irrigated rice area (Appendix B-C). The results suggest that the average minimum and maximum temperature are the weather parameters that have the most influence on rice production, with the highest number of provinces having statistically significant relationships. Detrending the data has not resulted in an increase in the statistical strength of the relationship with weather parameters suggesting that there may be specific phenological stages impacted by climate change and may be influenced on residuals.

Table 3.2 shows the provinces and the precipitation and temperature metric that had the highest significant correlation. It is clear that the mean minimum and mean maximum temperatures have the highest number of significant relationships with rice production. It is also clear that the vast majority (75%) of provinces with significant correlations between weather variables and rice production are not irrigated, which suggests that irrigation effectively mitigates the potential impact of climate. A number of other studies have found the benefits of irrigation systems in reducing the hydro-environmental limits which are impact the crop from climate change, e.g. groundwater recharge (Kumar, 2016), mitigate the irrigation water requirement (Boonwichai et al., 2018; Wang et al., 2014), and reducing water deficit level (Nikolaou et al., 2020). Thus, the extension of irrigation to crop field areas is vital for maintaining the potential crop yield.

In the following section, the spatial distribution of the weather parameters with the highest number of provinces with significant relationships (cumulative rainfall, the average number of rainy days, average mean minimum temperature, and average mean maximum temperature) are assessed. In all figures, the colours indicate the level of correlation, whilst the blue circles are those provinces with significant relationships (P = 0.05). Figure 3.12 shows the provincial-level variations in correlation between total rainfall and rice yield, and rice production during the wet season. Note that only those provinces with >40% rice cultivated area, and which have a weather station are included.

a) Amount of rainfall and rice yield

b) Amount of rainfall and rice production

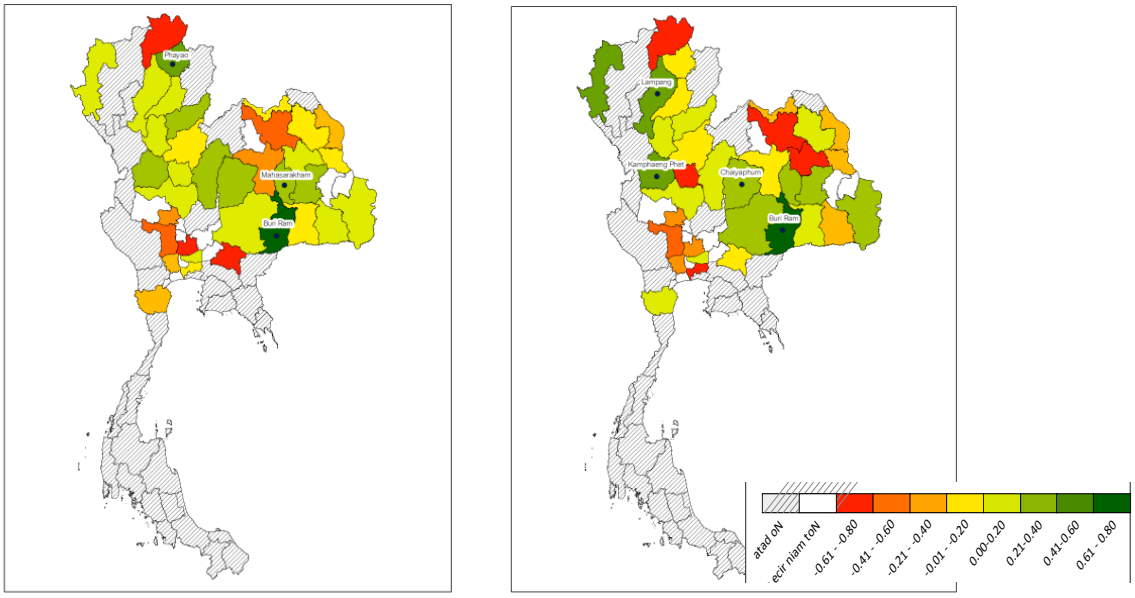

Figure 3.12 Correlation between rice yield, rice production, and cumulative of rainfall between May and October.

The relation between the amount of rainfall for rice yield and rice production is 3 (all of the significant provinces located in non-irrigated rice) and four provinces (1 province in irrigated rice and three provinces located in non-irrigated rice), respectively. To study the factors that influence rice production, box plots of the correlation coefficient for each significant parameter are shown in boxplot, which describes the distribution and skewness of the data.

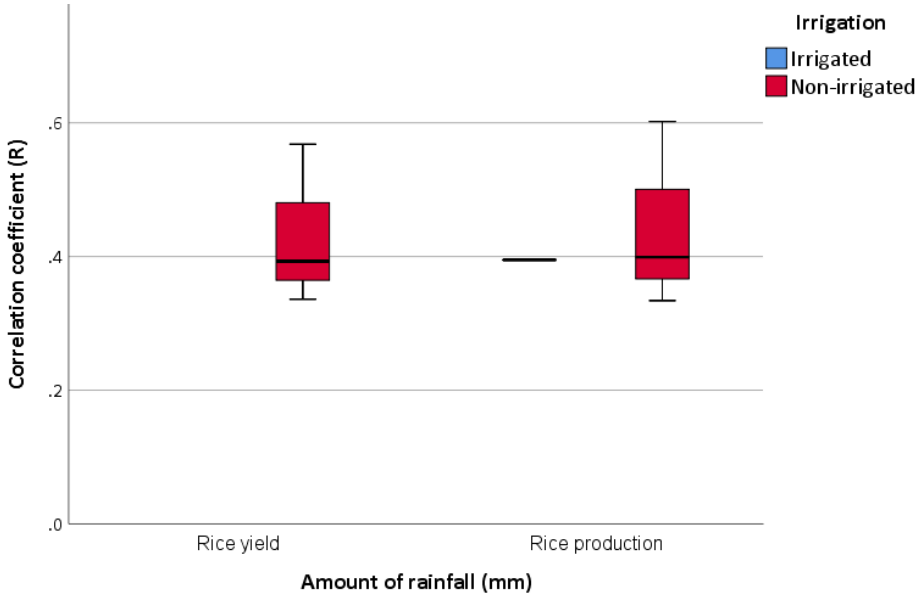

Figure 3.13 Correlation coefficient of rainfall with rice agricultural area over 40% with different irrigation systems.

Figure 3.13 indicates the positive correlation between rainfall and rice production was highest, ranging between 0.33-0.6; the correlation was lower in some provinces in irrigated and non-irrigated areas (ranging from 0.3 to 0.4). The correlation between rainfall and rice yield was found in non-irrigated areas and marginally lower (0.34-0.57). Buri Ram is highest on both rice yield and rice production correlation; however, there is a slightly higher correlation on rice production (r = 0.57 for rice yield correlation and r = 0.6 for rice production at sig. 0.000).

With regards to rainy day variables, Table 3.2 demonstrates that average rainy day and rice yield/production were correlated with rice productivity and yield. Figure 3.14 shows the provincial-level variations in correlation between the average number of rainy days and the rice yield and rice production during the wet season.

a) Average rainy day and rice yield

b) Average rainy day and rice production

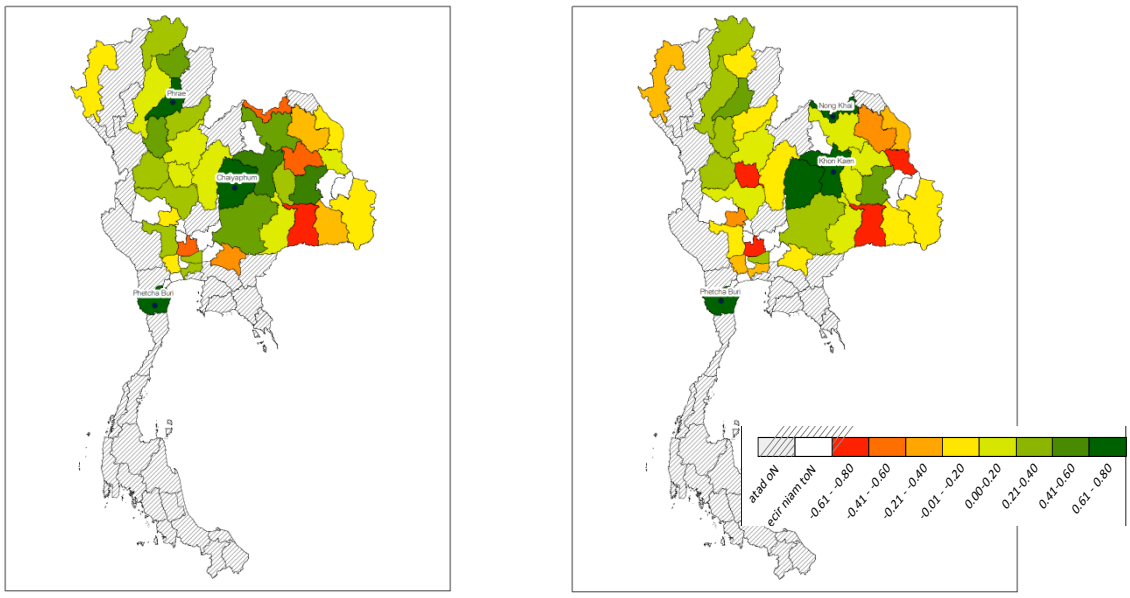

Figure 3.14 Correlations between rice yield and rice production and average rainy days between May and October.

The relation between the average rainy day for rice yield and rice production is 3 (all of significant provinces located in non-irrigated rice) and four provinces (all significant provinces located in non-irrigated rice), respectively. The range of correlation coefficient on rice yield is 0.34-0.38 whilst the range of correlation coefficient of rice production is 0.4-0.45. Further, the present study investigates the factors that influence rice production; a box plot of the correlation coefficient for each significant parameter with rice yield and rice production is shown in box plot, which describes the distribution and skewness of the data.

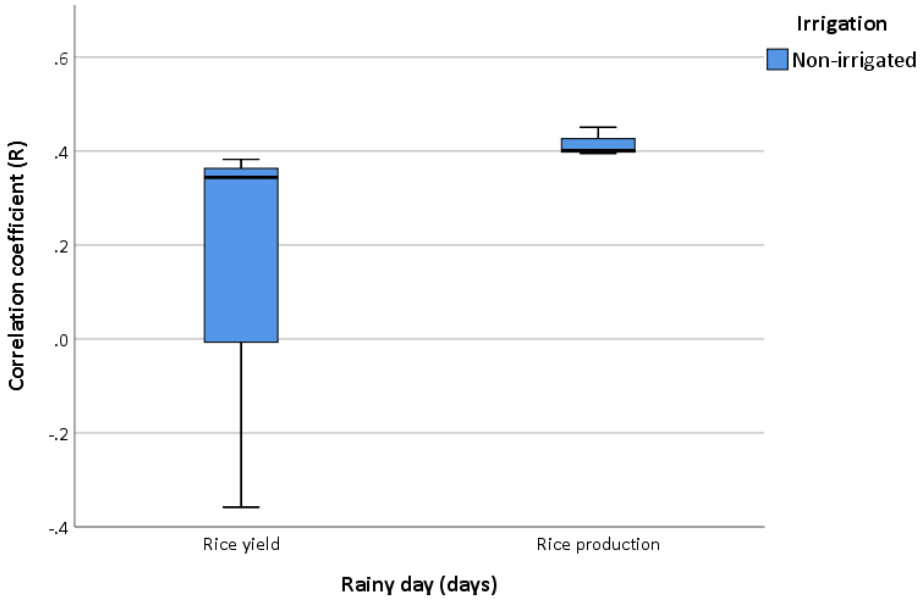

Figure 3.15 Correlation coefficient of rainy day with rice agricultural area over 40% with different irrigation systems.

Figure 3.15 indicates that rice production has a high correlation with a narrow correlation (~0.4-0.45) on the rainy day variable. However, the correlation on rice yield is slightly lower (~0.34-0.38) than rice production, but there is a wide correlation compared with other weather variables. This evidence may be the result of various rice varieties with differing rice productivity. Finally, the correlation between rainy days and rice yield has a large gap and outlier values.

With regards to the significant temperature variables, Table 3.2 demonstrates that the mean minimum temperature and mean maximum temperature were correlated with rice productivity and yield in the greatest number of provinces and, to a greater extent, than precipitation parameters. The correlations between the mean minimum and mean maximum temperature and rice yield, rice production, and detrended rice yield and rice production are shown at the provincial level in Figure 3.16.

a) Mean minimum temperature and rice yield b) Mean minimum temperature and rice production

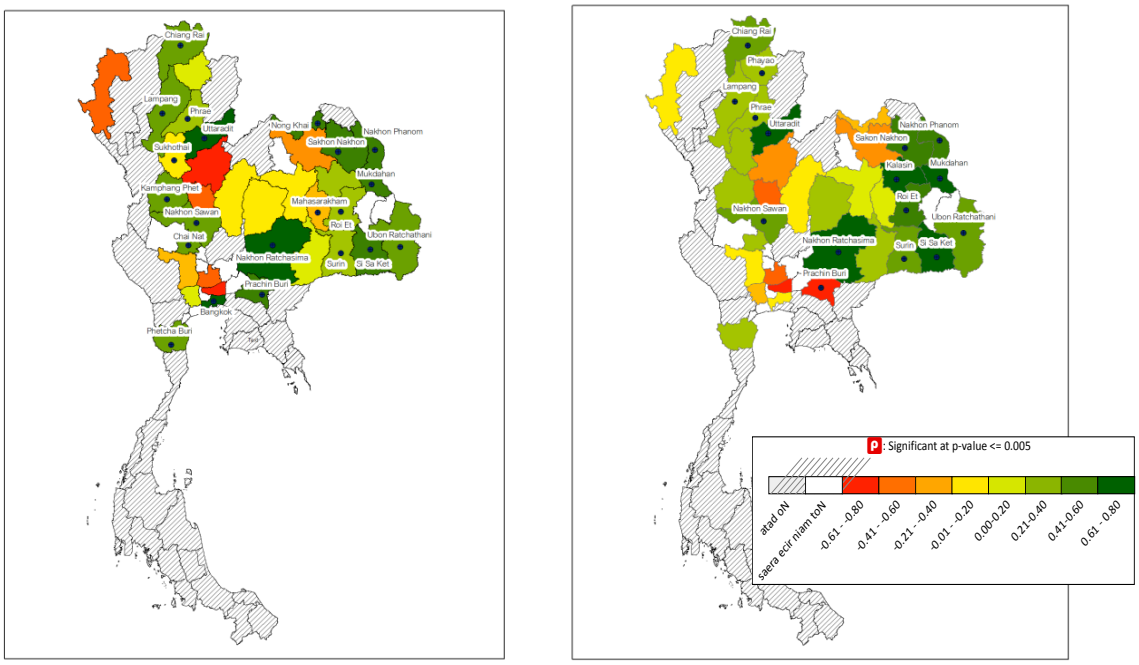

Figure 3.16 Correlations between rice yield, rice production, and cumulative mean minimum temperature using data between May and October.

Figure 3.16 (and listed in Table 3.2) shows the spatial distribution of the provinces with the significant statistical agreement between the mean minimum temperature and rice yield with 18 provinces across irrigated and non-irrigated areas, of which 3 are in irrigated areas and 15 are in non-irrigated areas.

Regarding rice yield, the correlation (r) in irrigated rice areas ranged between 0.45 and 0.72, while the non-irrigated rice area was between 0.40 and 0.66. The positive correlations suggest that increases in the mean minimum temperature led to an increase in rice yield and production. The three provinces with the highest correlation on rice yield were Nakhon Ratchasima, Uttaradit, and Sakhon Nakhon, with 0.66, 0.64, and 0.61, respectively. The majority of these provinces are photoperiod-sensitive rice varieties which are commonly planted in non-irrigated rice areas and sensitive to photoperiod. Regarding the correlation with rice production, the correlation was found in 16 provinces, and all located in non-irrigated rice areas, which ranged from -0.44-0.76. In addition, there is only Prachin Buri with a negative correlation (r =-0.44). Two main factors are stimulating rice productivity, i.e. geography and temperature, especially in the day length. Notably, the highest correlations are found in the north-eastern region, which is close to the Mun river (located in the Mun basin) and the Phu Phan mountain range (Natawa et al., 2005). The Mun basin consists of 31 tributary basins. Furthermore, these provinces may also be influenced to a greater extent by the south-western monsoon, which brings humid air mass from the India Ocean to Thailand and causes clouds and high rainfall to cover the country. The spatial distribution of the

correlation coefficient for the temperature and rice yield and rice production area is largely similar.

The correlation coefficients are shown as box plots in Figure 3.17 for two main groups in irrigated and non-irrigated rice areas. The range in correlation coefficients for mean minimum temperature and rice yield was broad (r = 0.45 - 0.72) for irrigated rice areas. The correlation coefficient for non-irrigated rice areas is slightly lower (r= 0.4-0.66) due to the limited number of provinces (4). In the correlation between rice production, all of the correlation is non-irrigated rice area and ranging between – 0.44 (outlier value) - 0.76.

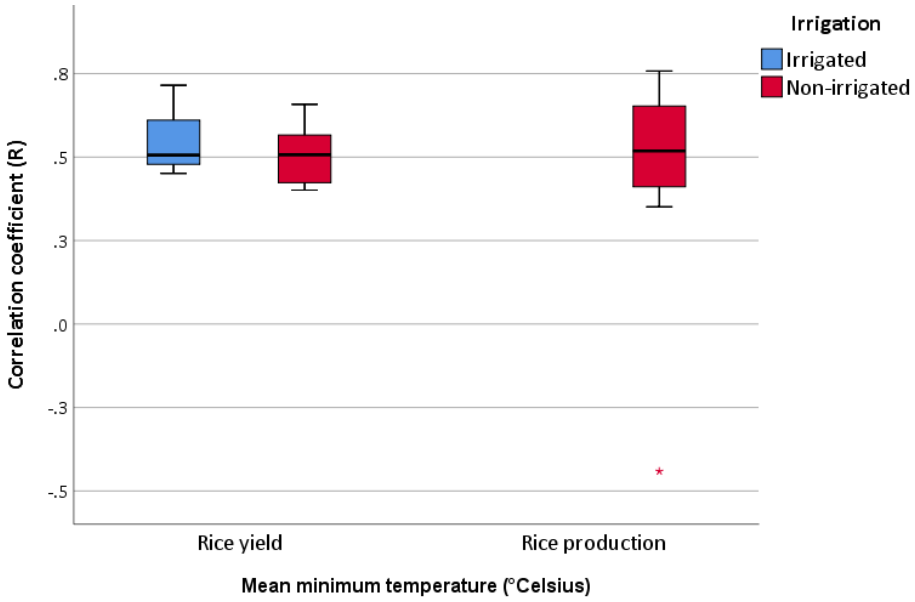

Figure 3.17 Correlation coefficient variation between the mean minimum temperature and rice production with >40% rice cultivated area (star symbols describe outlier value).

The afterwards analysis, shown in Figure 3.17, is the variation in the correlation coefficient between the mean maximum temperature and rice yield and rice production. Again, only those provinces that had statistically significant results and those areas where cultivated rice area is more than 40% are displayed.

a) Mean maximum temperature and yield

b) Mean maximum temperature and rice production

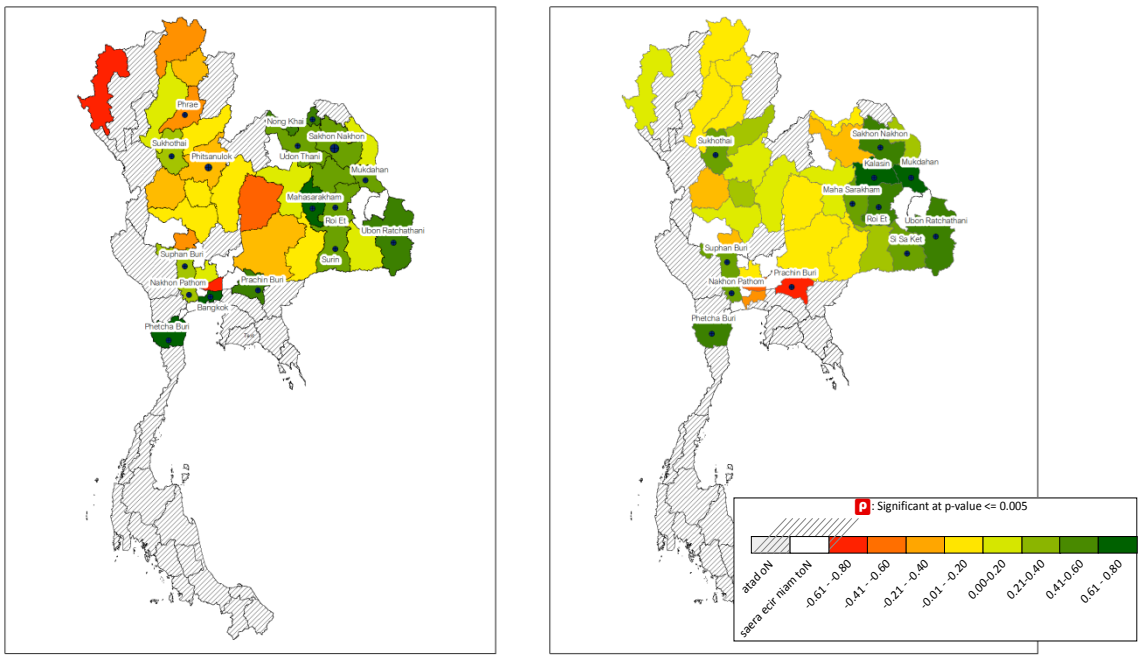

Figure 3.18 Correlations between rice yield, rice production, and mean maximum temperature during May and October.

The correlation between mean maximum temperature and rice yield reveals that only three and eleven provinces had significant statistical relationships in irrigated and non-irrigated rice areas over 40% of rice cultivated area, respectively. The highest correlation was found in non-irrigated areas- Phetcha Buri, Maha Sarakham, and Ubon Ratchathani provinces with r = 0.66 (sig. 0.000), 0.59 (sig. 0.000), and 0.54 (sig. 0.001), respectively. While the correlation in irrigated areas was highest in Bangkok, Suphan Buri, and Nakhon Pathom provinces, with r = 0.68 (sig. 0.000), 0.37 (sig. 0.032), and 0.36 (sig. 0.030), respectively. Another correlation is mean maximum temperature and rice production reveals that only two and ten provinces had significant. Regarding the irrigated area, Nakhon Pathom and Bangkok provinces, with r = 0.43 (sig. 0.009) and 0.38 (sig. 0.025), while in non-irrigated areas reveals a high correlation in Kalasin, Mukdahan, and Ubon Ratchathani with r = 0.72 (sig. 0.001), 0.62 (sig. 0.007), and 0.57 (sig. 0.000), respectively.

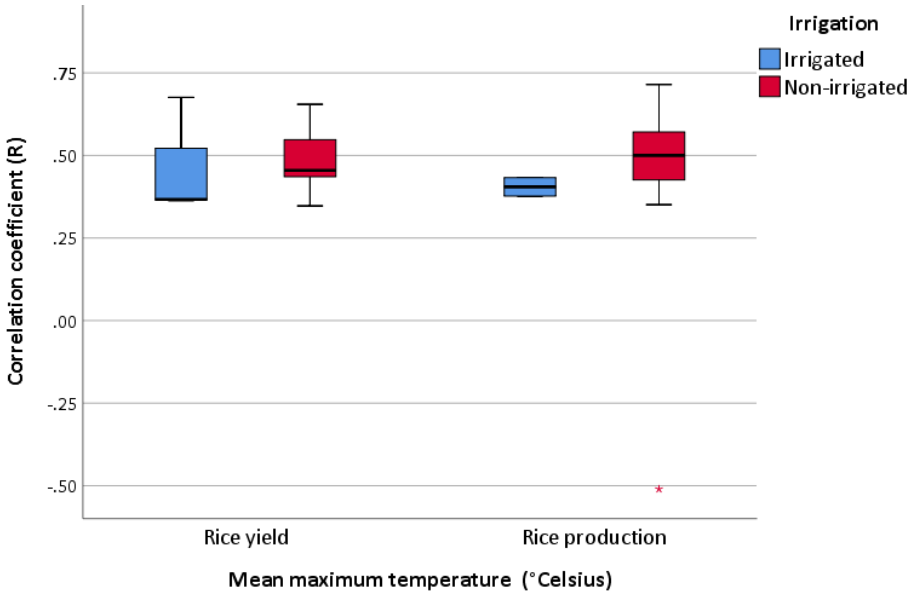

Figure 3.19 Correlation coefficient of mean maximum temperature with rice agricultural area over 40% in different irrigation systems.

A box plot analysis of the correlation coefficient (Figure 3.19) indicates that the mean maximum temperature and rice yield have a similar range (r = 0.35-0.68) of correlation coefficient values in irrigated and non-irrigated areas. As evident previously, the correlation coefficient between mean maximum temperature and rice production reveals a similar correlation range with rice yield; however, the correlation is a slightly narrow correlation in the irrigated area. Also, there is one province with a negative correlation with rice production in Prachin Buri in the same pattern as the mean minimum temperature (r = -0.51 sig. 0.002).

The latter significant weather parameter is the difference between the mean maximum and mean minimum temperature and only focusing on those provinces that had statistically significant results and those areas where cultivated rice area is more than 40%. The correlation between the difference between mean maximum and mean minimum temperature and rice yield is shown in Figure 3.20.

a) Difference mean maximum and minimum temperature and rice yield

b) Difference mean maximum and minimum temperature rice production

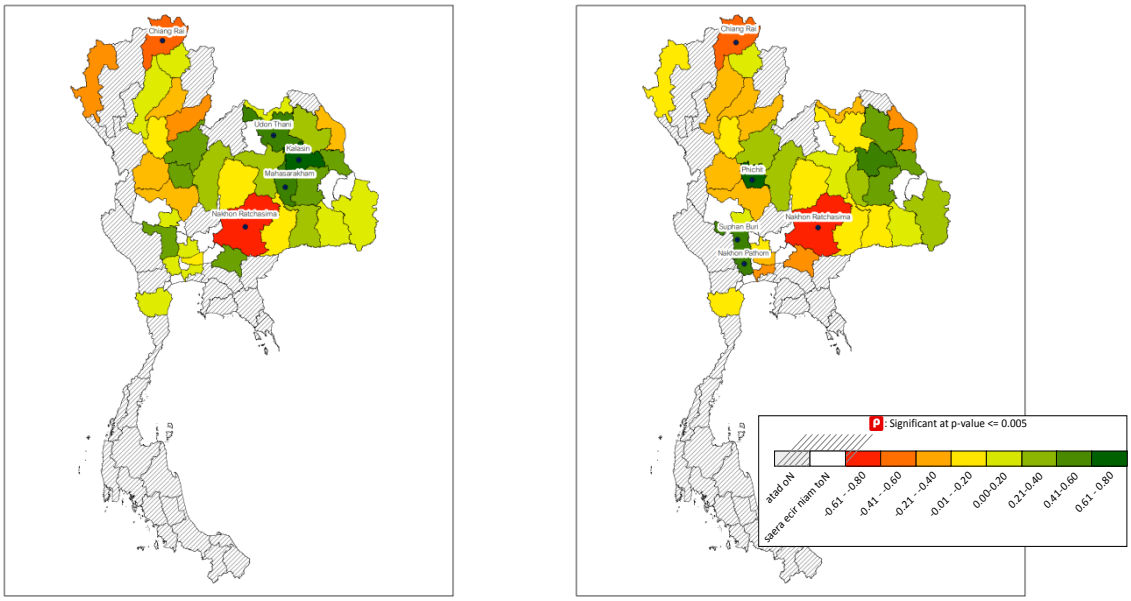

Figure 3.20 Correlations between rice yield, rice production, and difference between mean maximum and mean minimum temperature during May and October.

The correlation between the difference in mean maximum and mean minimum temperature and rice yield reveals that only five provinces had significant statistical relationships with non-irrigated rice areas over 40% of rice cultivated area. There are extremely highest correlations in both positive and negative correlations, Kalasin has the highest positive correlation with r = 0.6 (sig. 0.011), and Nakhon Ratchasima has the highest negative correlation with r = -0.57 (sig. 0.000). The correlation between differences of mean maximum and mean minimum temperature and rice production was significant in three provinces located in irrigated areas and two provinces located in non-irrigated areas. The range of correlation for irrigated areas (Nakhon Pathom, Phichit, and Suphan Buri) is 0.38-0.61, and Phichit has the highest correlation (sig.0.002). Conversely, the correlation for non-irrigated areas (Chiang Rai and Nakhon Ratchasima) is a negative correlation with a range of -0.41- -0.56. As evident, two provinces are significant for both rice yield and rice production in Chiang Rai and Nakhon Ratchasima (non-irrigated rice cultivated area); however, there are slight improvements in their correlation for rice production.

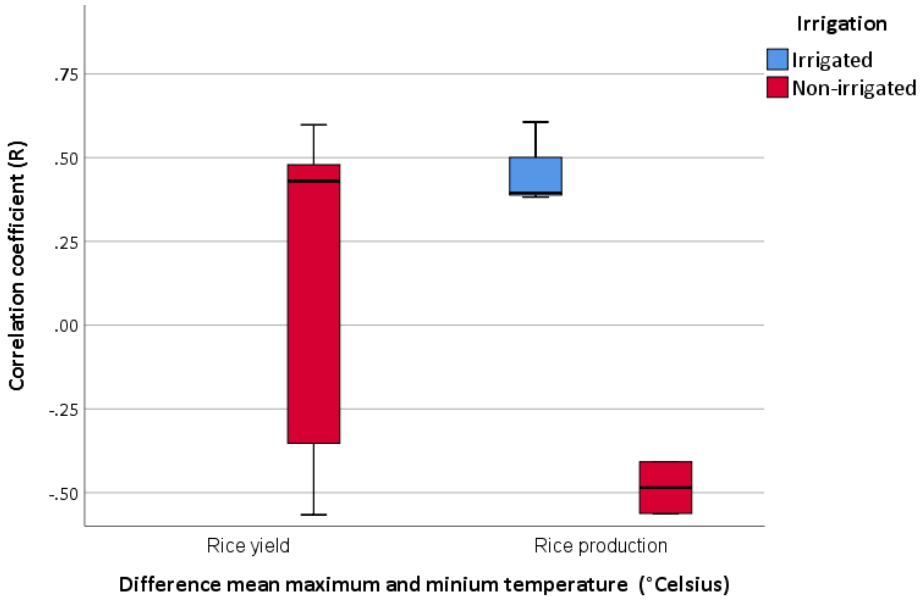

Figure 3.21 Correlation coefficient of difference between mean maximum and mean minimum temperature with rice agricultural area over 40% in different irrigation systems.

A box plot analysis of the correlation coefficients (Figure 3.21) indicates that the difference between mean maximum and mean minimum temperature and rice yield have a significant only non-irrigated area with a correlation range (r = -0.57-0.60). Regarding the correlation based on the difference between the mean maximum and minimum temperature and rice yield have significance for non-irrigated areas whilst the rice production is relative in both irrigated rice and non-irrigated rice area. The correlation in irrigated areas for rice production is 0.38-0.61. Rice production correlation is highest in Phichit province with r = 0.61 (sig.0.002), whilst the other two provinces in irrigated areas range between 0.38-0.39. The relationship for non-irrigated areas reveals negative correlation ranges from -0.41- -0.56 (in Chiang Rai and Nakhon Ratchasima province). All correlation shown as Appendix D.

As mentioned above, the rainfall in terms of cumulative rainfall and average rainy day have a positive correlation for both rice yield and production. The results are able to assume higher amounts of rainfall or rainy days, increasing rice productivity for all irrigation systems. Whilst the correlation between mean minimum temperature and mean minimum temperature proves a positive correlation for rice yield even though one province proved a negative correlation (Prachin Buri located in non-irrigated rice). The latter correlation is the difference between the mean minimum and mean maximum temperature that proved both positive and negative correlation for rice yield and production. Besides, the negative correlation found only two provinces in the non-irrigated areas (i.e. Chiang Rai and Nakhon Ratchasima). There are slightly more impacts on rice production and severe impacts on rice production than rice yield. Also, there are seriously impacted in the northeast region (Nakhon Ratchasima) than the north region (Chiang Rai).

3.3.3 Spatial autocorrelation

The contiguity edge method is applied for the weather parameters with the most significant trends, which are the average (temperature and rainfall) and cumulative rainfall. When considering the P-value, the present study determines the Z-score and P-value for accepting the study hypothesis. Our result reveals that there is no spatial auto-correlation with neighbouring provinces. Based on geographic information system (GIS) technology, this study is an analysis of the significant weather parameters for achieving the weather pattern at each location for 35 years. The result of spatial autocorrelation reveals the significant geography location and clustered pattern for the average temperature and cumulative rainfall in 1992. However, Moran's I index is absolutely low this year. For example, the average temperature is clustered with Moran's I index of 0.15 shown as Appendix E.

Table 3.3 Result of Moran's I index in significant weather parameter at significant year during study period.

Weather parameter	Year	Clustering pattern	Moran's index	Expected index	Variance	Z-Score	P-Value
Cumulative rainfall	1992	Random	0.149	-0.013	0.005	2.241	0.025
Average temperature	1992	Clustered	0.149	-0.013	0.005	2.241	0.025

a) Cumulative rainfall

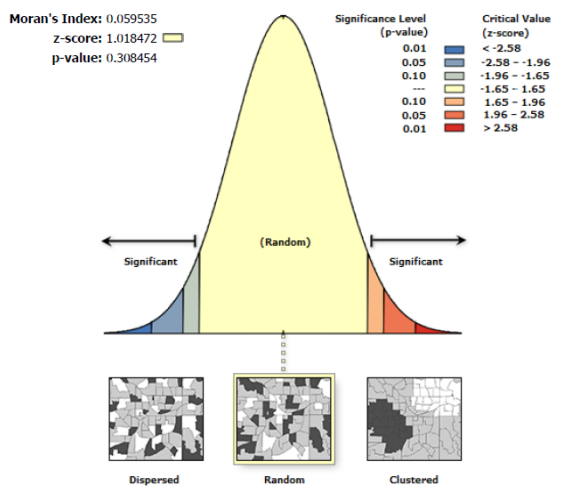

b) Average temperature

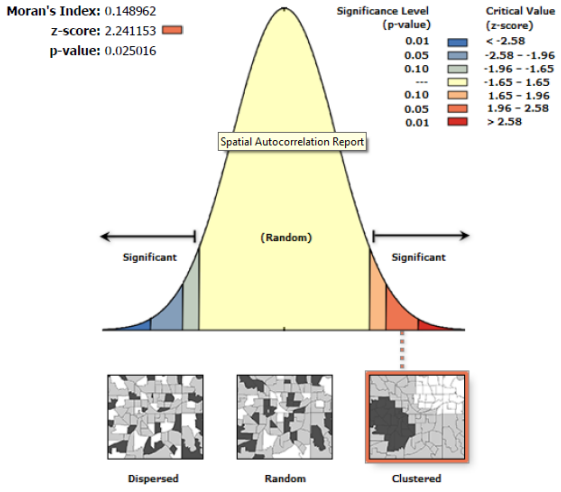

Figure 3.22 Result of spatial autocorrelation using Global Moran's I index demonstrated in a significant year.

Figure 3.22 suggests the results of the spatial autocorrelation at each location in 1992 for both cumulative rainfall and the average temperature at a certain significant level. Moran's Index of cumulative rainfall is 0.149, the Z-score is 2.241, and the P-value is 0.025. The critical value (Z-score) was less than 2.58 but greater than 1.96; thus, the result of the clustered pattern is a result of a random chance. The other factor proving slightly significant is the average temperature. Moran's Index of average temperature is 0.149, the Z-score is 2.241, and the P-value is 0.025. The critical value (Z-score) was less than 2.58 but greater than 1.96; thus, the result of the clustered pattern is a result of a clustered chance. The pattern of spatial autocorrelation is displays in the small box for each weather parameter.

3.3.4 Summary the susceptible provinces on climate change

The analysis presented in the previous sections has highlighted that a number of provinces have significant correlations between rice production variables and climatic variables; this is more evident in those regions that do not use irrigation. In overall, there are 30 provinces (6 provinces in irrigated areas and 24 provinces in non-irrigated or 85.71%) that show a significant relationship between rice production variables and climatic variables (Figure 3.23). The correlations were largely positive for rainfall and temperature; thus, the result suggests that high temperature and high rainfall have a positive impact on rice production and rice yield.

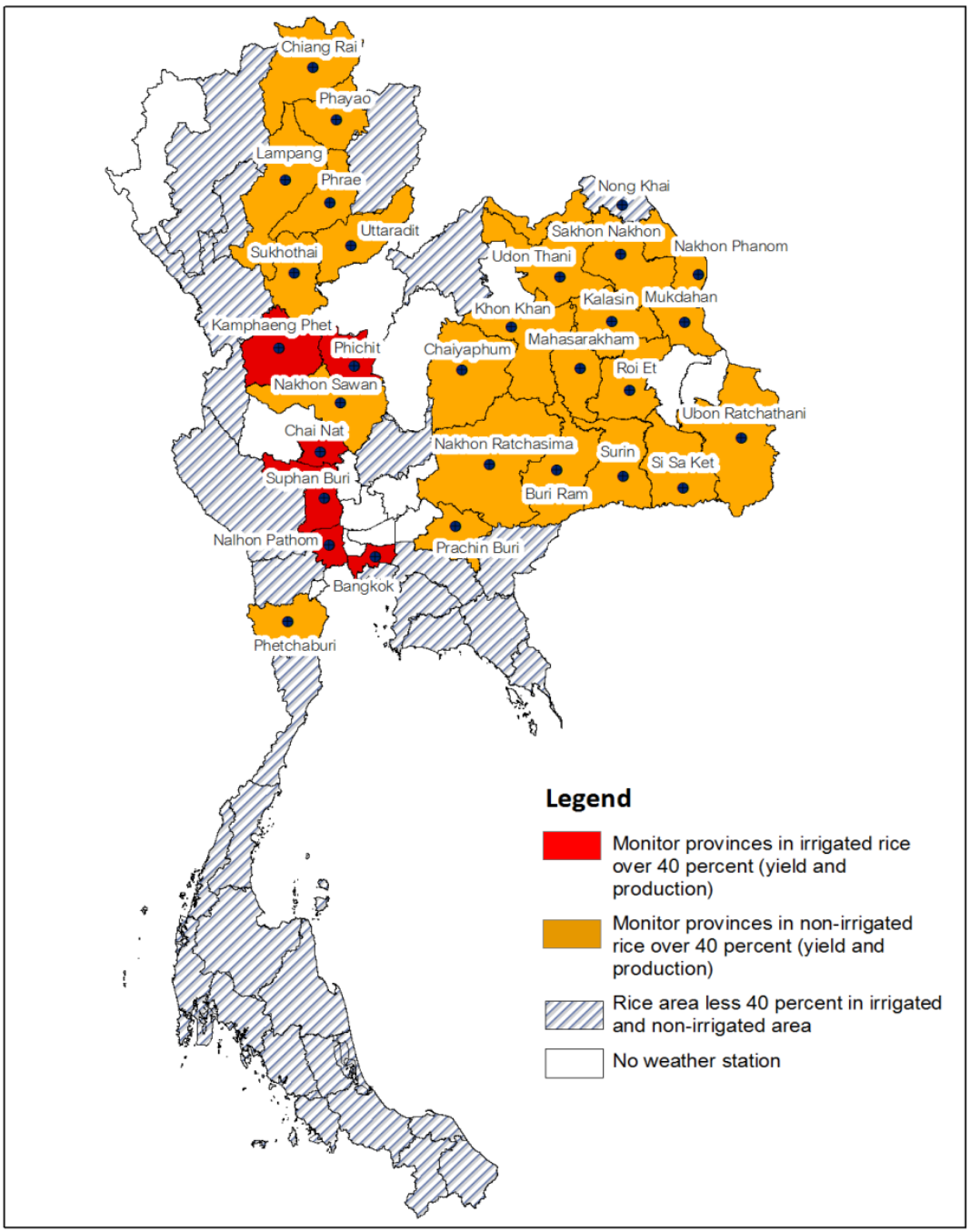

Figure 3.23 Monitored provinces' rainfall, mean minimum temperature and mean maximum temperature, specific to rice production and rice yield (irrigated in red colour and non-irrigated in orange colour).

Most provinces where there is a relationship between rice production and weather parameters don't use irrigation (Figure 3.23). The results revealed most correlation is a positive correlation among significant weather parameters with rice yield and production, except for some provinces is a negative correlation between mean minimum temperature, mean maximum temperature, and the difference between the mean maximum and mean minimum temperature. The Department of Disaster Prevention and Migration (DDPM) announced drought disaster areas in

25 provinces, and these provinces are relevant to the present study (16 provinces significant) (DDPM, 2020). These are able to interpret that higher global temperature corresponds with weather estimation on IPCC's Fourth Assessment Report (IPCC, 2007); thus, rice productivity tends to increase. However, some provinces found a negative correlation- Prachin Buri is only one negative correlation between the mean minimum and mean maximum temperature. However, there are differences significant negative correlations in difference mean minimum and mean maximum temperature in two provinces for rice yield and rice production (i.e. Chiang Rai and Nakhon Ratchasima) with slightly higher correlation on rice production. One of the reasons for this is that the northeast region of Thailand experiences higher annual precipitation (15-20%) than the irrigated regions found in central Thailand. Thus, precipitation is influencing rice planting in this region. Due to the most susceptible provinces located in northeast Thailand, the resilience to climate change in non-irrigated areas could be reduced by irrigation infrastructure improvement (Elliott et al., 2014) and by adopting drought-resistant rice varieties (Kumar et al., 2014; Todaka et al., 2015). Our results suggest that agricultural policymakers should monitor these susceptible provinces by combining the information between weather and rice productivity correlation. Beyond, the impacts of climate changes on rice productivity in Thailand are highly uncertain from weather parameters; thus, the simulation of climate change impacts on agriculture is challenging to investigate, and the suitable adaptation strategies are vital resilient to climate changes by integrated varied approach (e.g. economic approach) and climate modelling.

3.4 Discussion

This chapter analysed the relationship between climate and rice production parameters over the past 35 years. Located in a tropical zone, Thailand's paddies are impacted by increasing temperatures and precipitation. The cross-correlation between weather and rice production reveals that temperature is more significant than precipitation parameters, as observed in the number of provinces with significant correlation and values of correlation coefficients. When comparing the temperature parameters, the average minimum and maximum temperature have the greatest influence on rice production in a number of provinces. Also, the minimum temperature (referred to as night-time temperature) has more impact on rice production and rice yield than the maximum temperature (referred to as daytime temperature). Yenda et al. (2018) conducted the effect of weather parameters on rice yield during the Kharif season at the research farm at Orissa University of Agriculture and Technology, India, in 2016 under different planting conditions (e.g. puddled transplanting, unpuddled transplanting, and direct seeding). The puddled transplanted rice crop had the greatest grain yield, whilst the yield had a negative correlation with minimum temperature (-0.83) and rainfall (-0.59), a finding opposite to our study. Our findings

revealed the mean minimum and mean maximum temperatures definitely impact rice yield and production; however, they are necessary to determine which growth stage occurs. Sarker et al. (2012) supported our conclusions on the impacts of maximum and minimum temperatures and estimated the relationship between rice yields and climate variables by using time series data in Bangladesh. The result demonstrated the impacts of temperature (i.e. minimum and maximum temperature) and rainfall in 3 groups (i.e. Aus, Aman, and Boro rice, which Aus and Aman were planted in the wet season and Boro rice was planted in the dry season). The result proved a significantly positive correlation with the maximum temperature of Aus and Aman rice, whilst the Boro rice had adverse effects on rice yield. However, the minimum temperature had a negative effect on Aman rice; however, there was a significantly positive effect on Boro rice. Abbas & Mayo (2021) investigated the positive impacts between rice crops and minimum temperature at the replantation stage due to increasing the speed of leaf emergence and rainfall was positively significant for rice at the tillering and stem elongation stage by increasing tillering's rate. The growth stage of rice is crucial for their correlation. Research proved higher daily minimum temperature increased rice yield (Chen et al., 2016), which agrees with our study. The weather trends under the present study estimate that temperature in Thailand will rise in the near future; thus, it is recommended to breed new rice cultivars with temperature tolerance. Our results found limitations on detrending, the impact of rice variety, and the role of the irrigation system. Thus, we are clarified as following aspects.

3.4.1 Why does the detrended data have less weather agreement than raw data?

In this study, the underlying assumption was that government policies and technological developments might influence the ability to determine the influence of climate on the rice production time series. The pattern of historical yield data is calculated through detrending before analysis; this aims to reduce the effects of changes in agriculture technology development, such as agricultural machinery and rice seeds development.

The correlation between the raw and detrended rice yield and rice production data with weather data was analysed, with the results indicating weaker agreement between climatic variables and the detrended rice production data. The data in terms of rice yield and production are quite consistent over time (Figure 3.7); thus, creating a significant variation in their correlation. Key information assures the weaker signification on detrending is series on data quite fluctuating. Even though, this study is investigating cross-correlation without determining the differences on residuals of their relationships. Referring to significant rice production/yield variables, it is obviously seen that rice yield and production without detrending are increasing in significant provinces during the time period. The excessive temperature over the threshold level is the main

cause of crop growth, especially in the reproductive stage. Detrending rice yield was examined to eliminate the influences of agricultural technology (Rajavel et al., 2018). The limitation on detrending occurs in our study; thus, there are suggestions to adopt the appropriate detrended such as using fitting linear regression and applying residuals from the model (Wen, Ponnusamy, & Kang, 2019) or using a log-linear trend model (Vedenov & Sanchez, 2011) for accounting the effects between crop yield and weather. The detrend production index of crops may be preferable for analysis (Biswas et al., 2017).

3.4.2 Impact of rice variety

The aim of the research in this chapter is to investigate the correlation between weather and rice productivity in Thailand. However, the analysis ignores the impact that rice variety can have on yield and productivity. As mentioned in section 2.4.5, rice farmers plant rice in two main categories, photoperiod-sensitive and photoperiod-insensitive rice varieties, which vary with region and topography. For example, photoperiod-insensitive rice varieties are usually adopted in the Chao Phraya River delta due to the flowering response (not depending on day length and typically planted in the wet and dry seasons) (Vergara & Chang, 1985), and these typically provide higher yields (Kasetsart University, 2000). These areas are gradually replaced with high-yield rice varieties (HYRs) instead of local rice varieties (Molle et al., 2021). Meanwhile, photoperiod-sensitive rice varieties are normally used in the northeast region as these require more solar radiation for crop photosynthesis, which is sensitive in flower initiation, and this region of Thailand has lower annual precipitation and potentially less cloud cover. Different rice varieties have different growing season lengths from 99 days to 105 days (V et al., 2021), which can alter the annual production if multiple crops are planted. The yield can also vary by up to 50% amongst rice varieties (Bakare et al., 2017; Chowhan et al., 2017; Li et al., 2019), which can also influence the annual statistics for a particular province.

Our study investigated the relationship between weather and rice productivity data, which is not classified with rice variety. Thus, there may be distortion from analysis at the state level. The further study will suggest correlation investigation among different types of rice variety or select a specific dominant rice variety. One strategy to develop a rice variety referred to as a hybrid rice variety, which combines traditional varieties with those that are tolerant to diseases, pests, abiotic stress, heat, and droughts such as IR8, BR11, BBRI dhan28, and BBRI dhan29 varieties (Fen et al., 2015; Pandey et al., 2010; Yamano et al., 2016). Rice production depends on the cultivated area and cropping intensity, with the latter influenced by the rice variety. Consequently, rice production is higher in the Chao Phraya River delta, which has a different rice variety and a full irrigation system. This is in contrast to the northeast region, which has lower yields due to most

farmers' plant photoperiod-sensitive rice varieties (e.g. KDML105 and RD6) and together this type of variation distorts the findings of the impact of climate on rice productivity.

3.4.3 Role of irrigation in rice cultivation

Variability in rainfall distribution is the main restriction on rice planting, especially in tropical areas which depend on the monsoon rains. However, there is evidence of differences in water usage among irrigation farming systems (Taniyama, 2002). Analysis of the variation of monthly total rainfall indicates that precipitation has reduced in May relative to that found at the start growing season of the time series, which coincides with rice planting in the wet season. A research simulated model with rainfall data revealed a delay in the planting date due to the reduction of rainfall in the early season (Sujariya et al., 2020). A strategy for adapting to climate change adaptation is to shift the sowing date to an optimised time in order to increase rice yield (Ding et al., 2020). Yamauchi (2014) found that during times of insufficient precipitation, longer dry spells and a reduction of cumulative rainfall resulted in the rice transplanting date in the early wet season being delayed in non-irrigated rice areas; this led to drought risks and a decrease in rice production.

This analysis found a positive relationship between the average rainfall and rice yield, agreeing with previous studies that found cumulative rainfall has a positive effect on rice yield (Bhattacharya, 2013; Sarker et al., 2012; Saseendran et al., 2000). A higher number of provinces in non-irrigated areas have statistically significant correlations with rainfall which largely occurred in the northeast, which typically receives higher annual rainfall than more central regions. Therefore, a number of these provinces are more susceptible to changes in precipitation totals. In terms of the average number of rainy days, only non-irrigated provinces had statistically significant relationships with rice production, which might be evidence of insufficient precipitation before the growing season.

Temperature directly influenced crop photosynthesis and growth rate; Figure 3.11 illustrates the differences in average monthly temperature above the 35-year. This is most evident in the minimum and maximum average values but is also present, to a lesser extent, in mean temperature. Rice cultivation is optimal when temperatures range between 25° and 35°Celsius, and a number of studies have highlighted the negative impact that temperature can have on rice productivity (Ghadirnezhad & Fallah, 2014). Nagai and Makino (2009) assessed the impact of increasing daytime and night-time temperatures on rice and found biomass production and relative growth rate to be optimal at temperatures under 30/24°Celsius (day/night temperature), while the net assimilation rate of rice decreased at low temperatures (19/16°Celsius). Above

30°Celsius, crop photosynthesis is stimulated. This is supported by the present study, which found a positive correlation between temperature and rice production in almost all provinces. The minimum and mean temperatures during the rice growing season (May to October) are higher than the detrimental minimum values and within the range of optimum temperature. The temperature outside of the optimum temperature range has a serious impact during the reproductive stage by producing panicle sterility and lower grain production, and finally reduction in yield (Reyes et al., 2003; Nishad et al., 2018). Even though, fewer nearly or above optimum temperature ranges may not influence rice physiologically. Analysis of the temperature metrics (Section 3.3.1.2) indicates the mean temperature during the growing season falls within these bounds. A number of studies have found that temperature extremes or heat stress can increase water loss and death of seeding in the seeding stage, wither and yellow leaves, reduce tiller's rate, and reduce yield under heat conditions (40°Celsius at day/35°Celsius at night-time) (Xu et al., 2021). In addition, Rehmani et al. (2021) proved that extreme heat events coincided with the heat-sensitive reproductive growth period by using long-term meteorological data and considering stress days, i.e. higher daily maximum, high daily minimum temperature, and both critical temperature limits.

The correlation between rice production and the mean minimum and maximum temperature revealed 21 and 16 provinces, respectively had statistically significant relationships, and the majority of these were in non-irrigated areas. This, coupled with the analysis of precipitation, highlights the increased sensitivity of non-irrigated regions to climate change and that extending irrigation infrastructure and irrigated service areas may provide a means to mitigate climate change. Suwanmontri et al. (2020) investigated the factors based on changes in rice productivity from 1974-2018 using secondary data and compared two main regions (i.e. non-irrigated lowland-based northeast and irrigated lowland-based central Thailand). Their findings revealed irrigation water, especially in the dry season, was crucial for rice productivity. For example, rice yield increased more rapidly in the wet season (1.82-2.85 tonnes/ha) compared to the dry season (3.93-4.25 tonnes/ha), and rice production in the wet season was higher than in the dry season. The proportion of rice production was 26 million tonnes in 2011, of which 13 million tonnes was in the northeast and 5 million tonnes in the central region, and the rice cultivated area decreased during 2011-2016 in both the wet and dry seasons.

The remaining susceptible provinces (14.29%) reveal fewer impacts on rice productivity and weather correlation. In irrigated areas, the cumulative rainfall is found only in Kamphaeng Phet on rice production with low correlation coefficients. However, the temperature proves widespread on the mean minimum temperature (only specific to rice yield) and mean maximum temperature (both rice yield and rice production), which is observable from significant provinces. The dissimilar correlation

may be the reason for the critical temperature varied with rice variety and duration influences on physiological of rice plant. The result of the present study is in partial agreement with previous research. Bemal et al. (2009) investigated the Kharif season, which is sown in July-August and harvested in October-November, in two locations- Karnal and Hisar in India by adopting multiple regressions during 1992-2006. This agreement with positive correlation on maximum, minimum, and mean temperature whilst rainfall was a negative correlation in Karnal whilst there was a reversely impact in Hisar (positive correlation for rainfall and maximum/minimum/mean temperature was negative correlation).

3.4.4 Representative of weather data

The availability of weather station data is a limitation of this study. Most provinces only have one weather station, and it is generally located in a non-agricultural area which may not be representative of the weather throughout the province and may impact the analysis. A denser network of weather stations would alleviate this but would incur high operating costs at regional and country scales. An additional option is to use precipitation estimates from the Tropical Rainfall Measuring Mission (TRMM), which is objective to measure tropical and sub-tropical precipitation and is related with varied precipitation-related sensors. The format of TRMM level 3 product (3B43), which merges gauge and satellite analysis algorithm, contains 0.25° x 0.25° resolution for each month with a spatial coverage from 50° North to 50° South. The TRMM 3B43 is commonly analyses and integrated with other variables for meteorological monitoring (e.g. drought) and correlation with crop yield. The advantage of TRMM is coverage of large areas and substitution in the region with scarce weather stations; however, there is a limitation on the pixel size and poor accuracy for identifying precipitation in mountainous areas (Bharti & Singh, 2015).

The other reason for supporting our work is the optimum temperature for rice growth and the physiology activities of rice. The optimum temperature influences for crop photosynthesis is varied among regions and are relevant to normal rice development, Previous research has found the optimum temperature for rice growth is between 25° and 35°Celsius (Nishad et al., 2018) and that excessively high or low temperatures can induce plant stress which reduces plant growth and consequently yield (Krishnan et al., 2011; Shah et al., 2011). The level of crop stress is also influenced by the duration, intensity, and timing of stress, which can affect particular growth stages to a greater extent and which impact both grain quality and yield. The temperature stress may decrease the photosynthetic rate and the number of panicles in the panicle stage (Xu et al., 2021) in the reproductive stage, heat stress can inhibit flower initiation, pollen and spikelet development, flowering and anthesis, and grain yield (Hussain et al., 2019). The limitation of our study is weather data in seasonal; thus, more detail, especially each growth stage (i.e. tillering,

heading, flowering, milking, dough, and maturity), may improve the performance of correlation coefficients between weather and grain yield (Sattar et al., 2017).

Assessment of the spatial autocorrelation of the correlation between rice production and weather metrics revealed a random spatial distribution with respect to neighbouring provinces. The result reveals the significant geography location and clustered pattern for the average temperature and cumulative rainfall in 1992. The testing of Moran's I index the best solution if there is more information on the distance threshold or distance band between nearby objects. The further study proposed to assess other conceptualizations of spatial relationships such as Hot Spot Analysis (Getis-Ord Gi; (Getis & Ord, 2010)), Cluster and Outlier Analysis (Anselin Local Moran's I), and Local Indicators of Spatial Association (LISA) (Anselin, 1995). For example, LISA principally computes the similarity with its neighbours and test significance (i.e. high-high, low-low, high-low, and low-high). Thailand is located at latitude 5° to 23° North of the equator. The influences of topography and location may be impacted by the differences in weather conditions between the north region and the south region. Further research requires an ecophysiological model to reduce the uncertainty of climate change impacts assessment.

3.5 Conclusion

The main objective of this chapter was to investigate the variation of rice production in Thailand over the past 35 years and to assess the relationship between weather metrics, including rainfall (i.e. the amount of rainfall and number of rainy days) and temperature, with provincial level rice yield and production. The provinces with the most significant relationships were mostly (88%) found in areas which did not use irrigation, in part as these areas also typically experience higher annual rainfall. The result reveals minimum temperature, maximum temperature, and differences between maximum and minimum temperature have the highest correlation. The cumulative rainfall and rainy days are less correlated. Analysis at the provincial level of the relationship between rainfall and temperature and rice yield and production indicates that rainfall has a potential on rice productivity irrespective of whether the area is non-irrigated. The important temperature parameters impact rice yield and rice production are mean minimum temperature and mean maximum temperature due to their optimum temperature for crop growth. Finally, the study reveals no spatial correlation among weather parameters except in 1992.

The spatial variation of the area under rice cultivation is consistent with the implementation of government policies whereby the cultivated area was reduced in the central, east, and south regions through the implementation of agricultural zoning policies in 2009-2010 and 2012-2013 (Ministry of Agriculture and Cooperatives, 2014). The policies were designed to encourage

farmers to plant the optimal crops for their agricultural areas by considering the local environment (e.g. soil, land use, precipitation, forest, slope, and factory location) and using mechanisms of the provincial government (e.g. promote farmers who plant in low productivity to plant the other suitable crops instead or Thai government set the policy into area approaches and commodity approaches). The main objective of agricultural zoning is agricultural reform and sustainable agriculture. As a result of these policies, ~55% of provinces saw a >10% increase in rice cultivated area, 25% a decrease by >10%, and 20% of provinces saw changes +/- 10%. The magnitude of these changes illustrates the impact that the government can have on agricultural production, whilst the analysis of the influence of weather highlights the benefits of irrigation in rice cultivation and that 22% of provinces in Thailand are more susceptible to changes in climate.

Chapter 4 The dynamics of rice biophysical variables in irrigated and non-irrigated systems during the growing season

Southeast Asia accounts for 31% of the world's harvested rice area, with 48 million ha under rice cultivation (Redfern, Azzu, & Binamira, 2012). Concerning agricultural practices, 45% of this rice area is irrigated (18 million ha), 45% is non-irrigated (18 million ha), 5% is planted in deep water (3 million ha), and 5% is planted in non-irrigated upland areas (3 million ha). Thailand is the fourth-ranked country in terms of the use of irrigation in rice cropping (Mutert & Fairhurst, 2002) and is sixth-ranked in terms of rice exportation, with 33 million tonnes exported in 2017 (Fischer & Velthuizen, 2016). In 2012, the irrigated rice area covered 29.5 million rai or 4.7 million ha, which equates to 9% of the country's total land surface area (RID, 2013). Rice cultivation is mostly located in areas fully supported by irrigation systems (e.g. irrigation projects and canals). These areas typically have high planting densities where farmers can plant 2 or 3 rice crops per year (Pushpavesa, Somrith, & Petpisit, 1986). Thailand's main rice cultivated area is the Chao Phraya River delta, which accounts for 20-25% of rice production (OAE, 2017b). Information collected by the Rice Department, Ministry of Agriculture indicates that across Thailand there are 138 varieties of rice grown in various ecosystems and photoperiod sensitivities and which have specific characteristics such as pest/disease tolerance, being adaptive to local environments, having high yields, and cooking quality on consumer demands (Rice Department, 2016a).

Estimates of rice yield are based on Crop Cutting Experiments (CCE) and farmer interviews which are conducted close to harvesting. In Thailand, CCE is a reliable rice yield survey and estimation method used by the Office of Agricultural Economics (OAE). The main purposes of CCE are to measure rice yield to analyse the current annual statistical data. The CCE method is based on the farmer household, which is dependent on separating villages into irrigated and non-irrigated systems and their expected harvesting time. The CCE method identifies a sample village with three households selected randomly, from which two field sample plots are identified. The CCE process consists of 3 sections: 1) crop cutting survey (cutting all crop production within the sampling frame, i.e. rice stems and grains), 2) dyke survey, and 3) gleaning survey. These consist of measuring wet and dry grain yield over small (e.g. 1 m x 1 m) sampling areas at specific locations, which are then spatially aggregated to estimate yield at (ultimately) provincial scale. However, a limitation of using CCE to estimate yield is that the yield estimates are only available close to harvesting. In contrast, yield estimates earlier in the growing season would be

preferential for crop management and food security purposes. In addition to rice yield, other important biophysical variables include plant density, leaf area index (LAI), spikelet per m^2, and biomass accumulation. The plant density, which influences the seeding rate, is optimised to obtain the maximum yield and affects the kernel dimensions (Alipour Abookheili & Mobasser, 2021; Baloch et al., 2011). The LAI, which is defined as half the green leaf area per unit area (Zheng & Moskal, 2009), is a biophysical parameter that plays an essential role in the crop's photosynthesis and is commonly analysed concerning vegetation foliar cover, biomass, and crop productivity (Wang et al., 2018). Spikelet per unit area is related to number of filled spikelets (Takai et al., 2006). Finally, biomass is related to grain yield via harvest index (HI) (Zhang et al., 2008) and depends on the dry matter partitioning of crop leaves and panicles (Amanullah & Inamullah, 2016; Kondhia, Tabien & Ibrahim, 2015). Biophysical variables are often used to estimate yield either through parameterising crop growth or radiative transfer models or by developing an empirical relationship between the in-situ biophysical variable and remote sensing measurement (i.e. vegetation indices derived from airborne and satellite spectral (Campos-Taberner et al., 2016; Haboudane et al., 2004; Peng et al., 2021). Satellite data are routinely used to derive estimates of vegetation biophysical parameters such as LAI and biomass, and these in turn have been used to estimate rice yield (Clauss et al., 2018; Liu et al., 2015; Peng et al., 2014; Peng et al., 2021; Setiyono et al., 2018).

The analysis conducted in Chapter 3 found that mean minimum temperature, mean maximum temperature and amount of rainfall influence rice productivity. The spatial distribution of rice production is influenced by rainfall patterns, although areas with low rainfall can mitigate this uncertainty using an irrigation system. Photoperiod-sensitive rice varieties are closely related in their structure and dynamics to biophysical variables, with differences in the duration of panicle emergence among photoperiod-sensitive and photoperiod-insensitive varieties (Collinson, Ellis, Summerfield, & Roberts, 1992). The majority of rice varieties grown in the study area are photoperiod-sensitive rice. This chapter focuses on the second research question, which seeks to understand the influences of irrigation systems on rice biophysical characteristics such as LAI, biomass and yield and to investigate the relationship between rice biophysical variables at particular plant growth stages. This is believed to be the first investigation of its kind into the dynamics of rice biophysical characteristics with irrigation usage and rice variety. To meet these aims, field experiments were carried out at 21 irrigated and 7 non-irrigated sites in the Chao Phraya River delta, where measurements of a number of rice biophysical variables were made through the growing season.

4.1 Background of study area

The field sites were located in the Chao Phraya River delta (Figure 4.1), which covers 52,323 square km^2 in central Thailand. This delta comprises 11 provinces and has a tropical monsoon climate, with an average temperature of 33.8°Celsius and annual rainfall of 16,000 mm per year. The cultivated rice area is 164 million ha, producing 756.7 million tonnes of rice annually (OAE, 2017).

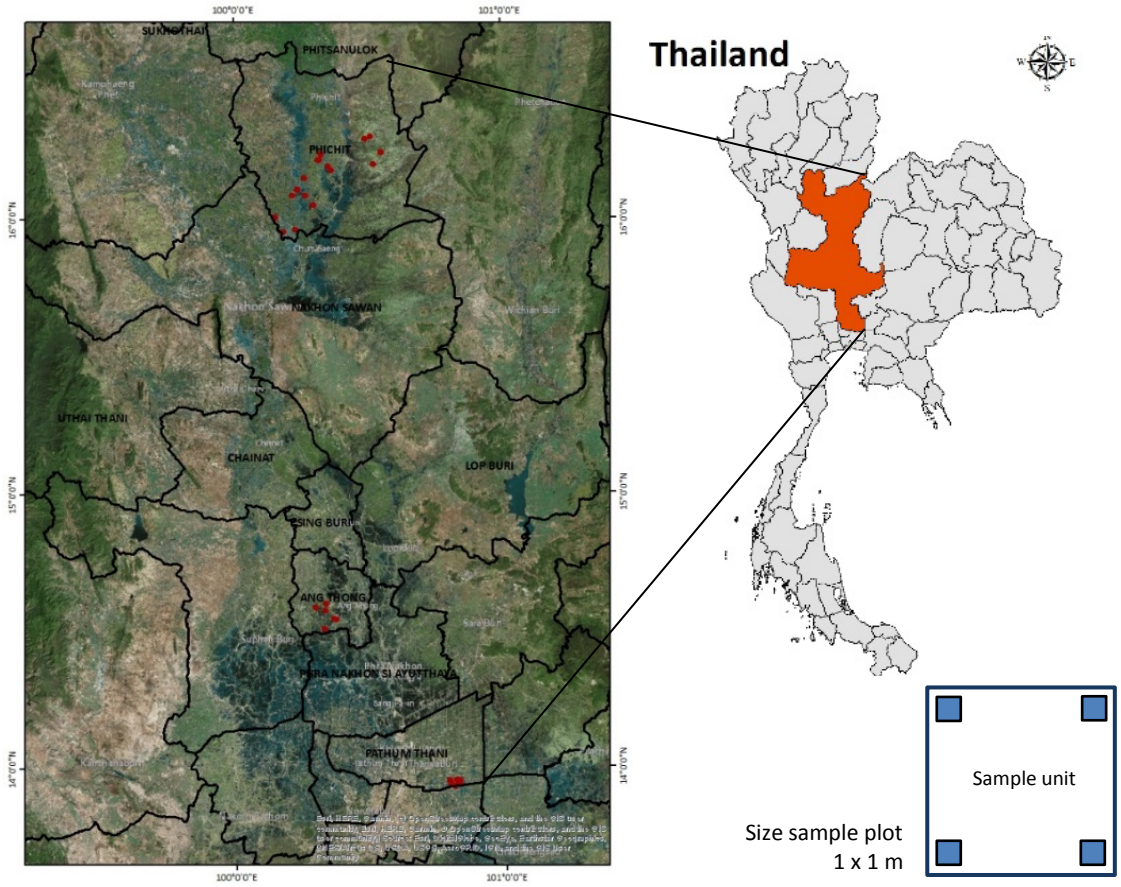

Figure 4.1 The Chao Phraya River delta, comprising 11 provinces in Central Thailand. The red circles on map on the left indicate the locations of the field experiments conducted in 2017.

Figure 4.1 shows the field experiment locations in three representative provinces located in the important rice-cultivated areas in the central region: Phichit (upper delta), Ang Thong (middle delta), and Pathum Thani (lower delta). The field experiments were collected in 28 fields, of which 16 were located in Phichit (Pho Tha Le and Ta Pan Hin amphoe), 6 in Ang Thong (Wisetchaichan amphoe), and 6 in Pathum Thani (Lam Luk Ka amphoe). Phichit contains irrigated and non-irrigated rice cultivation and field surveys were conducted in 9 irrigated and 7 non-irrigated fields. This enabled the impact of irrigation on rice biophysical variables to be assessed through the growing season under similar precipitation and temperature characteristics. However, a key

variable that influences rice biophysical development throughout the growing season is rice variety, which has been shown to increase yield by 26-40% and differs from rice ecosystems (Anisuzzaman, Kader, Ali, Haque, & Halder, 2016; Chhogyel & Bajgai, 2015).

Using the dataset described in Chapter 3, the annual rice productivity between 1981-2015 is shown in Figure 4.2 for each province studied in this chapter.

a) Average rice yield

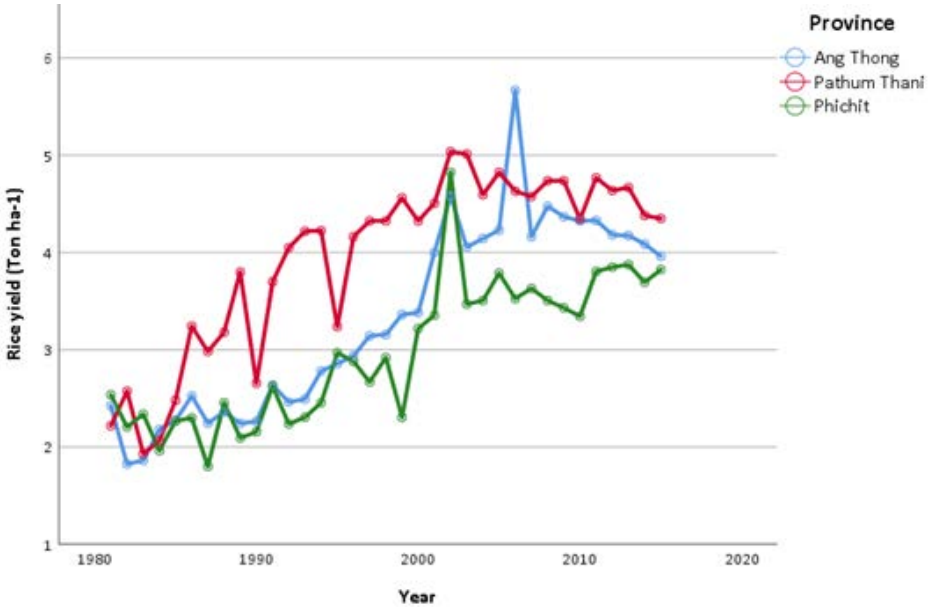

b) Average rice production

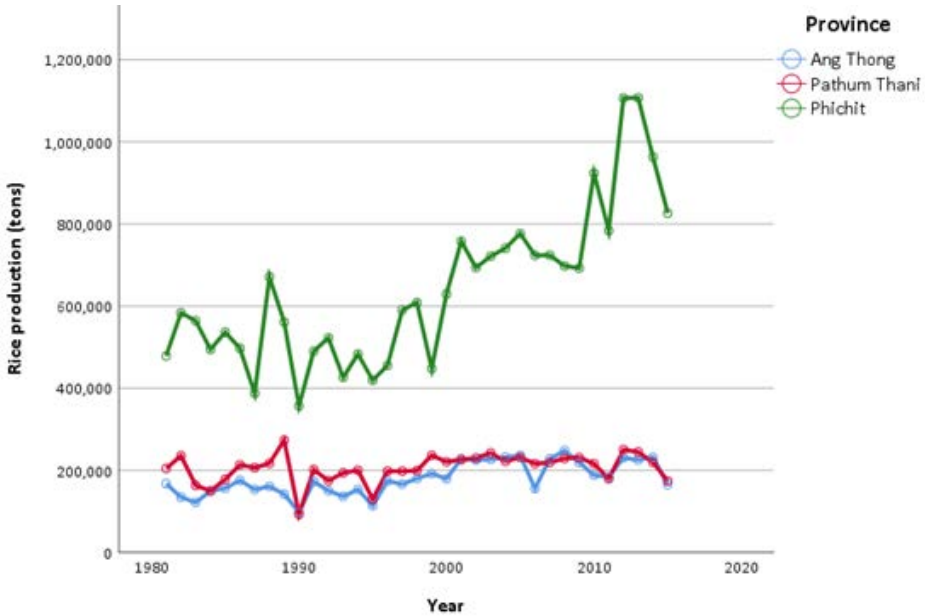

Figure 4.2 Time-series of rice yield and production during 1981-2015 for Phichit, Ang Thong, and Pathum Thani. a) Average rice yield and b) Average rice production.

Figure 4.2 illustrates the interannual variation in rice productivity and yield between 1981 and 2015 for Pathum Thani, Ang Thong, and Phichit, which have average rice yields of 3.9, 3.3, and 2.9

tonnes/ha, respectively. Rice yield has steadily increased over time, whereas total rice production (Figure 4.2b) has remained reasonably constant in Pathum Thani and Ang Thong. Rice cultivation in Pathum Thani, which has the highest yield, is predominantly (>25%) carried out in irrigated fields maximising agricultural effectiveness. The average rice production in Phichit is the highest, where 70.3% of agriculture is rice cultivation. However, the yield is the lowest which may result from rice cultivation being under both irrigated (23.3%) and non-irrigated (76.7%) land management. In Ang Thong province, rice cultivation is largely irrigated; although the yield was low between 1981-2000, it improved markedly after this to become comparable to that found in Pathum Thani.

Table 4.1 Characteristics of rice varieties planted in the study area (Rice Department, 2017).

Rice variety	Duration (days)	Dominant characteristics	Rice seed (mm)	Yield (tonnes/ha)	Planting area
RD31	111 (flooding) 118 (transplanting)	- Straight clumping and resistant for planthopper - Resistant to bacterial leaf blight disease	10.4x2.6x2 7.4x2.1x1.8	4.6 (flooding) 4.7 (transplanting)	Irrigated area in middle region
RD41	105	- Straight clumping and high grain when milling - Resistant to brown planthopper and blast disease	10.4x2.5x2 7.7x2.2x1.8	4.5	Irrigated area in lower north region
RD47	104-107 (flooding) 112 (transplanting)	- Strength stem, flag leaves broadleaf, long-grain, and resistant for planthopper and leaf blight disease - High grain quality (100% milled rice)	10.4x2.5x2 7.9x2.1x1.8	5	Irrigated area in lower north region
RD49	102-107	- Straight clumping and high density of rice grain - High grain quality (mill to 100% rice seeds)		4.6	Irrigated area
RD57	107-110 (flooding) 117-120 (transplanting)	- Straight clumping and leaves and strong stem and	10.8x2.5x2.1 7.4x2.2x1.9 7x2x1.8	4.5	Irrigated area

Rice variety	Duration (days)	Dominant characteristics	Rice seed (mm)	Yield (tonnes/ha)	Planting area
RD57 (Cont.)		medium rice grain density - Easily falling grain			
RD61	87	- Straight clumping and easily falling grain - Resistant to brown and white-backed planthopper		6.3	Irrigated area in lower north and middle region

It is essential to highlight the role of rice varieties in enhancing yield when assessing temporal trends in rice production. The intensive cropping and continuous planting in a few rice varieties lead to severe biotic stress and pest outbreaks (Berga & Tamb, 2012; Kumar et al., 2022). Between 1970 and the present, over 50 varieties of rice have been developed to be a pest- and diseases-tolerant (Leung et al., 2003; Wang et al., 2005). The traditional rice variety has developed the modern high-yield varieties (HYVs) for yield improvement in both the wet and dry seasons (Chaturvedi, 2005; Cheng et al., 2007; Qingquan, 2002). Table 4.1 lists the main rice varieties grown in the study area, their dominant characteristics, and their typical yield. All varieties are designed for irrigated areas, whereas some varieties, such as KDML105 (or jasmine rice) and RD6, are designed for non-irrigated cultivation (Rice Department, 2017). Rice varieties were developed to be resistant to insect pests such as the planthopper and diseases, which during severe outbreaks can be responsible for losses of up to 4 tonnes/ha (Heong et al., 2015) and are designed to increase yield potential by rice genetic improvement. It is clear from Table 4.1 that yield, and the length of the growing season can differ by a factor of 1.4 as a function of rice variety, which will directly impact the final provincial-level yield estimates. The table also highlights the influence of the rice planting method (i.e. flooding or transplanting), which influences the growing season length and which is influenced by precipitation patterns.

4.2 Methodology

4.2.1 Primary data

The primary data used in this chapter were collected during field experiments carried out during the wet season (May to October) in 2017, covering the main growth stages: seeding (in different cultural practices- both direct sowing and transplanting), tillering, panicle, flowering, and harvesting (Figure 4.3). The field surveys involved interviewing farmers to gain information on

their planting date, rice variety, fertiliser usage, post-harvesting yield, and irrigation location. The latter was then compared to irrigation boundaries derived from the Royal Irrigation Department (RID), which was used to identify sample site locations in irrigated or non-irrigated areas initially. In addition to interviewing farmers, several rice biophysical variables were measured throughout the growing season in large and homogenous fields. The latter requirements were to ensure sufficient satellite pixels fell within the fields with an average paddy size of 0.61, 0.86, and 2.9 ha in Phichit, Ang Thong, and Pathum Thani, respectively.

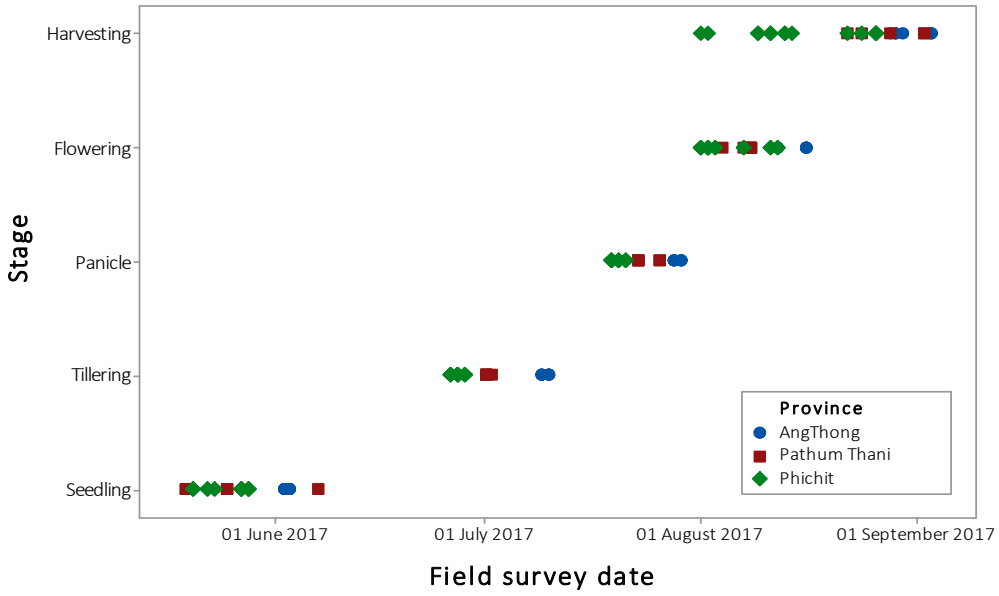

Figure 4.3 Field survey dates in Phichit, Ang Thong and Pathum Thani.

4.2.2 Research methodology

This chapter aims to investigate the variation in rice biophysical variables through the growing season from the seeding to harvesting stage.

4.2.2.1 Definition of rice phenology and sampling units

The field surveys were carried out throughout the growing season to measure rice biophysical variables at different growth stages. This study adopted the standardised scale of rice growth, 'Biologische Bundesanstalt, Bundessortenamt and CHemische Industrie (BBCH)', from the International Rice Research Institute (IRRI), which is measured phenological development information and relevance with satellite monitoring (Yuzugullu, Erten, & Hajnsek, 2015). Rice cultivation in Thailand can be single, double, or triple cropped, which differs among regions. The rice phenological cycle varies in length from 83 to 117 days, although the exact duration depends on rice variety (Table 4.1) and environment (Miranda et al., 2009; Li et al., 2018). Therefore, one of the criteria used in selecting the field sites was that the planting date among the paddy fields

enabled biophysical measurements to be made in all five growth stages. These growth stages are seeding (1-20 days), tillering (21-40 days), panicle (41-70 days), flowering (71-90 days), and harvesting (90-120 days), as shown in Table 4.2.

To ensure that the field sites were representative of rice cultivation in the region, it was necessary to exclude sample sites where hybrid rice varieties were grown that have short growing seasons to avoiding floods and for higher yields, and where rice was uprooted (called 'lodging') due to the occurrence of severe weather before harvesting. Six sample sites were found to be either lodging (PC6 and PC8), flooding (AT6), or to contain a hybrid rice variety (PC4, PC16, and PT6); all of which distorted the length of the growing season and were therefore excluded from our analysis.

Table 4.2 Rice phenological stages

Growth phase	Study stage	Example of paddy	Name
Vegetative	Seeding		Germination
			Leaf development
	Tillering		Tillering
			Stem elongation
			Booting
Reproductive	Panicle		Heading
	Flowering		Flowering
Maturity			Development of grain
			Ripening
	Harvesting		Senescence
Transplanting			Transplanting, recovery (rice)

4.2.2.2 Measurement of rice biophysical variables

At each field site, several measurements were made, including water depth, planting density, plant height, panicle length, above and below canopy Photosynthetically Active Radiation (PAR), canopy leaf area index (LAI), leaf chlorophyll content, wet and dry biomass, and post-harvest yield. The measurements at each field varied depending on the phenological stage, as indicated in Figure 4.4, with the measurements made listed in each corner.

a) Seeding (15 days) | b) Tillering (35 days) | c) Panicle (65 days) | d) Flowering (85 days) | e) Harvesting (90-120 days)

Seeding	Tillering	Panicle	Flowering	Harvesting
- General data on planting - Stem density - Water depth	- Stem density - Water depth - Height - PAR/LAI - Chlorophyll content	- Stem density - Water depth - Height - Panicle length (if) - PAR/LAI - Chlorophyll content - Biomass (if)	- Stem density - Water depth - Height - Panicle length - PAR/LAI - Chlorophyll content - Biomass	- Stem density - Water depth - Height - Panicle length - PAR/LAI - Chlorophyll content - Biomass - Yield - Moisture content

Figure 4.4 Field and plant measurements made at each growth stages.

In the seeding stage, measurements of stem density, water depth, and where possible, leaf chlorophyll content were made. In the remaining growth stages, measurements of stem density, water depth, height, above and below PAR, LAI, chlorophyll content and biomass were obtained as the canopy was more developed (Figure 4.4).

Rice height was measured to quantify the growth rate; it was measured from 3 randomly selected plants and defined as the height from the soil or water surface to the tip of the highest leaf. Water depth was measured from the soil to the water surface at two locations per sample plot for averaging. Due to variations in the paddy field surface topography, the water depth varies spatially and to capture this, several measurements are required. The water depth during the early growth stage depends on the planting method and influences the remotely sensed radiative measurements, mainly when the canopy is less dense. The PAR, which covers the visible spectrum (400-700 nm) where plants absorb solar energy for photosynthesis, was measured by taking ceptometer measurements using an AccuPAR instrument ~5 cm above the canopy and ~5 cm above the soil or water surface. The average PAR, measured under diffuse sky conditions where possible to avoid underestimation (Fang et al., 2014), was calculated for each field using 4 or 5 measurements made at each sampling location, of which were 4 in each paddy field (a totally 16-20 measurements per field). The PAR measurements were then converted to leaf area index (LAI) using the approach described by Samanta et al. (2019). The fraction of photosynthetically active radiation transmitted through the crop canopy is related to the leaf distribution and the leaf area within the rice canopy. The PAR measurements were used to calculate the LAI using the approach

proposed by Norman-Jarvis (Norman, 1974). The extinction coefficient (K) describes the proportion of radiation absorbed by the canopy at a specific solar zenith angle (θ) and leaf angle distribution (x).

$$K = \frac{(x^2 + tan^2\, q)^{1/2}}{x + 1.744\,(x + 1.182)^{-0.733}} \qquad \text{Equation 4.1}$$

The leaf angle distribution is a key canopy structural parameter that influences the radiative (reflectance and transmittance) properties of a canopy, and is often assumed to be spherical (Vicari, Pisek, & Disney, 2019). Under this case, K simplifies to:

$$K = \frac{1}{2\cos q} \qquad \text{Equation 4.2}$$

The leaf area index (L), which describes the one-sided green leaf area per unit ground surface area ($m^2\ m^{-2}$), is then calculated via:

$$L = \frac{\left|\left(1 - \frac{1}{2k}\right)\right| b - 1 \ln \tau}{A(1 - 0.47\,b)} \qquad \text{Equation 4.3}$$

where fb (beam fraction) is the ratio of the above and below canopy PAR, τ is the probability that a ray will penetrate the canopy, and A is leaf absorptivity, which is set to 0.9 following the approach of conversion factor in healthy green foliage (Barclay & Goodman, 2000).

a) Above PAR measurement

b) Below PAR measurement

Figure 4.5 Above (a) and below (b) canopy PAR measurement in the flowering stage.

Measurements of leaf chlorophyll content were made using a MultispeQ chlorophyll meter for 3 - 4 plants per sample plot (12-16 measurements in total). The MultispeQ indirectly estimates chlorophyll concentration using a standardised calibration and connecting with the PhotosynQ network (Kuhlgert et al., 2016). Finally, the wet and dry plant biomass, comprising of the total plant biomass, leaf-stem, and grain biomass, was measured through destructive sampling conducted over a 1 m x 1 m area where the biomass was harvested and measured immediately to prevent moisture loss. After removal, the wet biomass weight was separately measured for the rice stems and grains (Figure 4.6). For the dry biomass measurements, the moisture was removed through oven drying prior to conducting correlation analysis with other rice biophysical variables or remotely sensed data (Cheng et al.,2017). This process was repeated for each paddy field individually.

Figure 4.6 Destructive biomass measurement of a 1 m x 1 m sample plot.

The rice yield estimates were determined using the CCE method, which is used to estimate rice yield per unit area at district and regional levels by government agencies (FAO, n.d.). The rice stems and grains were dried separately at 80° Celsius for 48 hours and then weighed to determine the dry weight of the leaf, stem, and grain materials. The measurement locations in each field were recorded using a handheld GPS (WGS 84, Zone 47North) to locate them in the satellite data. The measured rice biophysical data was averaged at each of the four measurement locations in each field. Those where the standard deviation (S.D.) was > +/- 1 S.D. were assumed to be in error and removed, and the average recalculated.

Pearson's correlation coefficient was used to assess the relationship between the rice biophysical variables as a function of both the individual growth stage and overall growth stages (P = 0.05). The analysis was further stratified according to irrigated and non-irrigated methods. Finally, an analysis of the correlation between the rice biophysical variables and rice yield is carried out since

this research aims to develop a method which facilitates yield estimation using remotely-sensed data (discussed in Chapter 5).

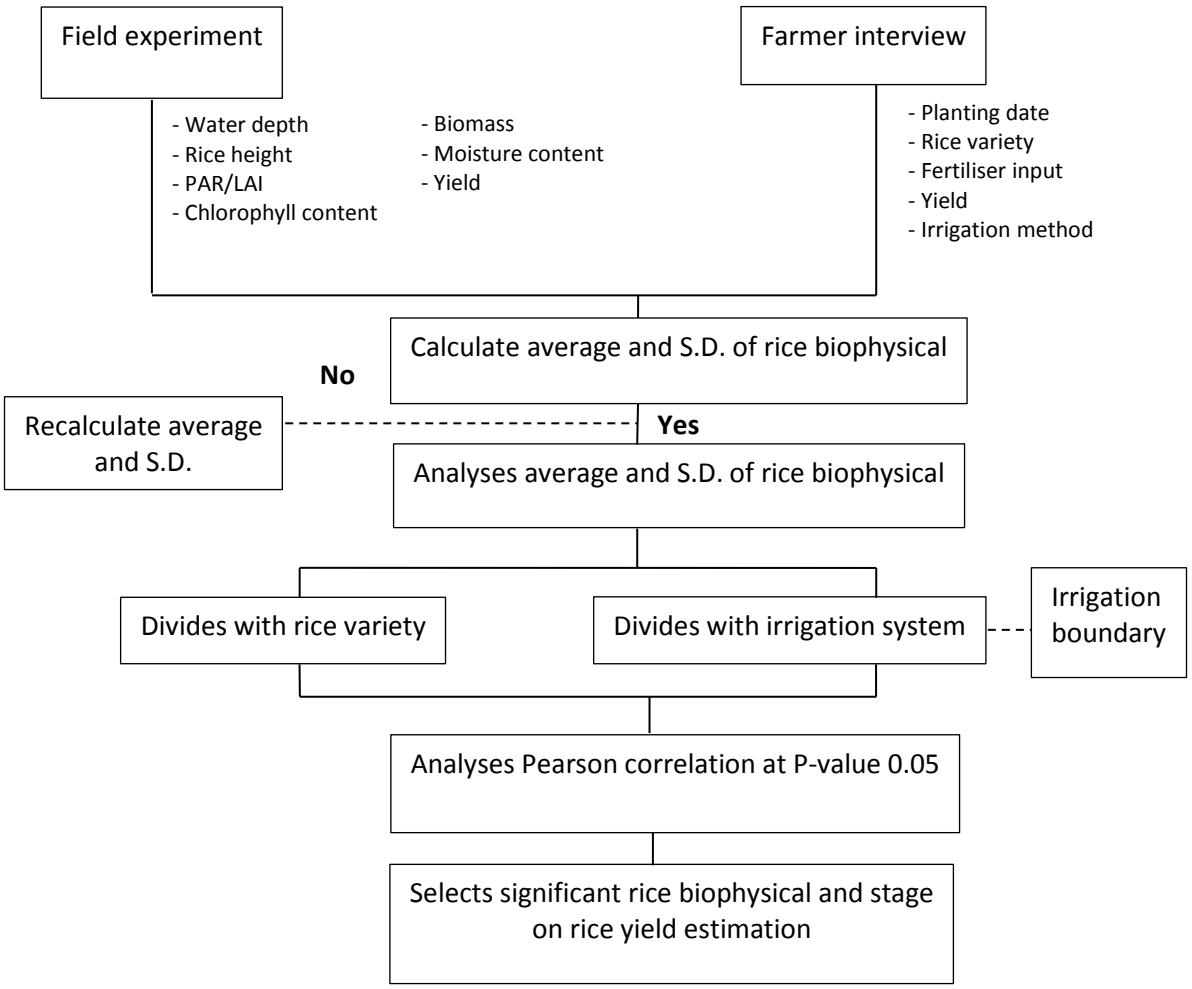

Figure 4.7 Flowchart illustrating the analysis.

4.3 Results

4.3.1 Rice planting characteristics

In the study area, the fields sampled contained eight main photoperiod-sensitive rice varieties (Figure 4.8) and one photoperiod sensitive variety (Khao Dawk Mali105 or called HomMali105). One characteristic of the HomMali105 variety is its long growing period of 115 - 120 days.

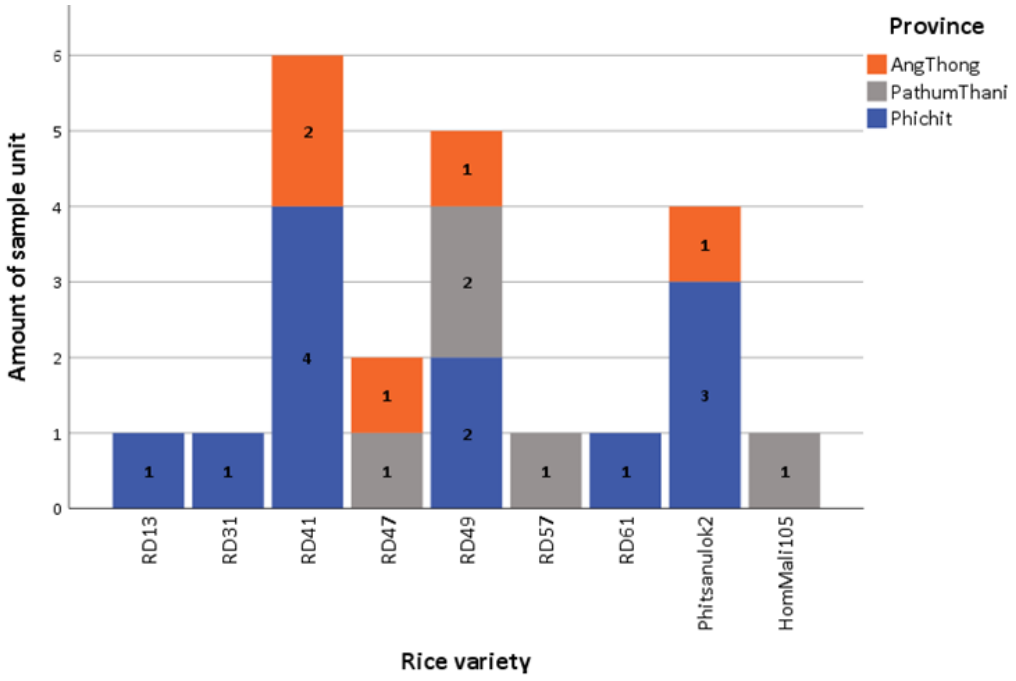

Figure 4.8 Rice varieties in study area: Phichit (blue), Ang Thong (orange), and Pathum Thani (grey).

As evident from Figure 4.8, many rice varieties are grown in irrigated and non-irrigated fields. Phichit is the only province that contains both irrigated and non-irrigated areas, where most (6) field sites were irrigated and contain the RD41 (6) rice variety (see Table 4.1 for more detail). However, the non-irrigated areas contained a more significant number of rice varieties (6). Ang Thong province contained four rice varieties in five sample fields, whilst in Pathum Thani there were four rice varieties across five sample fields. In all three provinces, the planting date varied between the 4th and 24th of May (see Table 4.3).

Table 4.3 Planting date of sampling fields in Phichit (PC), Ang Thong (AT), and Pathum Thani (PT).

Sample unit	Planting date	Irrigation system	Rice variety	Field size (Ha)
PC1	8 May 2017	Irrigated	RD41	0.61
PC2	16 May 2017	Irrigated	Phitsanulok2	0.22
PC3	5 May 2017	Irrigated	RD41	0.93
PC5	10 May 2017	Irrigated	RD41	0.63
PC7	12 May 2017	Irrigated	RD61	0.84
PC9	12 May 2017	Non-Irrigated	Phitsanulok2	0.25
PC10	4 May 2017	Non-Irrigated	Phitsanulok2	0.61
PC11	10 May 2017	Non-Irrigated	RD49	0.35
PC12	18 May 2017	Non-Irrigated	RD49	0.44
PC13	5 May 2017	Irrigated	RD41	0.25
PC14	18 May 2017	Non-Irrigated	RD13	1.52

Sample unit	Planting date	Irrigation system	Rice variety	Field size (Ha)
PC15	21 May 2017	Non-Irrigated	RD31	0.67
AT1	24 May 2017	Irrigated	RD41	0.95
AT2	22 May 2017	Irrigated	Phitsanulok2	1.15
AT3	24 May 2017	Irrigated	RD41	1.10
AT4	24 May 2017	Irrigated	RD49	0.65
AT5	20 May 2017	Irrigated	RD47	0.46
PT1	8 May 2017	Irrigated	HomMali105	2.19
PT2	8 May 2017	Irrigated	RD47	0.98
PT3	6 May 2017	Irrigated	RD49	1.78
PT4	20 May 2017	Irrigated	RD49	8.09
PT5	4 May 2017	Irrigated	RD57	1.46
Average field size in irrigated area (ha)				**1.39**
Average field size in non-irrigated area (ha)				**0.64**

Table 4.3 illustrates the average planting date in Phichit, Ang Thong, and Pathum Thani was 11th, 22nd and 9th May, respectively. In Phichit, the average of planting date varied by four days on average between irrigated and non-irrigated areas. The average field sizes in Phichit, Ang Thong, and Pathum Thani were 0.61, 0.86, and 2.9 ha, respectively, while irrigated areas (1.39 ha) were on average larger than non-irrigated areas (0.64 ha). The sample field sites contained two rice cropping patterns, direct seeding and transplanting. Direct seeding involves planting rice seeds directly into the paddy, either by ploughing or harrowing depending on the level of land preparation. Most farmers prepare pre-germinated seeds by soaking the rice seeds for one day, incubating them for two days, and then sowing them into the flooded or mud field ('*wet direct seeding'*), while some sow into dry soil ('*dry direct seeding'*). Transplanting involves soaking rice seeds for 24 hours until incubating for 48 hours until root emergence, then sowing the rice sprouts into dry or wet paddy fields. Irrespective of the planting method, rice sowing will either be conducted manually or by machine, which influences the stem density. In the study area, most farmers adopted direct seeding in well-puddled seedbeds or shallow standing water. The variation in agricultural practices employed in the study area is illustrated in Figure 4.9.

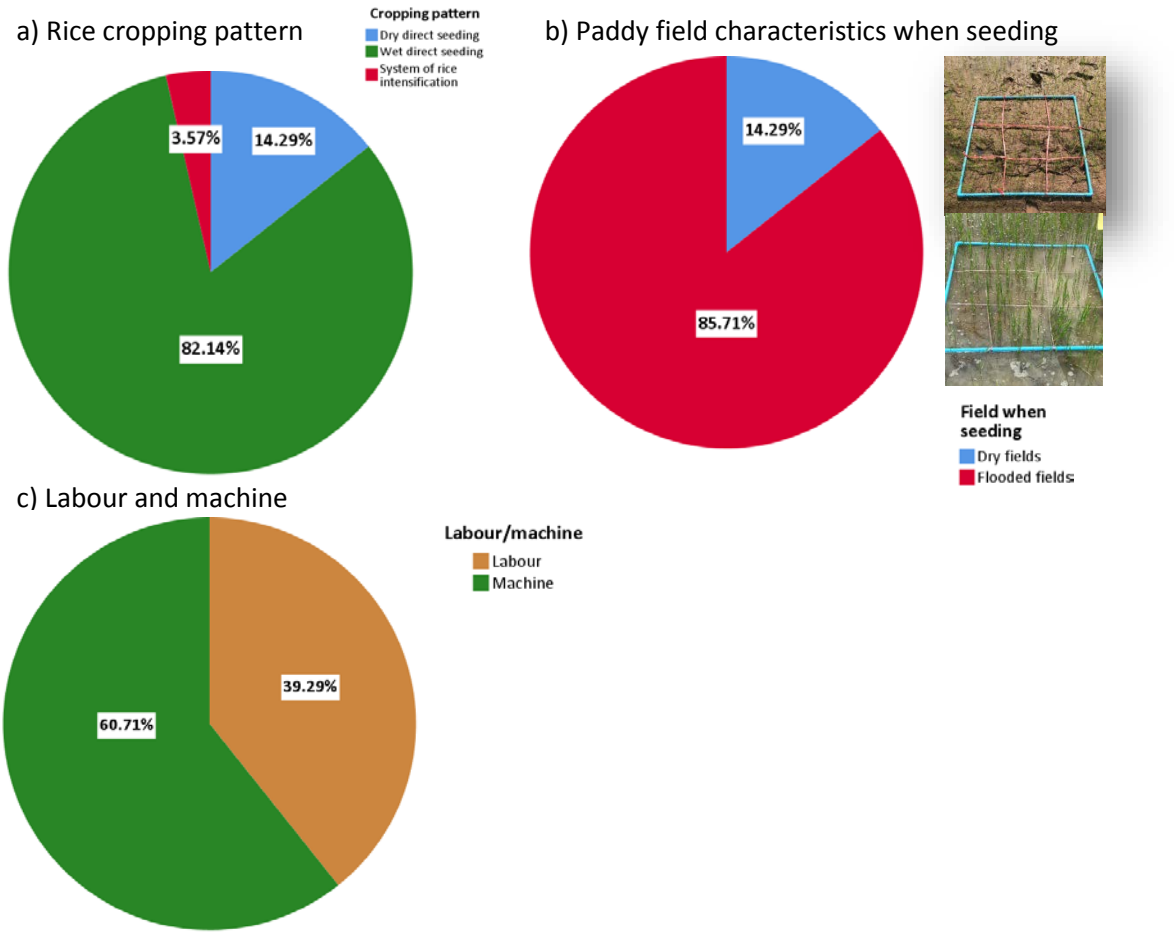

Figure 4.9 Rice cropping pattern in study area derived from farmer interviews.

Figure 4.9 indicates that the majority (82%) of the sampled fields utilised direct wet seeding, and therefore most fields are flooded (85%). Mechanisation, applied to enhance agricultural productivity in pre- or post-harvest, accounts for 50%, 66%, and 83% of rice planting in Phichit, Ang Thong, and Pathum Thani, respectively.

Most of the measurements collected in the field sites are rice biophysical variables (e.g. stem density, height, panicle length, PAR /LAI, chlorophyll content, wet and dry biomass, moisture content and yield), although measurements of water depth were also made, as water is released into the paddy fields for rice germination and then drained at the start of the panicle stage. Water depth was measured as it provides the background signal in remotely sensed measurements in the early growth stages and influences the amount of vegetative material visible above the water surface. The presence of water influences optical remote sensing measurements by reducing reflectance by up to 28% depending on view zenith angle due to changes in the surface anisotropy (Sun et al., 2017).

Temporal variations of water depth and rice height are analysed and presented in Figure 4.10 and Table 4.4. The average rice height in the tillering, panicle, flowering, and harvesting stages was 49.4, 80.9, 97.2 and 98.9 cm, respectively, and demonstrate the rapid development of height in the panicle stage. The average rice height in Pathum Thani in the harvesting stage was higher than in other provinces due to the use of the HomMali105 variety, which is taller than others. When assessed as a function of the irrigation method, the difference in rice height between irrigated and non-irrigated rice increases by 0.64, 1.22, 3.48, and 6.54 cm in the tillering, panicle, flowering, and harvesting stages, respectively. The average water depth in the seeding, tillering, panicle, flowering, and harvesting stages are 2.83, 4.69, 4.45, 3.66, and 1.5 cm, respectively. Surprisingly, the water depth difference between irrigated area and non-irrigated area reveals only minor variation of between 0.5 – 2.5 cm through the growing season. However, there is no water depth in non-irrigated areas during the flowering and harvesting stage. The slight difference in water depth is partly due to the field sites being in regions where precipitation is high (see Chapter 3, Figure 3.1).

a) Overall and differences in irrigation systems

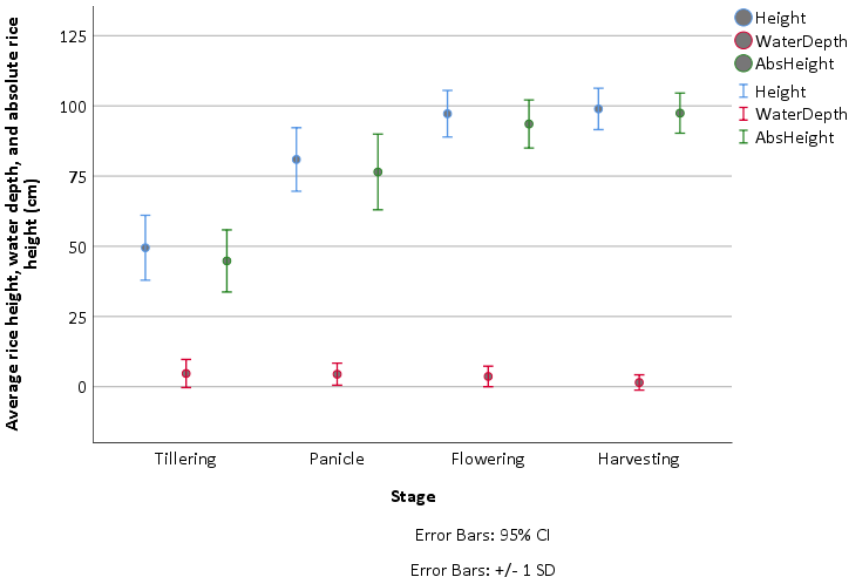

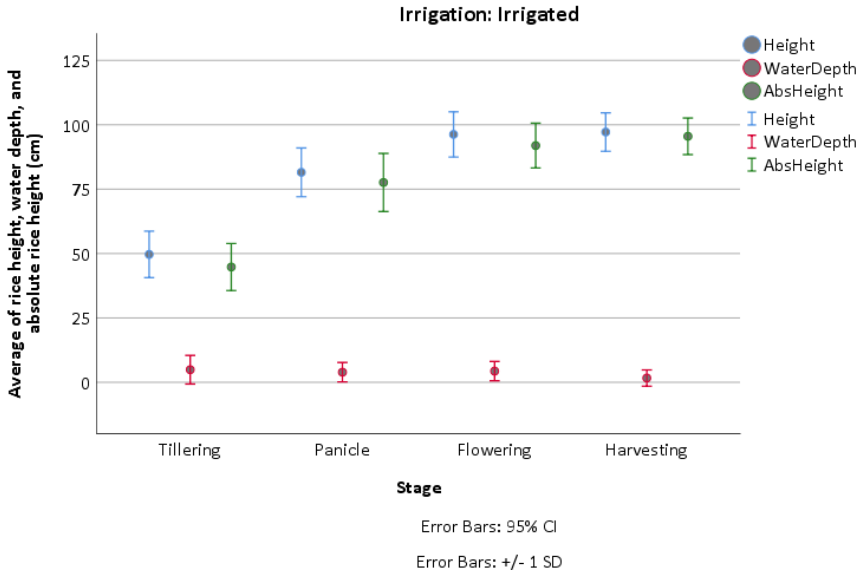
Irrigation: Irrigated
Average of rice height, water depth, and absolute rice height (cm)
125
100
75
50
25
0
Tillering
Panicle
Flowering
Harvesting
Stage
Height
WaterDepth
AbsHeight
Height
WaterDepth
AbsHeight
Error Bars: 95% CI
Error Bars: +/- 1 SD

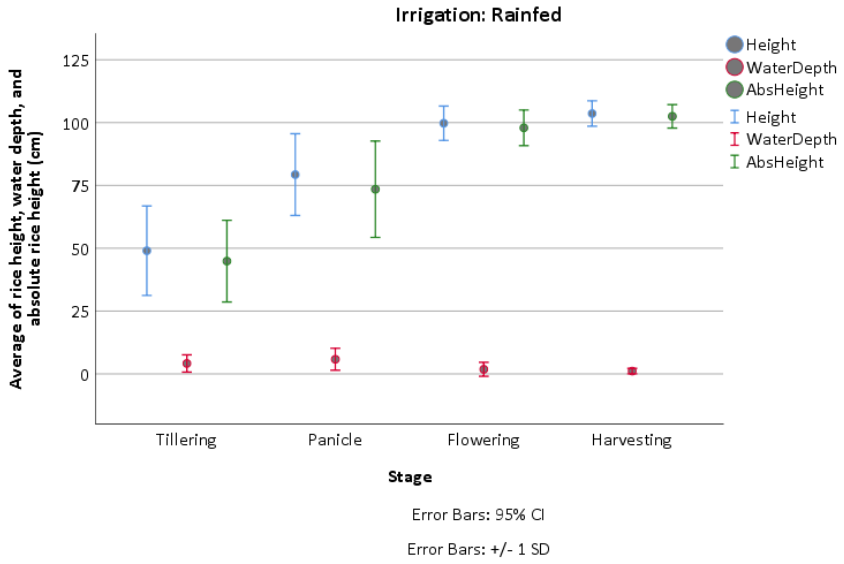
Irrigation: Rainfed
Average of rice height, water depth, and absolute rice height (cm)
125
100
75
50
25
0
Tillering
Panicle
Flowering
Harvesting
Stage
Height
WaterDepth
AbsHeight
Height
WaterDepth
AbsHeight
Error Bars: 95% CI
Error Bars: +/- 1 SD

b) Phichit

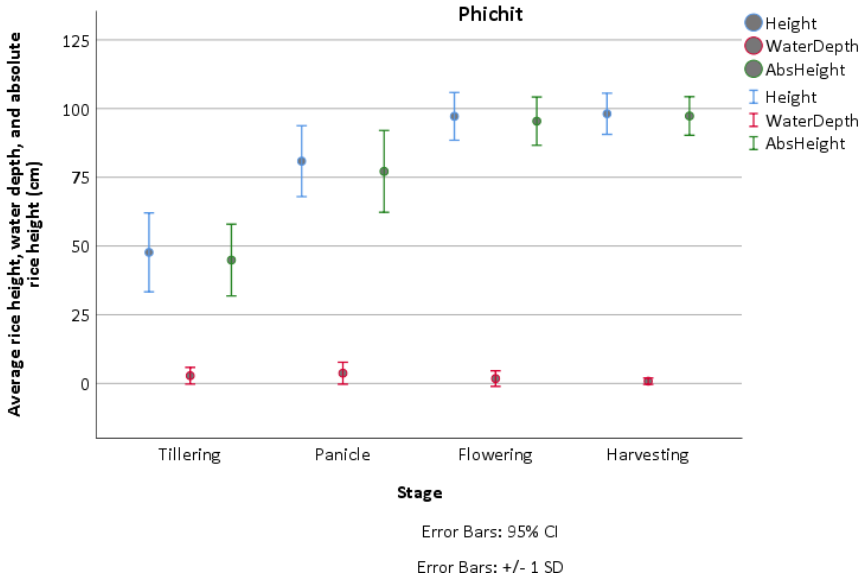
Phichit
Average rice height, water depth, and absolute rice height (cm)
125
100
75
50
25
0
Tillering
Panicle
Flowering
Harvesting
Stage
Height
WaterDepth
AbsHeight
Height
WaterDepth
AbsHeight
Error Bars: 95% CI
Error Bars: +/- 1 SD

c) Ang Thong

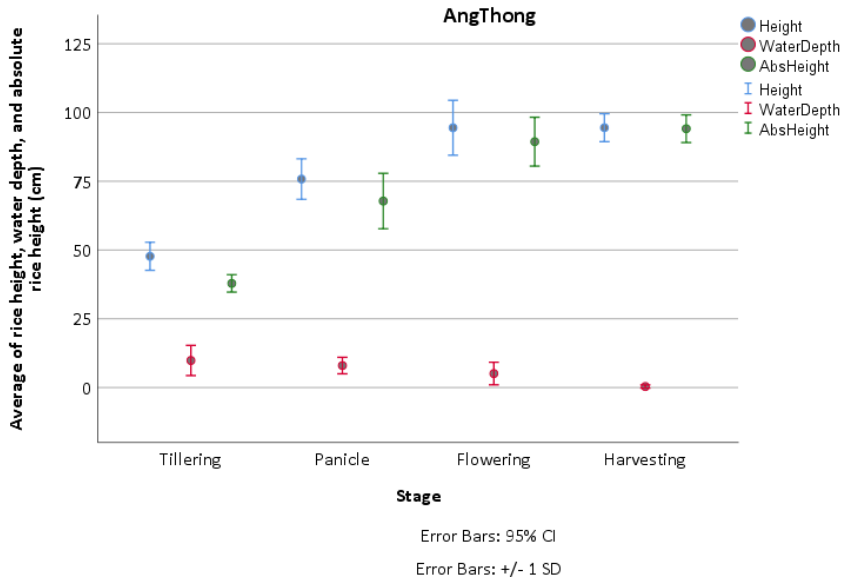

d) Pathum Thani

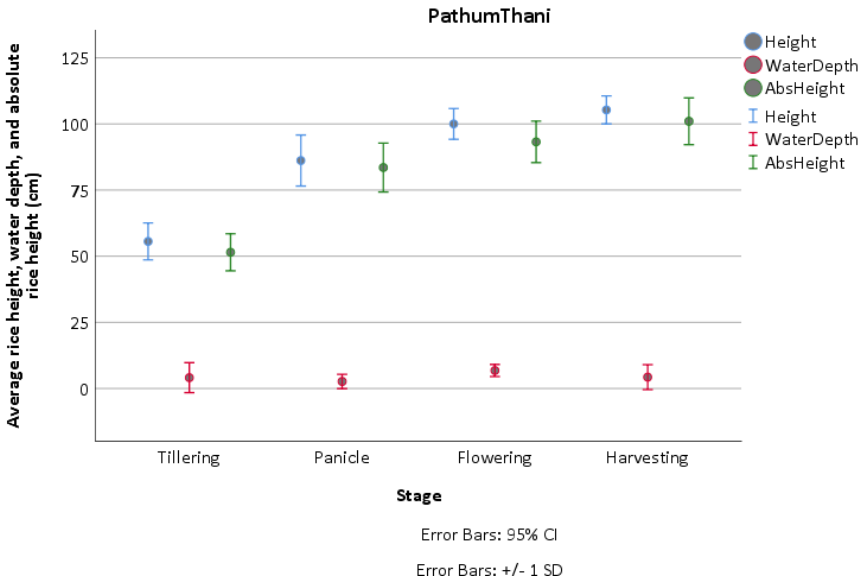

Figure 4.10 Average rice height (cm), water depth (cm), and height difference between rice height and water depth (cm). a) Overall provinces and different irrigation system, b) Phichit, c) Ang Thong, and d) Pathum Thani.

Table 4.4 Summary of rice height, water depth, and difference in rice height and water depth at different rice phenological stages.

Irrigation system	Seeding	Tillering			Panicle			Flowering			Harvesting		
	Water depth (cm)	Rice height (cm)	Water depth (cm)	Absolute height (cm)	Rice height (cm)	Water depth (cm)	Absolute height (cm)	Rice height (cm)	Water depth (cm)	Absolute height (cm)	Rice height (cm)	Water depth (cm)	Absolute height (cm)
Overall													
Mean	2.83	49.48	4.69	44.79	80.92	4.45	76.47	97.2	3.66	93.54	98.91	1.5	97.41
S.D.	0.85	2.47	1.07	2.36	2.41	0.84	2.87	1.77	0.78	1.83	1.57	0.58	1.52
Irrigated													
Mean	2.44	49.66	4.89	44.77	81.52	3.94	77.58	96.25	4.34	91.91	97.16	1.65	95.51
S.D.	0.9	2.25	1.39	2.28	2.37	0.94	2.82	2.2	0.94	2.17	1.86	0.79	1.77
Non-irrigated													
Mean	3.87	49.02	4.15	44.87	79.3	5.82	73.48	99.73	1.82	97.91	103.6	1.13	102.47
S.D.	2.11	7.27	1.41	6.63	6.64	1.78	7.82	2.79	1.13	2.89	2.07	0.44	1.9

4.3.2 Rice biophysical variable measurements

4.3.2.1 Stem density

Stem density influences the competition between rice plants and, along with the rice height and variety, can influence rice yield through competition for sunlight (Liu et al., 2017; Phan et al., 2017). Therefore, the appropriate method of determining plant population is to manually count total number of rice stems. The number of rice stems per unit area (1 m x 1 m) was measured at each growth stage using a quadrat divided into nine equal areas (Figure 4.9), with the inside diameter of 33.3 cm x 33.3 cm per small grid, as shown in Figure 4.11.

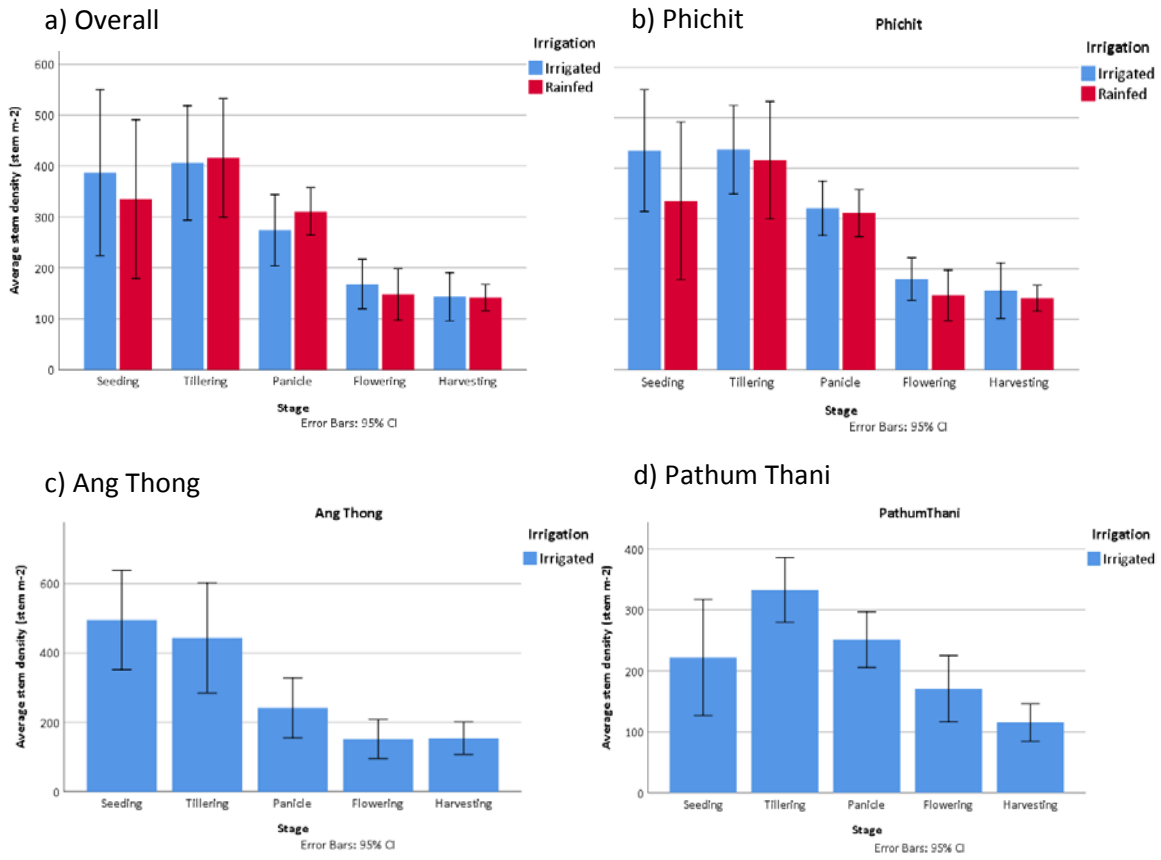

Figure 4.11 Rice stems density in all provinces (a), Phichit (b), Ang Thong (c), and Pathum Thani (d).

Stem densities are most remarkable in the seeding and panicle stage and vary between 250 and 500 stems m^{-2}, which reduces considerably to the harvesting stage (120 -150 stems m^{-2}). Stem density is higher in irrigated than the non-irrigated areas in most phenological stages, but the difference is reduced in the seeding stage to ~ 50 stems m^{-2}. The results indicate that irrigated areas have higher rice stem density, although it is yet to be seen how this translates into other biophysical parameters. The dramatic decrease in stem density between the tillering and harvesting stages is due to the development of flag leaves or uppermost leaves in the grain-filling

stage, which increases the competition for light between plants and ultimately reduces the number of plants (Whaley et al., 2000).

4.3.2.2 Dynamics of photosynthetically active radiation (PAR) and leaf area index (LAI)

The leaf area index (LAI) is an important variable in ecosystem function which is related to plant photosynthesis, respiration, and transpiration of crops (Gower, Kucharik, & Norman, 1999) and characterises the amount of green leaf material within the canopy per unit ground area (1 m x 1 m). It is now routinely estimated using remotely sensed data and is an essential climate variable (ECV). Furthermore, the LAI is a crucial parameter in agronomic research that is used for crop growth monitoring (Ali et al., 2020; Daniela Stroppiana et al., 2006) and dynamic simulation between water and nitrogen diagnosis in different irrigation system (Adeluyi et al., 2021; Liu et al., 2018). Estimates of LAI were derived using AccuPAR indirect optical measurements (SunScan ceptometer), which measure the canopy gap fraction or transmittance. Using the ceptometer, five reading were made under the canopy and one above the canopy, which measures the incident radiation (Casa, Upreti, & Pelosi, 2019). The LAI is derived from the PAR measurements using Equations 4.1-4.3 and measured from the tillering to harvesting stages (Table 4.5).

Table 4.5 LAI converted from PAR measurement.

Irrigation system	Statistic	LAI (m^2 m^{-2})			
		Tillering	Panicle	Flowering	Harvest
Overall	Average	2.36	3.65	4.3	3.89
	S.D.	0.16	0.23	0.23	0.19
Irrigated	Average	2.34	3.55	4.22	3.86
	S.D.	0.18	0.24	0.28	0.21
Non-irrigated	Average	2.39	3.93	4.53	3.98
	S.D.	0.37	0.58	0.41	0.43

Across all sites the LAI peaked in the flowering stage with an average LAI of 4.3 m^2 m^{-2} in all sites and 4.22 and 4.53 m^2 m^{-2} in irrigated and non-irrigated areas, respectively. The significant increase in LAI in the flowering stage is due to the production of flag leaves occurring in the transition from crop growth to grain production through their increased photosynthetic capacity (Acevedo-Siaca, Coe, Quick, & Long, 2021). The LAI in non-irrigated areas is only marginally higher than that found in irrigated areas, which also typically has a more significant standard deviation. It should be noted that integrated within the results shown in Table 4.5 is the influence of rice variety and their differing structural characteristics. This is illustrated in Figure 4.12, which shows the temporal dynamics of LAI as a function of the rice variety.

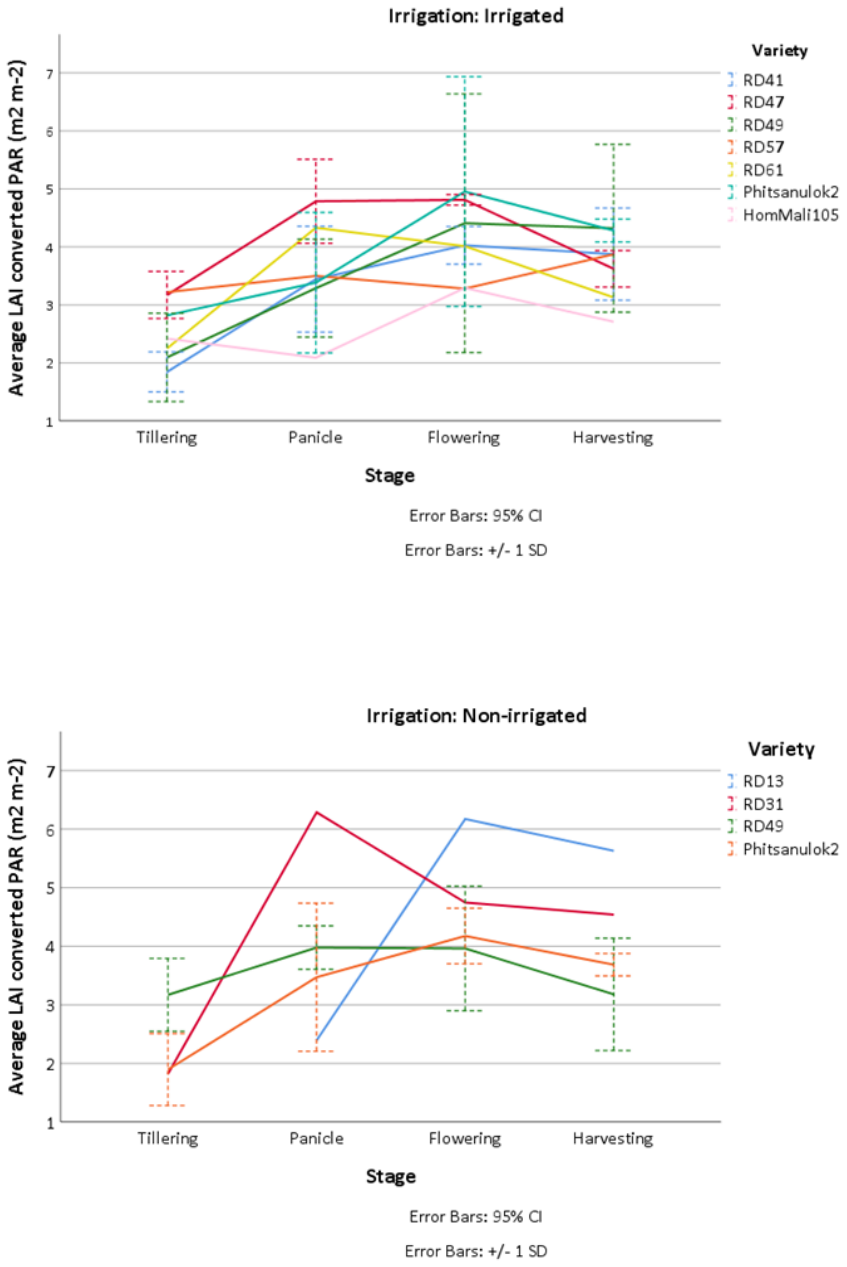

Figure 4.12 PAR-derived LAI for all field sites highlighting the influence of rice variety on the magnitude and seasonal evolution of LAI.

It is evident from Figure 4.12 that rice variety influences both LAI magnitude and its temporal dynamics, which has clear implications for estimating LAI using satellite observations. Overall field sites, the average LAI in non-irrigated areas was higher (3.7 m^2 m^{-2}) than in irrigated areas (3.55 m^2 m^{-2}). In the irrigated area, the RD47 rice variety LAI peaks in the panicle stage whilst the RD41 peaks in the flowering stage, and this difference is due to the shedding of rice leaves. This illustrates the variability in the structural characteristics of different rice varieties even though they were planted at the same time and under the same conditions. Nicknejad et al. (2009) noted that the variation in LAI from different rice varieties occurred due to differences in rice ripening. Only two rice varieties were planted in irrigated and non-irrigated areas, both found in two

sampling fields (Figure 4.8). The LAI of the Phitsanulok2 variety was greater in non-irrigated areas from the panicle (DOY 200) to harvesting (DOY 229) stages. The LAI of RD49 is higher in non-irrigated areas during the tillering (DOY 179) and panicle (DOY 200) stages but lower in the flowering (DOY 223) and harvesting (DOY 231) stages compared to LAI in irrigated areas.

The main rice variety in the study area is RD41 is found only in irrigated areas and has a peak LAI (4 $m^2 m^{-2}$) in the flowering stage (DOY 219). When analysed at the provincial level, the variation in the temporal dynamics of LAI was related to differences in agricultural practices, weather conditions, and rice variety. It is clear that LAI is strongly linked to rice variety and possibly the irrigation system used, with peaks in LAI occurring at different growth stages according to variety. Increasing rice height and LAI, especially the heading stage, improved rice yield on short-duration rice variety in tropical Asia by increasing the crop growth rate (CGR), net assimiliation rate (NAR), and mean LAI in the reproductive stage (Zhou et al., 2021). In all varieties, the maximum LAI was found in the flowering stage when rice plants develop grains before decreasing through to the harvesting stage. Similar seasonal dynamics in LAI and equally large variations in LAI magnitude were also found by Fang et al. (2014). They found that the AccuPAR-derived LAI was underestimated due to the influences of stem and yellow leaf area index, particularly at the end of the growing season. The lower LAI in the harvesting stage is due in part to leaf senescence which is detected as plant area index (PAI) by some methods (e.g. hemispherical photos), and some leaf fall as even the PAI reduces in this stage (Fang et al., 2014). It is also relevant to consider the influence of stem density (Figure 4.11), which was found to peak in the tilltering stage before reducing through the growing season in response to increased competition for light. In contrast, the LAI increases through the growing season and broadly peaks in the flowering stage when the total dry matter is also high (Moradpour et al., 2011). Most crops integrate the LAI into crop simulation models for yield estimation (Curnel et al., 2011; He et al., 2017; Zhao & Pei, 2013).

4.3.2.3 Chlorophyll content

Chlorophyll is a photosynthetic pigment that controls leaf photosynthetic capacity and plays an important role in the photosynthesis process and vegetation growth. Leaf chlorophyll concentration varies among rice leaves during the growing season, and studies have found a strong correlation between chlorophyll concentration and rice yield (Ramesh et al., 2002). Therefore, chlorophyll concentration was measured using an in-situ optical technique with MultispeQ during different growth stages. The results for all study sites and irrigated and non-irrigated sites are shown in Table 4.6 and Figure 4.13.

Table 4.6 Chlorophyll content as a function of growth stage for all field sites, irrigated and non-irrigated sites.

Irrigation system	Statistic	Chlorophyll content (µmol m^{-2})			
		Tillering	Panicle	Flowering	Harvest
Overall	Average	28.46	34.27	41.06	27.93
	S.D.	2.63	1.05	0.75	1.26
Irrigated	Average	25.28	35.05	41.27	27.32
	S.D.	3.19	1	0.85	1.58
Non-irrigated	Average	36.94	32.21	40.5	29.55
	S.D.	2.39	2.77	1.68	1.97

Table 4.6 illustrates the variation in chlorophyll content with growth stage and according to the irrigation system. Leaf chlorophyll content peaked during the flowering stage before decreasing in the harvesting stage, which matches the findings of Ata-Ul-Karim et al. (2016) and has similar dynamics to the LAI (Table 4.5). The variation in the average chlorophyll concentration as a function of irrigation is inconclusive, with rice cultivated in irrigated areas having higher chlorophyll concentrations in the panicle and flowering stages. However, there is a more excellent range of values in the non-irrigated sites.

a) Chlorophyll content over all field sites

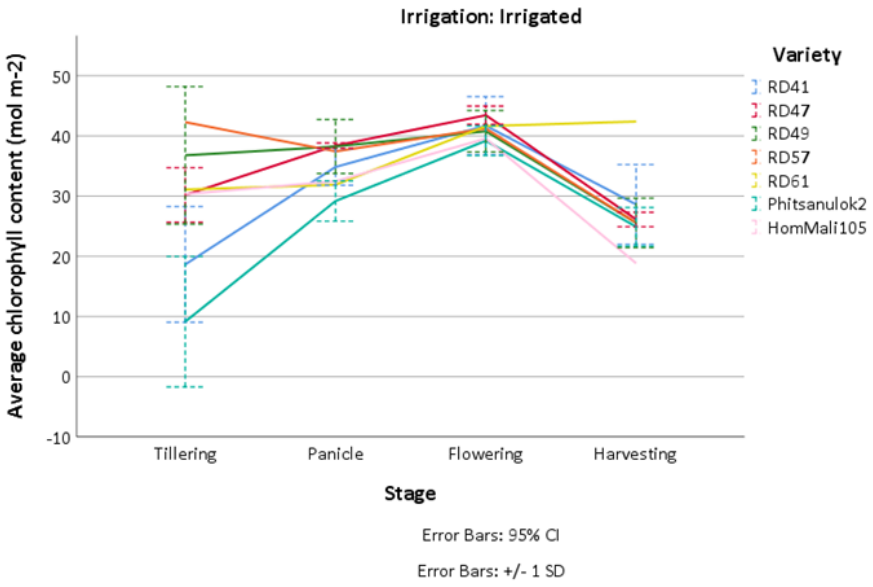

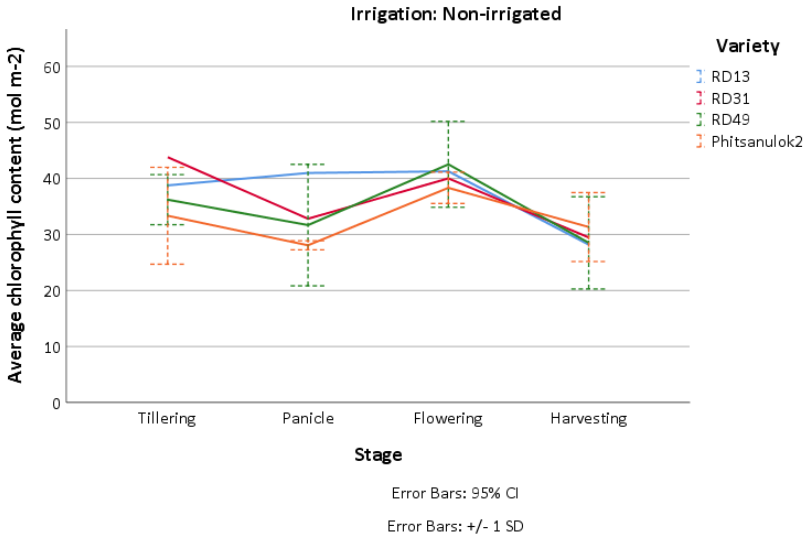

b) Chlorophyll content in Phichit

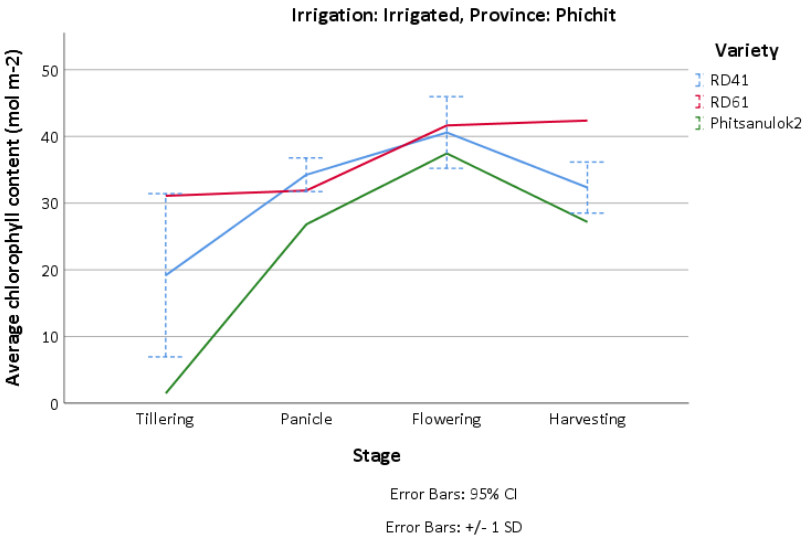

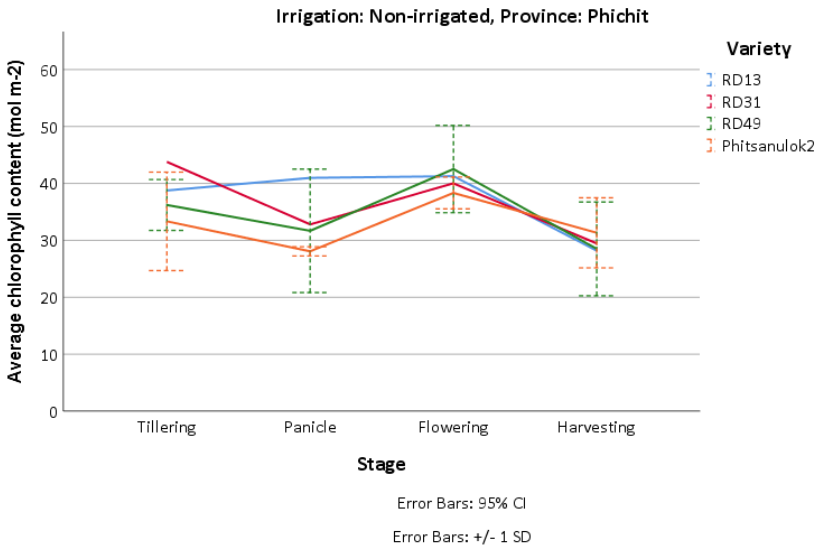

c) Chlorophyll content in Ang Thong

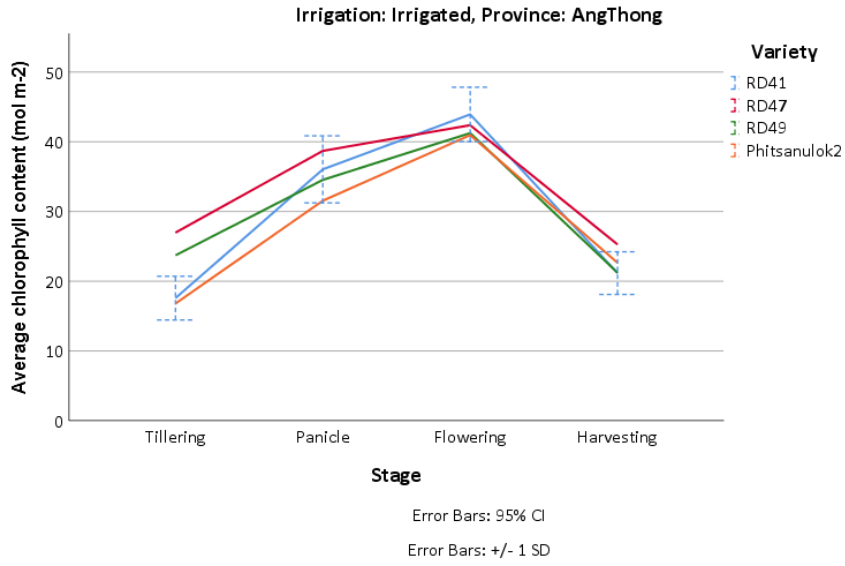

d) Chlorophyll content in Pathum Thani

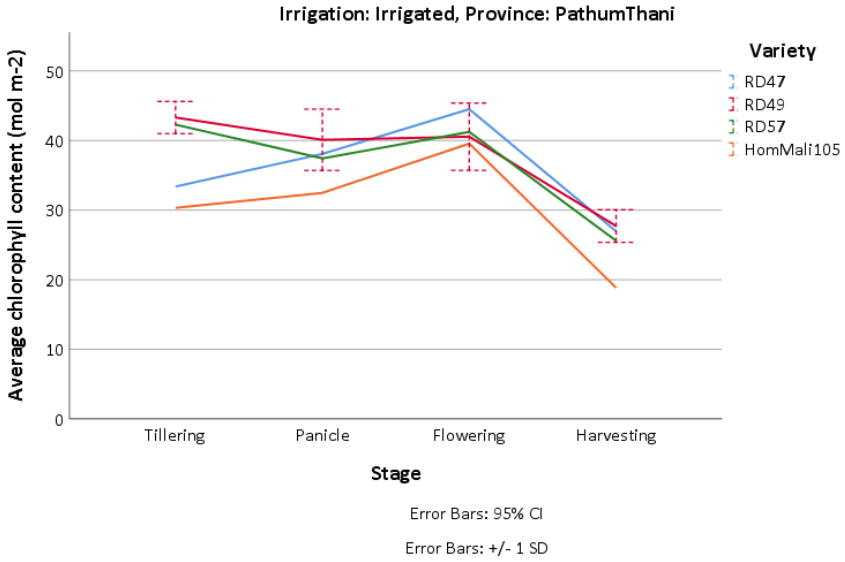

Figure 4.13 Chlorophyll content stratified according to rice variety and irrigation system. a) Chlorophyll content according to irrigation system (all sites), b) Phichit, c) Ang Thong and d) Pathum Thani.

The range of chlorophyll concentration in the irrigated and non-irrigated areas is influenced by the rice variety (Figure 4.13a), particularly in the tillering stage when the chlorophyll content varied by a factor of ~4. The chlorophyll concentrations found in irrigated and non-irrigated rice are broadly similar. However, the range of values is more excellent in irrigated areas, which have a more defined profile, and which show a significant decrease in the mature stages. Two rice varieties, Phitsanulok2 and RD49, are grown in irrigated and non-irrigated areas. The former has quite different chlorophyll values in the tillering stage, with a difference of 31.86 μmol m^{-2}, whilst the panicle, flowering, and harvesting stages are similar, at 1.26, 0.88, and 4.15 μmol m^{-2}, respectively. In both irrigated and non-irrigated areas, the chlorophyll concentration of RD49

displayed large fluctuations but tended to have higher concentrations when irrigated, with an average difference of 3.95 μmol m^{-2}. On a provincial level, the upturned bowl shape of chlorophyll concentration found in the irrigated areas is more apparent relative to the flatter profiles in non-irrigated areas. Ata-Ul-Karim et al. (2016) also found considerable seasonal variation between two rice varieties but also found that nitrogen fertilisation had an enormous impact on chlorophyll concentration, although a more modest impact on the temporal trend. The photosynthetic light use efficiency (LUE) refers to the efficiency of a plant's use of the absorbed radiation energy to produce biomass (Quero et al., 2019) and is influenced by the leaf chlorophyll concentration (Slattery et al., 2017; Zheng et al., 2021).

4.3.2.4 Wet and dry biomass

Theoretically, the above-ground biomass (AGB) is an advantage for rice yield estimation as it reflects rice growth status. Here, the AGB explore their potential for yield estimation derived from the ground- based and satellite platforms. After cutting rice roots, rice samples were oven dried until constant weight. Three main growth stages where wet and dry biomass was measured are the panicle, flowering, and harvesting stages (Figure 4.14).

a) Mean of wet and dry biomass in overall study area

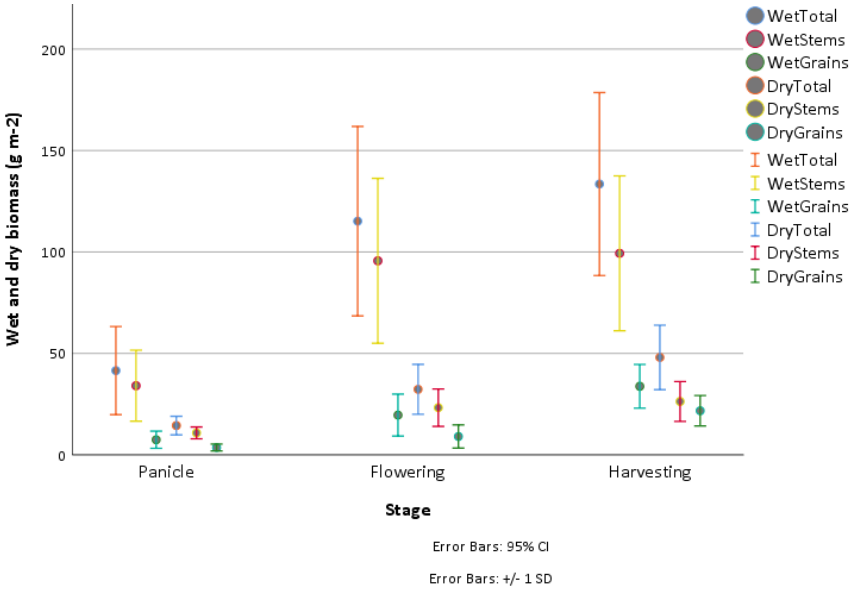

b) Mean of wet and dry biomass in different irrigation systems

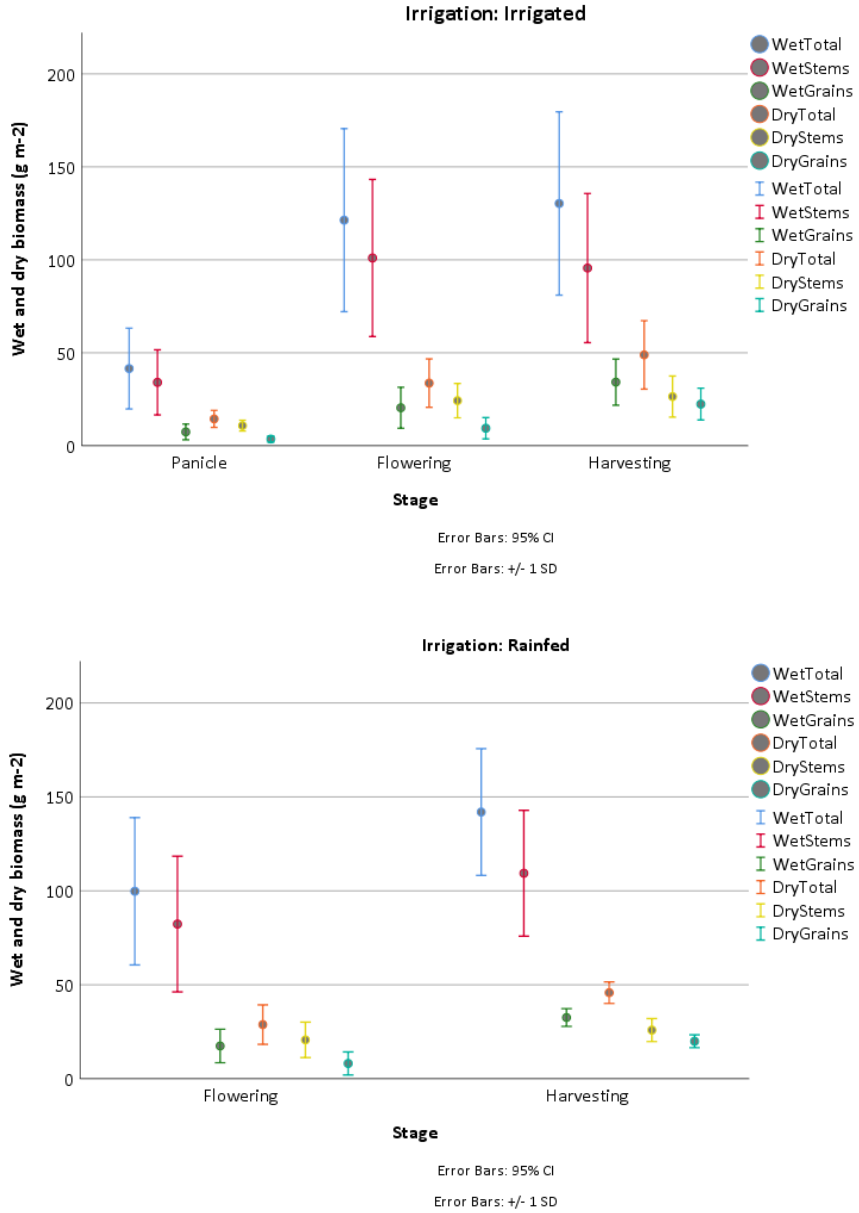

Figure 4.14 Wet and dry biomass. a) Mean of total wet and dry biomass in overall study area, b) Mean of total wet and dry biomass in different irrigation systems.

Figure 4.14 illustrates the variation in wet and dry rice biomass in the study area. Analysis of the entire dataset in the panicle stage indicates wet and dry biomass (in brackets) values of the total material, only the stems, and only the grain was 41.53 (14.44), 34.08 (10.82), and 7.44 (3.62) g m^{-2}, respectively. Biomass increases through the flowering stage, peaking in the harvesting stage with wet and dry biomass (in brackets) values of 133.48 (48.02), 99.33 (26.29), and 33.77 (21.74) g m^{-2} for the whole rice plant, stems, and grains, respectively. This differs from the LAI, which was lower in the harvesting stage due to the influence of senescent (non-green) leaves that are not photosynthetically active. Irrigation systems influence on plant biomass, with the biomass in irrigated areas being 21.5 g m^{-2} greater than that found in non-irrigated areas in the flowering stage and 11.6 g m^{-2} in the harvesting stage. In the case of dry biomass, the differences between

irrigated and non-irrigated areas were 4.88 and 3.05 g m^{-2} in the flowering and harvesting stages, respectively. A more excellent range in biomass was found in each growth stage in irrigated systems, particularly in the harvesting stage, which varied between 50-250 g m^{-2} and 100-180 g m^{-2} in irrigated and non-irrigated areas, respectively. The influence of rice variety on wet and dry biomass in the overall study area and different irrigation systems is shown in Figure 4.15.

a) Wet and dry biomass in overall study area

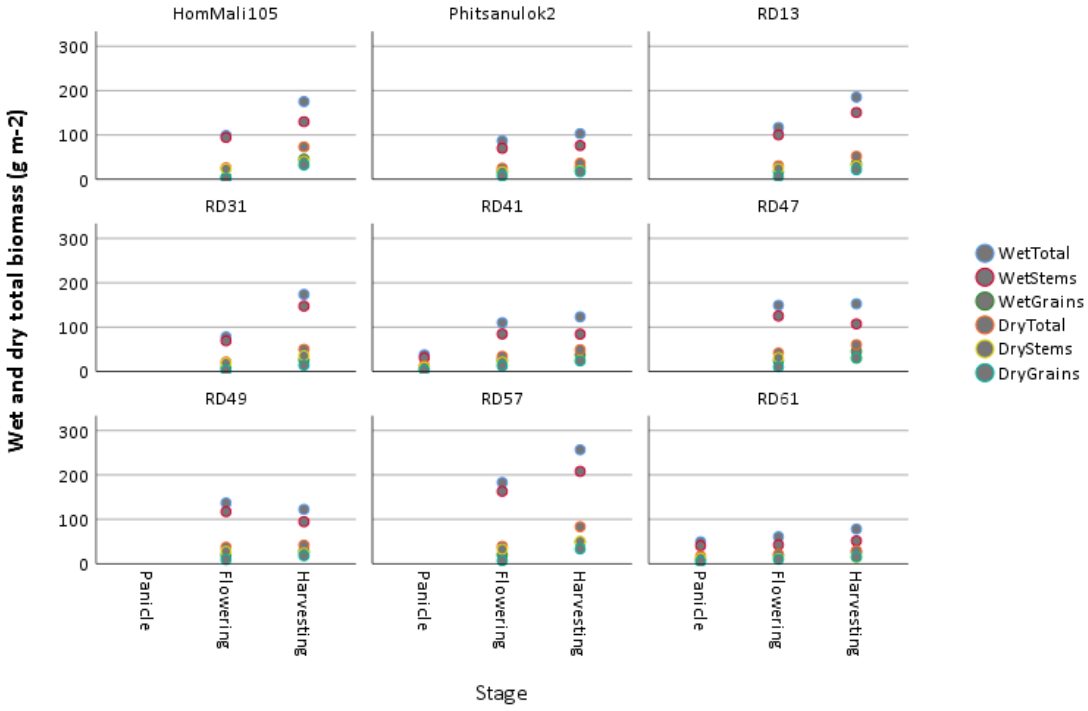

b) Wet and dry biomass in different irrigation systems

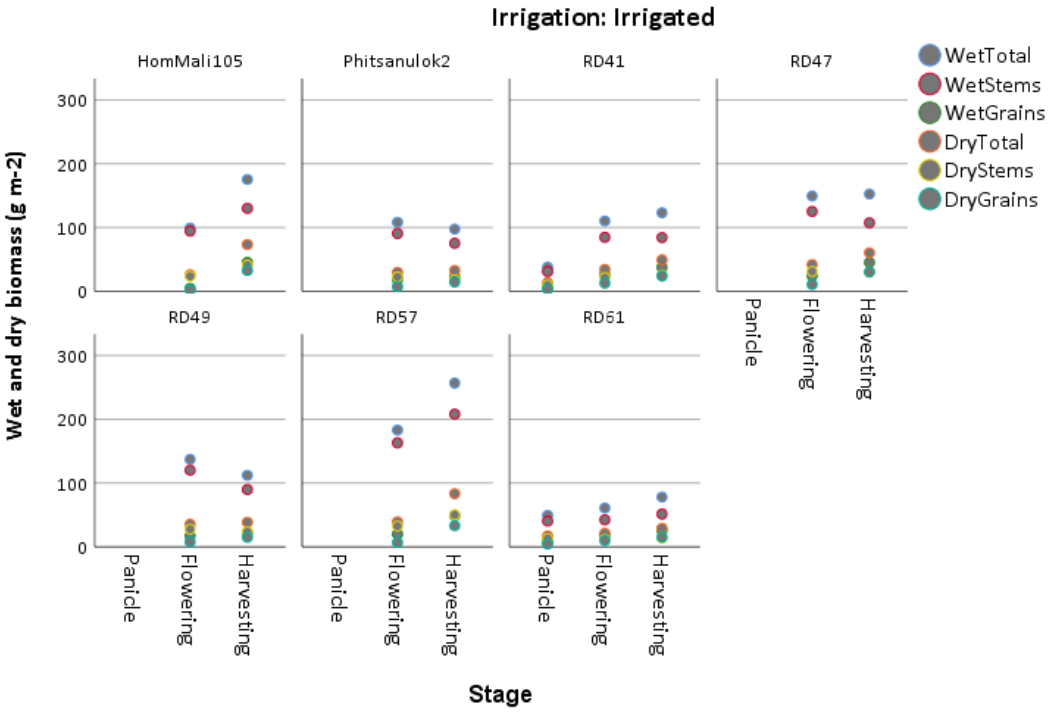

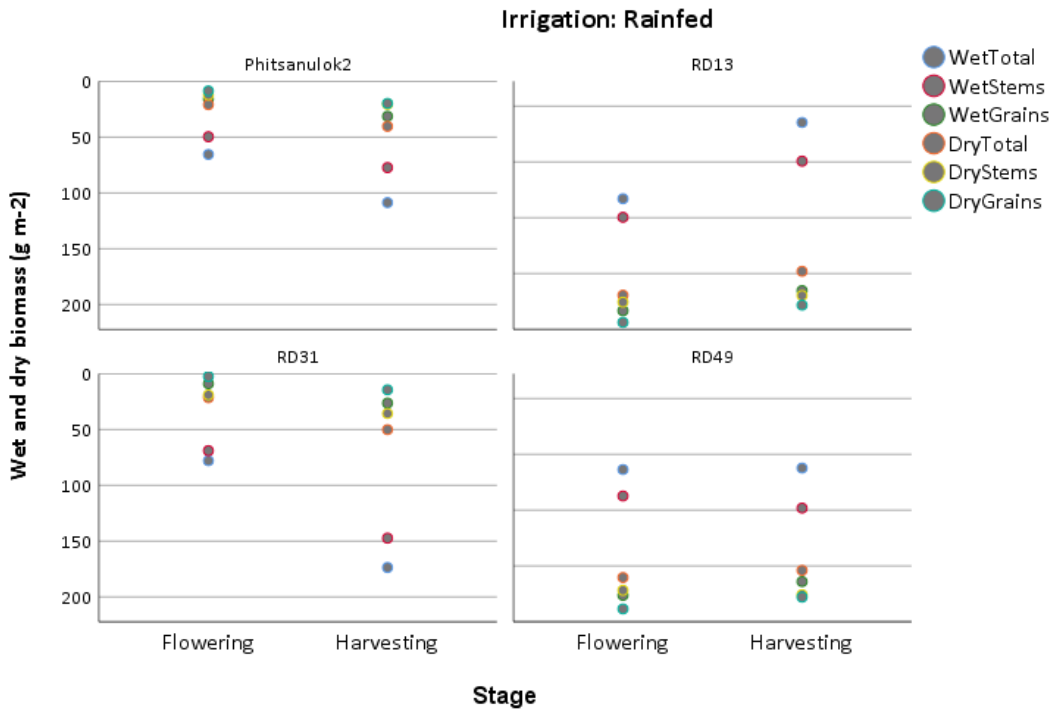

Figure 4.15 a) Wet and dry biomass in overall study area, b) Wet and dry biomass in the different irrigation systems by specific rice variety.

Figure 4.15 illustrates the variation in wet and dry biomass for different rice varieties. Rice biomass in irrigated areas was typically higher than that in non-irrigated areas in the flowering stage, with average wet total biomass and dry biomass in brackets 121 (34) and 100 (29) g m^{-2}, respectively. In comparison, rice biomass in irrigated areas was lower than biomass in the non-irrigated areas in the harvesting stage with average wet total biomass and dry biomass in brackets 130 (49) and 142 (46) g m^{-2}, respectively. Even the grain biomass is higher in the irrigated areas (34 g m^{-2}) than in non-irrigated areas (32 g m^{-2}) (He et al., 2022). Sufficient water is impacted on grain development. The grain panicle seems to initiate in the panicle stage for irrigated areas while the grain occurs in the flowering stage for non-irrigated areas. The biomass is highest in the harvesting stage, whilst LAI or stems density reduce in the same growth stage (Choudhury et al., 2007; Li et al., 2020). The reason for lower LAI after flowering is saturation and increased non-photosynthetic active plant tissue (Jonckheere et al., 2004; Leblanc & Chen, 2001). Typically, wet biomass varied between 41.5 and 130.3 g m^{-2} in irrigated areas and 99.8 and 141.9 g m^{-2} in non-irrigated areas. The wet biomass for RD49 and Phitsanulok2 rice varieties was broadly similar, with an average difference of 25 and 1.3 g m^{-2} in irrigated and 10.7 and 43.2 g m^{-2} in non-irrigated areas, respectively. Figure 4.15 illustrates the variation in rice biomass by growth stage but also shows that different rice varieties have different temporal dynamics. For example, the biomass for RD31 (Figure 4.15a) increased through the growing season, whilst RD49 decreased in the harvesting stage. As noted with the LAI, the influence of rice variety on biomass has implications

for using EO data to estimate rice biophysical variables. The minimum and maximum wet biomass is 14.27% and 215.45% of the average total wet biomass (119.13 gm^{-2}), whilst the minimum and maximum dry biomass are 23% and 215.36% of the average total dry biomass (38.65 g m^{-2}). Knowledge of the rice variety being grown would help reduce this uncertainty, and this variation should be taken into account when collecting field data for use in developing and validating EO-derived biophysical parameter estimates.

4.3.2.5 Rice yield

The results reveal that irrigated and non-irrigated areas have similar productivity where the average rice yield was 4.87 tonnes/ha and 4.78 tonnes/ha, respectively. When accounting for all agricultural land under irrigated and non-irrigated rice production, the total production would be 787,794 tonnes in irrigated area and 542,516 tonnes in non-irrigated area with a difference of ~245,000 tonnes. These results show that there is a yield gap among different irrigation systems.

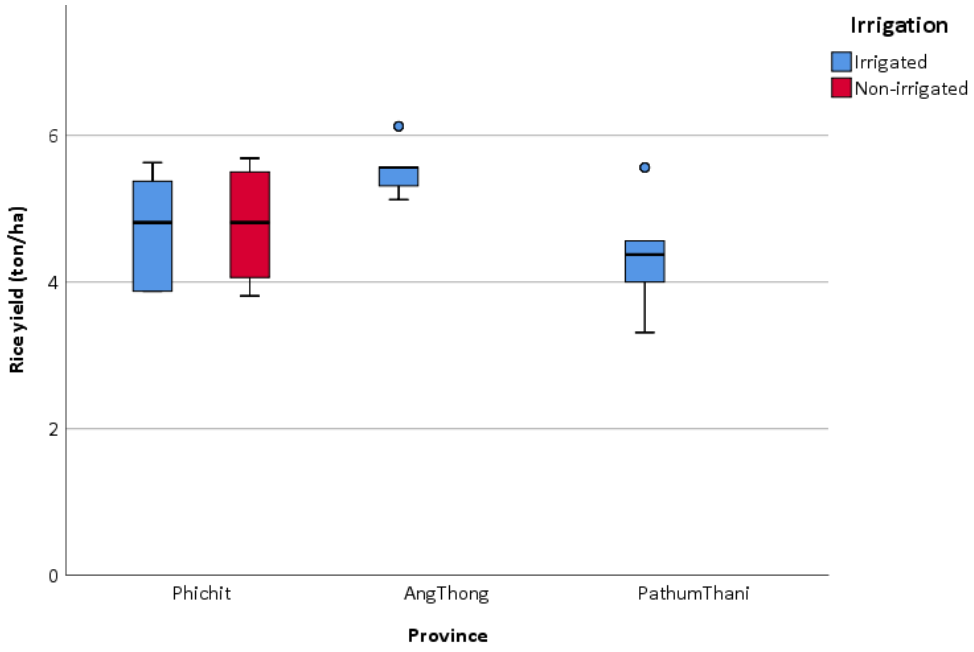

Figure 4.16 Rice yield separate by the irrigation system and province

4.3.3 Correlation on rice biophysical variables

The following section investigates the correlation among rice biophysical variables at each growth stage and overall growth stage, to determine which might be the best predictor of rice yield and the extent to which this depends on irrigation system. Doing so allowed different stages of growth would allow assessment of the potential to estimate yield using a particular biophysical parameter earlier in the growing season and therefore aiding early yield prediction. The rice biophysical variables assessed include stem density, height, water depth, awns length, LAI, wet

and dry biomass (total, stem, and grain), and yield. The selected results of the significance statistical analysis are presented in Table 4.7 and that the rest of the results can be found in Appendix E.

Table 4.7 Correlation between yield and rice biophysical variables as a function of growth stage.

Area	Rice variable	Correlation	Stage					
			Seeding	Tillering	Panicle	Flowering	Harvesting	Overall
Overall area	Height	r sig.	NA	**0.37*** **(0.09)**	0.07 (0.77)	-0.19 (0.4)	-0.1 (0.66)	0.03 (0.78)
	Wet grain biomass	r sig.	NA	NA	0.95 (0.21)	**0.45**** **(0.04)**	0.30 (0.17)	**0.27*** **(0.07**
	Dry grain biomass	r sig.	NA	NA	0.94 (0.22)	**0.43**** **(0.05)**	0.28 0.21	0.21 0.16
Irrigated Area	Stem density	r sig.	**0.45*** **(0.08)**	0.23 (0.39)	-0.39 (0.16)	**-0.46*** **(0.08)**	0.2 (0.46)	0.08 (0.47)
	Wet grain biomass	r sig.	NA	NA	0.95 (0.21)	**0.47*** **(0.08)**	0.37 (0.15)	**0.31*** **(0.08)**
Non-irrigated area	Height	r sig.	NA	**0.74*** **(0.09)**	0.35 (0.5)	-0.37 (0.47)	**0.81**** **(0.05)**	0.19 (0.38)
	Chlorophyll content	r sig.	NA	-0.38 (0.46)	-0.8 (0.6)	-0.58 (0.22)	-0.09 (0.86)	**-0.36*** **(0.08)**
	Chlorophyll content	r sig.	NA	-0.38 (0.46)	-0.8 (0.6)	-0.58 (0.22)	-0.09 (0.86)	**-0.36*** **(0.08)**
	Wet total biomass	r sig.	NA	NA	NA	-0.44 (0.38)	**-0.97**** **(0.00)**	**-0.58**** **(0.05)**
	Wet stem biomass	r sig.	NA	NA	NA	-0.57 (0.24)	**-0.95**** **(0.00)**	**-0.69**** **(0.01)**
	Dry total biomass	r sig.	NA	NA	NA	-0.23 (0.66)	**-0.97**** **(0.00)**	-0.32 (0.31)
	Dry stem biomass	r sig.	NA	NA	NA	-0.63 (0.18)	**-0.93**** **(0.00)**	**-0.69**** **(0.01)**

Where *, ** value significant at the 0.05 and 0.01 probability level (2-tailed)
NA No measurement

The correlations presented in Table 4.7 illustrate that none of the rice biophysical variables significantly correlated in the seeding, tillering or panicle stages. When assessing the correlation using data from all areas, only wet grain biomass in the flowering stage had a significant but weak correlation (r = 0.45). The situation was similar in irrigated areas, where no parameters had a significant relationship with the yield at any growth stage. In non-irrigated areas, significant correlations were found between rice yield and total wet biomass, wet stem biomass, total dry biomass, and dry stem biomass: -0.97, -0.95, -0.97, and -0.93, though all in the late stages of the growing season. The results indicate that none of the rice biophysical variables offered a consistent way to estimate rice yield, particularly earlier in the growing season, which would be advantageous for crop management and food security. However, as evident from previous analysis, the influence of rice variety could be significant, and therefore it is vital to conduct this analysis as a function of the two rice varieties with the most samples and irrigation method.

Table 4.8 Correlation between yield and rice biophysical variables as a function of rice variety in irrigated areas.

Rice variable	Correlation	HomMali 105	Phitsanulok2	RD41	RD47	RD49	RD57	RD61
Chlorophyll content	r sig.	.[c]	0.21 (0.63)	-0.11 (0.61)	-0.17 (0.69)	**-0.52*** **(0.08)**	.[c]	.[c]
Wet total biomass	r sig.	.[c]	0.29 (0.71)	**0.64**** **(0.02)**	-0.54 (0.46)	0.19 (0.72)	.[c]	.[c]
Wet stem biomass	r sig.	.[c]	0.26 (0.74)	**0.65**** **(0.02)**	-0.52 (0.48)	0.17 0.75)	.[c]	.[c]
Wet grain biomass	r sig.	.[c]	0.4 (0.6)	**0.54*** **(0.06)**	-0.29 (0.72)	0.16 (0.76)	.[c]	.[c]
Dry total biomass	r sig.	.[c]	0.36 (0.64)	**0.63**** **(0.02)**	-0.39 (0.61)	0.25 (0.63)	.[c]	.[c]
Dry stem biomass	r sig.	.[c]	0.37 (0.64)	**0.7**** **(0.01)**	-0.52 (0.48)	0.3 (0.56)	.[c]	.[c]
Dry grain biomass	r sig.	.[c]	0.19 (0.81)	**0.5*** **(0.08)**	-0.22 (0.79)	-0.06 (0.92)	.[c]	.[c]

Where *, ** value significant at the 0.05 and 0.01 probability level (2-tailed)

NA No measurement

Table 4.8 demonstrates the relationship between rice yield and other rice biophysical variables in irrigated areas (i.e. RD41 (6 sample units), RD47 (2 sample units), RD49 (3 sample units), Phitsanulok2 (2 sample units), and RD57/RD61/HomMali105 (1 sample unit each)). Again, the results reveal the strongest correlations with RD41 variety for total wet biomass (r = 0.64), wet stem biomass (r = 0.65), total dry biomass (r = 0.63), and dry stem biomass (r = 0.7), which has the most samples. The findings for non-irrigated areas are presented in Table 4.9 but have poor relationships between yield and rice biophysical variables.

Table 4.9 Correlation coefficient between yields with rice biophysical variables in non-irrigated areas for different rice varieties.

Rice variable	Correlation	Phitsanulok2	RD13	RD31	RD49
Wet total biomass	r sig.	0.2 (0.8)	.[c]	.[c]	**-0.97**** **(0.03)**

Where *, ** value significant at the 0.05 and 0.01 probability level (2-tailed)

NA No measurement

The correlation coefficients are weak and variable for all biophysical parameters as a function of both rice variety and irrigation approach, although the number of samples in both instances is small. Further analysis of the relationship between yield and biophysical variables for the specific rice variety RD41, which has the most (6) samples, for different growth stages was carried out (Table 4.10).

Table 4.10 Correlation of RD41 overall and in each growth stage.

Rice variable	Correlation	Seeding	Tillering	Panicle	Flowering	Harvesting	Overall
Stem density	r	0.05	0.4	0.11	**-0.86***	0.15	**-0.79****
	sig.	(0.93)	(0.43)	(0.84)	**(0.03)**	(0.77)	**(0.00)**
Height	r	NA	0.47	0.04	0.36	0.21	**0.67****
	sig.		(0.35)	(0.93)	(0.48)	(0.69)	**(0.00)**
Chlorophyll content	r	NA	-0.72	-0.06	0.49	-0.04	**0.64****
	sig.		(0.11)	(0.91)	(0.32)	(0.93)	**(0.00)**
Wet total biomass	r	NA	NA	**1.00****	0.62	**0.87****	**0.67***
	sig.				(0.26)	**0.02**	**(0.01)**
Wet stem biomass	r	NA	NA	**1.00****	0.62	**0.85****	**0.69****
	sig.				(0.27)	**(0.03)**	**(0.01)**
Wet grain biomass	r	NA	NA	**1.00****	0.63	**0.83****	**0.57****
	sig.				(0.26)	**(0.04)**	**(0.04)**
Dry total biomass	r	NA	NA	**1.00****	0.67	**0.94****	**0.62****
	sig.				(0.22)	**(0.00)**	**(0.02)**
Dry stem biomass	r	NA	NA	**1.00****	0.68	**0.89****	**0.67****
	sig.				(0.21)	**(0.02)**	**(0.01)**
Dry grain biomass	r	NA	NA	**1.00****	0.65	**0.87***	**0.52***
	sig.				(0.24)	**(0.03)**	**(0.07)**

Where *, ** value significant at the 0.05 and 0.01 probability level (2-tailed)
NA No measurement

The result in Table 4.10 indicates that yield is best related to wet and dry biomass in the harvesting stage, where the correlation (r) ranges between 0.83 and 0.94. The relationship between rice yield and total dry biomass was strong, although there were only six data points.

a) Dry total biomass

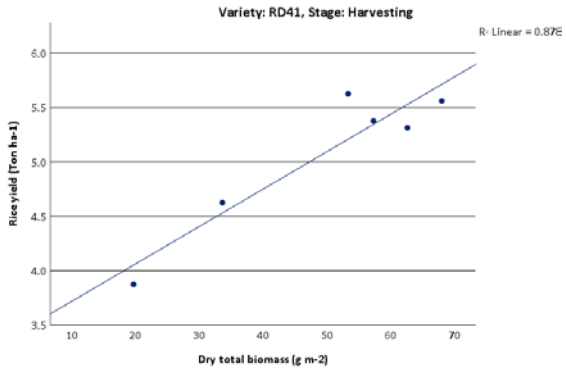

b) Dry stem biomass

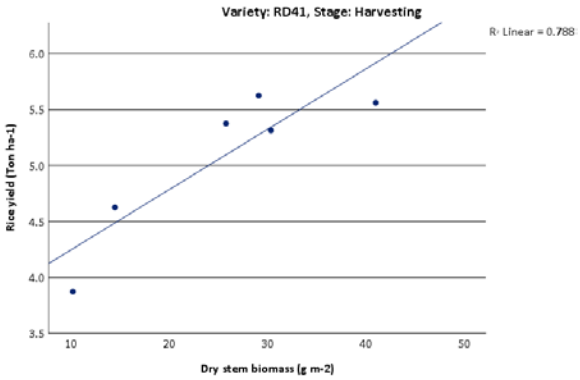

c) Dry grain biomass

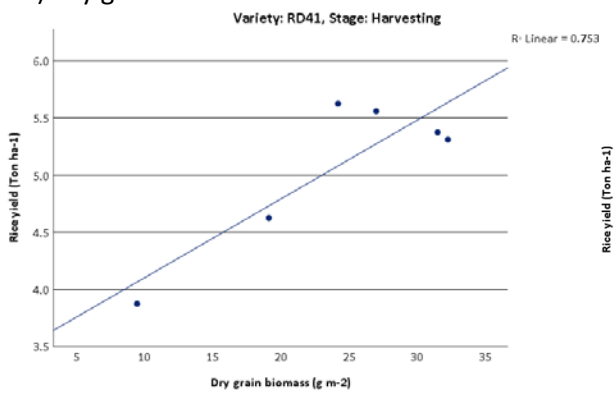

d) Wet total biomass

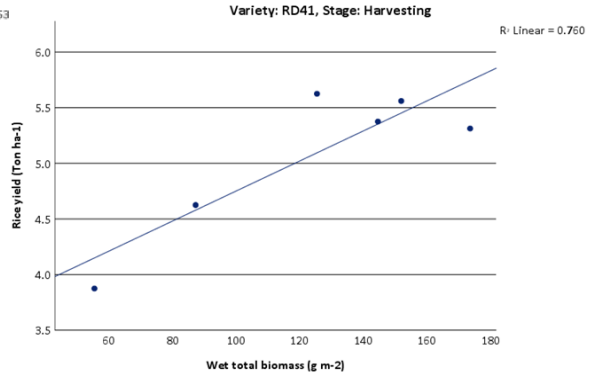

Figure 4.17 Correlation between yield and wet and dry biomass for the RD41 rice variety.

4.4 Discussion

This chapter investigated the variation in rice biophysical variables throughout the growing season as a function of irrigation method and rice variety. One of the aims of this study was to assess the relationship between various biophysical and structural characteristics and rice yield. The purpose of doing so is the potential to estimate rice yield using more easily obtained biophysical parameters and be able to do so earlier in the growing season. An extensive dataset of rice biophysical parameters was collected through the growing season and under different land management practices. To the best of our understanding, this is the first to do so, considering the irrigation methods and rice variety. The results indicate that the temporal dynamics of rice biophysical parameters and rice structural characteristics are influenced by environmental conditions, irrigation system, and rice variety. The findings indicate that rice height and biomass peak in the harvesting stage, whist the planting density is highest in the seeding and tillering stage and tends to decrease through the growing season as the rice matures (Figure 4.11). The more leaf area indicates the high absorb capability to capture solar radiation for crop photosynthesis (Ermanto et al., 2021). Rianto et al. (2019) proved influences on rice varieties and planting cropping patterns with the percentage of canopy cover. Increasing LAI depends on the increased tiller number and lengths of rice leaves, which is the tiller's rate different with rice variety. Research investigated the differences of LAI in various rice varieties on Tarom, Neda, Shafagh, and Fajr varieties were 3.97, 5.09, 4.24, and 4.9 m^2 m^{-2} (Nicknejad et al., 2009). The LAI (Table 4.5 and Figure 4.12) displays considerable variability in its dynamics through the growing season due to the influence of rice variety. It is often highest in the flowering stage in all regions and irrespective of irrigation system, although some rice varieties (e.g. RD47, RD61) peak in the panicle stage due to their dominant rice characteristics.

Other studies have found LAI to vary with rice variety (Bronge & AB, 2004; Chen et al., 2007; Leonenko et al., 2013; Zheng & Moskal, 2009). Rice height and leaf area distribution impacted the competition for light and nitrogen; then, they are effect on the growth of rice biomass in the final (Burgos et al., 2006; Graf et al., 1990). In addition, the competition for light on rice proved changes in morphological traits for light capturing and absorbing water and nutrients (Schaedler, Taborda, Goulart, Chiapinotto, & Pinho, 2020). A research analysed the LAI development in different irrigation and irrigation management; the result revealed the LAI under shallow water depth (SWD) in paddies were different compared with the continuous flooding (CF), with the varied correlation between LAI and treatment ranged 0.46-0.88 (Maftukhah et al., 2019) and coherent with tillering's rate (Zhong et al., 2002).The limitation of LAI is the foliage in the paddy. The relationship between LAI and foliage area index (FAI) had been investigated and the LAI-FAI estimation was significantly correlated with rice grain yield (Aschonitis et al., 2014). Finally, the

correlation between rice yield and biophysical parameters is typically poor although marginally better for wet and dry biomass in the flowering stage, which is close to panicle emergence.

Earth observation data has been widely applied to map areas of rice production (Kuenzer & Knauer, 2013; Oyoshi, Tomiyama, Okumura, & Sobue, 2013; Stroppiana et al., 2019; Zhang et al., 2015; Zhang et al., 2018; Zhao et al., 2016) and to estimate rice biophysical parameters using optical and radar observations. One of the objectives of this research was to investigate the correlation between rice yield and other biophysical parameters, particularly chlorophyll content and LAI. The LAI is a vital plant canopy structural parameter which plays an important role in the land-atmosphere energy exchange. As a result, LAI has been routinely estimated using remotely sensed data using parametric and physically-based retrieval methods (Verrelst et al., 2015). The LAI of rice canopies has been successfully estimated using a wide range of methods, including vegetation indices (Ali et al., 2020; Son et al., 2013; Wang, Huang, Tang, & Wang, 2007; Yeom et al., 2021) and radiative transfer models (Aboelghar et al., 2010; Adeluyi et al., 2021; Campos-Taberner et al., 2016, 2018; Darvishzadeh et al., 2012). Gong et al. (2021) investigated the poor correlation (not exceeding 0.4 correlations) between eight VIs, LAI, and height because they varied on rice varieties (48 rice varieties) in pre- and post-heading. Therefore, determining whether LAI correlates with yield would be advantageous and support using EO-derived LAI to estimate yield. Our findings indicate that LAI is weakly correlated with yield in all growth stages.

Rice yield is an essential parameter in quantifying rice productivity when combined with the area under rice cultivation. Several approaches utilise EO data to estimate yield using canopy reflectance (Chang et al., 2005; Nuarsa et al., 2011; Rahman et al., 2012), time-series analysis (Fermandez et al., 2021; Son, Chen, & Chen, 2022), regression models (Paul, Saha, & Hembram, 2020)**,** and rice growth simulation models (Kandiannan et al., 2002). In addition, radar data have been used to estimate rice biomass (Li et al., 2016; Ndikumana et al., 2018), from which yield can be estimated. Our analysis indicates that yield is poorly correlated with all the biophysical parameters, including LAI and chlorophyll content. This is in contrast to several studies that have found a good correlation between LAI and yield (Noureldin et al., 2013). However, LAI is a commonly used as an input to a crop growth model from which yield is estimated (Curnel et al., 2011; Dente, Satalino, Mattia, & Rinaldi, 2008; He et al., 2017; Maki et al., 2017) rather than a direct approach to estimate yield.

The results in this chapter have highlighted the influence of rice variety and irrigation systems on rice biophysical parameters and their temporal dynamics. Furthermore, the results indicate that rice variety can result in large differences in biophysical parameters at a given growth stage. For example, the average LAI peaked in the flowering stage. However, the LAI varied from 2.5 $m^2 m^{-2}$

to 6.9 $m^2 m^{-2}$ depending on the rice variety, and some rice varieties peaked in the panicle or harvesting stages.

To remove the influence of rice variety on the biophysical parameter analysis, we focus on the rice variety with the most significant number of samples, which was RD41 with 6 samples. The RD41 rice variety is characterised by straight clumping, strong and green leaves, straight flag leaves, and tolerance to the planthopper pest and irrigation planting in the central areas. The results of the correlation analysis are improved when using only RD41, particularly the wet and dry biomass (i.e. overall, stem, and grain) in the harvesting stage, which might benefit on yield estimation. Irrigation systems provide sufficient water for crop growth and ensure rice production efficiency, and our results support this where rice yield is ~55-60% higher (Nonvide, 2017). Irrigation development, therefore, allows improved high agricultural yield and contributes to government development plans/policies.

4.5 Conclusion

The research described in this chapter aimed to investigate the influence of irrigation and rice variety on rice biophysical variables, which were measured through the growing season during an extensive field campaign. Although it is difficult to disentangle due to the small sample size, our findings indicate that rice variety significantly influences the magnitude and dynamics of rice biophysical parameters. As a result, attempts should be made to account for rice variety when using remotely sensed data to estimate biophysical parameters such as LAI. One of the study's aims was to investigate the correlation between the biophysical parameters and yield at different growth stages to determine whether they could use to estimate yield earlier in the season. Additionally, if LAI or chlorophyll were correlated with yield, EO-derived LAI or chlorophyll estimates may be used to calculate yield. However, in all cases, the correlations were typically low and insignificant. When focussing on the most common rice variety in our study area (RD41), the most promising correlation with yield were found with total dry biomass and dry stem biomass in the harvesting stage, albeit still relatively weak relationships. Therefore, this rice variety will be the focus of the next chapter, which investigates rice yield estimation using EO data.

Chapter 5 The potential of optical and radar satellite observations to estimate rice biophysical variables and rice yield estimation

5.1 Introduction

The previous chapter investigated the temporal pattern and correlation between essential rice biophysical variables in the Chao Phraya River delta, Thailand. The results show how the pattern of rice biophysical variables, particularly LAI, biomass, and yield, differ with irrigation systems and that rice variety is also essential. The result of the analysis revealed a strong positive correlation between rice height, and wet and dry grain biomass with yield but also suggested that; rice variety also plays a vital role in the relationship between biophysical variables. At individual growth stages, significant correlations between rice biophysical variables were found in the tillering and flowering stages. However, the relationship's strengths varied, with a stronger correlation found between some biophysical variables than others depending on the growth stage. Thus, the results suggest that rice yield estimation is optimal using biophysical variables in the panicle, flowering, and harvesting stages. However, an additional complication is that the correlation between rice biophysical variables and growth stages varied across irrigation systems and rice variety. Among nine rice varieties in the study area, the RD41 shows the highest correlation with biomass. Therefore, it is essential to investigate the potential of using rice biophysical variables at particular growth stages to estimate yield. The acquisition of rice growth stage data is vital to select the appropriate growth stage to utilise different satellite sensors in rice yield estimation effectively. Earlier achieving agricultural information, especially rice yield and production, are advantageous for agricultural policy planning and ensuring global food security.

Remote sensing has the potential to provide information on crops, including their seasonal dynamics and the aerial extent, and has been widely applied for rice monitoring and yield estimation. Many studies have investigated the association between satellite data and crop growth which, in some cases, use satellite-derived rice biophysical variables to estimate potential yield (Aboelghar et al., 2010; Campos-Taberner et al., 2017; Gnyp et al., 2014; Hosseini et al., 2015; Jia et al., 2014; V. Kumar et al., 2013). Vegetation indices, which are designed to maximise sensitivity to the vegetation characteristics whilst minimising external perturbations (e.g. soil background and atmospheric effects) The vegetation indices have been widely applied to monitor vegetation and to identify crop characteristics such as crop status, stress, water status, phenology and crop yield (Bolton & Friedl, 2013; Lopresti et al., 2015; Sjöström et al., 2011; Son et al., 2014).

The most commonly used vegetation index is the Normalized Difference Vegetation Index (NDVI, Rouse Jr, Haas, Schell, & Deering, 1974), which exploits the contrasting response of red and near-infrared wavelengths to healthy vegetation. The NDVI has been routinely used for crop mapping and monitoring regional and global scales (Guan, Huang, Liu, Meng, & Liu, 2016; Nguyen, De Bie, Ali, Smaling, & Chu, 2012; Pan et al., 2015). By exploiting frequent observations, a time-series of NDVI measurements have been used to monitor crop productivity, biomass, and crop phenology (Bro-Jørgensen, Brown, & Pettorelli, 2008). The Enhanced Vegetation Index (EVI) builds on the NDVI but designed to improve sensitivity over high biomass regions and be more resistant to atmospheric effects. The EVI has been widely adopted for crop mapping and monitoring (Gusso et al., 2012; Peng et al., 2011; Shihua et al., 2014; Zhang et al., 2015).

In addition to monitoring and mapping crop dynamics and aerial extent, vegetation indices have also been used to estimate crop biophysical variables, including Leaf Area Index (LAI) and Fraction of Absorbed Photosynthetically Active Radiation (fAPAR; Fuster et al. (2020); Zhou et al. (2017)). Vegetation indices have also been successfully applied to empirically estimate crop yield empirically using regression models derived from single- or multi-date data (Bolton & Friedl, 2013; Harrell et al., 2011; Liu et al., 2015; Noureldin et al., 2013; Panda et al., 2010). For example, Padilla et al. (2012) developed a model to estimate LAI through the growing season based on the relationship between LAI and the NDVI, which was subsequently used to parameterize the GRAMI rice model (Maas, 1992). A constraint to using optical data for crop monitoring occurs in regions of more persistent cloud cover, which can be overcome by exploiting the all-weather capability of radar imagery. The backscatter of Synthetic Aperture Radar (SAR) signals is related to the surface characteristics, the canopy structure and canopy water content (Kobayashi & Ide, 2022; Phan et al., 2021; Soria-Ruiz et al., 2007; Verma et al., 2019). Radar backscatter is sensitive to crop structural characteristics such as height, shape, leaves size, and stem density (Choudhury & Chakraborty, 2006; Kim, Hong, & Lee, 2008; Koppe et al., 2012; Sudarmanian & Pazhanivelan, 2019; Wu et al., 2020; Zhang et al., 2017). Additionally, the behaviour of backscatter from rice canopies varies with growth stage due to the change in vegetation structure (e.g. plant density, height, leaf and panicle initiation) and moisture content, soil moisture, and surface roughness (Martinez-Agirre, Álvarez-Mozos, & Lievens, 2017; Bindlish & Barros, 2001; Zhao & Cui, 2013). Consequently, SAR has the potential to provide information on vegetation dynamics and canopy structure. Several studies have investigated the utility of integrating optical and SAR data to monitor crop phenology and estimate biophysical parameters at different growth stages (Biswal et al., 2019; Guissard et al., 2006; Lopez-Sanchez et al., 2017; Park et al., 2018; Soria-Ruiz et al., 2007). For example, Clevers and Van (1996) developed a reflectance model and backscatter model to estimate LAI, which was then used as an input to a crop growth model. The benefit of

using optical and radar data is that measurements are available throughout the growing season, which can be used to parameterize crop simulation models.

This chapter addresses two research questions. The first objective is to investigate the relationship between rice biophysical variables, spectral vegetation indices, and radar backscatter at different growth stages and irrigation methods. The second research area will develop a linear regression model that relates the satellite measurements with rice yield to estimate yield over a large spatial extent and potentially earlier in the growing cycle. The results will be validated with official statistical data at the amphoe and provincial levels.

5.2 Methodology

5.2.1 Data

5.2.1.1 Primary data

The primary data used in this analysis are satellite data and field survey data. Due to the small size of rice fields in Thailand (~0.61 hectares), coarse spatial resolution satellite data, such as MODIS, are not appropriate despite their daily overpass frequency. Therefore, this study focused on medium resolution satellite data from the European Space Agency (ESA) Sentinel programme. This includes optical data from the Sentinel-2 Multi-Spectral Instrument (MSI) and SAR imagery from space-borne Sentinel-1.

The MSI onboard Sentinel-2 A and B, which were launched on 23rd June (2015) and 7th March (2017), respectively, provide global data every ~5 days (or less) at the equator under cloud-free conditions. The MSI contains 13 spectral wavebands between 0.44 um to 2.19 um, a swath width of 290 km and spatial resolution of 10 m (four visible and near-infrared bands), 20 m (six red edge and shortwave infrared bands), and 60 m (three atmospheric correction bands- aerosols, water vapour, and cirrus). The Sentinel-1 comprises two polar-orbiting satellites (e.g. ascending and descending) operating day and night and collecting measurements using a dual polarisation C-band imager. Sentinel-1 has a temporal resolution of 6 days for two combined constellations or 12 days with one at the equator, and a spatial resolution of acquisition modes: strip map (SM; 5 m x 5 m), interferometric wide swath (IW; 5 m x 20 m), extra-wide swath (EW; 20 m x 40 m), and wave (WV; 5 m x 5 m). Sentinel-1 produces dual polarisation polarimetry data in vertical and horizontal transmission and receives responses in vertical and horizontal waves. Polarisation illustrates the orientation of the plane of oscillation of the propagation signal. Four possible polarisations are delivered on different transmissions and receive signals: HH (horizontal transmit and receive), VV (vertical transmit and receive), HV (horizontal transmit, vertical receive), and VH (vertical

transmit, horizontal receive) (Lusch, 1999). In this analysis, only VV and VH polarised data were used as these have been provided in the Southeast Asia region and prove the best correlation with rice biophysical. The incidence angle range is 29.1° – 46° and right look direction (side-looking). The incidence angle is defined as the angle by the radar beam and perpendicular to the surface. In principle, the return of microwave signals is strong at a low incidence angle. All Sentinel data were directly downloaded from ESA, and only imagery acquired within a week of a field campaign in a specific growth stage was selected for processing. Details of image pre-processing are provided in **Section 5.2.4**.

The other primary data used in this chapter are the field experiment data which was the focus of analysis in Chapter 4 (page 100-105 details the data collection methodology). In addition, measurements of several rice biophysical variables were collected at crucial growth stages throughout the wet growing season (May to October) in 2017. GPS measurements at the sampling locations allow these measurements to be col-located with the satellite measurements.

5.2.1.2 Secondary data

The secondary data used in this chapter are derived from two primary sources at the Office of Agricultural Economics (OAE): official statistical data of the area under agricultural production and its yield. Besides, the spatial data of rice cultivated areas have been derived through the interpretation of Landsat 8 data at the amphoe and provincial levels. The statistical data consists of rice production and yield estimates at the amphoe and provincial levels during the 2017 wet growing season. These data enable validation of our rice yield estimates. In addition, the spatial data allows masking Sentinel imagery into the rice and non-rice cultivated areas. The latter is helpful for rice production calculation in the three provinces (i.e. Phichit, Ang Thong, and Pathum Thani) representing the upper, middle, and lower Chao Phraya River delta. The other secondary data is the spatial dataset of the irrigation boundary, which allows the identification of irrigated and non-irrigated rice paddies.

5.2.2 Satellite data and statistic data preparation

5.2.2.1 Satellite data download and preparation

The satellite image acquisition dates are those closest to the time of the field sampling campaign. The acquisition dates of Sentinel imagery are shown in Table 5.1 and are largely +/- 7 days from the field surveying date to avoid the distortion due to rice growth. This was not always possible with Sentinel-2 MSI imagery, particularly during the monsoon (mid-May to mid-October). In this case, the nearest available image was used as long as the temporal gap to the next growth stage

was 20-35 days, the lengths of which depends on the growth stage (Figure 4.4). In the case of Sentinel-1, imagery cycle in the ascending and descending orbits was downloaded in VV and VH polarisations. The field survey dates and associated downloaded satellite data are shown as Table 5.1.

Table 5.1 Field survey and acquisition dates of satellite data.

Growth stage	Field survey date	Satellite download date		
		Sentinel-2	Sentinel-1	
			Ascending	Descending
Seeding	20 May – 7 Jun 2017	7 May, 27 May, 30 May, and 6 Jun 2017	22 May 2017	26 May 2017
Tillering	26 Jun – 10 Jul 2017	26 Jun, 6 Jul 2017	27 Jun 2017	1 Jul 2017
Panicle	19 – 30 Jul 2017	24 Jul, 31 Jul 2017	21 Jul 2017	25 Jul 2017
Flowering	1 – 16 Aug 2017	13 Aug, 20 Aug 2017	2 Aug 2017	6 Aug 2017
Harvesting	9 Aug – 3 Sept 2017	25 Aug, 9 Sept and 14 Sept 2017	26 Aug 2017	30 Aug 2017

The larger number of Sentinel-2 images in the seeding stage is due to the wide range of planting dates in the study area, which varied from the beginning of May until the beginning of June 2017. The satellite data did not acquire the full scene for analysis and was excluded from the analysis. In each growth stage, approximately 13 Sentinel-2 and 5 Sentinel-1 scenes were downloaded, and which covered the entire study area (Figure 5.1).

a) Sentinel-2 b) Sentinel-1

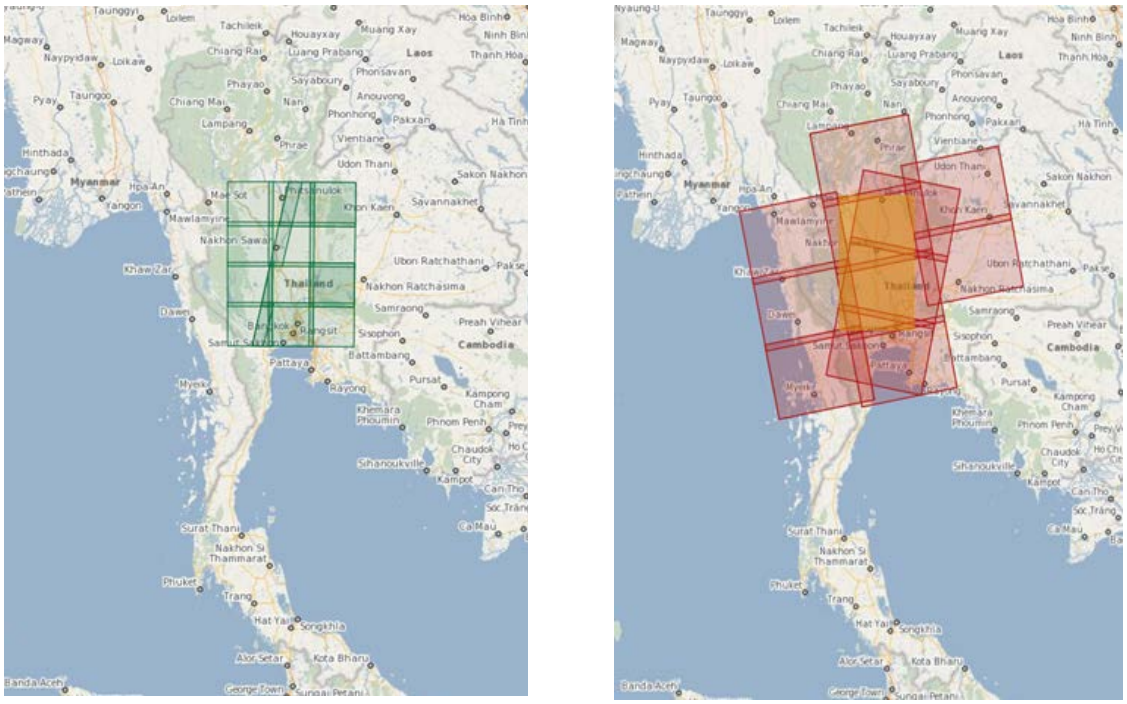

Figure 5.1 Location of the Sentinel-2 (left) and Sentinel-1 (right) image tiles over the study area.

5.2.2.2 Statistical data preparation

The yield estimated using satellite data will be validated using the yield information provided by OAE, which is the agency responsible for collecting and publishing agricultural statistics in Thailand. The OAE official statistics are calculated using field survey data at the commune level, which is then aggregated to the district, province, regional, and country levels. The official rice yield and production are stratified in two administrative levels for validating the remotely sensed yield estimates: amphoe and province level. In 2017, rice production and yield (shown in the brackets) in the Phichit, Ang Thong, and Pathum Thani was 876,596 tonnes (3.77 tonnes/ha), 230,547 tonnes (4.16 tonnes/ha), and 223,167 tonnes (4.49 tonnes/ha), respectively. Rice yield and production in 2017 are shown in Table 5.2.

Table 5.2 Rice yield and rice production statistics in 2017 in three representative provinces (OAE, 2017a).

Province/Amphoe	Rice harvested area (ha)	Rice yield (tonnes/ha)	Rice production (tonnes)
Phichit	**232,536**	**3.77**	**876,596**
Muang Phichit	23,669	3.98	94,084
Taphan Hin	25,984	4.09	106,373
Bang Mun Nak	22,600	3.88	87,716
Pho Thale	26,821	4.09	109,632
Pho Prathap Chang	19,274	3.84	74,083
Sam Ngam	21,524	3.74	80,445
Wang Sai Phun	17,983	3.42	61,478
Thap Khlo	24,612	3.48	85,525
Sak Lek	6,919	3.08	21,277
Bueng Na Rang	13,718	3.97	54,444
Dong Charoen	14,745	3.39	49,947
Wachirabarami	14,688	3.51	51,592
Ang Thong	**55,421**	**4.16**	**230,547**
Muang Ang Thong	3,916	4.12	16,131
Chaiyo	2,885	3.84	11,089
Pa Mok	593	3.80	2,252
Pho Thong	13,508	4.13	55,719
Wiset Chai Chan	15,342	4.12	63,190
Samko	7,798	4.24	33,093
Sawaeng Ha	11,379	4.31	49,073
Pathum Thani	**49,657**	**4.49**	**223,167**
Muang Pathum Thani	3,099	4.31	13,363

Province/Amphoe	Rice harvested area (ha)	Rice yield (tonnes/ha)	Rice production (tonnes)
Pathum Thani (Cont.)			
Khlong Luang	8,066	4.58	36,903
Thanyaburi	1,484	4.51	6,687
Lat Lum Kaeo	11,548	4.63	53,408
Lam Luk Ka	11,846	4.50	53,307
Sam Khok	2,892	4.47	12,924
Nong Suea	10,722	4.34	46,575

5.2.3 Field survey data collection

The field survey collected important rice biophysical variables from the seeding to harvesting stages. The latitude and longitude coordinates of each sample unit were recorded using a handheld GPS receiver, and within each there were four measurement plots. Coordinates were then generated with ArcGIS in point and polygon (rice parcel) format. The biophysical variables assessed in relation to the satellite data for each sampling unit were the average value of the centre pixels to account for any variability and to ensure the pixels were homogeneous (i.e. not mixed).

5.2.4 Digital image pre-processing

Image pre-processing was conducted according to the following sections, which are carried out for each Sentinel-1 and Sentinel-2 image prior to data extraction (Figure 5.2).

Sentinel-2 MSI optical data

The MSI product used for this analysis is the Sentinel-2 Top-Of-Atmosphere (TOA) Level-1C (L1C), geometrically corrected TOA radiance. To correct the data to surface reflectance, the Sen2Cor algorithm is used for atmospheric, terrain, and cirrus correction (Main-Knorn et al., 2017). The Sen2Cor toolkit provides Bottom-Of-Atmospheric (BOA) surface reflectance (Level-2A, L2A) in addition to various quality assurance data such as aerosol optical thickness, water vapour, scene classification, and quality indicators for cloud and snow probabilities. The surface reflectance derived from Sen2Cor has been validated over different land covers with good results ($r > 0.9$), and low root mean square errors (< 0.04) (Sola et al., 2018; Uwe et al., 2013). Cloud cover is a major limiting factor, with the cloud cover percentage varying from 5-77% per scene.

The Sentinel Application Platform (SNAP) is used to cloud mask the surface reflectance; resample the data to 20 m spatial resolution, and to calculate the NDVI and EVI vegetation indices. The

latter has been regularly used to analyse rice temporal dynamics (Domiri, 2017; Li et al., 2019; Shammi & Meng, 2021) and assess their relationship to biophysical variables (Aboelghar et al., 2011; Ali et al., 2020; Maki & Homma, 2014; Son et al., 2013).

The NDVI is defined by Rouse, Haas, Schell, & Deering (1974) and is calculated using the red (ρ_R) and NIR (ρ_{NIR}) wavebands via Equation 5.1.

$$NDVI = \frac{\rho_{NIR} - \rho_R}{\rho_{NIR} + \rho_R} \qquad \text{Equation 5.1}$$

According to Huete et al. (2002), the EVI is calculated as shown in Equation 5.2.

$$EVI = G\ x\ \frac{\rho_{nir} - \rho_r}{\rho_{nir} + C1 * \rho_r + C2 * \rho_b + L} \qquad \text{Equation 5.2}$$

Where ρ_b is the spectral reflectance in the blue band (B02), ρ_r is the spectral reflectance in the red band (B04), and ρ_{nir} is the spectral reflectance in the near-infrared band (B08). L is a constant that minimises the ground effect (L = 1), G is the gain factor (G = 2.5) and C1, C2 are adjustment factors to minimise the effect of aerosols in the atmosphere (C1 = 6.5 and C2 = 7.5).

In principle, the vegetation index values range between -1 to +1, where higher positive values signify healthy and denser green vegetation.

Sentinel-1 SAR data

Sentinel-1 C-band data were taken in various orbital directions with the ascending and descending orbits in 2017. The mode of SAR data identifies the S1-S6 beams for strip map products and provides different acquisition modes. The SAR Imagery in Interferometric Wide Swath (IW) mode has a spatial resolution of 5 m x 20 m in a single-look complex (SLC) was used in this analysis. SLC products are images in the slant range by azimuth imaging plane in the image plane of satellite data acquisition. Each pixel is represented by complex I (phase) and Q (quadrature) magnitude values and contains both amplitude and phase information. The amplitude measures the strength of the reflected signal at the sensor, while the phase is a measurement point along the wave of the reflected signal when received at the sensor. The phase of the SAR image is determined by the distance from the satellite antenna to the ground target. The amplitude measurement provides essential information on the roughness, geometry, wetness, and dielectric (or permittivity) constant of the ground surface. In pre-processing, the SAR data is geo-referenced using orbit auxiliary and attitude data, providing Zero-Doppler slant range geometry. Further, SAR products provide additional orbit state vector (OSV) information to improve location accuracy (Schubert, 2019).

The acquired Sentinel-1 SAR data were pre-processed using SNAP (Sentinels Application Platform) and Sentinel Toolboxes, which included applying precise orbit direction, thermal noise removal, and radiometric correction before sub-swath images were merged. In addition, pre-processing included deburst and speckle filtering to reduce the salt & pepper effect common in SAR imagery (Lee, 1980), multi-looking terrain correction, and the backscatter conversion to sigma nought (σ^0). A window of 7 x 7 pixels was used in the filtering was 7 x 7 as this has been found to provide the best noise reduction performance (Dasari & Anjaneyulu, 2017). The IW mode SAR data consists of three sub-swaths in IW1, IW2 and IW3, which have different incidence angles, ranges, and azimuth look bandwidths. The IW is a primary operational mode for Sentinel-1. Due to, there are compositions with three bursts on one image; thus, there are essential top-deburst data for the continuous images.

The data were radiometrically corrected to backscatter intensity using sensor calibration parameters in IW metadata. To ease processing, the data were resampled to a square grid raster (14.2 m x 14.2 m) and the set range looks, and azimuth looks to 4 and 1, respectively. A terrain correction was performed using the Range-Doppler method (Bayanudin & Jatmiko, 2016) and resampled Shuttle Radar Topography Mission (SRTM) 1 arc second (30 m) Digital Elevation Model (DEM) to integrate the SAR images. The final step is to convert the backscatter power to the backscatter coefficient using logarithm transformation. In principle, the radar backscatter consists of sigma-nought (σ^0), gamma-nought (γ^0), and beta-nought (β^0). Here, we use sigma-nought - σ^0_{VV} and σ^0_{VH} are referred to as VV and VH. A polarisation ratio of VV/VH (cross-ratio) was then calculated using VV and VH backscatter coefficients. The data pre-processing is shown in Figure 5.2. To account for any geometric uncertainty, the backscatter at each sample plot was averaged, which is discussed in more detail in **Section 5.2.6**.

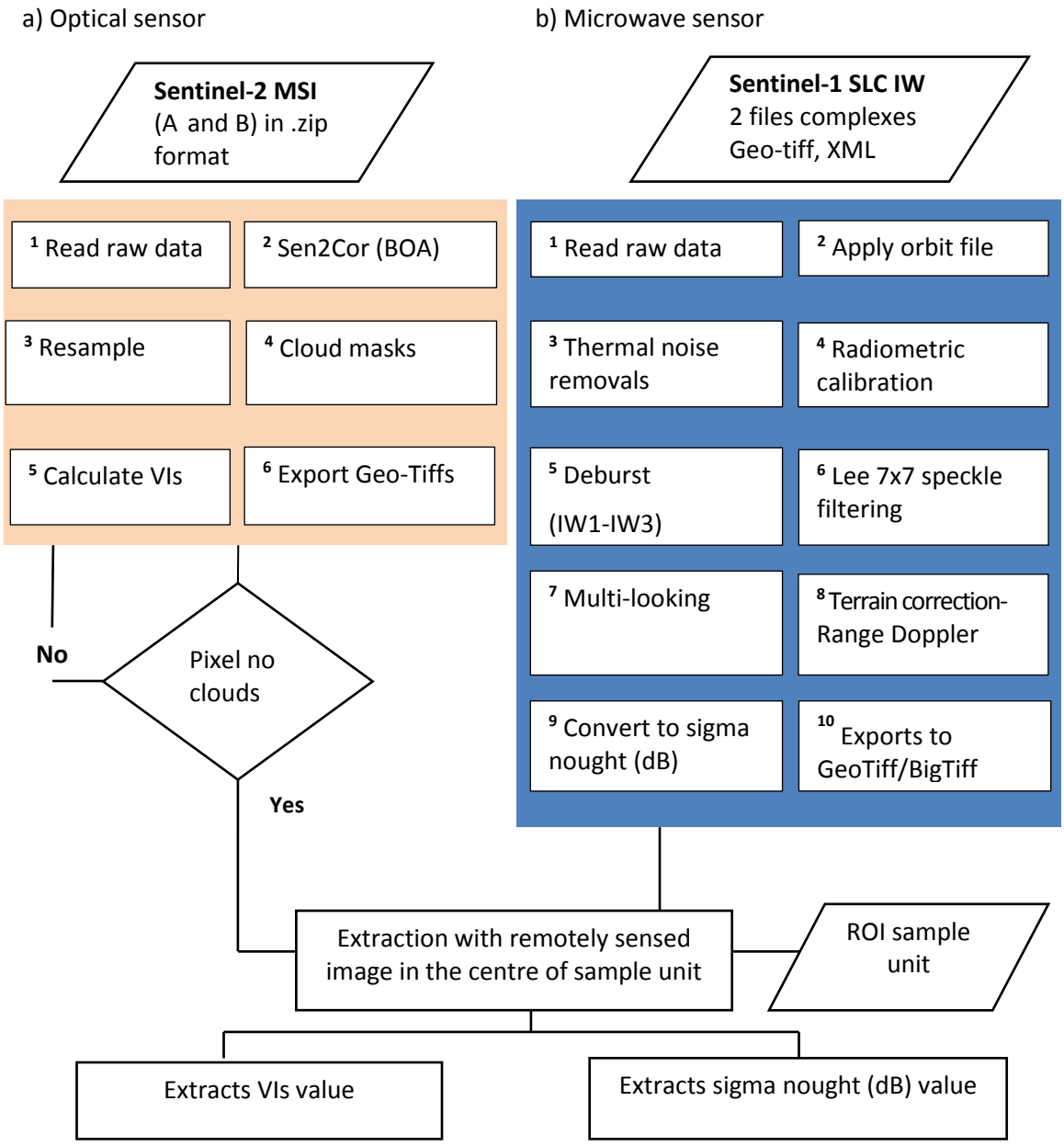

Figure 5.2 Flowchart of the data pre-processing applied satellite image data prior to relating satellite measurements with rice biophysical variables.

5.2.5 Vegetation indices and sigma nought backscatter value extraction (field level) and descriptive statistics

A region of interest (ROI) was drawn around each sampling unit and used to extract the image pixels. These extraction points were made at the sample centre on a pixel basis (~2-4 pixels inside the ROI) to avoid mixed pixels, especially at the paddy field corners. Finally, the vegetation indices (Sentinel-2) and backscatter coefficients (σ^0; Sentinel-1) at each sample plot (field level) were

averaged to provide a sampling site vegetation index and backscatter value for accounting geometric uncertainty.

5.2.6 Satellite data sample site averaging

Generally, the sampling unit consisted of more than one satellite pixel. In this section, we describe the process for calculating the average satellite-derived indicator using the pixels covering each paddy field. Figure 5.2 demonstrates the process using the backscatter coefficient in the ascending VV and VH, and NDVI) from one sampling unit in the panicle stage, which contains 3-4 pixels well within the field boundary to avoid the mixed pixels. The redline is the field boundary whilst the blue ROI is the central pixels which are averaged. The relationship between rice biophysical variables (Chapter 4) and the average vegetation index and backscatter coefficient (σ^0) at each phenological stage was investigated. This temporal analysis aimed to assess the influence of rice variety and irrigation on phenology and rice biophysical variables.

a) Sentinel-2 in NDVI

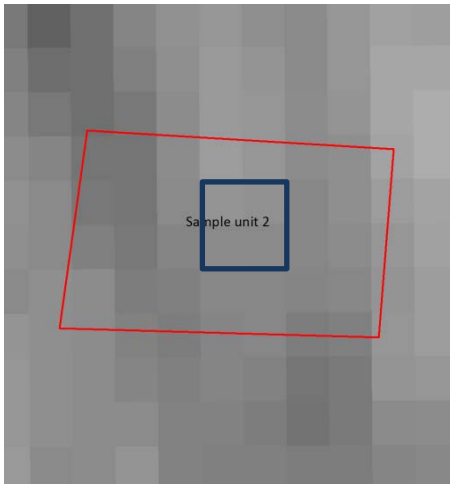

b) Sentinel-1 in ascending VH polarisation

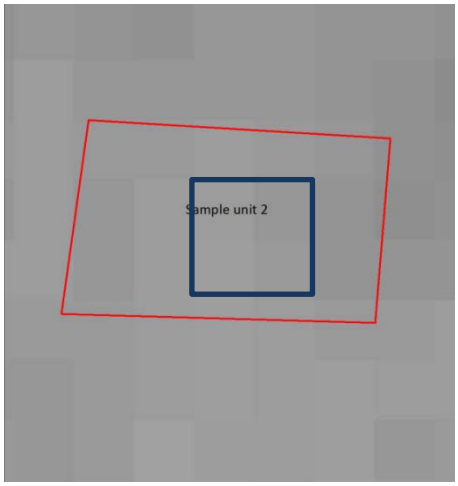

Sample unit	VI		Sigma nought (dB)	
	NDVI	EVI	Ascending VV	Ascending VH
2	*0.63*	0.7	-8.07	*-14.92*
	0.62	0.72	-8.96	*-14.20*
	0.63	0.70	-8.34	*-15.26*
	0.62	0.67	-8.45	*-14.85*
Average	***0.62***	**0.69**	**-8.46**	***-14.81***

Figure 5.3 Example of backscatter coefficients and NDVI subsets showing the locations of the sample points within a sample unit in the panicle stage.

5.2.7 Phenological trends of vegetation indices and backscatter coefficient

Prior to analysing the correlation between the satellite measurements and rice biophysical parameters, an analysis of the temporal dynamics of these metrics was carried out. In general, transplanting occurs from mid-May to the beginning of June, with a tillering stage in the end of June to the beginning of July, the maximum tiller number occurs around the end of July, the heading period in mid-August, and harvesting begins in September and early October. The satellite data were averaged in the sample unit for each growth stage and used to characterise the average rice phenology.

In Phichit, the minimum rice age is 4 days, and the maximum is 104 days, with mean of 62 days. In Ang Thong, the minimum rice age is 9 days and the maximum 104 days, with mean of 61 days. Finally, the minimum rice age in Pathum Thani is 11 days and the maximum of 117 days, with mean of 69 days. Figure 5.4 demonstrates the representative NDVI and backscatter coefficients in a sample unit located in Phichit. The average satellite values in each growth stage are examined and separated by rice variety. In the case of the VIs, the most outstanding values are found in the tillering and panicle stages, with the flowering and harvesting stages being much lower. The trends in the backscatter data are broadly similar in the VV polarised imagery, although increases in the harvesting stage are evident. The cross-polarised data show similar magnitudes between the tillering and flowering stages before decreasing in the harvesting stage.

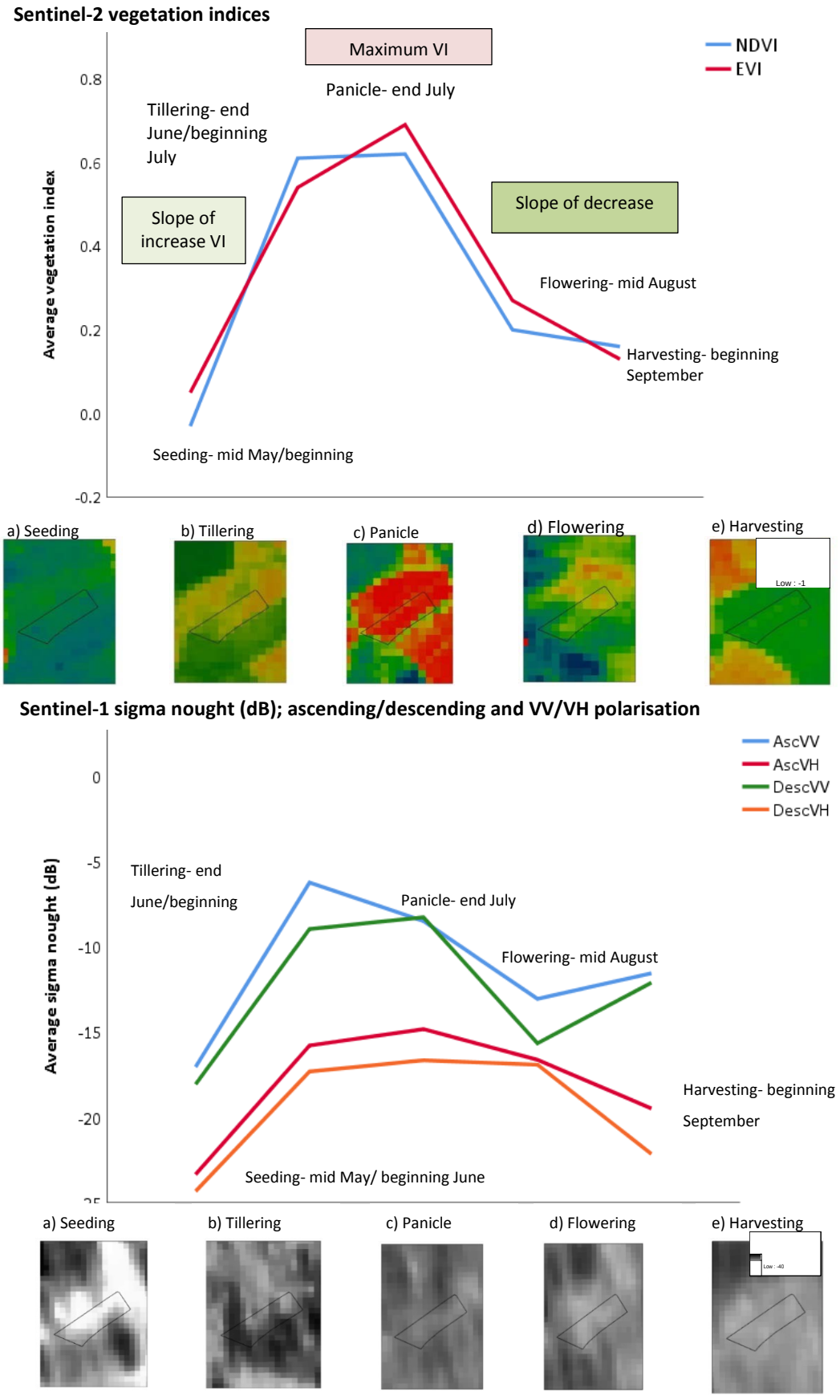

Figure 5.4 Comparisons of the phenological variations of vegetation indices (blue represents NDVI and red represents EVI) and radar backscattering for a selected field in Phichit.

5.2.8 Correlation analysis

The relationship between the satellite and rice biophysical variables was assessed using Pearson's correlation coefficient, which measures their relationship's statistical relationship and direction. The present study used a P-value at 0.05 to define the significance of the relationship. The correlation analysis was applied to rice yield and the satellite measurements- individually separated growth stages, overall growth stages, and irrigated and non-irrigated areas.

5.2.9 Estimation of rice yield using regression analysis

The vegetation indices and backscatter coefficients are set as independent variables in the regression model, whilst rice yield is the dependent variable. The yield data was used to build the yield estimation model derived from field. The previous chapter indicated that RD41 might be suitable for rice yield estimation as it has the largest number of samples. Therefore, the main approach explored to develop a rice yield estimation model using SAR and optical imageries is linear regression between yield, vegetation indices, and backscatter coefficients. In terms of rice yield estimation, a linear regression model was generated at the provincial level:

$$Y = a + bX \qquad \text{Equation 5.3}$$

Where Y is the predicted rice yield (ton/ha) in a given province, a and b are the coefficients, and X is a representative pixel. The simple regression relationships are used to calculate the correlation coefficients (r) of the model between rice yield and VIs or backscatter variables.

Rice-cultivated areas in the three representative provinces were masked in the satellite data using the OAE derived dataset discussed in section 5.2.1.2 and are displayed in Figure 5.5.

a) Phichit

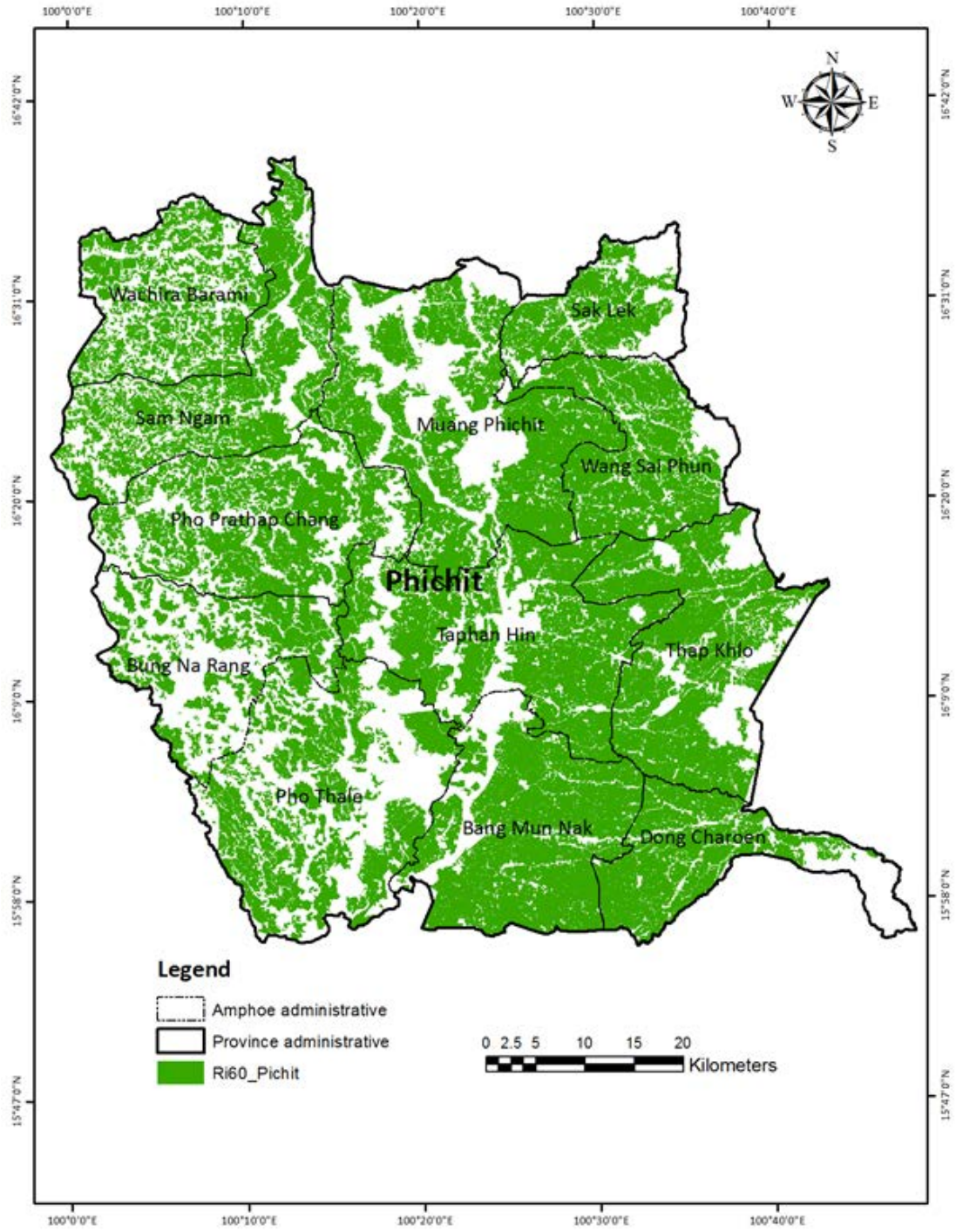
100°0'0"E
100°10'0"E
100°20'0"E
100°30'0"E
100°40'0"E
16°42'0"N
16°31'0"N
16°20'0"N
16°9'0"N
15°58'0"N
15°47'0"N
N
W
E
S
Wachira Barami
Sak Lek
Sam Ngam
Muang Phichit
Wang Sai Phun
Pho Prathap Chang
Phichit
Taphan Hin
Thap Khlo
Bung Na Rang
Pho Thale
Bang Mun Nak
Dong Charoen
Legend
Amphoe administrative
Province administrative
Ri60_Pichit
0 2.5 5 10 15 20
Kilometers

b) Ang_Thong

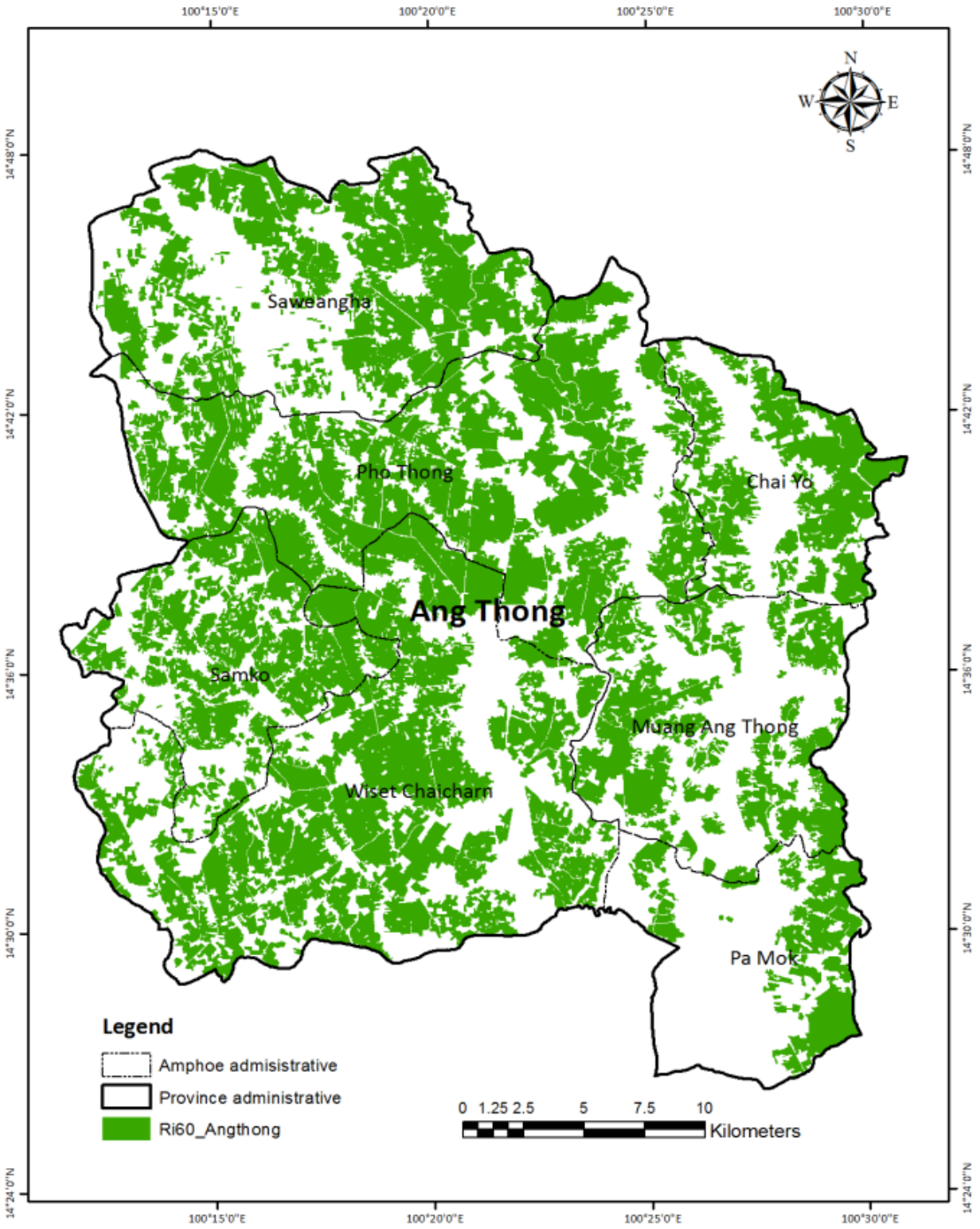
100°15'0"E
100°20'0"E
100°25'0"E
100°30'0"E
14°48'0"N
14°42'0"N
14°36'0"N
14°30'0"N
14°24'0"N
N
W
E
S
Saweangha
Pho Thong
Chai Yo
Ang Thong
Samko
Muang Ang Thong
Wiset Chaicharn
Pa Mok
Legend
Amphoe admisistrative
Province administrative
Ri60_Angthong
0 1.25 2.5 5 7.5 10
Kilometers

c) Pathum Thani

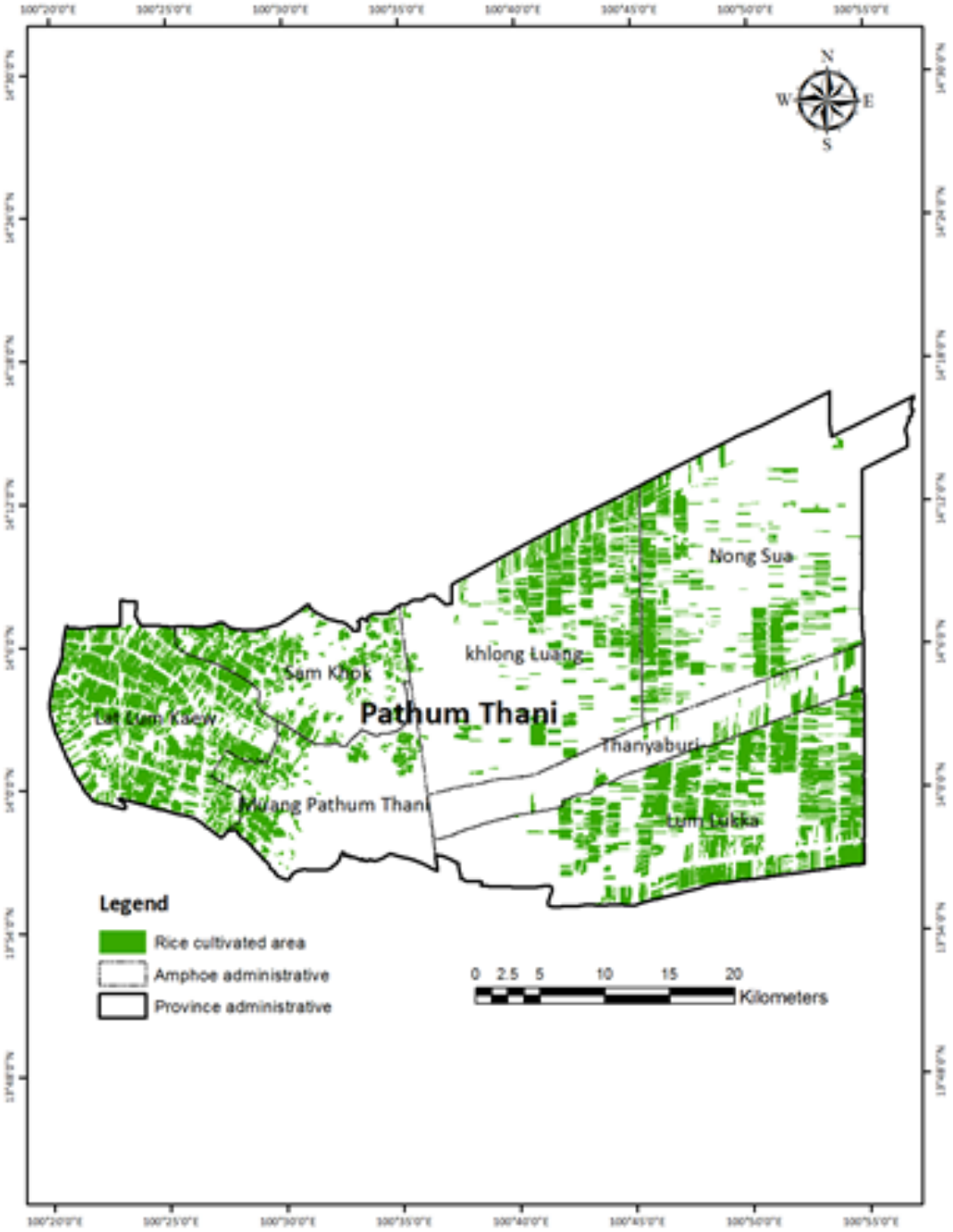

Figure 5.5 Rice cultivated areas in three representative provinces (Phichit, Ang Thong, and Pathum Thani) interpreted with Landsat 8 OLI/TIRS in 2017.

The most appropriate linear regression model was applied to the satellite imagery to derive estimates of rice yield per unit area for each administrative boundary. First, yield estimates were derived at the scale of the administrative boundary by aggregating yield estimates in rice cultivated areas and on a per-pixel basis. These were then aggregated to estimate rice production on the provincial scale (i.e. Phichit, Ang Thong, and Pathum Thani).

5.2.10 Model validation

Data from 2017 were used to assess the accuracy of the model prediction. Rice production was calculated by multiplying cultivated rice area by yield per unit area. Statistical indicators (i.e. root mean square error (RMSE) and mean absolute percentage error (MAPE)) were used to quantify the uncertainty of the predicted values, with the former indicating the variability of the prediction accuracy and the latter the mean or average of absolute error (MAE). The RMSE calculates the average error to measure the differences between estimated and actual yield:

$$RMSE = \sqrt{\frac{\sum_{i=1}^{n}(Y_i - Y_i')^2}{n}} \qquad \text{Equation 5.4}$$

Where n is the number of provinces used for validation, $\hat{y}$ is the estimated yield, and y_i is the observed rice yield.

The MAPE is an accuracy measure of the quality of forecasting model and was calculated via:

$$MAPE = \frac{1}{n}\sum_{i=1}^{n}\left|\widehat{Y}_i - Y_i\right| x\ 100 \qquad \text{Equation 5.5}$$

A flowchart illustrating the methodology for rice yield estimation is presented in Figures 5.6.

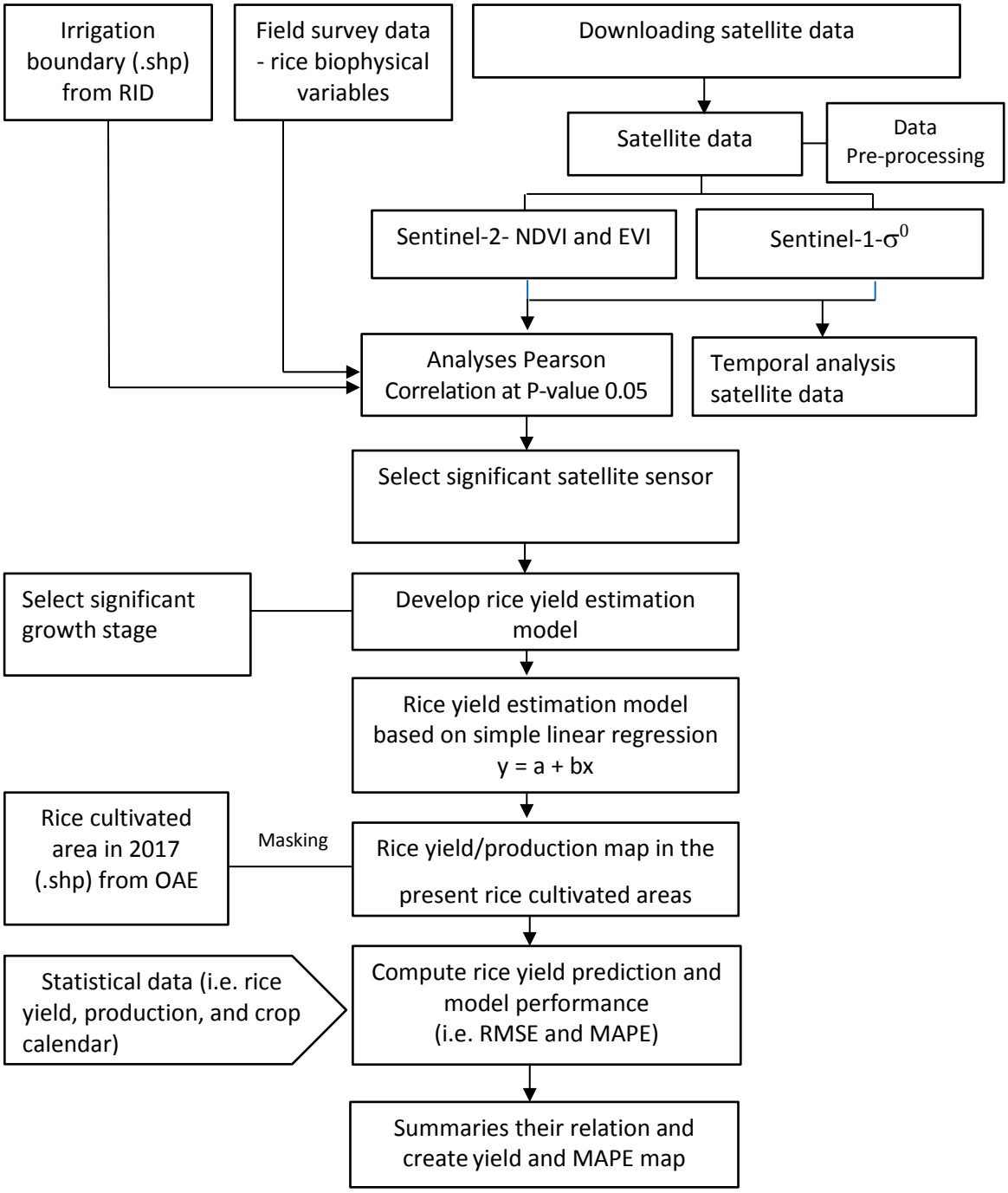

Figure 5.6 Research flowchart analysis.

5.3 Results

Two key objectives were the focus of this research: 1) to assess the potential of EO data for estimating rice biophysical variables and the influence of irrigation method on yield estimation, and 2) to determine the potential of estimating rice yield using rice biophysical variables and EO data. The results of this chapter concern the latter and are divided into four outputs: temporal pattern of vegetation indices and backscatter coefficients; the correlation between satellite measurements

and rice biophysical variables; the potential to estimate rice yield; and finally, validation of the predicted yield estimates.

5.3.1 Pattern of vegetation indices and backscatter coefficients

The research conducted in the previous chapter revealed the dynamics of rice biophysical variables on wet direct seeding. This study analyses the dynamics of vegetation index values and backscatter coefficients during the growing season.

5.3.1.1 Phenological profile of vegetation indices

An analysis of the temporal dynamics of the vegetation indices is presented in this section, characterised by the onset of greenness (SOS) in the seeding stage. Flooding is the main cause of low VI value during the seeding and transplanting stages. The VI values then increase throughout the growing season and peak in the panicle stage before declining in the flowering and harvesting stages, during what is termed the end of greenness (EOS). A summary of the average NDVI and EVI values for all areas (all 22 sampling units), irrigated (16 sampling units), and non-irrigated (6 sample units), is shown in Appendix J. Meanwhile, Figure 5.7 illustrates the temporal variation of the NDVI over a field sample plot during the different stages of plant growth.

The temporal trends in NDVI and EVI for all sites are shown in Figure 5.7. Note that the average is calculated for all sites, which include different rice varieties and irrigation systems.

a) Average NDVI and EVI phenological profiles for all field sites

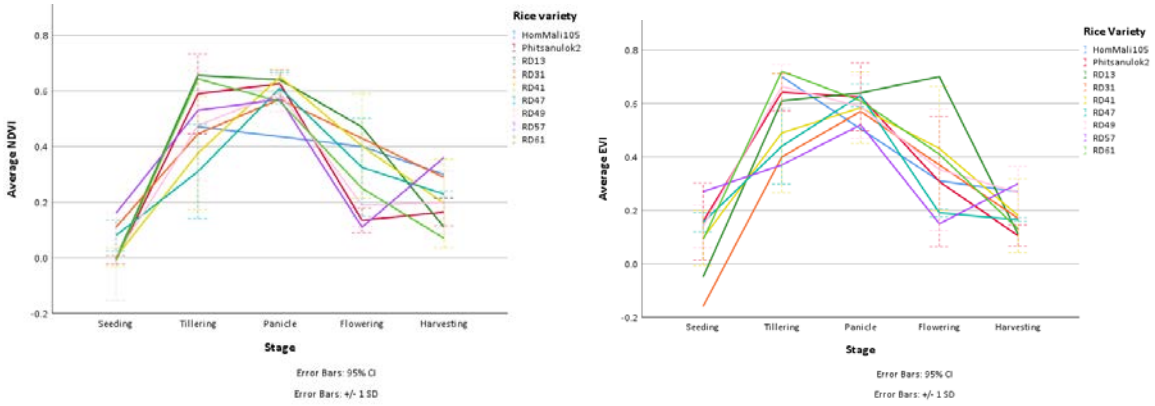

b) Average NDVI and EVI phenological profiles in Phichit

NDVI

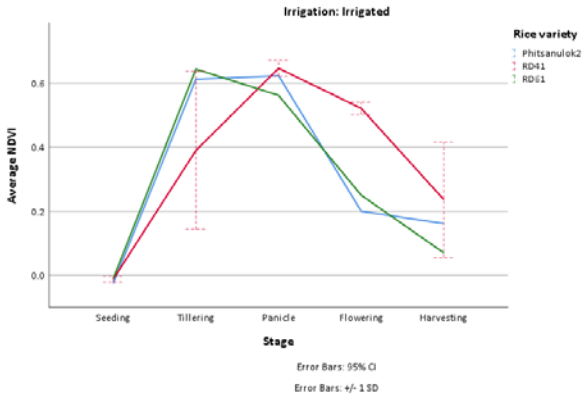

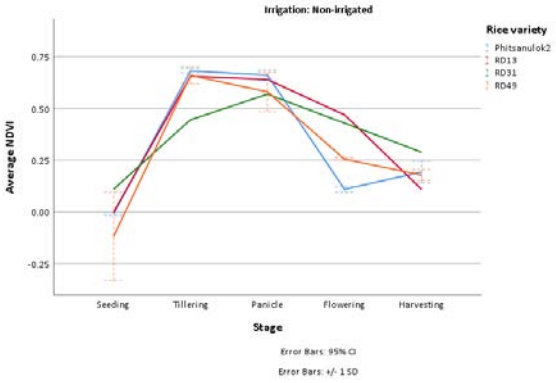

EVI

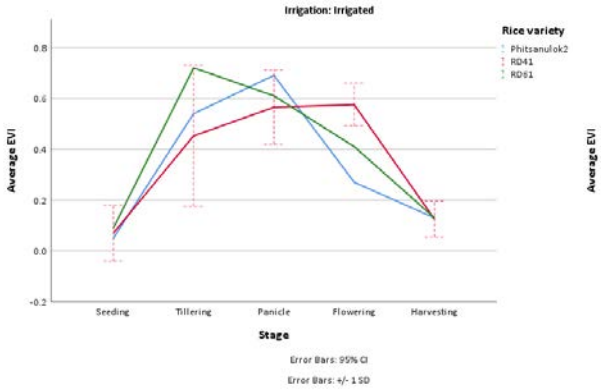

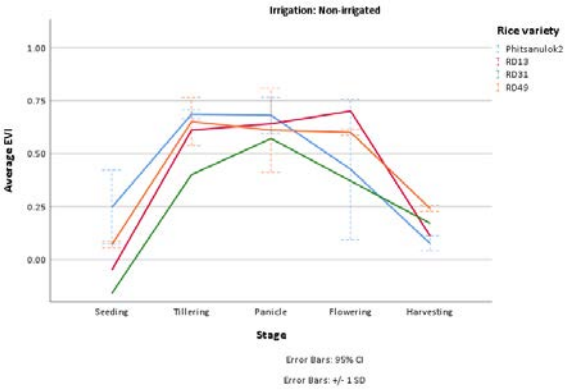

c) Average NDVI and EVI phenological profiles in Ang Thong

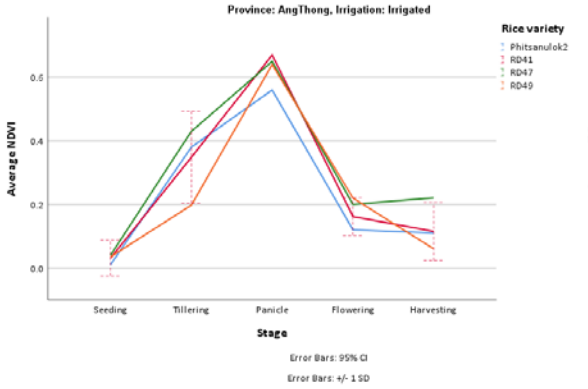

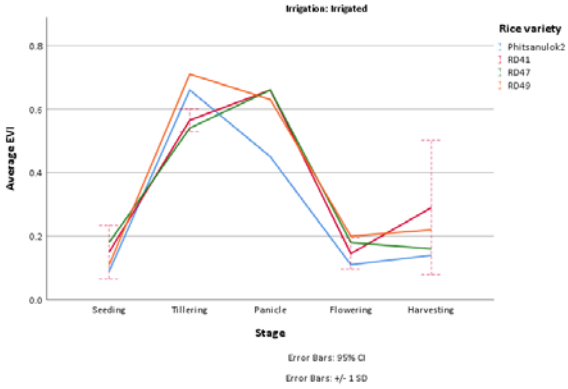

d) Average NDVI and EVI phenological profiles in Pathum Thani

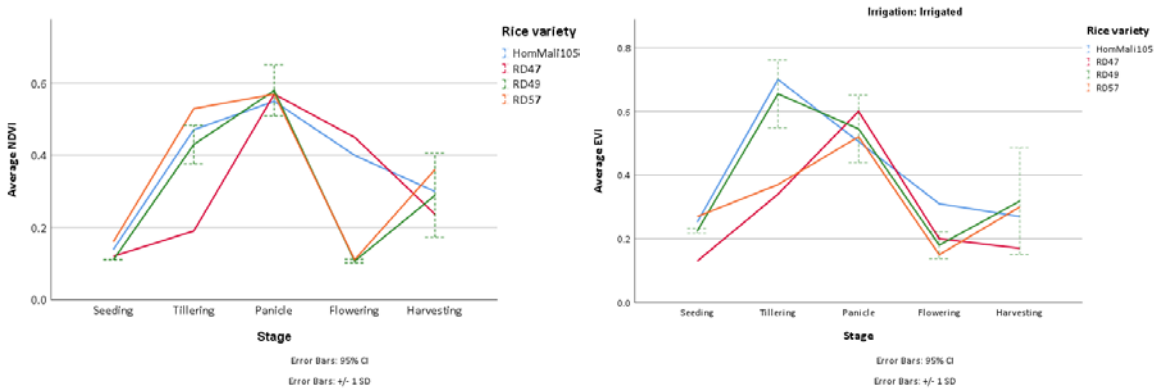

Figure 5.7 Seasonal NDVI and EVI phenological profiles in the study area. a) Average for all field sites, b) Average in Phichit, c) Average in Ang Thong, and d) Average in Pathum Thani.

In general, rice fields are flooded at the onset of rains. In the seeding stage (**DOY 134**), rice is short, and some paddy fields are flooded, which serves to lower VI values (~ 0.03 averages for NDVI and ~0.12 for EVI) due to the influences of the underlying water background. As the rice structure develops (e.g. the height and tiller's rate influenced by stem density, **DOY 180**), the vegetation index values increase (average ~0.47 for NDVI and ~0.57 for EVI) due to increased rice canopy cover and reduced background contribution (soil or water surface). In the panicle stage (**DOY 205-210**), rice develops flag leaves and initiates panicle, resulting in a higher leaf area of healthy green vegetation and consequently the vegetation index peaks in this stage (~0.61 averages for NDVI and 0.6 for EVI). In the flowering stage (**DOY 221**), rice develops into a milky and leaves begin to wither, causing a sudden decrease in NDVI (0.27) and EVI (0.36) values. Rice flowers and wither leaves in the flowering stage may impact the canopy reflectance and also impact both vegetation indices. Finally, the vegetation indices are lowest in the harvesting stage (**DOY 240**) when the rice grain ripens, which reduces the visibility of green leaves, and leaves continue to wither (NDVI ~0.20 and EVI ~0.19). Photographs in Table 4.2 (Chapter 4) highlight the changes in canopy characteristics and photosynthetic elements throughout the growing season that directly influence VI values. However, cloud cover is problematic and leads to fewer observations in the flowering to harvesting stages, coupled with the potential influence of undetected cloud, which may impact the averaging of the VI data.

It is obviously evident from Figure 5.7 that the temporal dynamics of the NDVI and EVI follow a similar trend but still differ, with the dynamics of the NDVI being more pronounced in some cases. For example, the vegetation indices of the Phitsanulok 2 variety in Phichit, which used a different irrigation system and a number of different rice varieties, indicates the NDVI peaked in the tillering stage in the irrigated areas whilst the NDVI peaked in the panicle stage in the non-irrigated areas. These illustrate the influence of irrigation where sufficient water availability

stimulates rice growth earlier. This difference in the peak vegetation indices pattern occurs in the EVI and is found to be slightly higher when compared with NDVI. The EVI is more responsive to canopy structure than the NDVI, therefore more responsive to changes in LAI (Figure 4.12). The EVI displayed better performance from the tillering to panicle stage, as indicated by more constant NDVI between the shifting on these two growth stages. The LAI was primarily high in the flowering stage, whilst vegetation indices tended to be low (NDVI and EVI), which may result from the impact of rice heads obscuring some of the rice leaves or from the increased cloud cover in the flowering stage, which reduced data availability.

In addition to the influences of rice variety, irrigation systems also influence rice development, therefore vegetation index values. Our results reveal that vegetation indices were slightly higher in non-irrigated areas due to differences in LAI (e.g. Table 4.5, Figure 4.12) which tended to be higher, and the use of different rice varieties, which influence the growing season length. It is evident, therefore, that irrigation method and rice variety play an essential role in the phenological cycle of rice, which may need to be accounted for when using satellite observations to monitor and quantify rice growth status.

5.3.1.2 Temporal pattern of backscatter coefficients (σ^0)

The temporal dynamics of the backscatter coefficients (σ^0) were investigated in the same manner as vegetation indices. Several factors influence backscatter behaviour, such as the dielectric constant of vegetation and the surface, leaf size and orientation, surface roughness, and canopy geometry (Agustan et al., 2015; Bamler & Hartl, 1998; Bindlish & Barros, 2001; Koppe et al., 2012; Mc Nairn & Brisco, 2004; Pazhanivelan et al., 2015; Sudarmanian & Pazhanivelan, 2019). This analysis investigated the backscatter coefficients in different orbit directions and polarisations and the ratio between different polarisation (VV/VH). The results indicate less variation in backscatter coefficients throughout the growing season compared with the vegetation indices, which had more pronounced phenological profiles. It is also evident that there are some minor differences in backscatter between ascending and descending orbits, particularly in the seeding stage, where the influence of the plant's vertical structure (rice height) is more apparent (Phan, 2018; Yuzugullu et al., 2017; Zhang et al., 2014). In addition, there are small differences between irrigated areas and non-irrigated areas. The variation of these figures is shown in Figure 5.8.

a) Temporal average backscatter coefficient in overall area

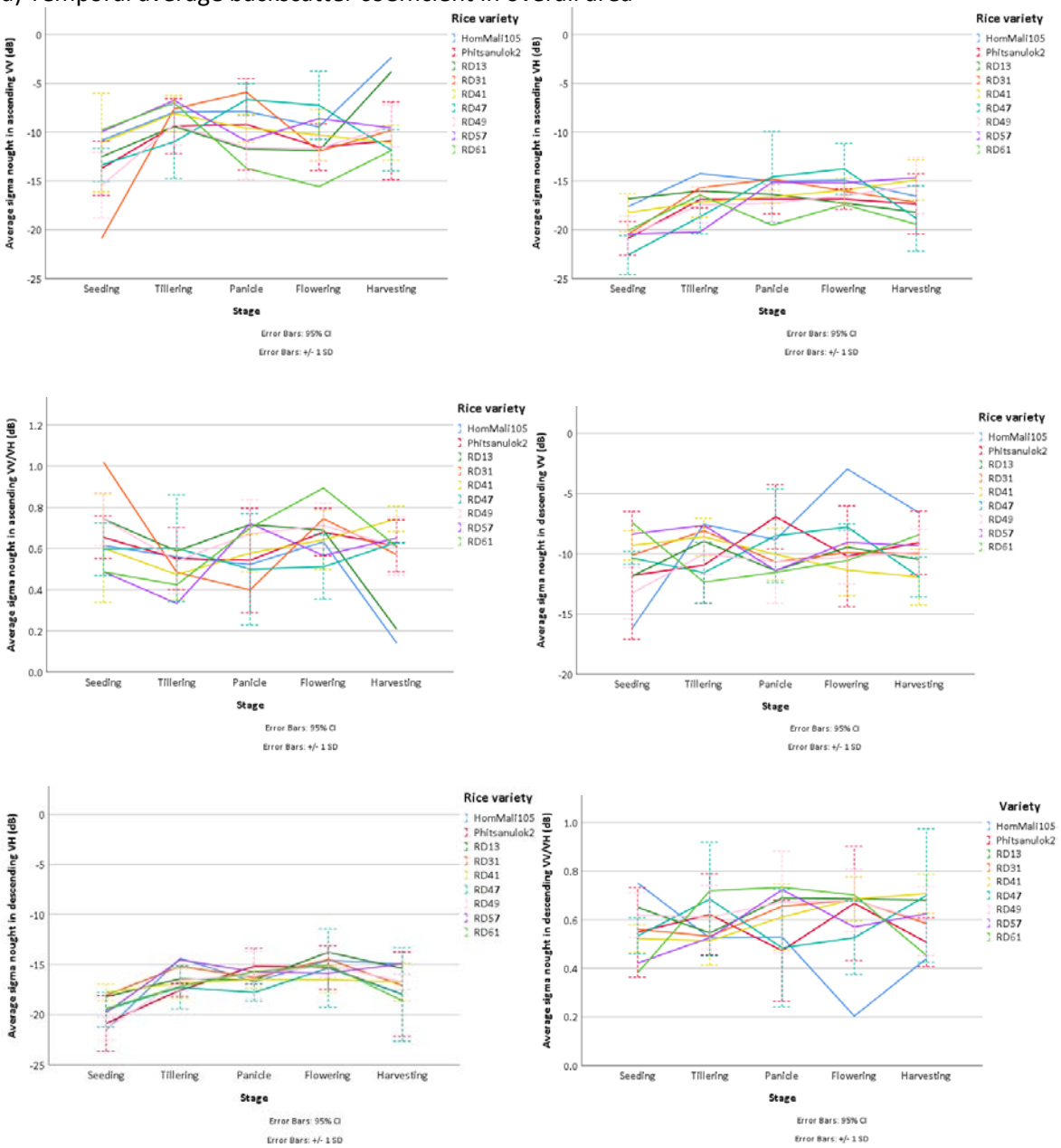

b) Average backscatter coefficient in Phichit

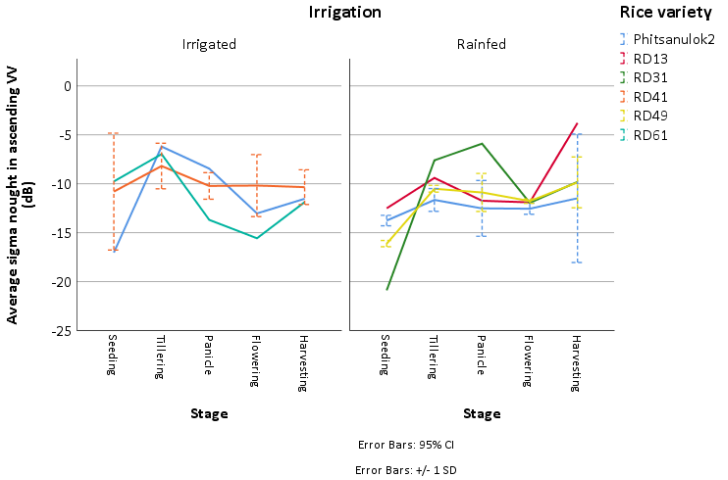

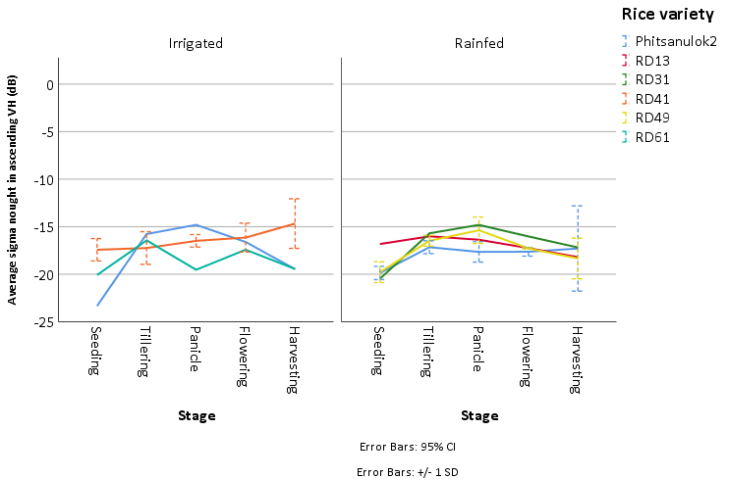
Rice variety
Phitsanulok2
RD13
RD31
RD41
RD49
RD61
Irrigated
Rainfed
Average sigma nought in ascending VH (dB)
0
-5
-10
-15
-20
-25
Seeding
Tillering
Panicle
Flowering
Harvesting
Stage
Error Bars: 95% CI
Error Bars: +/- 1 SD

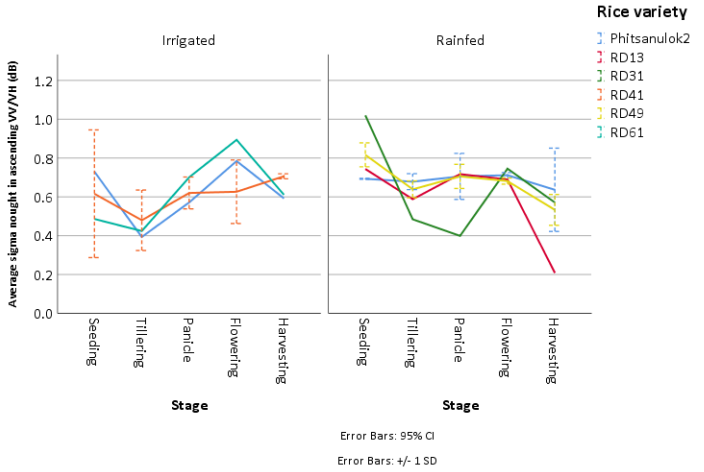
Rice variety
Phitsanulok2
RD13
RD31
RD41
RD49
RD61
Irrigated
Rainfed
Average sigma nought in ascending VV/VH (dB)
1.2
1.0
0.8
0.6
0.4
0.2
0.0
Seeding
Tillering
Panicle
Flowering
Harvesting
Stage
Error Bars: 95% CI
Error Bars: +/- 1 SD

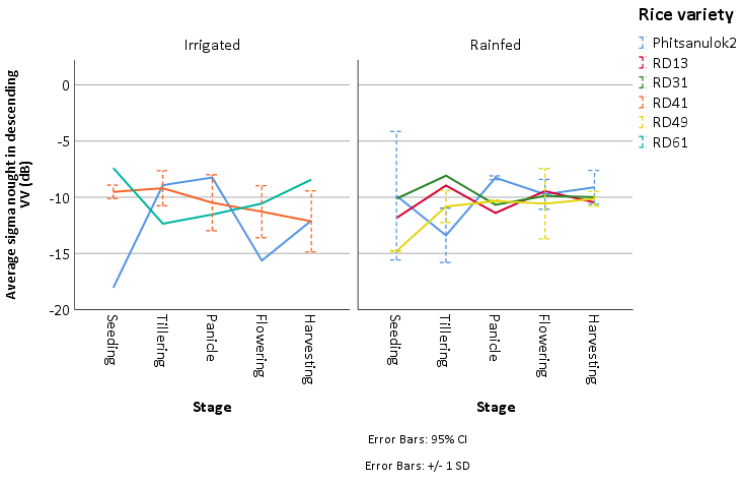
Rice variety
Phitsanulok2
RD13
RD31
RD41
RD49
RD61
Irrigated
Rainfed
Average sigma nought in descending VV (dB)
0
-5
-10
-15
-20
Seeding
Tillering
Panicle
Flowering
Harvesting
Stage
Error Bars: 95% CI
Error Bars: +/- 1 SD

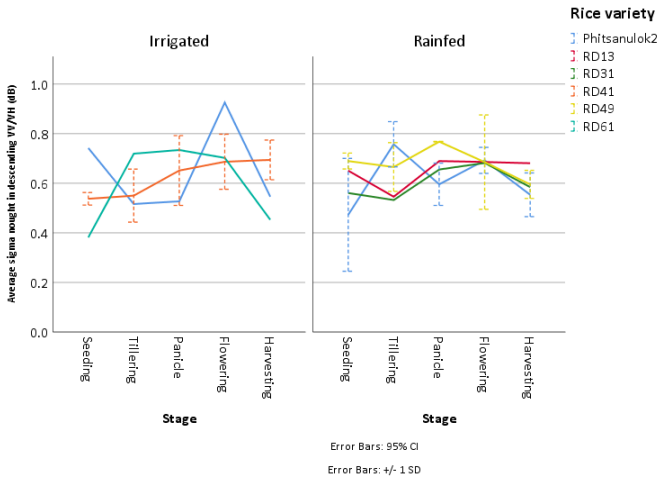

c) Average backscatter coefficient in Ang Thong

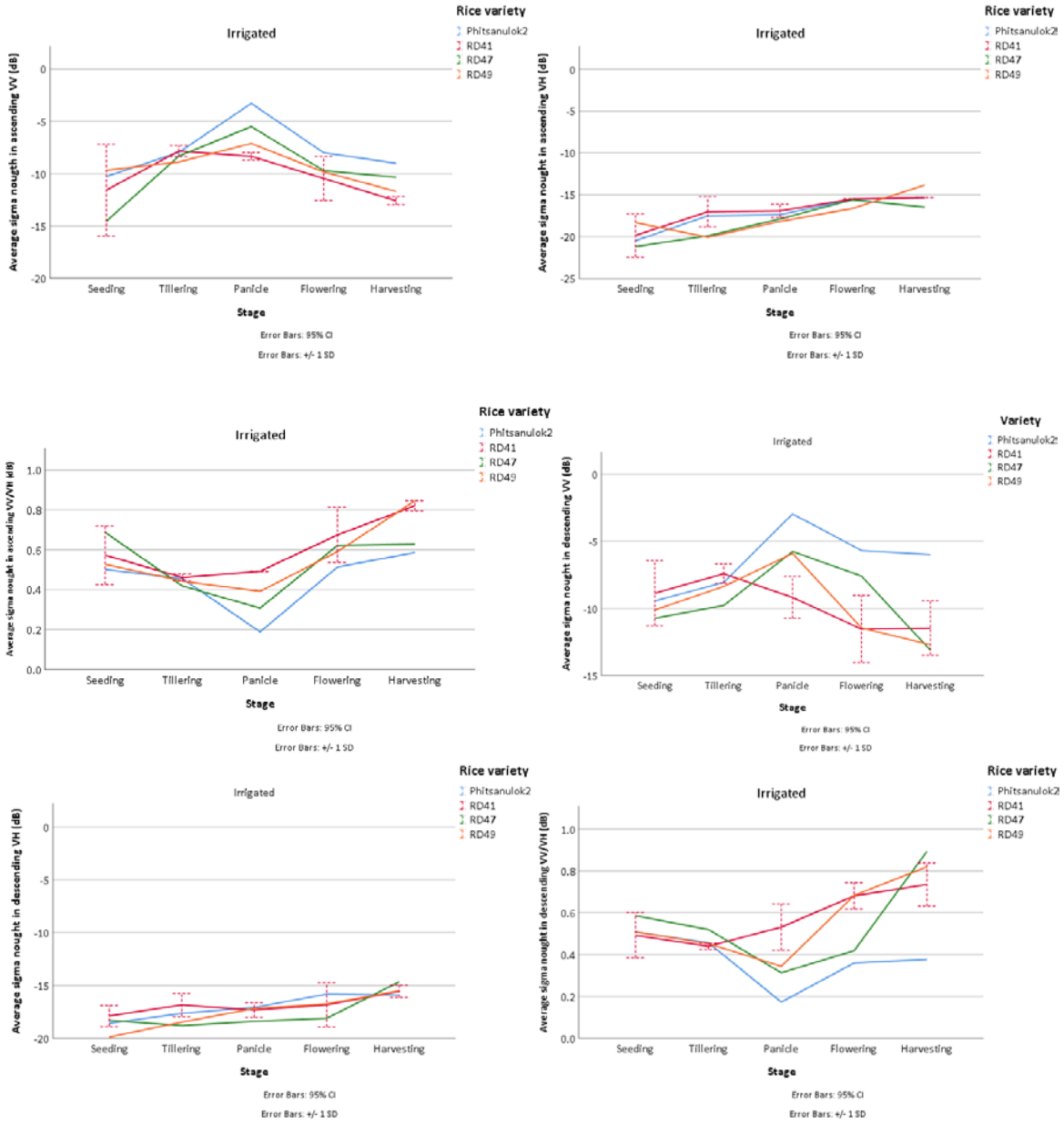

d) Average backscatter coefficient in Pathum Thani

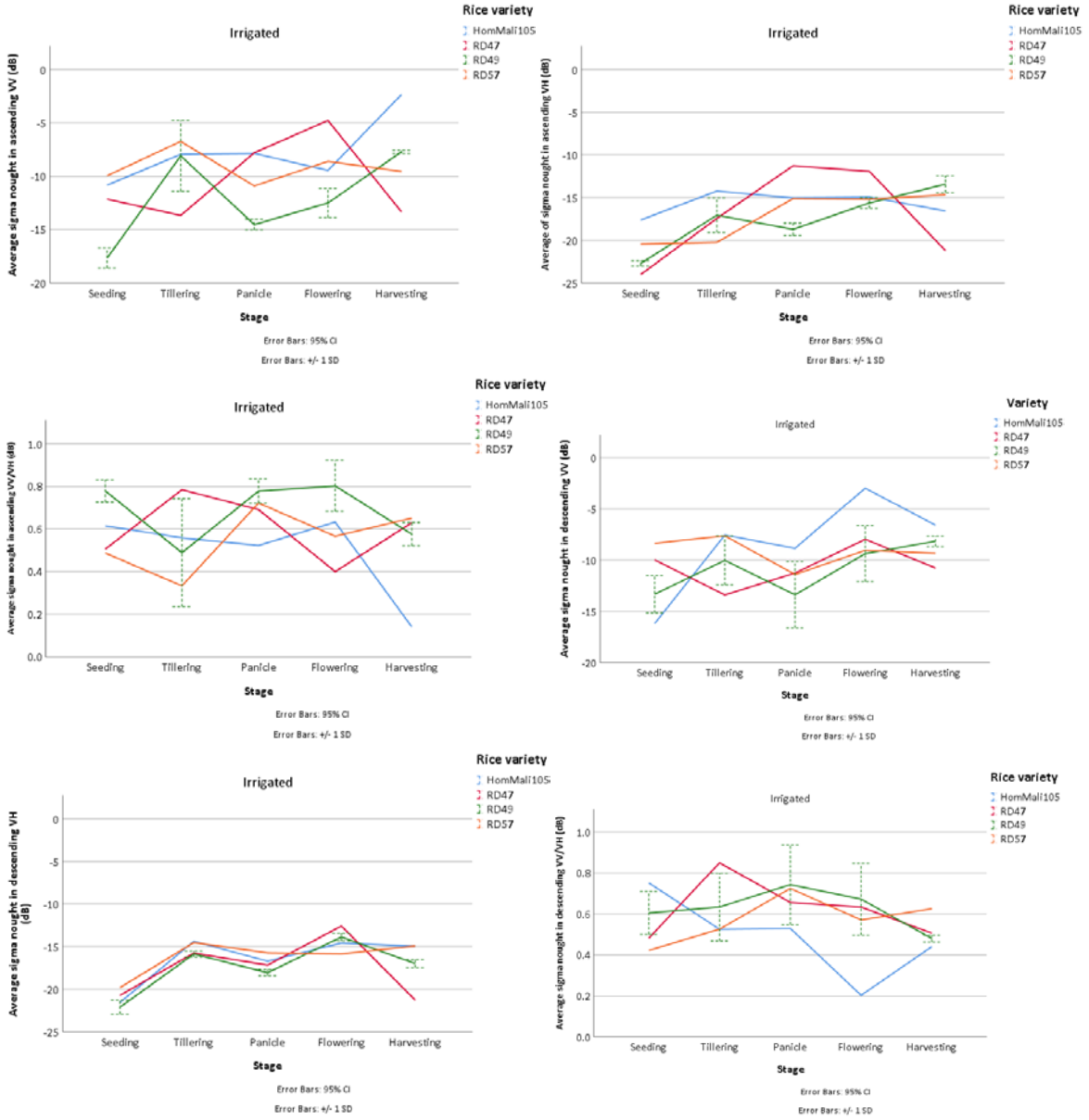

Figure 5.8 Temporal trend in the backscatter coefficients (sigma nought) for different orbital directions and polarisations for: a) Overall area, b) Phichit, c) Ang Thong, and d) Pathum Thani.

Figure 5.8 illustrates the behaviour of the backscatter coefficient (σ^0) in different orbital directions and polarisations over the study area in 2017. The structure of the rice canopy and paddy field background directly influence the backscatter coefficient. The surface scattering characteristic depends on the rice structure, such as the structural, morphological, and dielectric condition of the canopy. Thus, the variability of rice structure impacts rice biophysical variables (Inoue et al., 2014). The scattering mechanism of the vegetation canopy is dominated by the rice canopy's dielectric properties and geometric distribution (Arii, Yamada, Kojima, & Ohki, 2019), which influences backscatter magnitude. The dynamics evident in Figure 5.8 agree with those of Phan et al. (2018), who used X-band SAR in the VV polarisation. Rice plants are transplanted in mid-May,

and paddy fields are flooded (~2.83 cm) several days before transplanting. The dates of panicle initiation, flowering, and maturing stages are mid-July, mid-August, and begin-September. The backscatter coefficient in the sowing/seeding stage pattern reveals low backscatter coefficients due to the smooth ground surface, with a dielectric constant of water and a sparse rice canopy. When vertical rice structure develops and the tiller's rate, the backscatter coefficients increase in the ascending VV, VH, and descending VH. The volume scattering of the rice canopy is characterized by double-bounce scattering between the vertical rice plants and the ground surface. The phenological profile of ascending and descending VH polarised backscatter increased through the growing season, whilst the VV polarised backscatter largely remained flat, which occurs due to the strong attenuation of VV polarised light by vertical stems. Furthermore, the scattering mechanism among grain, stem, and leaf appeared in the late vegetative stage. In terms of dielectric properties, rice grains develop milky, dough (soft and hard dough), and the moisture content influences the backscatter coefficient in the flowering (reproductive stage) and harvesting (grain maturity) stages. The increased canopy density and biomass in the harvesting stage increase VH and VV backscatter. Similar dynamics were found by Bazzi et al. (2019) and Phung et al. (2020), who attributed the variations in volume scattering to changes in biomass and incidence angle.

There was a varying response in the backscatter coefficient as a function of the irrigation system, which had broadly similar magnitudes, but backscatter in VV polarisation decreased in the flowering stage. The VH polarisation proves saturation before the maturity stage, although the reason is uncertain as the vegetation structural parameters (Figures 4.4) and water depth are similar in the panicle and flowering stages. The lowest backscatter is observed within the seeding stage because of specular reflection from the flooded paddies. Meanwhile, the VV/VH signals typically decreased from the late vegetative until the harvesting stage; although some rice variety (HomMali105) suddenly decreased and ceased decreasing after senescence. The dominant pattern for vegetation indices and backscatter is that they vary with the growth stage following this development of the rice canopy. However, the results indicate that agricultural practices and rice variety play an important role which cannot be controlled in the present study.

5.3.2 Correlation between vegetation indices, backscatter coefficients, and rice biophysical variables

5.3.2.1 Correlation of vegetation indices and rice yield biophysical variables

The rice biophysical variables collected in different growth stages were analysed in Chapter 4 to assess the relationship among rice biophysical. In this section, we build on this by analysing the correlation between rice biophysical variables and vegetation indices. The results, shown in Table

5.3 for all areas combined and for each growth stage, is a regression analysis that could be carried out due to the limitation on cloud cover.

Table 5.3 Correlation between vegetation indices and rice biophysical variables in overall area, irrigated areas, and non-irrigated areas across growth stages.

Irrigated system	Stage	Rice biophysical variables	Statistical	Vegetation indices	
				NDVI	EVI
Overall	Panicle	Rice age	Pearson (sig. 2-tailed)	0.13 0.57	**-0.45*** **0.04**
	Flowering	Water depth	Pearson (sig. 2-tailed)	**-0.62**** **0.01**	**-0.59**** **0.01**
		Height	Pearson (sig. 2-tailed)	**-0.52*** **0.03**	0.05 0.83
	Harvesting	Stem density	Pearson (sig. 2-tailed)	**-0.57**** **0.01**	0.05 0.83
		Water depth	Pearson (sig. 2-tailed)	0.42 0.05	**0.47*** **0.03**
		Wet total biomass	Pearson (sig. 2-tailed)	0.30 0.17	**0.45*** **0.04**
		Wet stem biomass	Pearson (sig. 2-tailed)	0.34 0.12	**0.45*** **0.03**
		Dry total biomass	Pearson (sig. 2-tailed)	0.28 0.21	**0.43*** **0.05**
		Dry stem biomass	Pearson (sig. 2-tailed)	0.35 0.11	**0.46*** **0.03**
	Overall growth stage	Rice age	Pearson (sig. 2-tailed)	**0.27**** **0.01**	0.11 0.24
		Height	Pearson (sig. 2-tailed)	**-0.40**** **0.00**	**-0.48**** **0.00**
		Absolute height	Pearson (sig. 2-tailed)	**-0.39**** **0.00**	**-0.49**** **0.00**
		LAI	Pearson (sig. 2-tailed)	-0.21 0.07	**-0.25*** **0.02**

Where *, ** value significant at the 0.05 and 0.01 probability level (2-tailed)

NA No PAR measurement (in seeding stage)

The results shown in Table 5.3 are mixed, which very few variables are a significant correlation with the vegetation index measurements. Overall, three parameters had significant negative relationships with the NDVI: the water depth, rice height, and stem density. In particular, water depth and rice height showed significant negative correlations with the NDVI, while the EVI showed a significant negative correlation between water depth and the EVI in the flowering stage. This is because the monsoons hit the flowering stage and lead to flooding in almost paddy fields because farmers are not releasing water. In the harvesting stage, a negative correlation is found

between stem density and the NDVI; whilst a positive correlation is found in water depth and EVI. Additionally, the wet and dry total and stem biomass are related to EVI in the harvesting stage (~0.45). Finally, the chlorophyll content and LAI tend to be lower in the harvesting stage than in the flowering stage (Figure 4.12-4.13 and Table 4.5-4.6, Chapter 4). The weak correction found between the vegetation indices and chlorophyll content, LAI, and yield are surprising since many studies have found the inverse (e.g. Zhang et al. (2019)) and proved other vegetation index (Normalized Difference Red Edge: NDRE) better performance with agronomic parameters). Gao et al. (2013) proved that the vegetation indices, such as RVI, NDVI, and EVI, were not effective with maize in the heading stage due to the near-infrared reflectance saturation and dense coverage.

5.3.2.2 Correlation of vegetation indices and rice yield biophysical variables

Having assessed the temporal dynamics of the satellite metrics in relation to the rice phenological cycle, the following section presents an analysis of the correlation between satellite data and yield variables. The correlation was performed as a function of the irrigation method, at individual growth stages and across all growth stages. The results are summarised in Table 5.4.

Table 5.4 Correlation between vegetation indices and rice yield in overall area, irrigated areas, and non-irrigated areas across growth stages.

Irrigated system	Stage	Statistical	Vegetation indices	
			NDVI	EVI
Overall	Seeding	Pearson (sig. 2-tailed)	-0.20 0.39	**0.57**** **0.01**
Non- irrigated	Tillering	Pearson (sig. 2-tailed)	0.72 0.11	**0.84*** **0.04**

Where *, ** value significant at the 0.05 and 0.01 probability level (2-tailed)

NA No PAR measurement (in seeding stage)

The best agreement is found in the early rice growth stages, particularly for the EVI and rice yield in the seeding stage in non-irrigated areas. In contrast, more potent (but not significant) correlations are found in between the vegetation indices and yield in the flowering and harvesting stage. It is evident from phenological vegetation index profiles (Figure 5.7) that the vegetation index values at the end of the season, when the rice canopy structure is dense, are lower than those in the seeding stage when the canopy is less developed. It is believed that this is due to the increase in non-photosynthetic material in the canopy, which VIs is not sensitive.

a) EVI in the seeding stage

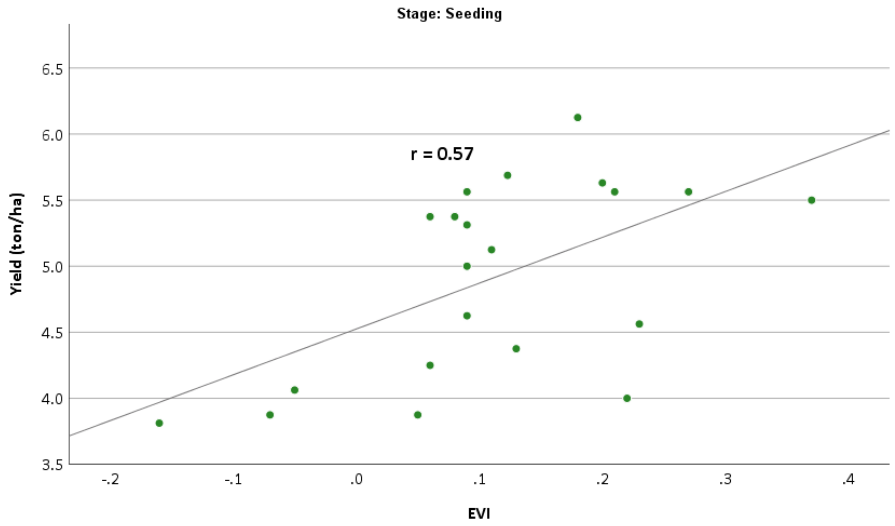

b) NDVI in the panicle stage

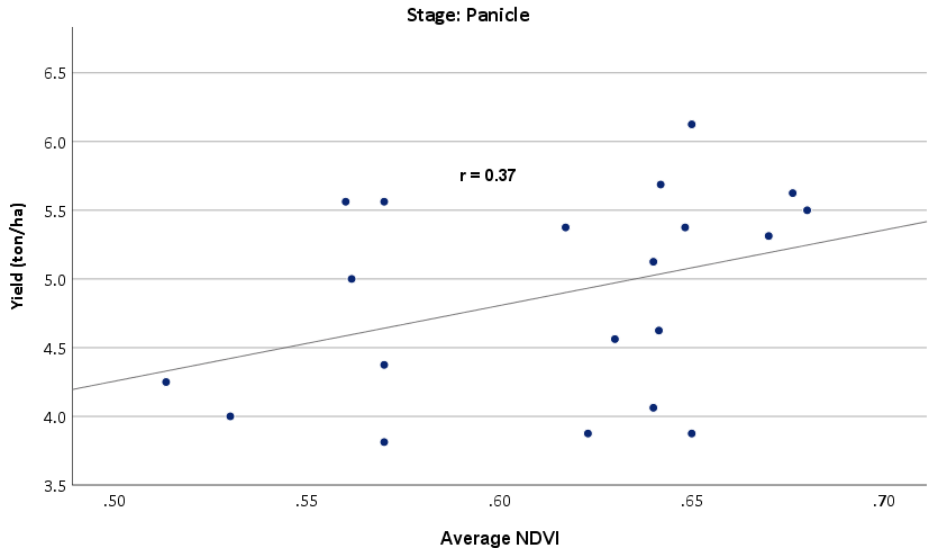

Figure 5.9 Scatter plots between observed rice yield and significant Sentinel-2. a) EVI in the seeding stage and b) NDVI in the panicle stage.

To determine the possible impact of rice variety on the correlation analysis, we carry out a similar analysis but focus on rice varieties with a sufficient number of samples for analysis (Table 5.5).

Table 5.5 Correlation between vegetation indices and rice yield in overall area, irrigated areas, and non-irrigated areas across growth stage specific growth stage.

Irrigated system	Stage	Statistical	Vegetation indice	
			NDVI	EVI
Phitsanulok2	Tillering	Pearson (sig. 2-tailed)	-0.09 0.91	**0.95*** **0.05**
RD41	Seeding	Pearson (sig. 2-tailed)	0.33 0.53	**0.86*** **0.03**

Where *, ** value significant at the 0.05 and 0.01 probability level (2-tailed)

NA No measurement

5.3.2.3 Correlation of SAR (Sentinel-1) backscatter coefficient and yield

A similar analysis to the previous section was carried out using the backscatter coefficient at different polarisations and orbital directions, with the results shown in Table 5.6.

Table 5.6 Correlation between backscatter coefficient and rice biophysical variables in overall areas, irrigated areas only, and non-irrigated areas.

Irrigated system	Stage	Statistical	Backscatter coefficient					
			AscVV	AscVH	AscVV/VH	DescVV	DescVH	DescVV/VH
Overall	Seeding	Pearson (sig. 2-tailed)	0.09 0.68	0.04 0.87	-0.05 0.81	**0.49*** **0.02**	**0.42*** **0.05**	**-0.44*** **0.04**
	Harvesting	Pearson (sig. 2-tailed)	**-0.44*** **0.04**	0.14 0.52	**0.54**** **0.01**	-0.24 0.27	0.21 0.36	0.39 0.07
Irrigated	Seeding	Pearson (sig. 2-tailed)	-0.01 0.96	0.07 0.79	0.09 0.73	**0.62**** **0.01**	**0.65**** **0.01**	-0.49 0.05
	Harvesting	Pearson (sig. 2-tailed)	-0.43 0.10	0.20 0.46	**0.57*** **0.02**	-0.33 0.21	0.28 0.29	**0.50*** **0.05**
Non-irrigated	Tillering	Pearson (sig. 2-tailed)	**-0.88*** **0.04**	-0.62 0.19	**0.90*** **0.02**	-0.70 0.12	-0.80 0.06	0.63 0.18
	Panicle	Pearson (sig. 2-tailed)	-0.47 0.35	-0.42 0.40	0.44 0.38	**0.84*** **0.04**	0.60 0.21	-0.35 0.50

Where *, ** value significant at the 0.05 and 0.01 probability level (2-tailed)

NA meant no PAR measurement (in seeding stage)

Regarding the relationship using all data, the relationship between backscatter and rice yield variables is significant only in the ascending direction for VV and VV/VH polarised data in the harvesting stage with negative (r = -0.44) and positive (r = 0.54) correlations, respectively. Conversely, significant positive and negative correlations are found in the seeding stage for all

descending polarised data (i.e. VV, VH, and ratio VV/VH). Overall, the ascending VV/VH ratio and ascending VV polarisation performed best, with higher correlations with rice yield.

In irrigated areas, significant correlations are found in the seeding stage on descending VV and descending VH with 0.62-0.65 correlation coefficient; however, the ratio VV/VH in both ascending and descending is 0.57 (ascending VV/VH) and 0.5 (descending VV/VH). In contrast, correlations found in non-irrigated areas had stronger relationships, but the strength of the relationship differed with polarisation. Finally, the tillering and panicle stage is significant, with rice yield in the non-irrigated areas for ascending VV and ascending VV/VH with -0.88 and 0.90 in the tillering stage. Meanwhile, the correlation coefficient in the panicle stage appears in the descending VV in the panicle stage (r = 0.84). These differences could be due to the sensitivity to volume scattering from rice canopy. In the vegetative phase, the backscatter coefficient in VH increased due to an increase in rice density and height, increasing double-bounce scattering between rice canopy and underlying surface. However, the VV backscatter gradually increased due to the impact of extinction on the vertical element of rice structure and orientation (e.g. stems and leaves). In the reproductive phase, the VH increased due to the denser plant canopy and the emergence of rice heads. The water content in rice heads has less impact on the vertical extinction and orientation of rice components; however, the VV polarised backscatter is reduced due to decreasing rice in the cylinder pattern (He et al., 2018).

a) Descending VV in the seeding stage

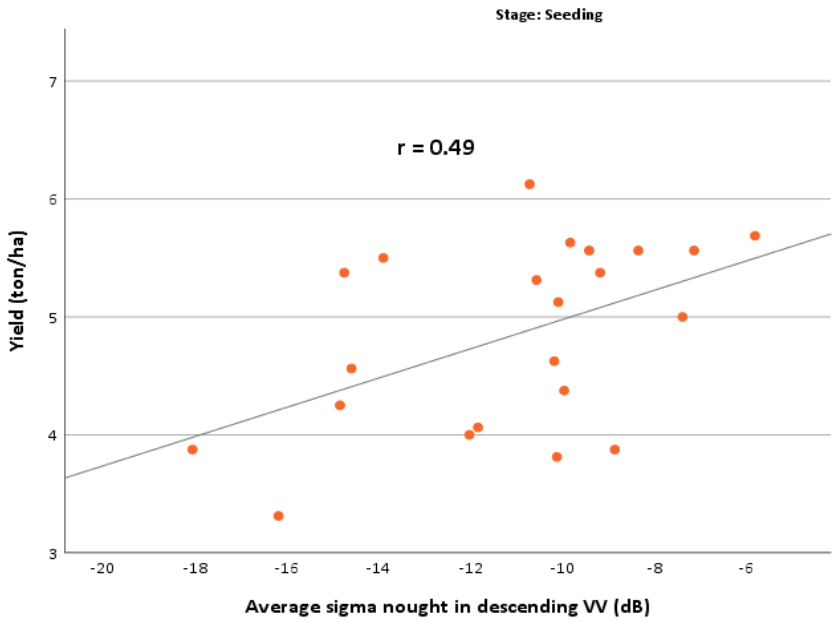

b) Ascending VV/VH in the harvesting stage

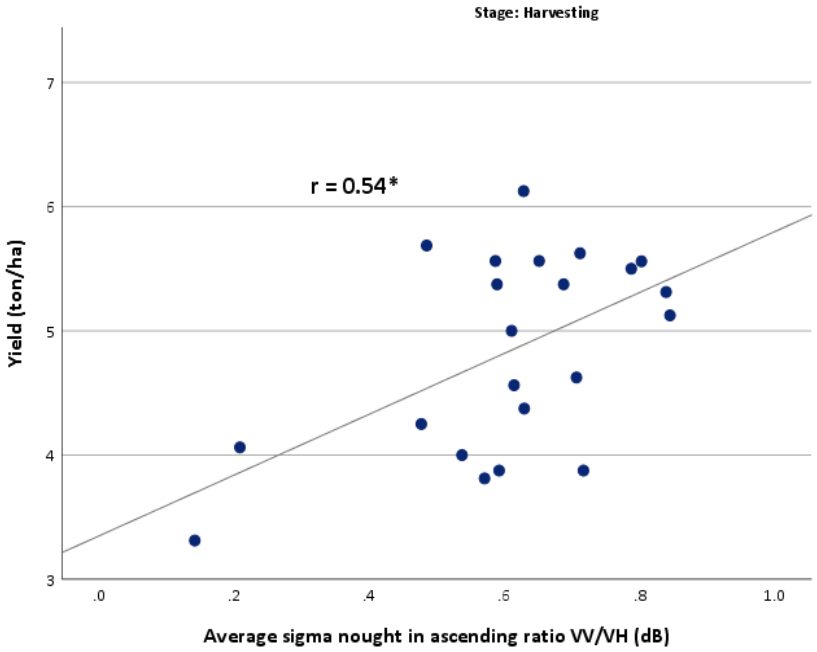

Figure 5.10 Scatter plots between observed rice yield and significant Sentinel-1. a) Descending VV in the seeding stage and b) Ascending VV/VH in the harvesting stage.

Table 5.7 shows the relationship for the most dominant rice varieties (i.e. Phitsanulok2, RD41, and RD49).

Table 5.7 Correlation between backscatter coefficients and rice biophysical variables in all areas, irrigated areas only, and non-irrigated areas sepreated rice varieties.

Irrigated system	Stage	Statistical	Backscatter coefficient					
			AscVV	AscVH	AscVV/VH	DescVV	DescVH	DescVV/VH
Phitsanulok2	Seeding	Pearson	0.79	**0.98***	-0.47	0.84	0.86	-0.76
		(sig. 2-tailed)	0.21	**0.02**	0.53	0.17	0.14	0.24
RD41	Flowering	Pearson	0.14	**0.81***	0.12	0.49	0.55	-0.37
		(sig. 2-tailed)	0.80	**0.05**	0.82	0.33	0.25	0.47
RD49	Seeding	Pearson	0.46	0.83	-0.12	0.08	**0.92***	0.22
		(sig. 2-tailed)	0.44	0.09	0.85	0.90	**0.03**	0.72
	Harvesting	Pearson	**-0.94***	-0.45	0.61	-0.77	0.51	0.74
		(sig. 2-tailed)	**0.02**	0.45	0.28	0.13	0.38	0.15

Where *, ** value significant at the 0.05 and 0.01 probability level (2-tailed)

NA meant no PAR measurement (in seeding stage)

Only three significant relationships were found between backscatter and yield, which were different regarding backscatter polarization and the growth stage. The results indicate that no growth stage or backscatter polarization performs with any consistency with moderate and weak negative and positive (non-significant) correlations in the majority of cases. The best results were found using the ascending orbit data and VV/VH backscatter ratio in the harvesting stage and this will be used to develop a linear regression model.

5.3.3 Develop simple linear regression model

Regression analysis analyses the relationship between one variable (set as a dependent variable) and a series of variables (set as independent variables). The following section describes the development of a simple linear regression model by setting the vegetation indices, and backscatter coefficients as independent variables and rice yield at a provincial level as the dependent variable. The best results found using the NDVI were in the panicle stage and for the EVI in the seeding stages, and these data were used to develop the regression model, detailed in Appendix J.

Referring to the EVI, the B value indicates that a difference of one unit increases approximately 3.469 tonnes of rice production, and the constant value is 4.525, which is significant in the seeding stage. Conversely, the NDVI identifies a difference of one unit result in their pixel 5.497 tonnes and constant 1.508 in the panicle stage. The Sentinel-1 SAR in the ascending and ratio of VV/VH polarisation and specific in the harvesting stage. The B value indicates that a difference of one unit increases approximately 2.447 tonnes of rice production based on the ascending ration VV/VH. The constant value is 3.351, which is significant in the harvesting stage. The rice yield model for the vegetation indices and backscatter is shown in Table 5.8.

Table 5.8 Model expression based on a simple regression model based on different remotely sensed data.

Factor	Growth stage	Model expression on rice yield predicted model	R	R^2	Std. error of estimation (SEE) (ton/ha)
Sentinel-2 optical					
- EVI	Seeding	Y = (EVI*3.469) +4.525	0.57	0.32	0.62
- NDVI	Panicle	Y = (NDVI*5.497) +1.508	0.37	0.14	0.70
Sentinel-1 SAR ascending VV/VH	Harvesting	Y = (ascending VV/VH*2.447) +3.351	0.54	0.29	0.68

Table 5.8 reveals the results from the linear regression models. The standard error of estimation (SEE) for the EVI and NDVI is 0.62 and 0.70 tonnes/ha, respectively, whilst the regression model found using the backscatter data (ascending VV/VH polarised data) has a SEE of 0.68 tonnes/ha. The SEE is similar for both the radar and optical data, suggesting neither outperforms the other, although an advantage of radar data is its all-weather capability. The simple linear regression models developed using SAR data performed better than optical data, and these use to estimate yield for other rice varieties and booting stage/maturity/ripening stage is advantages of yield estimation.

a) Panicle stage (booting and heading stage)

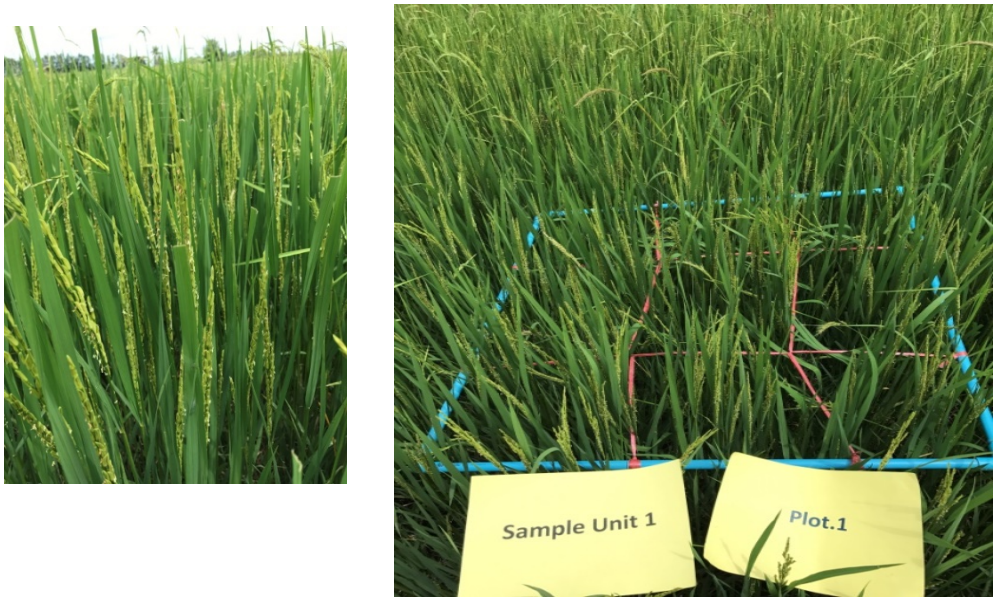

b) Harvesting (maturity) stage

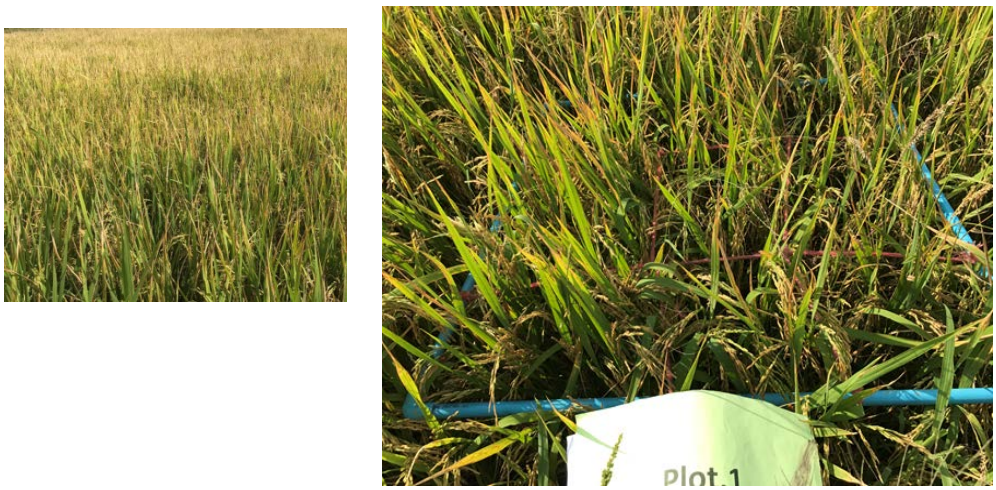

Figure 5.11 Photos of sample fields in the panicle (booting and heading) and harvesting (maturity) stage (example sample unit 1 in Phichit).

The figure 5.11 demonstrates that rice culms and grain development varied in the different growth stages. In the panicle stage, rice develops its flag leaf and initiates grains. The rice culms are vertical, and the green leaves suggest high chlorophyll content. This relationship is related to spectral reflectance (NDVI ~0.61 and EVI ~0.6), which is not saturated NDVI in this growth stage. The other critical growth stage for yield estimation is the harvesting stage. The vegetation indices have low values (NDVI ~0.2 and EVI ~0.1) due to lower chlorophyll contents and increased senescent material. Conversely, rice grains are hard dough and nearly to harvest if the moisture contents reach the standard.

5.3.4 Validation of yield estimates derived using the simple regression model

The regression models described in Table 5.8 are applied to satellite data to estimate yield across three provinces and which is validated using official yield data from 2017. The results are shown in Table 5.9.

Table 5.9 Accuracy assessments on a simple regression model based on ascending VV/VH and government's yield statistic in 2017.

Province/Amphoe	Government statistic yield (tonnes/ha)	EVI in seeding		NDVI in panicle		AscendingVV/VH in harvesting	
		Forecasting yield (tonnes/ha)	MAPE (%)	Forecasting yield (tonnes/ha)	MAPE (%)	Forecasting yield (tonnes/ha)	MAPE (%)
Phichit	**3.77**	**5.33**	**68.82**	**3.32**	**9.0**	**4.72**	**52.34**
- Bang Mun Nak	3.88	5.37	94.00	2.89	4.28	4.64	67.74
- Bung Na Rang	3.97	5.48	46.56	3.90	4.25	4.88	30.50
- Dong Chareon	3.39	5.26	64.60	3.16	1.08	4.65	45.48
- Muang Phichit	3.98	5.24	80.63	3.14	8.38	4.75	63.73
- Pho PrathapChang	3.84	5.28	74.11	3.71	22.43	4.86	60.25
- Pho Thale	4.09	5.32	17.10	3.97	12.54	4.84	6.59
- Sak Lek	3.08	5.18	131.29	2.56	14.50	4.55	103.27
- Sam Ngam	3.74	5.33	56.08	3.46	1.28	4.78	39.94
- Taphan Hin	4.09	5.62	77.30	3.29	3.96	4.73	49.31
- Thap Khlo	3.48	5.13	75.18	3.38	15.81	4.60	57.79
- Wachira Baramee	3.51	5.30	30.38	3.48	14.44	4.70	53.91
- Wang Sai Phun	3.42	5.51	78.16	2.94	4.99	4.63	49.55
Ang Thong	**4.16**	**5.59**	**93.53**	**4.45**	**62.14**	**4.87**	**71.88**
- Chai Yo	3.84	5.56	77.31	4.41	40.74	4.87	55.39
- Muang Ang Thong	4.12	5.53	56.65	4.35	23.21	4.76	34.82
- Pa Mok	3.80	5.70	440.98	4.34	311.64	4.79	354.82
- Pho Thong	4.13	5.62	26.47	4.47	0.58	4.94	11.04

Province/Amphoe	Government statistic yield (tonnes/ha)	EVI in seeding		NDVI in panicle		AscendingVV/VH in harvesting	
		Forecasting yield (tonnes/ha)	MAPE (%)	Forecasting yield (tonnes/ha)	MAPE (%)	Forecasting yield (tonnes/ha)	MAPE (%)
Ang Thong (Cont.)							
- Samko	4.24	5.52	17.62	4.70	29.83	5.00	25.35
- Sawangha	4.31	5.85	2.56	4.61	23.18	4.88	18.77
- Wiset Chaichan	4.12	5.36	33.11	4.26	5.81	4.83	2.98
Pathum Thani	**4.49**	**5.94**	**21.96**	**3.96**	**26.99**	**4.86**	**18.29**
- Khlong Luang	4.58	5.88	5.06	4.05	27.73	4.85	13.41
- Lam Luk Ka	4.50	5.90	28.77	3.80	17.04	4.87	6.26
- Lad Lum Kaeo	4.63	6.17	22.78	3.83	23.80	4.84	3.81
- Muang Pathum Thani	4.31	5.67	1.77	3.97	28.73	4.85	12.88
- Nong Suea	4.34	5.94	21.33	4.07	46.09	4.90	35.10
- Sam Khok	4.47	6.12	67.74	3.99	9.47	4.87	33.51
- Thanyaburi	4.51	5.93	6.25	4.04	36.10	4.86	23.07

Table 5.9 illustrates the MAPE in the amphoe; then, the average MAPE at the provincial level. The MAPE calculates from the absolute error of the differences between official yield and forecast yield (significant satellite in specific growth stage). The square error of absolute error is further analysed for the RMSE and MAPE, which is calculated from mean absolute error (MAE) and converted to percentage values. It is clear from the table that the vegetation index estimated yield is overestimated in nearly all cases with the MAPE ranging between 5.13 and 6.17 for the EVI and It is clear from the table that the vegetation index estimated yield is overestimated in nearly all cases, with the MAPE ranging between 1.77 to 440.98% for the EVI and 0.58 to 311.64 for the NDVI. The NDVI has a lower average MAPE (32.71%) compared to the EVI (61.44%) over all amphoes.

In the case of the EVI, the average satellite-derived yield in Phichit, Ang Thong, and Pathum Thani is 5.33, 5.59, and 5.94 tonnes/ha, which compares to the average government yield estimates of 3.77, 4.16, and 4.49 tonnes/ha, respectively. Consequently, the average MAPE of the EVI-derived yield estimates in Phichit, Ang Thong, and Pathum Thani is 68.8%, 93.5%, and 21.9%, respectively. The NDVI performs slightly better with average estimated yield in Phichit, Ang Thong, and Pathum Thani of 3.32, 4.45, and 3.96 tonnes/ha, respectively, compared to the average government yield estimates of 3.77, 4.16, and 4.49 tonnes/ha, respectively. As a result, the RMSE and MAPE (in brackets) in the following provinces are 82.82 tonnes (9%), 6,805 tonnes (62.1%), and 10,899 tonnes (26.9%), respectively. Finally, the yield estimated using the VV/VH backscatter data provides estimates ranging between 4.57 and 5 tonnes/ha. The average MAPE of the yield estimates in Phichit, Ang Thong, and Pathum Thani is 52.34%, 71.88%, and 18.29%, respectively.

Table 5.9 is a result of applying the developed rice yield estimation model based on simple linear regression to the output of masking rice areas using the raster calculator function. Then, the results are clipped into the amphoe level and summation the rice yield at the same administrative level. The rice yield forecasting based on the Sentinel-1 in the ascending in the ratio of VV/VH polarisation in the Phichit, Ang Thong, and Pathum Thani is 4.72, 4.87, and 4.86 tonnes/ha, respectively. Then, rice yield applies to the rice production in these provinces. The results are also revealed the overestimation of rice yield for all provinces. The rice production from the yield estimation model and official rice production (in brackets) in the Phichit, Ang Thong, and Pathum Thani is 1,301,420 tonnes (876,596 tonnes), 236,964 tonnes (230,547 tonnes), and 204,240 tonnes (223,167 tonnes), respectively. The RMSE perform better in the rice irrigated areas with less variance on the backscatter (Figure 5.8). The MAPE is calculated to compare actual rice yield and forecasts rice yield for percentage error estimation. The result of the MAPE in the Phichit, Ang Thong, and Pathum Thani is 52.34%, 71.88%, and 18.29%, respectively. The output of rice

cultivated areas may be some mix-pixels classification of OAE spatial data. Obviously, some provinces have higher MAPE values such as Sak Lek, Bang Mun Nak, and Muang Phichit (in Phichit) and Chaiyo, Pa Mok (in Ang Thong). Conversely, the MAPE is slightly lower MAPE (<35%) and suitable to estimate yield. The latter is essential for the delivery of timely and accurate agricultural information derived from remotely sensed images for mid-season yield forecasts of the national rice production, which is beneficial for agriculture resource management, food security, and agricultural policy formulation. The MAPE is illustrated into the amphoe level in each province to recognize easy the error of the yield estimation model based on the NDVI in the panicle stage and the ascending ratio of VV and VH polarisation in the harvesting stage as shown in Figure 5.12-5.13.

a) Phichit

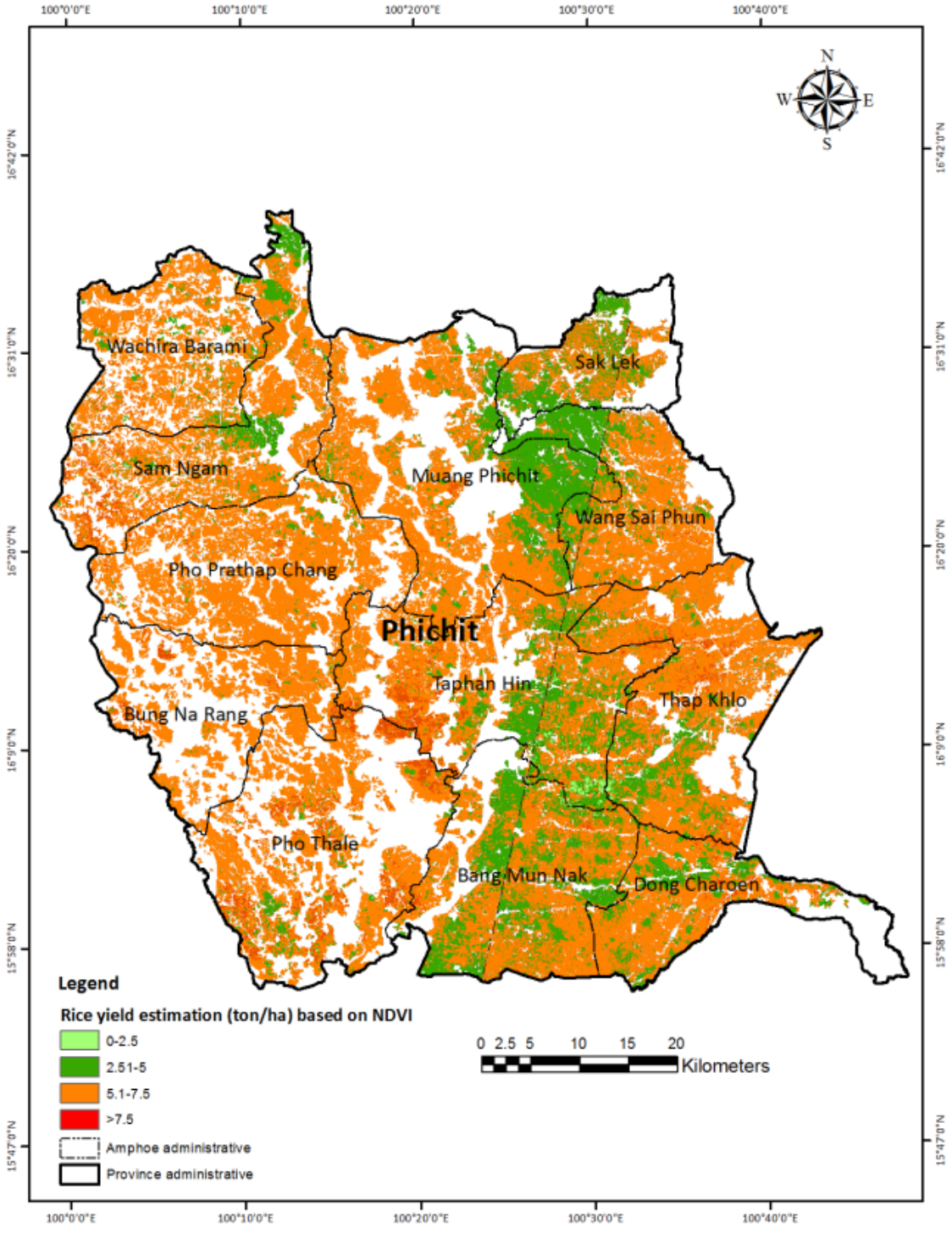
100°0'0"E
100°10'0"E
100°20'0"E
100°30'0"E
100°40'0"E
16°42'0"N
16°31'0"N
16°20'0"N
16°9'0"N
15°58'0"N
15°47'0"N
N
W
E
S
Wachira Barami
Sak Lek
Sam Ngam
Muang Phichit
Wang Sai Phun
Pho Prathap Chang
Phichit
Taphan Hin
Thap Khlo
Bung Na Rang
Pho Thale
Bang Mun Nak
Dong Charoen
Legend
Rice yield estimation (ton/ha) based on NDVI
0-2.5
2.51-5
5.1-7.5
>7.5
Amphoe administrative
Province administrative
0 2.5 5 10 15 20
Kilometers

b) Ang Thong

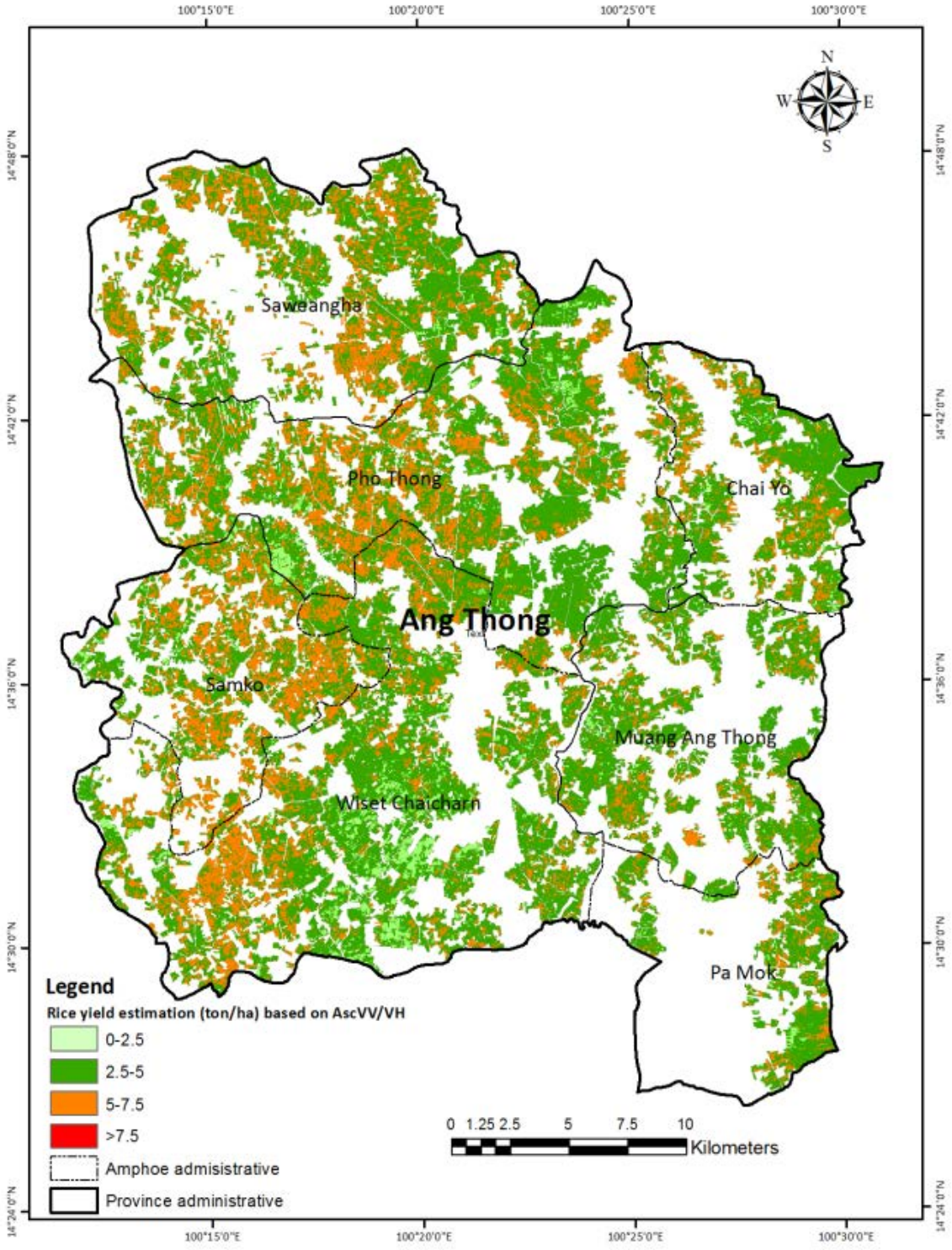
100°15'0"E
100°20'0"E
100°25'0"E
100°30'0"E
14°48'0"N
14°42'0"N
14°36'0"N
14°30'0"N
14°24'0"N
N
W
E
S
Saweangha
Pho Thong
Chai Yo
Ang Thong
Samko
Muang Ang Thong
Wiset Chaicharn
Pa Mok
Legend
Rice yield estimation (ton/ha) based on AscVV/VH
0-2.5
2.5-5
5-7.5
>7.5
Amphoe admisistrative
Province administrative
0 1.25 2.5 5 7.5 10
Kilometers

c) PathumThani

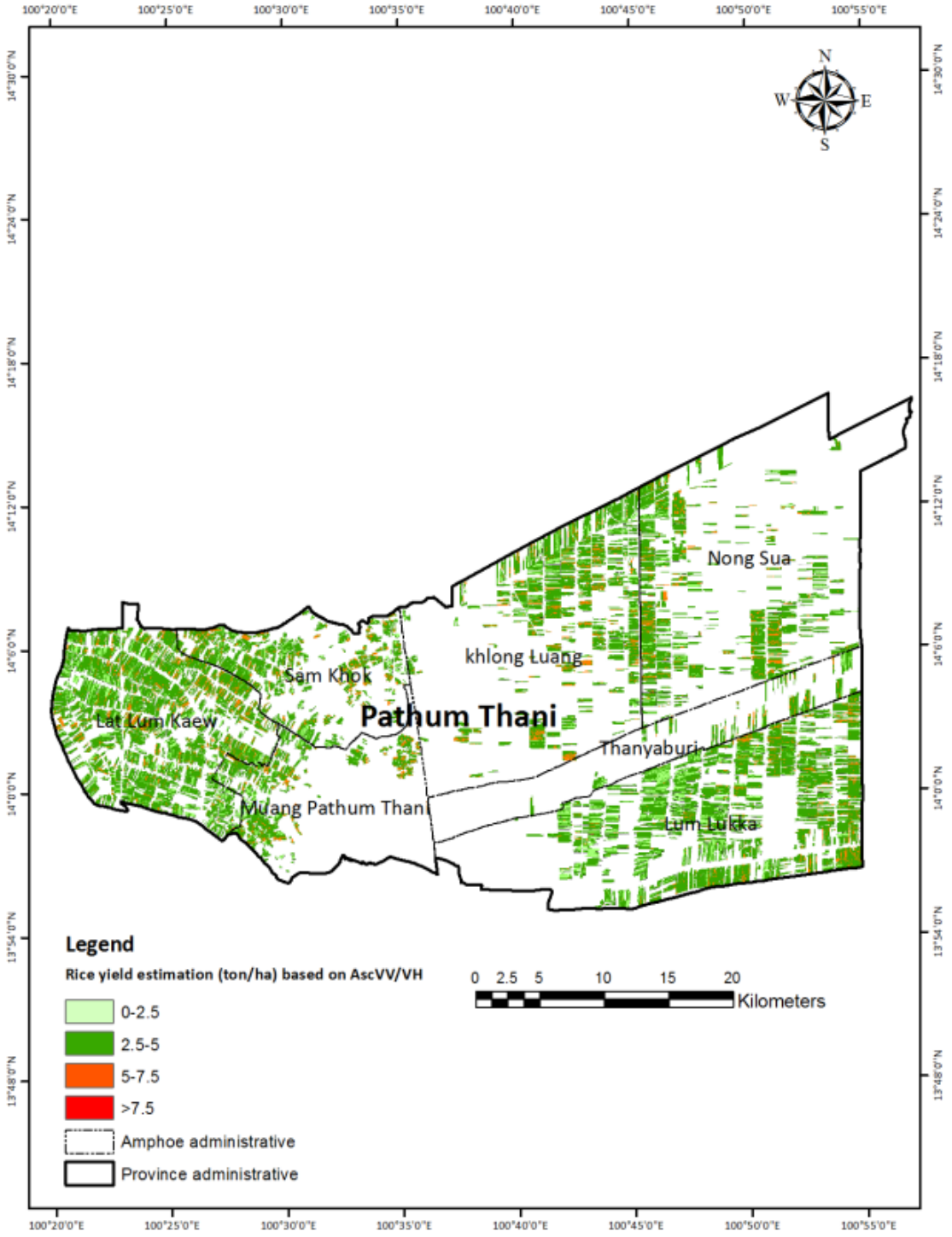

Figure 5.12 Rice yield estimation and MAPE in three representative provinces by applying simple linear regression model to optical imageries with NDVI in the panicle stage.

a) Phichit

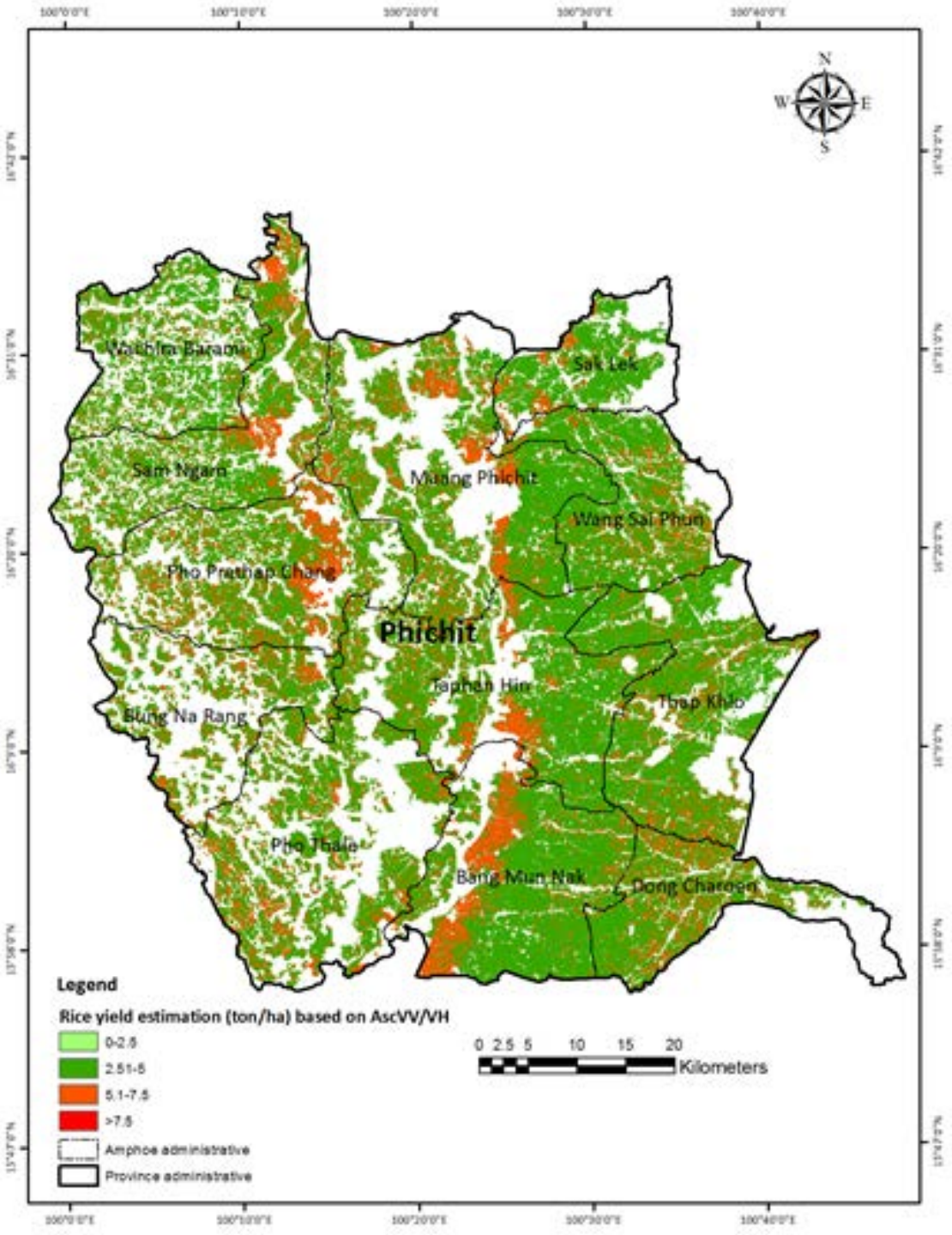
N
W
E
S
Wachira Barami
Sak Lek
Sam Ngam
Muang Phichit
Wang Sai Phun
Pho Prathap Chang
Phichit
Taphan Hin
Thap Khlo
Bung Na Rang
Pho Thale
Bung Mun Nak
Dong Charoen
Legend
Rice yield estimation (ton/ha) based on AscVV/VH
0-2.5
2.51-5
5.1-7.5
>7.5
Amphoe administrative
Province administrative
0 2.5 5 10 15 20
Kilometers

b) Ang Thong

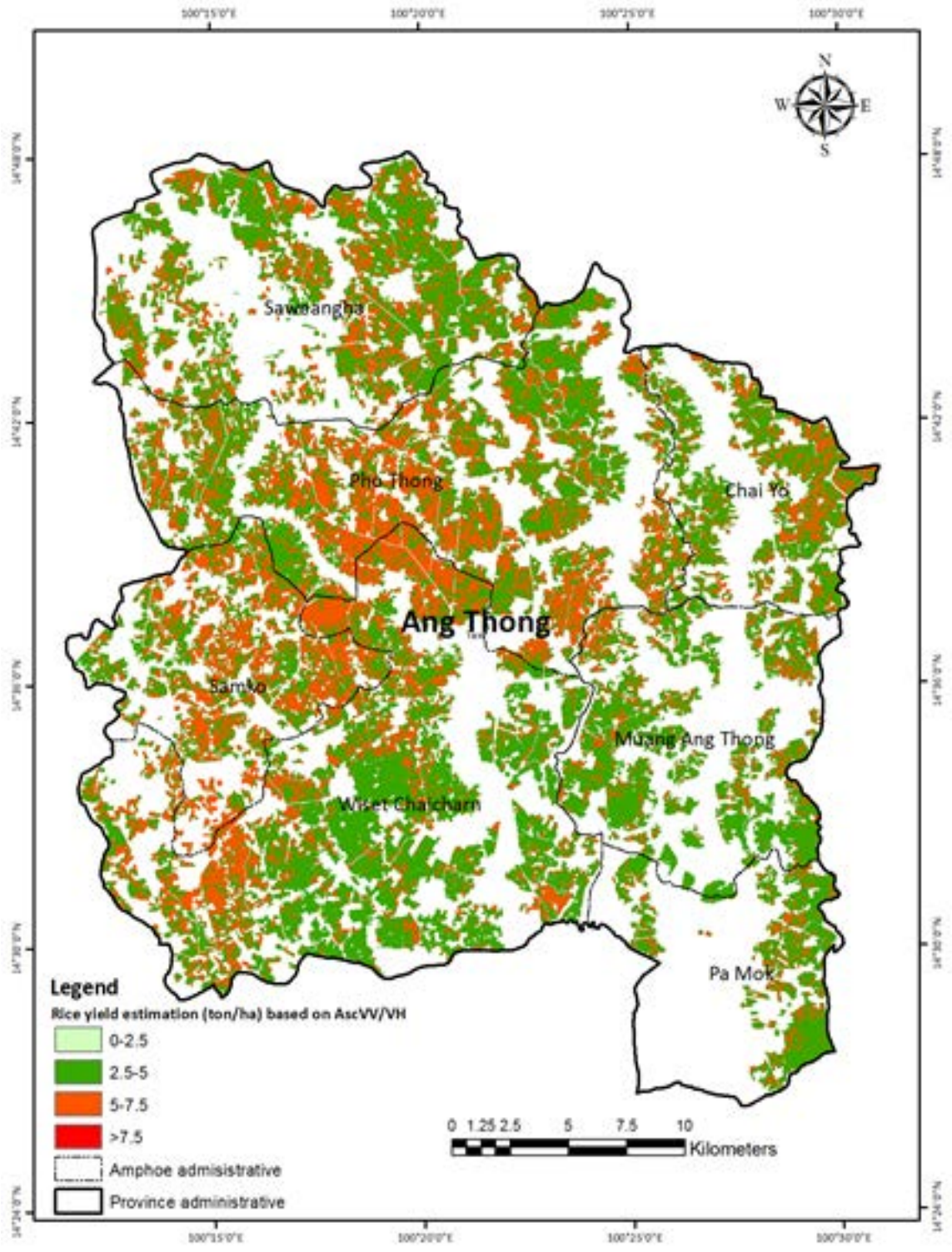
N
W
E
S
Sawangha
Pho Thong
Chai Yo
Ang Thong
Samko
Muang Ang Thong
Wiset Chaicharn
Pa Mok
Legend
Rice yield estimation (ton/ha) based on AscVV/VH
0-2.5
2.5-5
5-7.5
>7.5
Amphoe admisistrative
Province administrative
0 1.25 2.5 5 7.5 10
Kilometers

c) Pathum Thani

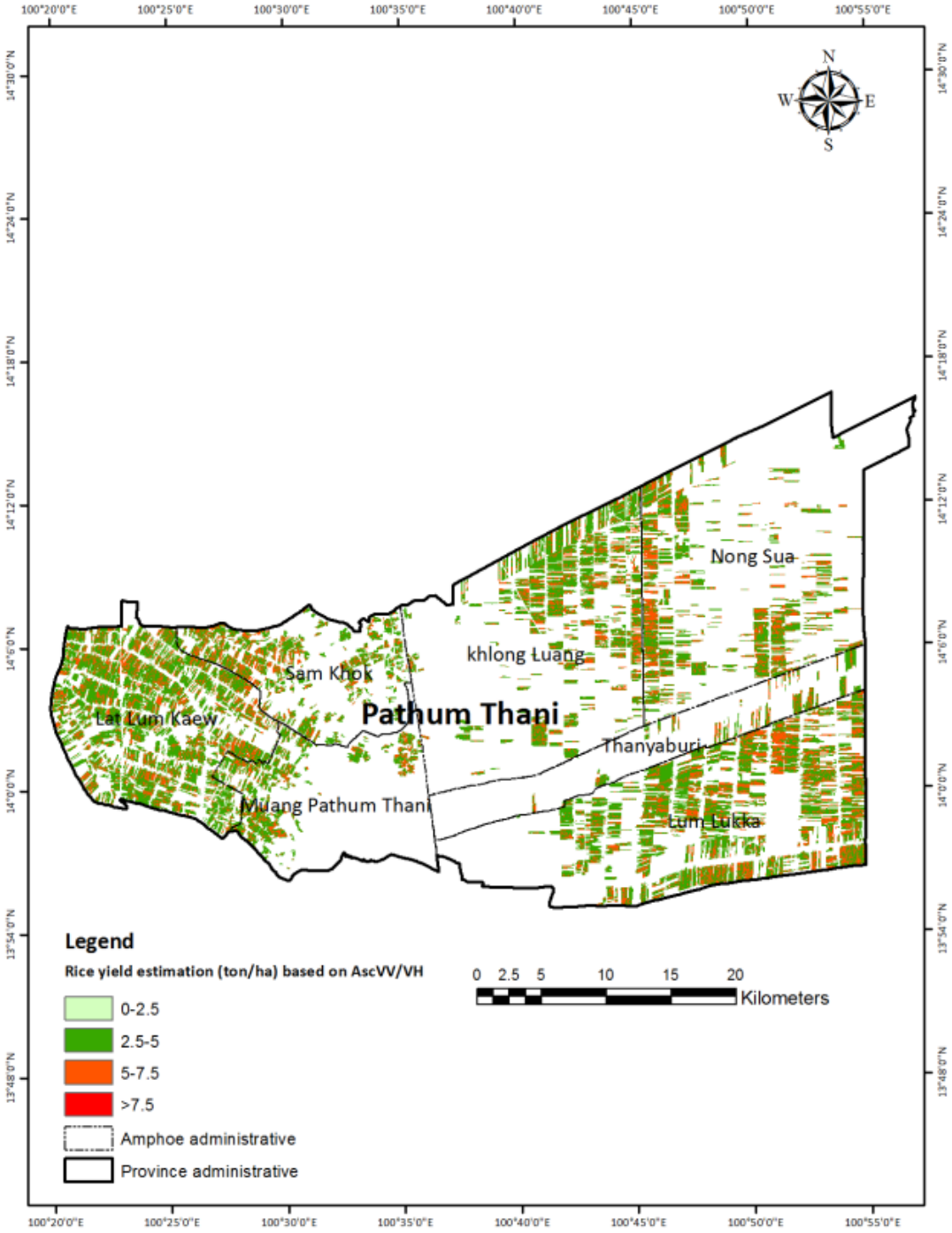

Figure 5.13 Rice yield estimation and MAPE in three representative provinces by applying simple linear regression model to SAR imageries in the harvesting stage.

5.4 Discussion

5.4.1 Seasonal changes in satellite data according to rice growth

Analysis of the temporal dynamics of vegetation indices and backscatter through the growing season indicates that the vegetation indices have a defined seasonal cycle, particularly the NDVI, which recorded the highest values in the panicle stage. Rice characteristics begin with flooding (inundation) and transplanting; thus, the vegetation indices are pretty low at these stages. Then, NDVI increases following rice growth and leaf greenness. This agrees with numerous studies that found the highest NDVI values before the ripening phase by analysing the MODIS-based vegetation and water indices, reconstructed NDVI temporal profile, and setting thresholds such as Otsu's method and LSWI + 0.05 $\geq$ NDVI (or EVI) for flooding and transplanting pixel (LI et al., 2020; Peng et al., 2011). Xiao et al. (2002) proved that the LAI of rice peaked two months after transplanting. The temporal dynamics of the EVI were similar to the NDVI, which may reflect the greater sensitivity of the EVI to the canopy structure rather than the vegetation vigour (Mondal et al., 2014). As the rice canopy grows and matures, LAI increases, whilst the development of flowers and seeds changes the composition of photosynthetic and non-photosynthetic material (Chang et al., 2016). Other studies have investigated the rice phenological cycle by extracting remote sensing data. Zhou, Liu, and Liu (2019) assimilated rice phenological from the MODIS in EVI product to identify three phenological dates (transplant date, heading date, and maturity date) into the World Food Study (WOFOST) model. The correlation (r) ranged from 0.8-0.82 and proved efficiency for rice phenological simulation. Other research created rice phenology using object classification (pixel-based classification) from Sentinel-1/2 and estimated the proper time window in time-series VIs and PhenoRice algorithm. These combinations of methods help in define the start of the season (SoS), flowering (or peak of the season: PoS), and cropping intensity during the growing season (Xiao, Xu, & He, 2021). In summary, the vegetation index has successfully tracked the rice phenological cycle or dynamics for the wet season, even though some data in the flowering stage may be missing. The rice variety indicated the variation of vegetation and varied with the growth stage.

Meanwhile, the temporal backscatter of rice displays the cross-ratio (VV/VH) as excellent performance. The backscatter for each of the growth stages is agreed with previous research. Backscatter in both VV and VH polarisation in the transplanting period shows the lowest backscatter related to the specular reflection of the water surface in the paddy field. After the transplanting, rice roots develop their nodes and density. Some research suggested excluding C-band SAR data in the seeding stage because there are effects from ridge appearing on the water surface (Kobayashi & Ide, 2022). In the tillering stage, the backscatter of VV increased more

rapidly than VH polarisation because of the increased rice height and caused the vertical structure development. In addition, there are influences from double-bounce scattering between rice plants and the water surfaces. In the panicle stage, rice develops its stems and panicle initiation and causes microwave attenuation by vertical plant structures. In the flowering or ripening stage, SAR signals are quite sensitive to moisture contents for vegetation and soils, called dielectric constant. Finally, the harvesting stage is a slight change in rice structure, and the backscatter is dropped due to senescence. The result explores the different backscatter patterns between two orbits and polarisations, agreed with Wali et al. (2020) and consistent with crop phenological changes. However, the present study's limitations are the wide range of planting dates (4 – 24 May 2017 with ~20 days) which causes a slightly distortion of vegetation indices (NDVI and EVI).

The SAR phenological cycle is less pronounced than the vegetation indices, with the VV polarised backscatter consistent throughout the season, whilst the VH polarised backscatter typically increased. Other studies have found similar trends (He, Li, Wang, Dai, & Lin, 2018). As the same result with the present study showed that the backscatter coefficient in VH polarisation was relatively low (-20 dB) in the transplanting phase, whilst the flooding water in VV polarisation was higher (-13 dB). Furthermore, it was difficult to classify the phenological phase of HH or VV polarisation. Polarisation is one crucial factor impacting the strengths of the backscatter (CEOS, 2018) and its interaction with vegetation structure. In principle, the total backscatter of a rice canopy is primarily from volume scattering due to the ears, leaves, and stems, multiple scattering between the canopy and underlying ground surface, and surface scattering by the ground surface (soil or flooded water). In the sowing and transplanting stages, the ground surface is a smooth surface, with a dielectric constant of water; at this point, the signal is no return, and the backscatter coefficient is called "specular reflection" and causes the SAR images to dark. The rice canopy contains three layers (i.e. ears, leaves and stems). In particular, rice ears and stems are short cylinders and have narrow leaf's structure. Further, the leaf angle distribution varies by growth stage and is expressed by specific probability distribution functions (Verma et al., 2019). The SAR phenological cycle is less pronounced than the vegetation indices, with the VV polarised backscatter consistent throughout the season, whilst the VH polarised backscatter typically increased. Other studies have found similar trends (He, Li, Wang, Dai, & Lin, 2018). The same result with the present study showed that the backscatter coefficient in VH polarisation was relatively low (-20 dB) in the transplanting phase, whilst the flooding water in VV polarisation was higher (-13 dB).

5.4.2 Relation between rice yield variables and satellite

The relationship between the rice yield variables and satellite-derived measurements was investigated for different growth stages of the growing season. Our study reveals that the VIs peaked in the panicle stage and that the NDVI is typically slightly higher than EVI. The irrigation system appears to influence the temporal dynamics of the vegetation indices. For example, VI values in non-irrigated areas were higher than in irrigated areas in the panicle stage. This likely to be due to differences in the planting dates influence the growth stage and the availability of a consistent water supply. The lower correlation between VIs and rice yield variables found in non-irrigated areas is believed to be due to the influence of non-photosynthetic materials. Xu et al. (2020) found that NDVI tends to saturate at high effective LAI values due to non-photosynthetic vegetation (NPV). The study contributed green vegetation (GV) and NPV by Plant Area Index (PAI) measurement and found a weak correlation between NDVI and PAI with higher rice residue in the paddy field. Due to the non-photosynthetic vegetation, several researchers have applied the other seasonal NDVI pattern. Ajith et al. (2017) developed rice yield prediction using time-series of MODIS-NDVI (MOD13Q1) data from the beginning to the end of the growing season and found a high correlation with rice yield based using the NDVI summation ($\sum$NDVI; $R^2 = 0.75$). Specific rice variety (RD41) had the highest correlation between rice yield and EVI in the seeding stage, whilst Phitsanulok2 is the highest correlation among the two parameters in the tillering stage.

Furthermore, it was difficult to classify the phenological phase of HH or VV polarisation. Polarisation is one crucial factor impacting the strengths of the backscatter (CEOS, 2018) and its interaction with vegetation structure. In principle, the total backscatter of a rice canopy is primarily from volume scattering due to the ears, leaves, and stems, multiple scattering between the canopy and underlying ground surface, and surface scattering by the ground surface (soil or flooded water). In the sowing and transplanting stages, the ground surface is a smooth surface, with a dielectric constant of water; at this point, the signal is no return, and the backscatter coefficient is called “specular reflection” and causes the SAR images to dark. The rice canopy contains three layers (i.e., ears, leaves, and stems). In particular, rice ears and stems are short cylinders and have narrow leaf’s structure. Further, the leaf angle distribution varies by growth stage and is expressed by specific probability distribution functions (Verma et al., 2019). The moisture content of rice panicles decreases in the ripening stage and leads to a slight reduction of the backscatter coefficient (Nelson et al., 2014). SAR data is more influenced by the vegetation canopy structure and surface moisture content. This is reflected in our results, which show the strongest correlations with rice yield in the ascending orbit direction with the ratio of VV/VH. This agrees with previous research that has found a high correlation between the C-band backscatter coefficient and rice biophysical variables. However, there are limitations as the backscatter can

saturate when the LAI is >3 $m^2 m^{-2}$ and the total biomass (320 gDW m^{-2}) (Inoue et al., 2014). Further, the correlation between the backscatter coefficient and rice biophysical variables in the overall area agrees with previous research that found LAI, FPAR, biomass, and rice height were related to the ratio of VV/VH polarisation (Li et al., 2016). The result of our study indicates that rice yield had a high correlation with the backscatter coefficient in the ascending ratio of VV/VH polarisation in the harvesting stage. Finally, the RD41 variety improved the correlation of rice yield with ascending VH polarisation in the flowering stage. The results agree with Lam-Dao et al. (2011) previous study on using the ratio HH/VV of multi-date TerrSAR-X for multiple linear regression model in the Mekong Delta even though there was utilise the several multi-date band combinations of TerraSAR-X data of X-band. The result proved the relationship between in-situ yield and polarisation ratio data was a high positive correlation with a correlation coefficient of 0.892 in case 1 and 0.884 in case 7 (Lam-Dao et al., 2011). The results agreed with (Kobayashi & Ide, 2022) that suggested the potential of C-band SAR data of properly in the harvesting stage for yield estimation because of less affected by the surface to resonate of panicle conditions; in addition, the stable signal in ratio VV/VH after heading period.

The results of the comparison between satellite metrics and rice biophysical variables also highlight the role of the irrigation method, even when the rice variety is the same. As shown in Figure 5.7, peak vegetation index values occurred in the tillering stage in irrigated areas but in the panicle stage in non-irrigated areas. The irrigation method influences vegetation health and land surface temperature (LST) (Ambika & Mishra, 2019). Kamthonkiat et al. (2005) also found the NDVI to be higher in irrigated rice areas (ranged 0.64-0.77) than in non-irrigated areas (ranged 0.58-0.63), which suggests irrigation may play an important role in improving crop development and food security.

5.4.3 Potential of satellite data to develop rice yield estimation model based on simple linear regression

Numerous methods exist for estimating yield, such as seasonal crop growth, crop growth model, rice biophysical relevant to LAI and grain, and remotely sensed data (Fernandez-Beltran et al., 2021; Huang et al., 2013; Kim et al., 2017; Noureldin et al., 2013). In this study, linear regression and multiple regression models were developed using satellite and field measurements to predict yield. The results indicate that the least error found using a linear regression model was VV/VH polarised ascending backscatter in the harvesting stage, which had a SEE of 0.68 tonnes/ha. Noureldin et al. (2013) developed simple and multiple regression models using individual spectral bands and several vegetation indices (i.e., GVI, DVI, IPVI, RVI, NDVI, SAVI) using SPOT data. The most accurate yield estimates were found using the red, NIR and VIs (R^2 > 0.8), and the highest

accuracy between NDVI and LAI parameters. The lower error was found using a regression model developed using in-situ LAI measurements in the panicle stage. However, a limitation of this is the requirement to use surface measurements despite the benefit of being able to estimate yield earlier in the growing season than can be currently achieved.

Chapter 4 investigated the variation of biophysical variables through the growing season for different rice varieties grown in irrigated and non-irrigated areas. The results highlighted the vital role that rice variety has on rice plant structural development. These differences have important implications for estimating biophysical parameters and yield using satellite imagery. Modern rice varieties aim to maximise biomass production. Huang, Yin, Jiang, Zou, and Deng (2015) investigated two rice varieties (GLY2 and YXYZ) and found significant differences in high grain yield, spikelet per m^2, spikelet filtering percentage, LAI, and leaf N content. Crop photosynthesis depended on traits for potential yield improvement. This study also found that rice varieties lead to varied correlations between biophysical parameters and satellite data, even when planted in the same period. In addition to rice variety, the irrigation system also impacts both Sentinel-2 and Sentinel-1, as shown in Figure 5.7 and Figure 5.8, which is a high gap noticeable in the satellite values. However, to get a clear picture of the influence of rice variety and irrigation methods, a more significant number of samples of rice variety are needed.

The other study interest is investigating the total backscatter coefficient from of rice canopy (σ^0 total) and MIMICS model (Michigan's Microwave Canopy Scattering Model) (i.e. crown region, trunk region, and underlying ground region) (Steele-Dunne et al., 2017). In principle, the backscatter coefficient from crop canopy is expressed as the volume scattering with crop canopy and ground surface; thus, the backscatter coefficient should be determined as the total backscattering coefficient of crop canopy as defined in σ_{Total} (Verma et al., 2019). In addition, rice development in each growth stage responds differently with SAR signal. For example, the σ_{Total} signals in the harvesting stage impacted with surface, stem, leaves, and panicle grains. Because there are several layers and should investigate on the relationship with other microwave indices such as the Radar Vegetation Index (RVI) (Kim et al., 2012; Mandal et al., 2020) with essential rice biophysical variables. Future work may investigate the multiple linear regression model based on the polarisation ratio of multi-date and image combination of SAR images (Lam-Dao et al., 2011). Further work should be investigated the other vegetation indices such as the modified chlorophyll absorption ratio index/second modified triangular vegetation index (MCARI/MTV12) and transformed chlorophyll absorption in reflectance index/optimized soil-adjusted vegetation index (TCARI/OSAVI) for better performance. The other factors influences with crop and the present study did not collect is leaf water contents and panicle water contents, which influences with SAR signals (Kobayashi & Ide, 2022). Also, future works are focusing on using other shallow incidence

angle (>45°) because there has a stronger scattering with crop canopy and panicle. Besides, the combining of multi-frequency of radar backscattering or full polarisations is challenge for derive rice biophysical and yield estimation (Kim, Hong, & Lee, 2008).

5.5 Conclusion

This chapter builds on Chapter 4 by investigating the relationship between rice biophysical variables at different growth stages and satellite-derived vegetation indices and backscatter coefficients. Analysis of the temporal dynamics of vegetation indices and backscatter through the growing season indicates that satellite-derived measurements are suitable for characterising rice phenology. However, the vegetation index measurements had a more defined seasonal cycle but also appeared to be influenced by the development of flowers during the flowering stage, as the VI values were typically low here.

Regression models developed using satellite measurements in the harvesting stage provided the best approach to estimate rice yield. However, this is towards the end of the growing season and not a significant temporal advancement than in-situ measurement approaches. The best-performing regression model was developed using the NDVI in the panicle stage, which had a SEE of 0.70 tonnes/ha. The SAR based on ascending ratio VV/VH measurements in the harvesting stage is also better due to penetrating cloud cover, with a SEE of 0.68 tonnes/ha. The present study proves that the significance of SAR data in the ascending ratio VV/VH is better than the NDVI in the Pathum Thani (MAPE for the NDVI in panicle 27% and 18.29% MAPE for the ascending VV/VH). On the contrary, the MAPE based on NDVI in the panicle stage in Phichit and Ang Thong fits with 9% and 62.14%. The MAPE based on the ascending VV/VH in the harvesting stage in Phichit and Ang Thong is fits with 52.34% and 71.88%. A limitation of using regression models is the reliance on field measurements in their development, but it does provide a means to estimate the yield on a broader scale.

A key challenge highlighted in this chapter is the role of rice variety and irrigation system, which influences the structural characteristics of canopy and temporal dynamics of growth. This has implications for using satellite data to estimate rice yield where significant variation in the correspondence between satellite metrics and rice biophysical variables was evident. Therefore, future studies should investigate the influence of rice variety on satellite radiometric signals, as this may improve the development of methods for estimating yield using EO data.

Chapter 6 Discussion and conclusions

6.1 Summary of findings

The following sections summarise the main findings of this research, which centre on three main areas: 1) the influences of precipitation and temperature on rice production in Thailand; 2) the dynamics of rice biophysical variables and the role of irrigation in controlling them; and 3) the potential of optical and radar data to estimate rice yield.

6.1.1 Analysis of the impact of rainfall and temperature on rice production

This study investigated the influence of weather (temperature and precipitation) on annual rice yield and production at the provincial level in Thailand over the past 35 years (1981-2015). It was achieved by assessing the impacts of precipitation (amount of rainfall and average rainy days) and temperature (minimum temperature, maximum temperature, mean temperature, mean minimum temperature, mean maximum temperature, and difference in temperature) on rice yield and production. To remove the influences of changes in agricultural policy and developments in agricultural technology and seed developments, rice yield and production data were detrended by differentiating between original rice production/yield in the observation year and rice production/yield observation in the previous year in the time-series datasets. In 2015, the main rice cultivated area is located in the northeast with low productivity (~1.9 tonnes/ha) due to poor soil fertility. On the contrary, the rice cultivated areas in the central regions represent high productivity (~4.5-5 tonnes/ha) due to adequate irrigation and fertile soil.

The changes in rice cultivated areas over the period revealed that 55% of the provinces saw an increase of >10% in cultivated areas, 25% a decrease in cultivated areas by >10%, and 20% of provinces saw changes less than +/-10%. Analysis of the temporal dynamics of precipitation on a monthly basis revealed declining trend of average rainfall in May (~60 mm). This is important on rice production in Thailand, as it can influence the rice planting date in the wet growing season in terms of shifting the planting date, especially in the non-irrigated areas corresponding with the onset of monsoon. The rainfall variation in terms of standard deviation (S.D.) is highest from June-August. Besides, the number of rainy days gradually increases ~3-5 days per month and peaks during August-September.

The temperature in terms of mean minimum temperature in January around 18-19°Celsius; then, the temperature is slightly increased until April (~25°Celsius) and certainly steady until August-September. On the contrary, the mean maximum temperature is the distinctive pattern from the

mean minimum temperature. For example, the mean maximum temperature in January is 32°Celsius and sharpens increasing in April; then, the temperature reduces until the end of the year. Obviously, there is an enormous fluctuation between mean maximum and mean minimum temperature (defined as differences in temperature) at the beginning of the year (January-April). After October, the difference in temperature reveals higher trends of mean minimum temperature. The present study is agreeable with the IPCC weather trends forecasts (Solomon, 2007) and weather data derived from TMD, Thailand, that reveals the increasing temperature trends over the study period.

The correlation between rice and weather variables revealed that mean minimum temperature, mean maximum temperature, and cumulative rainfall adversely affected rice yield and production. The impact of climate on rice production also varies by level of irrigation. In general, the temperature-derived variables such as mean minimum and mean maximum temperature had a more considerable impact than rainfall variables. Some key findings from this study can be summarised as:

1) In the non-irrigated area, the mean minimum temperature has a significant positive relationship with rice yield for 15 provinces, whist in the irrigated area only 3 provinces recorded a significant relationship between rice yield and mean minimum temperature. Whereas there are 16 provinces is significant with rice production in the non-irrigated area (positive correlation 15 provinces and negative correlation 1 province).
2) In the non-irrigated area, the mean maximum temperature has a significant positive relation with rice yield for 11 provinces, whilst in the irrigated area only 3 provinces Contrary, the positive significant on rice production 2 provinces in irrigated areas and 10 provinces in non-irrigated areas (positive correlation 9 provinces and negative correlation 1 province).

3) In the non-irrigated area, the cumulative rainfall is positive. There are significant 3 provinces for rice yield. However, the positive significant with rice production found 1 province in irrigated rice and 3 in non-irrigated rice. The result demonstrates the influences of irrigation on rice production.

Furthermore, the present work determines the spatial autocorrelation with Global Moran's I index to study the systematic spatial variation pattern (i.e., cluster, random, disperse) with neighbouring provinces by assigning the feature location and weather data from their weather attribute. The test is set to share an edge with the target polygon in the conditions and considers the Z-score and P-value to accept the null hypothesis. The output identifies less spatial autocorrelation between share edge provinces. The result reveals that cumulative rainfall and average temperature are significant with the random and clustered pattern (Moran's I index ~0.15). Moreover, the result indicates some influences on the other variables.

An increase in water efficiency through irrigation supports long-term crop productivity (Winterbottom et al., 2013) by ensuring adequate water supply as per the requirement of the crop. The development of engineering irrigation structures (e.g. dams, conveyers and canals) is important in the redistribution water resources to agricultural areas (Ozdogan et al., 2010). Thus, improving water management provides better access to adequate water supplies and the ability to grow rice even in the dry season. The result reveals the influences of irrigation systems on rice productivity in the study area. To assess the impacts of predicted climate change on rice development, Horie (2019) grew rice under different environmental conditions and found that excessive temperature (>28°Celsius) reduced the panicle dry weight, which is important for biomass production and relative rice yield because of heat-induced spikelet sterility of rice. Predictions of future climate change based on the latest Global Climate Model (GCM) climate projection in Coupled Model Intercomparison Project Phase5 (PrCMIP5) suggest that the temperature in Thailand will increase during the 21st century. The national average temperature at baseline (1980-1999) is 25.2°Celsius; the future average temperature (2080-2099) will be 28.6°Celsius. The increasing temperature influences the Agricultural Ecology Zone (AEZ); the largest temperature increase has been found in the northern region of Thailand (> 4°Celsius). The precipitation trend has increased from 1,819 mm/year to 2,046 mm/year, while Asian monsoons influenced the difference in rainfall in the wet and dry seasons. The monsoons delays are explicitly impacted the beginning planting date even though the pattern of precipitation is uncertain (Kiguchi et al., 2020).

Overall, 30 provinces showed the impact of climatic variables on rice production – 6 provinces in irrigated areas and 24 in non-irrigated areas. Precipitation data used in the analysis in Chapter 3 were annual and therefore only applicable to the wet season rice; it prevents assessment of the influences of temperature or precipitation on rice planted in the different seasons. This may partly explain the limited correlation between precipitation and yield, particularly in non-irrigated regions. In addition, the data collection on rice yield and production data was averaged at the provincial level by neglecting the differences in irrigation systems. A province is only classified as irrigated if more than 50% area of the province is irrigated. Improved data collection separated by irrigation cultivated areas would improve the correlation analysis.

Secondly, the current study did not account for extreme events such as drought and flooding which usually depend on the lengths and intensity of extreme events. The extreme events seriously impact crop production especially when they occur close to harvesting period. The present study supports previous research that indicated the Aus and Aman rice (planted in the wet season) with a positive correlation; oppositely, the Boro rice (planted in the dry season) found a negative correlation. These correlations were related to the development of the speed of leaf emergence and rainfall affected tillering and stem elongation (Abbas & Mayo, 2021). The period

under the present study corresponds with the correlation results in Aus and Aman rice, which is planted in the wet season and a positive correlation. Similarly, Chowdhury and Khan (2015) monitored rice yield in Bangladesh between 1972 and 2014 and found maximum temperature to have a negative effect on yield in all three rice planting seasons: Aus (March-July), Aman (June to November), and Boro (November to May). This research also found that rainfall had a positive effect on yield when planted in the Aus and Aman seasons and an adverse effect when planted in the Boro season. To mitigate the adverse effects of excessive temperature on rice production especially during grain filling that reduced on non-structural carbohydrates in the sink (Chaturvedi et al., 2017) and spikelet fertility (Chidambaranathan et al., 2021).It is important to develop and cultivate temperature or heat-tolerant genetic rice varieties to ensure sustainability (Hakata et al., 2017; Khan et al., 2019; Kilasi et al., 2018). Further study should be investigated on the other methods of detrended such as fitting linear regression, applying residual for model, and log-linear trend model for better performance on detrended analysis. Also, the optimum temperature for rice development is ranged 25-35°Celsius (Nishad et al., 2018) and the effects on rice production in terms of net assimilation rate on rice and biomass, especially when the optimum temperature occurs in the reproductive stage should be investigated. Finally, the cumulative rainfall is a positive and proves agreeable because most provinces located in the northeast region are non-irrigated areas that require sufficient rains for their planting.

The location of the weather station may be limited because most of them are not located in the agricultural areas and there was the limitation of excellent representative of weather data. Besides, the spatial autocorrelation will be improved if we know the exact distance threshold of the distance band for our analysis, which is interpreted as less correlation on the spatial dimension. The unpredictability climate change seems to greatly impact especially in developing countries. The result identifies the average minimum and maximum temperature vital influences on rice yield/production. Thus, suitable agricultural adaptation strategies and developing new heat stress-tolerant rice varieties should be adopted for climate change resilience.

6.1.2 Dynamics of rice biophysical variables in irrigated and non-irrigated systems during the growing season

Due to the various rice ecosystem and photosensitive rice varieties, several rice biophysical variables such as density, Leaf Area Index (LAI), spikelet per m^2, and biomass accumulation varied with yield. Rice biophysical variables from in-situ measurement enable it to relate with remote sensing data products. Several studies estimated essential crop biophysical variables (LAI and biomass) and ultimately related them with yield. The present study aims to study the dynamics of rice biophysical in the overall and identify differences due to irrigation systems and rice variety. A

field campaign was conducted in 2017, during which time several rice biophysical variables were measured throughout the growing season to investigate their variations by rice variety. Besides, the present study aims to develop and validate models to predict rice yield using satellite data in the Chapter5. The present study collects rice biophysical variables with in-situ measurement of 28 sample units with different irrigation systems (21 sample units located in irrigated areas and 7 sample units located in non-irrigated areas in Phichit, Ang Thong, and Pathum Thani). Rice biophysical measurement is defined as five main growth stages: seeding (1-20 days), tillering (21-40 days), panicle (41-70 days), flowering (71-90 days), and harvesting (90-120 days). Besides, the rice biophysical variables differ with growth stage depending on their rice structure development, consisting of the water depth, stem density, height, Leaf Area Index (LAI), chlorophyll contents, wet and dry biomass, and yield.

The result presents two approaches via the dynamics of rice biophysical variables and their correlation with rice yield. The assessment was undertaken at various growth stages, irrigation systems, and rice varieties during the growing season. The irrigation influences rice development such as rice height found differences in height in the tillering, panicle, flowering, and harvesting with 0.64, 1.22, 3.48, and 6.54 cm, respectively. Besides, the differences that occur in the water depth in different irrigation in the seeding, tillering, panicle, flowering, and harvesting are 2.83, 4.69, 4.45, 3.66, and 1.5 cm, respectively (average differences in water depth 0.5-2.5 cm). There are some remarkable facts that no water in the paddy fields in the non-irrigated was found after the flowering stage. The stem density is a key variable closely associated with the tiller's rate of rice and flag leaf development. The stem density is highest during the seeding to panicle stage, approximately 250-500 stem/m^2. Then, the stem density is reduced by ~120-150 stem/m^2. The LAI variable, which indicates the ability of crops to absorb solar energy for biomass production, provides beneficial information on rice growth and yield evaluation. Our result shows that differences in LAI development depend on rice variety. Most rice varieties in the study peaked in LAI value in the flowering stage with 4.3 $m^2 m^{-2}$ (e.g. RD41, RD47, and HomMali105 in irrigated areas, RD13 in non-irrigated areas, and RD49 and Phitsanulok2 in both irrigated and non-irrigated areas). However, some rice varieties peaked earlier in the panicle stage (e.g. RD13 in non-irrigated areas and RD61 in irrigated areas) or later in the flowering stage (e.g. RD57 in irrigated areas). The shifting LAI development influences other rice biophysical and remotely-sensed data. In addition, the LAI in the non-irrigated areas is higher than in irrigated areas ~0.31 $m^2 m^{-2}$. The main reason for the high values of LAI in the flowering stage is the development of rice flag leaves and found the variation in the panicle stage in the non-irrigated areas. The LAI is usually a peak in the flowering stage, which develops the milky in rice grains. The chlorophyll content is one key variable reflected on the photosynthetic pigments and peaks in the flowering and sharp drops in

the harvesting. The amount of chlorophyll content in the irrigated areas is higher than in the non-irrigated areas during the panicle until the flowering stage. However, the chlorophyll content proves high chlorophyll content in the tillering stage (RD57, RD49, and RD47). The comparison of chlorophyll content in rice varieties planted in both irrigation and non-irrigation systems (Phitsanulok2 and RD49) found the large differences in the tillering, panicle, flowering, and harvesting stage with 31.86, 1.26, 0.88, and 4.15 μmol m^{-2}, respectively. The wet and dry biomass collects in the panicle until the harvesting stage. The biomass is highest in the harvesting stage, and the biomass in overall, stem, and grains in the harvesting stage (bracket shown the dry biomass) is 133.48 (48.02), 99.33 (26.29), and 33.77 (21.74) g m^{-2}, respectively. In the harvesting stage, the total wet biomass is highest with 119.13 g m^{-2} (minimum and maximum wet biomass of average total wet biomass 14.27% and 215.45%). The stem density and LAI tend to decrease whilst the biomass is increasing. The biomass in the RD49 and Phitsanulok2 found the differences on wet biomass with 25 g m^{-2} and 1.3 g m^{-2} in the irrigated areas and 10.7 g m^{-2} and 43.2 g m^{-2} in the non-irrigated areas. Rice variety is influence on the biomass, for example, and there was slightly higher wet total biomass in the Phitsanulok2 (49.25 g m^{-2}) than in RD41 (37.67 g m^{-2}). Regarding rice characteristics, the dominant characteristics in RD41 are straight clumping, hard stem, green rice leaves, straight flag leaves, and short ears of rice from flag leaves, which is outstanding with remotely sensed data, especially the vegetation index. There are differences in grain dormancy between rice varieties: the result shows that grain dormancy for RD13 and RD41 is 3 weeks and 9-10 weeks, respectively (Rice Department, 2016). Consequently, the yield for these varieties differed based on grain dormancy, with 4.06 and 5.06 tonnes/ha, respectively.

The results have shown a correlation in rice yield in overall growth stages in the entire study area and the irrigated areas. In the entire study area, significant rice biophysical at each growth stage was different. These findings prove a significant positive relationship with rice height stage (r= 0.37), wet grain and dry grain biomass (r = ~0.43-0.45) in the tillering stage and yield. There was preferably significant wet grain biomass in the overall growth stage (r = 0.27). In addition, the relationship between rice yield and other rice biophysical variables diversified among irrigation systems. In irrigated areas, the significance is found in the seeding, panicle, flowering, and overall growth stage. In seeding, the stem density is correlated with rice yield (r = 0.45). The LAI is correlated with rice yield in the panicle stage (r = 0.57). While in the flowering stage, stem density (r = -0.46) and wet grain biomass (r = 0.47) were significantly related to yield. In the overall areas, the wet grain biomass is significant with wet grain biomass (r = 0.31). Finally, there is a different significant growth stage with rice biophysical variables in non-irrigated areas. In the tillering stage, rice height is significant with rice yield (r = 0.74). The rice height is significant in the harvesting stage with yield (r = 0.81). The high negative correlation is all of the biomass (i.e., total, stem wet

and dry biomass) (r > -0.93). In the overall growth stage, the correlation is significant with chlorophyll content (r= -0.36), total wet biomass (r= -0.58), and wet and dry stem biomass (r = -0.69). All evidence supports the important role of rice variety and irrigation in the study area. The majority of rice development found in non-irrigated areas higher develops than the irrigated areas such as rice height (absolute rice height), stem density, LAI, chlorophyll content, and grain emergence. There was observed a delay in rice emergence in the non-irrigated areas, which may be from soil nutrients and water availability during the growing season. Here, rice biophysical reveals an increasing rice development in irrigated areas, such as water depth and yield. Some fluctuations in rice growth among different irrigation systems and various developments initiate. Our study suggests the significant rice biophysical on dry total and stem biomass on RD41 in the harvesting stage.

Retrieving biophysical variables from remote sensing data is vital for rice yield estimation before harvesting. Previous studies have proven the influence of rice variety on their biophysical variables, which increases the difficulties of using remote sensing estimating rice biophysical variables. Maftukhah et al. (2019) investigated the differences in LAI among different rice varieties (IR64 > Hitam and Mutiara variety approximately 1 m^2 m^{-2}). Thus, the study summaries the influences of rice varieties and irrigation water on physiological and biochemical behaviours in rice. Huang, Yin, Jiang, Zou, and Deng (2015) investigated two rice varieties (GLY2 and YXYZ variety), finding influences on different biophysical variables such as grain yield, spikelet per m^2, spikelet filtering percentage, LAI, and leaf nitrogen content. These researchers agreed with the present study that differences in rice variety reveal the different rice characteristics even when planted in the same period. Another research determined the association between rice yield and other essential agronomic traits in different ecotypes – Indica and Japonica inbred/hybrid and found various significant traits. For example, the Japonica inbred and hybrid was significant only high panicle number per area (Li et al., 2019). Chu et al. (2018) investigated the different rice varieties in Indica-Japonica hybrid rice (IJHR) and Japonica inbred rice (JIR) in two irrigation situations, such as the continuous flooding (CF) and alternate wetting and severe drying (AWSD). The result proved rice yield decrease in AWSD pattern for both IJHR and JIR varieties.

6.1.3 Potential of optical and radar satellite observation in rice yield estimation

Remote sensing is an effective instrument for crop monitoring and yield estimation because of its various advantages on spatial coverage, temporal, and spectral characteristics. Satellite data have been widely applied to estimate rice yield via empirical models using spectral vegetation indices (Huang et al., 2013; Ji et al., 2021; Mosleh et al., 2016; Noureldin et al., 2013; Son et al., 2014; Harrell et al., 2011; Zhang et al., 2019) and crop growth model parameterised with satellite

observations (Li et al., 2015; Machwitz et al., 2014; Setiyono et al., 2018; Singh et al., 2014; Son et al., 2016). In Chapter 5, both optical (Sentinel-2) and radar (Sentinel-1) data were used to monitor rice throughout the growing season and analyse the correlation between rice yield and Earth Observation (EO) data to develop yield estimation model. Several spectral vegetation indices were developed to increase vegetation sensitivity and reduce the other factors (soil backgrounds and atmospheric effects). Using the Sentinel-2 data, the NDVI and EVI were used to monitor the rice phenological cycle throughout the growing season, which found high VI values occurring in the panicle stage for both vegetation indices. Analysis of the LAI throughout the growing season (Chapter 4, Table 4.6) revealed that the highest LAI typically occurred in the flowering stage before decreasing in the harvesting stage. The temporal pattern of the vegetation index is shown lower in the seeding stage due to the bare soils or flooded field; then, the vegetation index is sharpened increases in the tillering stage due to the dense and green vegetation. The profile of the vegetation index is still increasing until the panicle stage, and there are slightly increasing in EVI in the panicle stage. Afterwards, the vegetation index suddenly decreased in the flowering and harvesting index due to their senescence. One of the reasons for lower VI values in the flowering stage, despite the higher LAI, is influenced by non-photosynthetic materials, such as flowers have impacted the radiometric signal (see Figure 4.4). This decrease in vegetation index values during the flowering stage has been observed in several other studies (Boschetti, Stroppiana, Brivio, & Bocchi, 2009; Mosleh et al., 2016; Son et al., 2014), which impacted the accuracy of LAI estimation using vegetation index measurements during the flowering stage.

The Synthetic Aperture Radar (SAR) data is quite relevant in terms of canopy characteristics and water contents on the crop. The capability of signal penetration on SAR signals depends on microwave signals. In present study focuses the backscatter coefficients in terms of sigma nought (σ^0). Analysis of the temporal dynamics of VV and VH radar backscatter in the ascending and descending orbits revealed that backscatter peaks in the tillering stage with the VV polarised data decreasing. At the same time, VH observations tended to remain flat (Figure 5.8). These trends are believed to be due to volume scattering in the rice canopy (consisting of rice ears, leaves, and stems), multiple scattering or called “double bounce” scattering between canopy layer and underlying ground surface, and surface scattering (soil or flooded water) (Verma et al., 2019) which have been observed in other studies. Volume scattering from crop canopies is comparatively low, with the backscatter coefficient largely influenced by the surface underneath the canopy (Choudhury & Chakraborty, 2006; Liu et al., 2019; Phan, 2018). These scattering effects reflect the different signals that occur during growing season, since they are influenced by the rice canopy structure composed of stem, stalk, and grain (Inoue et al., 2014; Yuzugullu et al., 2016). Furthermore, the moisture contents, which is the important factors in terms of dielectric

contents, of the rice panicle decreased in the ripening stage and led to a slight reduction of backscatter coefficient (Nelson et al., 2014). The temporal of backscatter indicates the low backscatter in the seeding stage, which is lower on the VH rather than VV polarisation. The result proves a lower backscatter in the descending than ascending in all growth stages. The low backscatter coefficient in the seeding stage is because of the specular reflection or "mirror", which is no response signal and is seen darken on SAR images. Then, the backscatter increases in the tillering stage because rice develops its tiller's rate. In the panicle stage, the backscatter coefficient decreases. In the flowering stage, the backscatter is reduced and relatively lowers for VV because of the dielectric of rice. The result proves the sensitivity with grain and moisture contents in the descending mode. Finally, the VV and VH polarisation in the harvesting stage slightly decreases. Conversely, the backscatter for VV on both ascending and descending orbit directions indicates an increasing backscatter; however, the backscatter in the descending is lower than the ascending on both VV and VH polarisation because of the influences on attenuation. The profile for both satellite data is advantageous for rice monitoring.

An important finding in Chapter 4 was the influence of rice variety, which can see significant differences in canopy biophysical variables. For example, the maximum average LAI in RD41 and RD49 was 4.03 m^2 m^{-2} and 4.23 m^2 m^{-2} (4.41 m^2 m^{-2} in irrigated area and 3.96 m^2 m^{-2} in the non-irrigated area), whilst the yield differed by 0.41 tonnes/ha (differences 0.51 tonnes/ha in irrigated area and 0.25 tonnes/ha in non-irrigated area). These differences in biophysical traits have implications for estimating biophysical parameters and yield using remotely sensed data. Current methods for estimating yield in Thailand are through crop cutting experiments (CCE) conducted at the end of the growing season, which is limited by the large number of manual efforts required to do so and that the yield estimates are derived late in the growing season. One of the aims of this research was to develop an approach to estimate rice yield using remotely-sensed data as early as possible in the growing season. To do so, a range of simple regression models were developed to estimate rice yield using field and satellite measurements.

Of the two best-performing models based on simple linear regression model in the significant satellite measurement and growth stage are shown as follows.

1) Optical data regarding vegetation index- EVI in the seeding and NDVI in the panicle stage measurements. The validation of EVI and NDVI with rice yield had an RMSE of 0.57 with SEE 0.62 tonnes/ha and RMSE of 0.37 with SEE 0.7 tonnes/ha, respectively.

2) SAR data in the ascending VV/VH measurements in the harvesting stage with rice yield had an RMSE of 0.54 with SEE 0.68 tonnes/ha.

The empirical models that utilise satellite and field measurements have been widely applied to estimate yield and have typically done so with lower error. For example, Noureldin et al. (2013) developed a rice yield estimation model in a linear regression models and multiple linear regression models by using SPOT4 data in August 2008 and August 2009. The model input the individual band (e.g. green, red, near-infrared, and middle-infrared spectral band), vegetation indices (e.g. Green Vegetation Index (GVI), Ratio Vegetation Index (RVI), Infrared Percentage Vegetation Index (IPVI), Difference Vegetation Index (DVI), Normalised Difference Vegetation Index (NDVI), and Soil Adjusted Vegetation Index (SAVI)), and leaf area index (LAI), which was measured 90 days after sowing, or the maximum vegetative growth stage. The highest accuracy was achieved by the multiple linear regression model integrating NDVI and LAI with $R^2 = 0.96$ and standard error of estimation (SEE) of 0.49 in 2008 and 0.529 in 2009, respectively. The rice yield estimation model based on SAR is advantageous for predicting rice yield during the growing season based on Sentinel-1 due to eliminating the effects of cloud cover problems on optical data. However, the seeding stage has a poor relationship with yield in Sentinel-1 data because there are ridges in the flood paddies in this growth stage. To improve the performance of rice yield estimation based on satellite data, the determination of rice biophysical variable selects on the yield estimation model. Besides, the mixed the irrigation system may be distorted the yield estimation model, as noticeable in the higher MAPE in the Phichit. Wang et al. (2019) analysed the Ground Range Detected (GRD) of multi-dates Sentinel-1 in IW model with VV and VH polarisations – end of tillering stage of vegetative phase and end of the grain filling stage of reproductive phase. This study developed the single VV and VH polarisation, the cross ratio VV/VH in tillering and grain filling stage, simple ratio, and SAR normalized Difference Index relate with rice yield. The outputs of backscatter in the VV and VH in the tillering stage is positive whist negative correlation in the grain filling and the excellent backscatter is SSD_{VH} (different between σ_{VV} in the grain filling σ_{VV} in the tillering stage) with $r^2 = 0.65$ and RMSE 0.74 tonnes/ha. Hoang-Phi et al. (2021) estimated rice yield using Sentinel-1 for Winter-Spring rice yield in An Giang province in 2018 by developing the multivariate regression model of VH backscatter. The output of linear regression equation $r^2 = 0.6$ and standard deviation estimate 0.33 tonnes/ha compared with in-situ yield. The estimated and survey yield results were 6.5 and 6.66 tonnes/ha with the standard deviation 0.80 tonnes/ha. Meanwhile, the present study proves that the ascending VV/VH polarisation in the harvesting stage and the NDVI in the panicle stage are preferable for rice yield estimation. The estimates of rice yield compared with official statistical yield (in bracket) reveal that rice yield based on NDVI in the panicle stage in Phichit, Ang Thong, and Pathum Thani are 3.32 (3.77), 4.45 (4.16), and 3.96 (4.49) tonnes/ha, respectively. Further, the estimated rice yield compared with official statistical yield (in bracket) reveals rice yield based on ascending VV/VH

polarisation in the harvesting stage in Phichit, Ang Thong, and Pathum Thani are 4.72 (3.77), 4.87 (4.16), and 4.86 (4.49) tonnes/ha, respectively.

A limitation of the models that performed best in this research is that they need to improve upon current methods (e.g. crop cutting) in a meaningful way, since the models either utilise field measurements or provide estimates of yield late in the growing season. Also, the variances of planting dates are impacted by the vegetation index/backscatter values of satellite data in the extraction paddy fields. The growth stage is critical for developing rice yield estimation by considering the initiation of rice grains (panicle stage) or maturity of rice grains (harvesting stage), which are related to satellite sensors. Even though, the vegetation index values tend to saturation at high LAI (> 3 m^2 m^{-2}) that may be the limitation and the influences of non-photosynthetic materials on rice fields. The SAR signal proves their sensitivity on rice canopy better than the performance on spectral measurement. In summary, the EO data has the potential to tracking the rice phenological profiles and rice yield estimation especially utilising the SAR data for rice yield estimation in the Chao Phraya River delta. In addition, the current study found that the rice yield estimation should be after the heading in the reproductive phase to the ripening or nearly senescence in the maturity phase for estimating rice yield at the provincial scale. The result of validation that compared the estimated rice yield and official statistical yield had high reliability with MAPE ranging 9-62% for NDVI and 18-72%, even though there was some variation of MAPE in the amphoe level.

6.2 Limitations

The following section outlines the limitations of the data and analyses conducted as part of this research on a chapter-by-chapter basis.

Chapter 3

Chapter 3 analysed the annual dynamics of rice yield and production alongside precipitation and temperature data to assess whether climate influenced rice crops in Thailand. The present study created a series of weather data by aggregating monthly, seasonal, and annual data.

The rice production and yield data used in this analysis were available at the provincial level. They had been aggregated into a single rice yield annual estimate that failed to account for the influences of rice variety. Analysis in Chapter 5 revealed that the yield could vary from 3.31-6.13 tonnes/ha across irrigation systems depending on the rice variety, which could result in large annual variations depending on the extent of cultivation of particular varieties. Research has found that fertility and rice varieties are crucial factors to yield and yield attributes (e.g. number

of effective m^{-2}, number of seeds per panicle, 1,000-grain weight, spikelet sterility, grain/straw yield, and harvest index) (Kumar et al., 2017). When analysing a long time-series of data, information on the time of development of a particular variety and the extent to which it is cultivated annually across Thailand is needed to account for changes in rice variety when assessing the influence of climate. The result of spatial autocorrelation using the Global Moran's Index proves there was less significance with Moran's Index of 0.15 and only significance in 1992 with cumulative rainfall (random pattern) and average temperature (clustered pattern) parameters. However, the spatial autocorrelation is lacking information on the threshold or significant distance to fix into our analysis for precise results.

Chapter 4

Despite careful planning, several limitations with the collection of measurements during the field campaign are central to the analysis in subsequent chapters.

Analysis of the field measurements revealed the immense impact that rice variety can have. It would have been preferable to collect field measurements for a smaller number of rice varieties in a more significant number of fields to improve the sample size. This would enable a more conclusive assessment of the impact of rice variety on structural characteristics and biophysical properties. In contrast, in the present study, the number of rice varieties was measured in only one field. However, due to the constraints of the fields which could be measured, it was not feasible to do so.

Chapter 5

A further difficulty with the field campaign concerned collocating satellite overpasses with the date of field data collection, particularly during the panicle to the harvesting stages. Most studies (Mosleh & Hassan, 2014; Wang et al., 2019; Zhao et al., 2021) divided the paddy rice growing season into 3-4 stages: sowing to transplanting (1 month), transplanting to heading stage (1.5-3 months), heading to reproduction stage with flowering (1 month), and flowering to maturity (1 month), while the three-growth stage defines in the initial/transplanting stage (1-32 days after sowing), peak stage (81-112 days after transplanting), and harvesting stage (129-161 days). However, the duration of each stage is influenced by rice variety and environmental conditions (De Datta, 1981), which adds some uncertainty in relating satellite measurements to the correct growth stage, particularly towards the start or end of a growth phase.

Finally, a difficulty in using satellite data to monitor rice paddies is the paddies' small size relative and limitation to the spatial resolution of the imagery. Despite the Sentinel data having a spatial resolution of 5 m x 20 m (single look complex) and 20 m for Sentinel-1 and -2 data, respectively,

relating image pixels to the corresponding locating in the paddy field is uncertain. As shown in Figures 5.5 and 5.8- in particular, the former- image pixels often fall on field boundaries within the field boundary. Depending on the surface characteristics of the surrounding fields, such as their growth period if cultivated, the relationship between the radiometric data and surface measurements will be compromised. Similar issues with mixed pixels have been noted in other studies using Sentinel (Misra, Cawkwell, & Wingler, 2020; Ramadhani et al., 2020; Son et al., 2021) and Landsat (Liao et al., 2018; Park et al., 2018; Zhang et al., 2018) imageries. The mixed pixel 30 m spatial resolution images and segment areas of Landsat 8 pixel and small rice field increase the probability of high mixed pixels. Also, clouds and cloud shadow seriously impact the contamination of pixels and misclassification. To account for some of the variation in the field and satellite measurements, the four rice biophysical measurements in each field were averaged; those with >1 S.D. from the mean were removed and the average recalculated. The satellite data extracts in the centre of the sample to avoid the mix-pixel values. Also, there may be some influences in the flooding in the flowering stage that coincides with monsoon, and the flooding in the paddy field influences the soil moisture (dielectric content) and impacts the backscatter or intensity in the final.

6.3 Future works

Based on the findings in Chapters 3 - 5 the following recommendations are suggested for future research.

- Analysis of the relationship between rice yield and precipitation, and temperature should use indices such as the Standardized Precipitation Index (SPI) and Diurnal Temperature Range (DTR), which have been shown to monitor drought conditions in different time-scale and drought types. These indices could be used alongside the Rice Productivity Index (RPI), which has been used to assess the correlation between rice productivity and climate variation (Patel, Chopra, & Dadhwal, 2007; Rahman et al., 2017). The RPI is the photochemical reflectance index and covers physiological and biochemical characteristics. However, a challenge in this analysis remains the underlying influences of rice variety on yield statistics, as different varieties have differing yield potentials. For example, Li et al. (2019) investigated the influences of agronomic traits and yield in the four different ecotypes (e.g. the inbred and hybrid for Indica and Japonica). They found differing rice characteristics such as filled grain number per panicle, 1,000-grain-weight, plant height, panicle length, grain per panicle, etc. The Japonica rice proved the dominant characteristics of high panicle number per unit area and extended growth period to improve high grain yield. Similar studies that have been analysed the influences of climate on rice production have seen the impact of weather in terms of time-series on temperature (April-October) and

rainfall (total rainfall all year responded with water usage within seasons and inter-seasonally) and rice yield at the district level by using Cobb-Douglas (CD) and Linear Quadratic (LQ). The results revealed that climate change impact rice yield and yield variability by 10-20%, and average rice yield was affected positively by temperature and negatively by rainfall, leading to fluctuation in rice production (Kim, 2009). Oort et al. (2016) revealed the impact of climate change on rice yield in the irrigated and non-irrigated systems for wet and dry seasons by simulating rice yield with varieties under high-temperature conditions in 4RCP. The high temperature negatively impacted rice yield, especially the photosynthesis rate (-24% in RCP 8.5 by 2070, compared with the baseline in 2000). Thus, this study suggested adaptation strategies (e.g. shifting sowing/planting dates suitable for monsoon onsets) and the serious impacts varied with East or West Africa. To account for the potential variation in rice yield, information on rice variety and its cultivated extent on an annual basis are needed.

- Chapter 4 revealed the considerable variation in the structural attributes of different rice varieties, which presents a challenge to the application of remotely sensed data to estimate biophysical variables over large spatial extents. Only a few studies using remote sensing data have explicitly accounted for rice variety. Ten rice varieties characterised the key phenological stages of rice, such as emergence, heading, and maturing using the signal of MODIS NDVI 16-day from 2001-2005 (Boschetti, Stroppiana, Brivio, & Bocchi, 2009). Further research is needed to understand the influences of rice variety on deriving estimates of yield or other biophysical parameters using remotely-sensed data. To do so, measurements of rice biophysical parameters throughout the growing season for a limited number of rice varieties but over a more significant number of paddy fields are needed.
- Chapter 5 revealed that the models developed to estimate rice yield was successful but may result in partly from the influences of rice varieties and irrigation that exhibit different structural characteristics. The best-performing models either required field measurements or provided yield estimates late in the growing season, neither of which offers significant benefits over the current methods implemented by the government (i.e. CCE). Accounting for the influences of rice variety mentioned previously may enable improved regression models to be developed. An alternative approach would be to employ crop growth simulation models, such as the SIMRIW (Simulation Model for Rice-Weather relations) (Horie et al., 1995), ORYZA (Yuan et al., 2017) or WOFOST model (Huang et al., 2015), parameterised using satellite-derived biophysical variables to estimate yield. LAI estimates could be derived from the Sentinel-2 Land bio-physical Processor (SL2P), which uses the PROSAIL canopy reflectance model (Baret, Jacquemoud, Guyot, & Leprieur, 1992) and which is suitable for describing the horizontally homogeneous structure of rice canopies. This approach has been applied to reliably estimate LAI with typically low errors of 1.55 – 6.98 $m^2 m^{-2}$ (MAPE 6.76% of the field measured LAI). Crop growth models may facilitate earlier

yield estimation, although the analysis should assess their suitability when applied to different rice varieties. The pattern of NDVI in rice peaked in the heading stage (Ali et al., 2021). On the contrary, our result indicated an earlier peaked NDVI in the panicle stage (**DOY 205-210**).

The study explored the correlation between rice biophysical variables and remotely-sensed data, proving the benefits of developing rice yield estimation models based on remotely-sensed data. There are different significant growth stages and remotely-sensed data in yield estimation. If the study develops yield estimation in the panicle stage, our study suggests the NDVI, while the ascending and VV/VH polarisation suggests yield estimation in the harvesting stage. The booting and post-heading stage is effective for yield estimation; however, differences in rice variety improve the accuracy of yield estimation throughout the growing season. This information can be incorporated into agricultural decision-making based on remotely-sensed data and is absolutely advantageous on improving agronomic services. Thailand should apply EO data for crop mapping and yield estimation. The proper satellite platform is necessary to determine their utilisation, while there is concern over cloud cover, especially in the rainy season; thus, our study recommends the Sentinel-1 in SAR for yield estimation.

Research using such models to estimate yield, Maki et al. (2017) directly integrated the parameters and remotely-sensed data to driven crop model “Simulated Model for Rice-Weather Relation (SIMRIW) - RS” such as transplanting date, leaf area index (simulated LAI or field measured LAI), amount of nitrogen, and meteorological data. These were essential data to readjust parameters. Other excellent research used non-remote sensing data (e.g. meteorological, soil, and agronomic management) and remote sensing data (e.g. MODIS and Sentinel-1 for start of season (SoS) and peak of season (PoS) rice estimation) for the ORYZA crop growth model (Setiyono et al., 2018). Zhou, Liu, and Liu (2019) proposed the assimilation technique with EVI time-series to extract essential phenology development (e.g. transplant date, heading date, and maturity date) and meteorological data (daily maximum/minimum temperature, solar radiation, wind speed, actual vapour pressure, and precipitation) into the WOFOST model. However, the entire above integrating remotely-sensed data and crop growth model seem to neglect rice variety determination. The further analysis should be investigated the other dual-polarisation in the HH or HV polarisation to determine the H transmission signal and whether it impacts on rice structure. Furthermore, the incidence angle, which describes the angle between the sensor and the ground, should be investigated by the other incidence angle of different SAR sensors. Research is being extended for the entire Chao Phraya River delta to apply the optical and radar remotely sensed data for rice monitoring and yield.

In the future, the Thai government, via the Ministry of Agriculture and Cooperatives, aims to utilise the advantage of remotely-sensed data in crop monitoring. One of the most important programmes- which involves cooperation between fourteen developing countries, the United Nations Conference on Trade and Development (UNCTAD), and the Aerospace Information Research Institute (AIR) Chinese Academy of Sciences (CAS)- is the CropWatch Innovative Cooperation Programme (CropWatch-ICP). This programme applies EO data on crop monitoring at a national and global scale to improve food security and operate towards the Sustainable Development Goals (SDGs) of zero hunger.

6.4 Conclusions

Rice is the world's major staple food crop and paddy fields account for over 12% of the global cropland area (FAOSTAT, 2010): close to 90% of the world's rice is produced in Asia (FAO, 2000). In Thailand, rice accounts for 46% of the cultivated area (OAE, 2020a) and is a major agricultural commodity, increasing production from 6.74 to 24.93 million tonnes between 1960 and 2020. As a result, the export of rice and its products now accounts for 10.69% of the export value of major agricultural product in Thailand (OAE, 2020b).

Analysis of the temporal dynamics of rice production and temperature and precipitation indicates that temperature and total rainfall influence rice production in the wet season. The irrigated areas proved resilient to changes in climatic variables. In comparison, the non-irrigated areas mostly in the northeast region are affected by changes in climate. Future predictions of climate change in Thailand suggest that rainfall will decrease, and temperature will increase. These changes highlighted the critical role that agricultural developments such as environmentally tolerant rice varieties can play in ensuring sustainable rice production when the world population is expected to increase to 9.8 billion by 2050 (United Nations, 2017).

Current methods for estimating rice yield in Thailand are based on conducting crop cutting experiments across a sample of areas under rice cultivation, which is laborious and time-consuming. On the other hand, satellite observations have been widely applied to map areas under agricultural land use, monitor their growing cycles and estimate rice yield and other biophysical parameters in many parts of the world. In the present study, Sentinel-1 and -2 observations were used to track the phenological cycle of rice using backscatter and vegetation index measurements, respectively. In the case of the vegetation indices, the values peaked in the panicle stage, where, while the LAI was not the highest, the development of flowers served to reduce vegetation index values. The backscatter coefficient also peaked in the panicle stage. However, it remained less variable in the flowering and harvesting stages when the canopy LAI

displayed less variation (+/- 0.5 $m^2 m^{-2}$) than the tillering and panicle stages and where the backscatter was responsive to the senescence leaves in the harvesting stage, unlike the NDVI.

Using field measurements collected throughout the growing season, empirical models were developed to estimate rice yield using satellite data. The best performing models estimated yield with RMSE of 0.54 with SEE 0.68 tonnes/ha and were limited by the requirement of either field measurements of ascending ratio VV/VH polarisation in the harvesting stage or that the rice yield estimates were best predicted late in the growing cycle. Also, the optical measurement in NDVI indicated excellent performance with NDVI in the panicle stage with the RMSE of 0.37 with SEE 0.7 tonnes/ha. When considering the SEE explained how large the prediction error is, the result proves that the SAR signal is better sensitive to rice canopy than spectral measurement. One of the issues in developing empirical models using satellite and field measurements is the influence of rice varieties with different biophysical attributes and temporal dynamics, adding variability to developing models at different growth stages. Further research is needed to investigate the spatial and temporal dynamics of different rice varieties in Thailand, to understand their influence on rice production and to assess the ability of satellite data to detect different rice varieties.

Appendix A Average seasonal temperature in different seasons in Thailand

Temperature	Region	Seasonal Temperature (°Celsius)		
		Winter	**Summer**	**Rainy**
Average Temperature	North	23.4	28.1	27.3
	Northeast	24.2	28.6	27.6
	Central	26.2	29.7	28.2
	East	26.7	29.1	28.3
	South			
	• East Coast	26.3	28.2	27.8
	• West Coast	27.0	28.4	27.5
Average Maximum Temperature	North	31.1	36.1	32.4
	Northeast	30.6	35.2	32.6
	Central	32.3	36.2	33.4
	East	32.0	34.1	32.3
	South			
	• East Coast	30.4	33.0	32.7
	• West Coast	32.0	34.1	31.6
Average Minimum Temperature	North	17.5	21.8	23.8
	Northeast	18.7	23.2	24.4
	Central	21.2	24.6	24.8
	East	22.3	25.2	25.2
	South			
	• East Coast	22.8	24.1	24.4
	• West Coast	23.2	24.0	24.3

Appendix B Summary of Pearson's correlation and P-value between temperature metrics and weather parameters at provincial level

Weather parameter	Number of significant provinces across the four groups (Specific significant group 1/3)			
	yield	Detrended yield	Production	Detrended production
Amount rainfall (Average)	2 provinces (0/2 provinces)	1 province (0/1 provinces)	4 provinces (1/3 provinces)	2 provinces (0/2 provinces)
Amount rainfall (Cumulative)	3 provinces (0/3 provinces)	1 province (0/1 province)	4 provinces (1/3 provinces)	2 provinces (0/2 province)
Rainy day (Average)	3 provinces (0/3 provinces)	1 province (0/1 province)	4 provinces (0/4 provinces)	2 provinces (1/1 provinces)
Rainy day (Cumulative)	2 provinces (0/2 provinces)	2 provinces (1/1 province)	4 provinces (0/4 provinces)	3 provinces (1/2 provinces)
Extra-maximum temperature (Average)	12 provinces (2/10 provinces)	3 provinces (1/2 provinces)	11provinces (2/9 provinces)	5 provinces (2/3 provinces)
Extra-minimum temperature (Average)	16 provinces (3/13 provinces)	3 provinces (0/3 provinces)	14 provinces (1/13 provinces)	4 provinces (0/4 provinces)
Mean temperature (Average)	5 provinces (2/3 provinces)	2 provinces (1/1 province)	4 provinces (0/4 provinces)	5 provinces (1/4 province)
Mean maximum temperature (Average)	14 provinces (3/11 provinces)	7 provinces (1/6 provinces)	12 provinces (2/10 provinces)	5 provinces (2/3 province)
Mean minimum Temperature (Average)	19 provinces (3/16 provinces)	4 provinces (1/3 province)	16 provinces (0/16 provinces)	4 provinces (1/3 provinces)
Difference in extra-maximum/minimum temperature (Average)	2 provinces (0/2 provinces)	3 provinces (1/2 province)	5 provinces (2/3 provinces)	2 provinces (0/2 province)
Difference in mean maximum/minimum temperature (Average)	5 provinces (0/5 provinces)	5 provinces (1/4 province)	5 provinces (3/2 provinces)	7 provinces (0/7 provinces)

Appendix C Correlation coefficient of significant weather and rice yield and rice production

C.1 Correlation coefficient of significant weather and rice yield

Weather parameter	Rice yield		
	Province	Irrigation system	Correlation coefficient (r)
Amount rainfall (Cumulative)	Buri Ram	Non-irrigated	0.568** (Sig.0.000)
	Maha Sarakham	Non-irrigated	0.336* (Sig. 0.048)
	Phayao	Non-irrigated	0.393* (Sig. 0.020)
Rainy day (Average)	Chaiyaphum	Non-irrigated	-0.358* (Sig.0.035)
	Phetcha Buri	Non-irrigated	0.344* (Sig.0.043)
	Phrae	Non-irrigated	0.382* (Sig.0.024)
Mean minimum temperature (Average)	Bangkok	Irrigated	0.715** (Sig.0.000)
	Chai Nat	Irrigated	0.451** (Sig.0.006)
	Kamphaeng Phet	Irrigated	0.506** (Sig.0.002)
	Chiang Rai	Non-irrigated	0.420* (Sig.0.012)
	Mukdahan	Non-irrigated	0.427* (Sig.0.011)
	Nakhon Phanom	Non-irrigated	0.526** (Sig.0.001)
	Nakhon Ratchasima	Non-irrigated	0.658** (Sig.0.000)
	Nakhon Sawan	Non-irrigated	0.488**(Sig.0.003)
	Nong Khai	Non-irrigated	0.549**(Sig.0.001)
	Phectcha Buri	Non-irrigated	0.440**(Sig.0.008)
	Phrae	Non-irrigated	0.401*(Sig.0.017)
	Prachin Buri	Non-irrigated	0.529**(Sig.0.001)
	Roi Et	Non-irrigated	0.404*(Sig.0.016)
	Sakhon Nakhon	Non-irrigated	0.612**(Sig.0.000)
	Si Sa Ket	Non-irrigated	0.583**(Sig.0.000)
	Surin	Non-irrigated	0.411* (Sig.0.014)
	Ubon Ratchathani	Non-irrigated	0.470** (Sig.0.004)
	Uttaradit	Non-irrigated	0.643**(Sig.0.000)

Appendix C

Weather parameter	Rice yield		
	Province	Irrigation system	Correlation coefficient (r)
Mean maximum temperature (Average)	Bangkok	Irrigated	0.676**(Sig.0.000)
	Nakhon Pathom	Irrigated	0.363*(Sig.0.032)
	Suphan Buri	Irrigated	0.367*(Sig.0.030)
	Maha Sarakham	Non-irrigated	0.585**(Sig.0.000)
	Mukdahan	Non-irrigated	0.443**(Sig.0.009)
	Nong Khai	Non-irrigated	0.547**(Sig.0.001)
	Phetcha Buri	Non-irrigated	0.655**(Sig.0.000)
	Prachin Buri	Non-irrigated	0.548**(Sig.0.001)
	Roi Et	Non-irrigated	0.428*(Sig.0.010)
	Sakhon Nakhon	Non-irrigated	0.455**(Sig.0.006)
	Sukhothai	Non-irrigated	0.347*(Sig.0.041)
	Surin	Non-irrigated	0.418*(Sig.0.012)
	Ubon Ratchathani	Non-irrigated	0.540**(Sig.0.001)
	Udon Thani	Non-irrigated	0.450**(Sig.0.007)
Difference mean maximum and minimum temperature (Average)	Chiang Rai	Non-irrigated	-0.353*(Sig.0.037)
	Kalasin	Non-irrigated	0.598*(Sig.0.011)
	Maha Sarakham	Non-irrigated	0.479**(Sig.0.004)
	Nakhon Ratchasima	Non-irrigated	-0.566**(Sig.0.000)
	Udon Thani	Non-irrigated	0.430**(Sig.0.010)

C.2 Correlation coefficient of significant weather and rice production

Weather parameter	Rice production		
	Province	Irrigation system	Correlation coefficient (r)
Amount rainfall (Cumulative)	Khamphaeng Phet	Irrigated	0.395**(Sig.0.019)
	Buri Ram	Non-irrigated	0.602** (Sig. 0.000)
	Chaiyaphum	Non-irrigated	0.334* (Sig 0.050)
	Lampang	Non-irrigated	0.399* (Sig 0.018)
Rainy day (Average)	Chaiyaphum	Non-irrigated	0.451** (Sig.0.007)
	Khon Kaen	Non-irrigated	0.395* (Sig.0.019)
	Nong Khai	Non-irrigated	0.401* (Sig.0.017)
	Phetcha Buri	Non-irrigated	0.402*(Sig.0.017)
Mean minimum temperature (Average)	Chiang Rai	Non-irrigated	0.490**(Sig.0.003)
	Kalasin	Non-irrigated	0.758**(Sig.0.000)
	Lampang	Non-irrigated	0.370*(Sig.0.029)
	Mukdahan	Non-irrigated	0.653**(Sig.0.000)
	Nakhon Phanom	Non-irrigated	0.610**(Sig.0.000)
	Nakhon Ratchasima	Non-irrigated	0.653**(Sig.0.000)
	Nakhon Sawan	Non-irrigated	0.437**(Sig.0.009)
	Phayao	Non-irrigated	0.385*(Sig.0.022)
	Phrae	Non-irrigated	0.351*(Sig.0.039)
	Prachin Buri	Non-irrigated	-0.441**(Sig.0.008)
	Roi Et	Non-irrigated	0.546**(Sig.0.001)
	Sakhon Nakhon	Non-irrigated	0.519**(Sig.0.001)
	Si Sa Ket	Non-irrigated	0.659**(Sig.0.000)
	Surin	Non-irrigated	0.518**(Sig.0.001)
	Ubon Ratchathani	Non-irrigated	0.449**(Sig.0.007)
	Uttaradit	Non-irrigated	0.659**(Sig.0.000)
Mean maximum temperature (Average)	Nakhon Pathom	Irrigated	0.433**(Sig.0.009)
	Suphan Buri	Irrigated	0.377*(Sig.0.025)
	Kalasin	Non-irrigated	0.715**(Sig.0.001)
	Maha Sarakham	Non-irrigated	0.447**(Sig.0.007)
	Mukdahan	Non-irrigated	0.624**(Sig.0.000)
	Phetcha Buri	Non-irrigated	0.506**(Sig.0.002)
	Prachin Buri	Non-irrigated	-0.510**(Sig.0.002)
	Roi Et	Non-irrigated	0.512**(Sig.0.002)

Appendix C

Weather parameter	Rice production		
	Province	**Irrigation system**	**Correlation coefficient (r)**
Mean maximum temperature (Average) (Cont.)	Sakhon Nakhon	Non-irrigated	0.494**(Sig.0.003)
	Si Sa Ket	Non-irrigated	0.426*(Sig.0.013)
	Sukhothai	Non-irrigated	0.351*(Sig.0.039)
	Ubon Ratchathani	Non-irrigated	0.571**(Sig.0.000)
Difference mean maximum and minimum temperature (Average)	Nakhon Pathom	Irrigated	0.395*(Sig.0.019)
	Phichit	Irrigated	0.606**(Sig.0.002)
	Suphan Buri	Irrigated	0.382*(Sig.0.024)
	Chiang Rai	Non-irrigated	-0.408*(Sig.0.015)
	Nakhon Ratchasima	Non-irrigated	-0.562**(Sig.0.000)

Appendix D Correlation between rice yield/production and weather in significant provinces

D.1 Cumulative rainfall

a) Amount of rainfall and rice yield

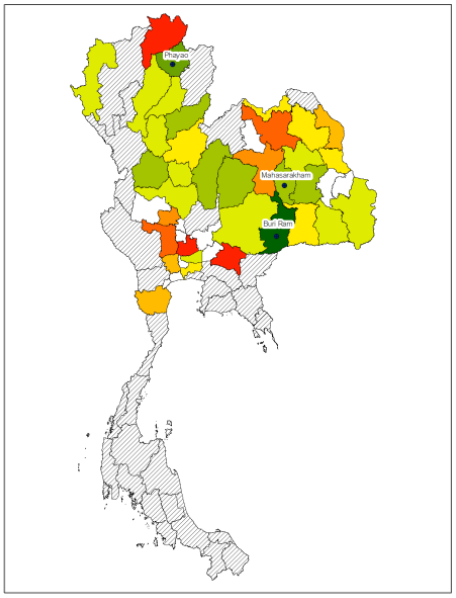

b) Amount of rainfall and detrended rice yield

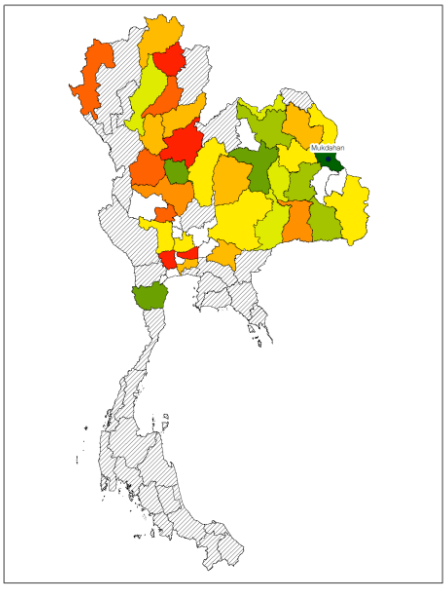

c) Amount of rainfall and rice production

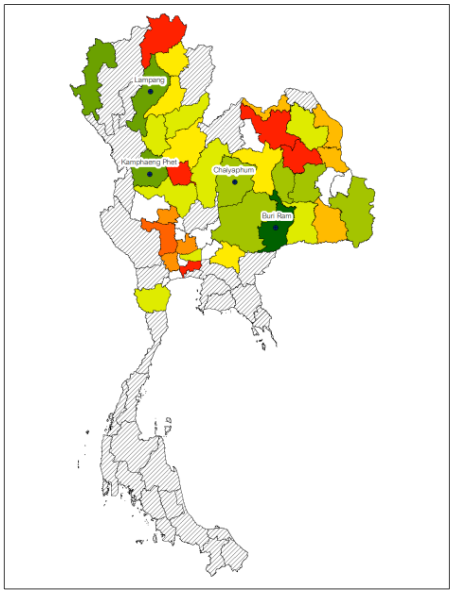

d) Amount of rainfall and detrended rice production

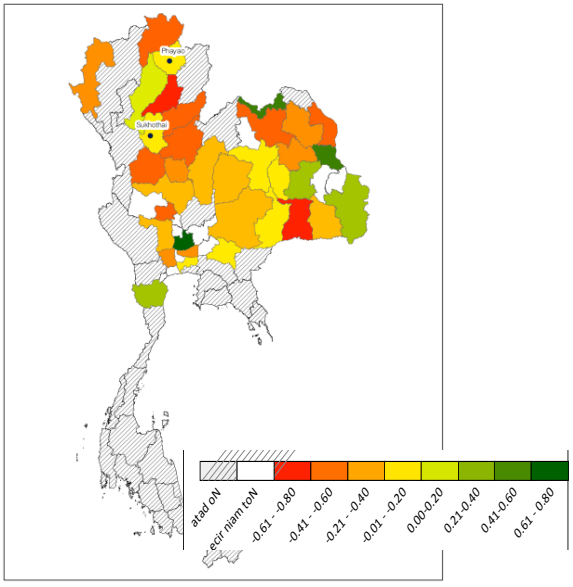

D.2 Average rainy day

a) Average rainy day and rice yield

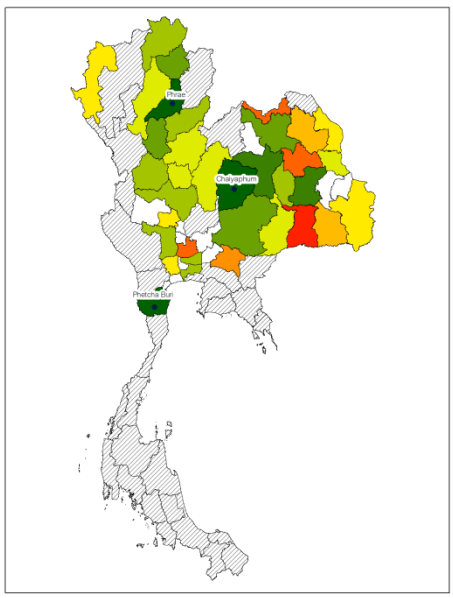

b) Average rainy day and detrended rice yield

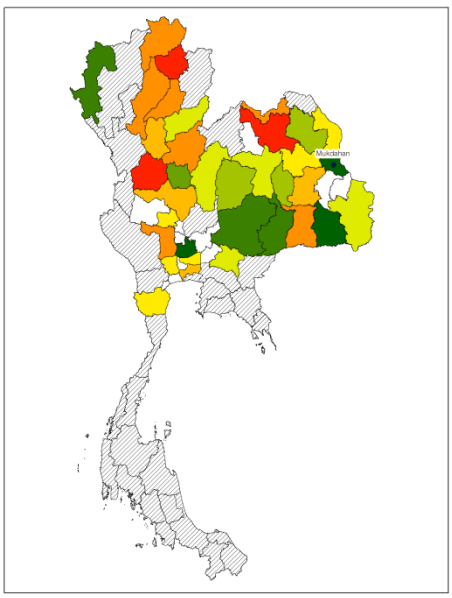

c) Average rainy day and rice production

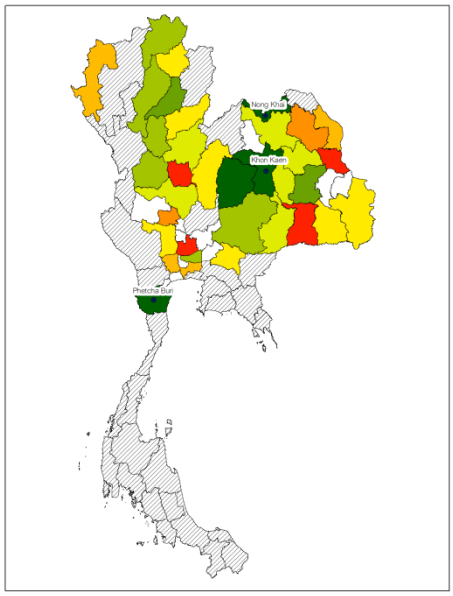

d) Average rainy day and detrended rice production

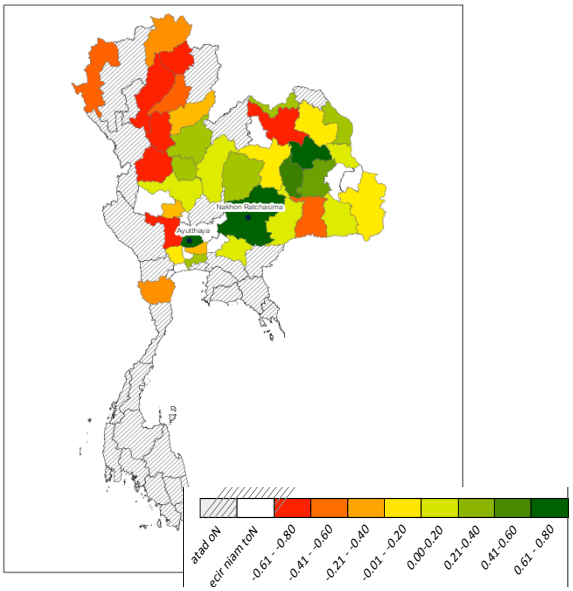

D.3 Mean minimum temperature

a) Mean minimum temperature and rice yield

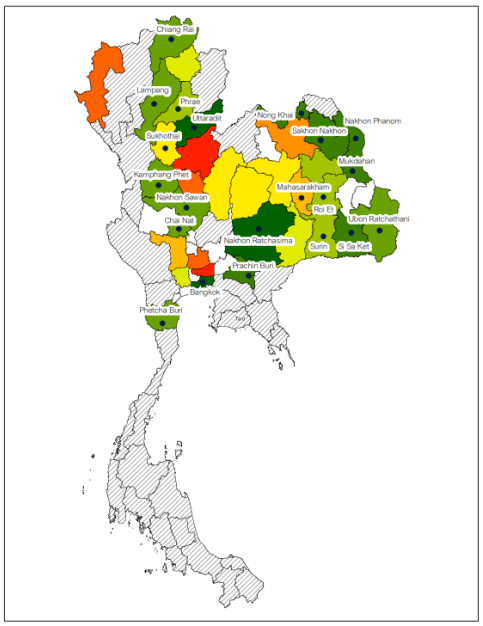

b) Mean minimum temperature and rice yield

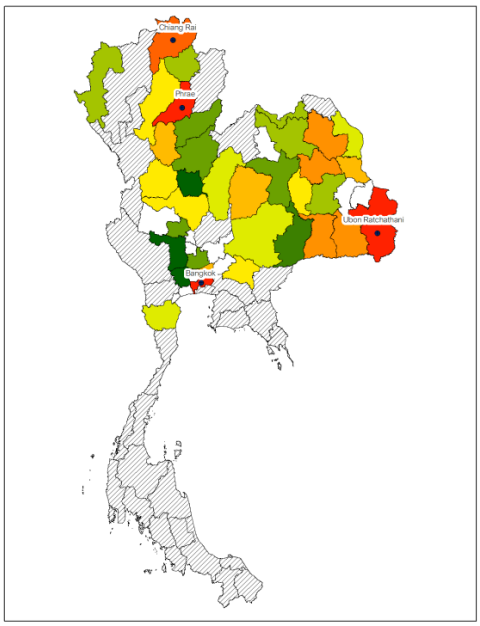

c) Mean minimum temperature and rice production

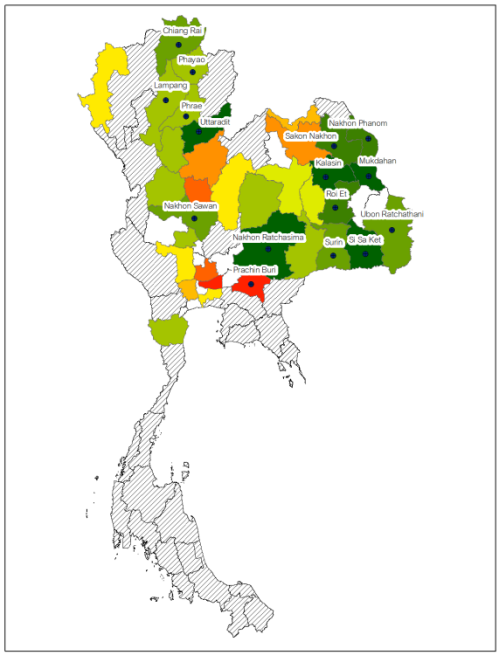

d) Mean minimum temperature and detrended rice production

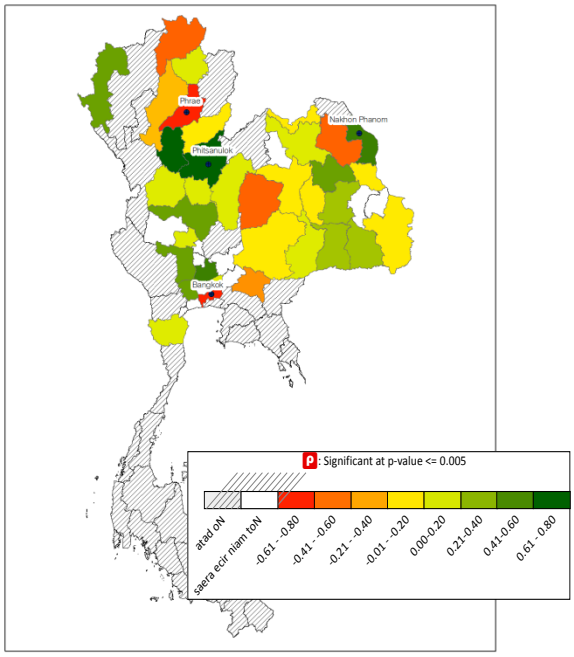

D.4 Mean maximum temperature

a) Mean maximum temperature and yield

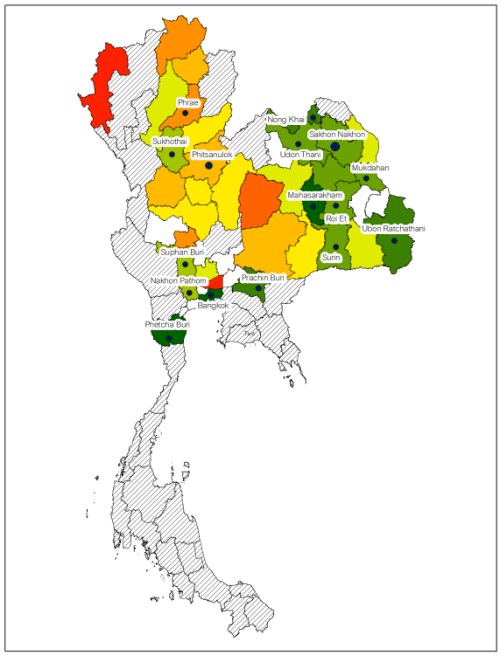

b) Mean maximum temperature and detrended yield

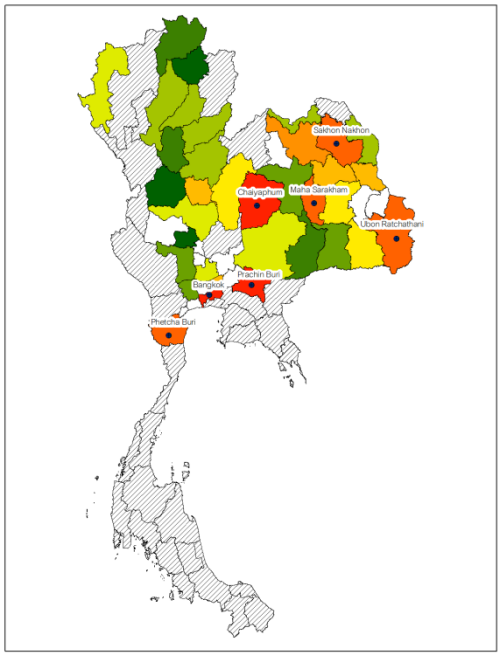

c) Mean maximum temperature and rice production

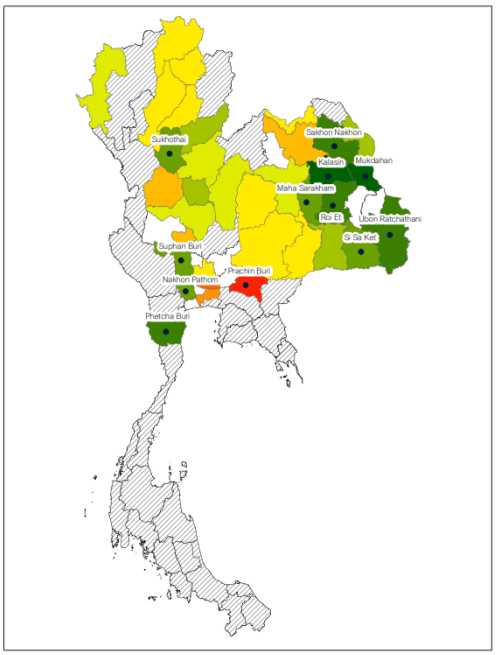

d) Mean maximum temperature and detrended rice production

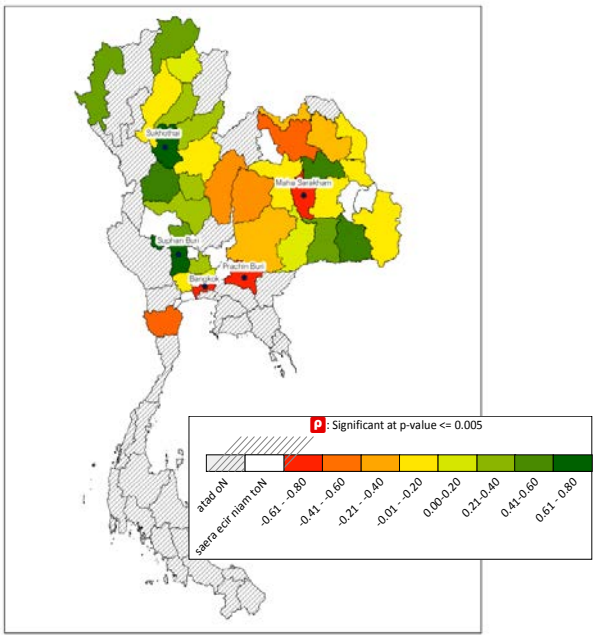

D.5 Differences between mean maximum and mean minimum temperature

a) Difference mean maximum and minimum temperature and rice yield

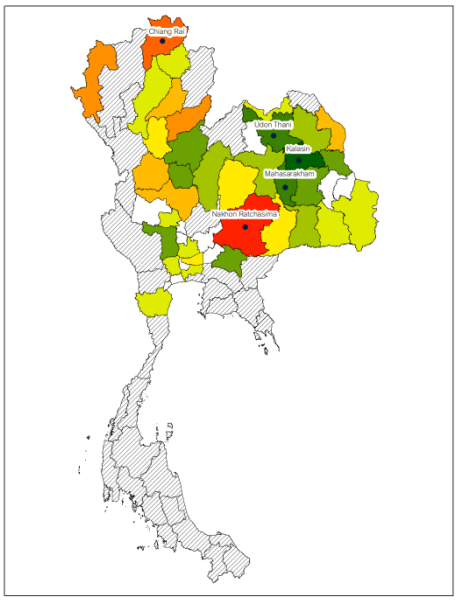

b) Difference mean maximum and minimum temperature and detrended rice yield

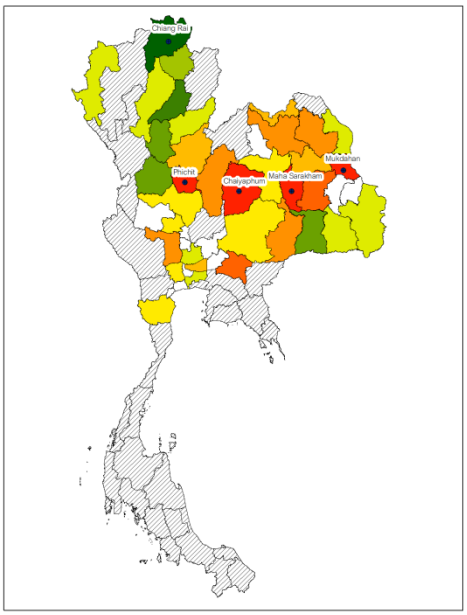

c) Difference mean maximum and minimum temperature rice production

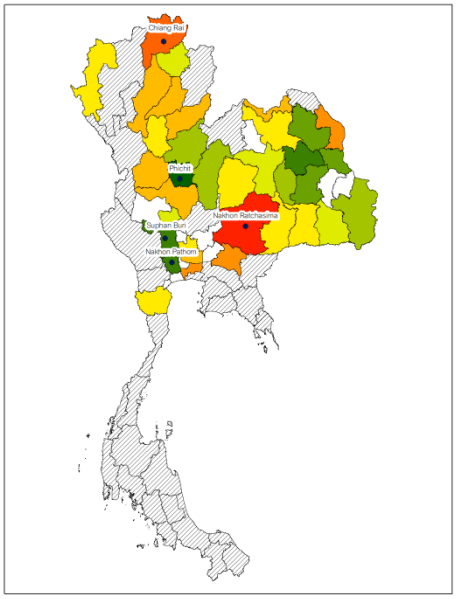

d) Difference mean maximum and minimum temperature and detrended rice production

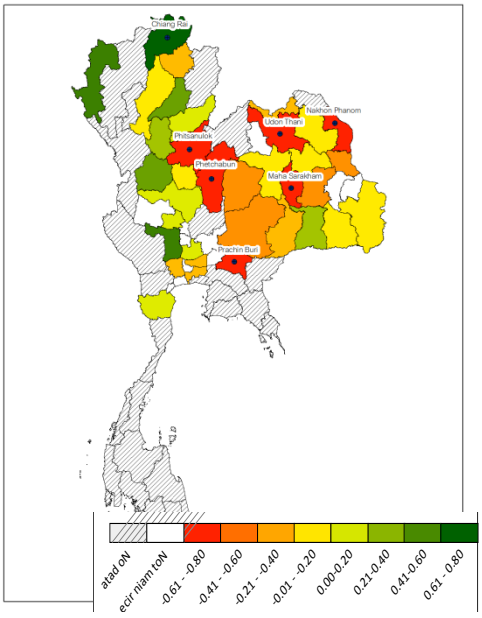

Appendix E Spatial auto-correlation with Moran's I index

E.1 Moran's I index of average rainfall

Year	Clustering pattern	Moran's Index	Expected index	Variance	Z-score	P-value
1981	Random	0.05	-0.01	0.01	0.95	0.34
1982	Random	0.08	-0.01	0.01	1.25	0.21
1983	Random	-0.01	-0.01	0.01	0.02	0.98
1984	Random	0.04	-0.01	0.01	0.76	0.45
1985	Random	0.04	-0.01	-0.01	0.75	0.45
1986	Random	0.05	-0.01	0.00	0.91	0.36
1987	Random	0.05	-0.01	0.01	0.90	0.37
1988	Random	0.01	-0.01	0.00	0.40	0.69
1989	Random	0.06	-0.01	0.00	1.02	0.31
1990	Random	0.04	-0.01	0.01	0.76	0.45
1991	Random	0.07	-0.01	0.00	1.25	0.21
1992	Random	0.06	-0.01	0.01	1.09	0.28
1993	Random	0.02	-0.01	0.01	0.43	0.67
1994	Random	0.02	-0.01	0.00	0.52	0.60
1995	Random	0.00	-0.01	0.00	0.25	0.81
1996	Random	0.03	-0.01	0.01	0.67	0.51
1997	Random	0.10	-0.01	0.00	1.58	0.11
1998	Random	0.01	-0.01	0.01	0.26	0.80
1999	Random	-0.05	-0.01	0.00	-0.48	0.63
2000	Random	0.02	-0.01	0.01	0.53	0.60
2001	Random	0.03	-0.01	0.00	0.69	0.49
2002	Random	0.04	-0.01	0.01	0.68	0.50
2003	Random	-0.01	-0.01	0.01	0.04	0.97
2004	Random	0.07	-0.01	0.01	1.14	0.25
2005	Random	-0.02	-0.01	0.01	-0.08	0.94
2006	Random	0.00	-0.01	0.00	0.22	0.83
2007	Random	0.03	-0.01	0.01	0.62	0.54
2008	Random	-0.04	-0.01	0.01	-0.36	0.72
2009	Random	-0.07	-0.01	0.00	-0.75	0.45
2010	Random	-0.09	-0.01	0.01	-1.11	0.27
2011	Random	0.02	-0.01	0.01	0.48	0.63
2012	Random	0.03	-0.01	0.00	0.62	0.53
2013	Random	0.07	-0.01	0.01	1.11	0.27
2014	Random	0.10	-0.01	0.00	1.59	0.11
2015	Random	0.12	-0.01	0.00	1.87	0.06

E.2 Moran's I index of cumulative rainfall

Year	Clustering pattern	Moran's Index	Expected index	Variance	Z-score	P-value
1981	Random	0.08	-0.01	0.01	1.33	0.18
1982	Clustered	0.11	-0.01	0.01	1.74	0.08
1983	Random	0.09	-0.01	0.01	1.48	0.14
1984	Random	0.09	-0.01	0.01	1.45	0.15
1985	Random	0.09	-0.01	0.01	1.46	0.14
1986	Random	0.09	-0.01	0.01	1.44	0.15
1987	Random	0.07	-0.01	0.01	1.14	0.26
1988	Random	0.09	-0.01	0.01	1.47	0.14
1989	Random	0.04	-0.01	0.01	0.70	0.49
1990	Random	0.09	-0.01	0.01	1.39	0.16
1991	Random	0.10	-0.01	0.01	1.53	0.13
1992	Clustered	0.15	-0.01	0.01	2.24	0.03
1993	Random	0.00	-0.01	0.01	0.13	0.90
1994	Random	0.02	-0.01	0.01	0.47	0.64
1995	Random	0.02	-0.01	0.01	0.47	0.64
1996	Random	0.02	-0.01	0.01	0.50	0.62
1997	Random	0.02	-0.01	0.01	0.47	0.64
1998	Random	-0.04	-0.01	0.01	-0.40	0.69
1999	Random	-0.01	-0.01	0.01	0.05	0.96
2000	Random	-0.01	-0.01	0.01	0.02	0.99
2001	Random	-0.01	-0.01	0.01	0.00	1.00
2002	Random	-0.01	-0.01	0.01	0.03	0.98
2003	Random	-0.01	-0.01	0.01	0.08	0.94
2004	Random	-0.01	-0.01	0.01	0.00	1.00
2005	Random	-0.01	-0.01	0.01	0.04	0.97
2006	Random	-0.02	-0.01	0.01	-0.03	0.97
2007	Random	-0.01	-0.01	0.01	0.00	1.00
2008	Random	-0.01	-0.01	0.01	0.03	0.98
2009	Random	-0.01	-0.01	0.01	0.06	0.95
2010	Random	-0.01	-0.01	0.01	0.10	0.92
2011	Random	-0.01	-0.01	0.01	0.00	1.00
2012	Random	-0.02	-0.01	0.01	-0.04	0.97
2013	Random	-0.02	-0.01	0.01	-0.04	0.97
2014	Random	-0.02	-0.01	0.01	-0.07	0.94
2015	Random	-0.02	-0.01	0.01	-0.05	0.96

E.3 Moran's I index of average temperature

Year	Clustering pattern	Moran's Index	Expected index	Variance	Z-score	P-value
1981	Random	0.08	-0.01	0.01	1.33	0.18
1982	Clustered	0.11	-0.01	0.01	1.74	0.08
1983	Random	0.09	-0.01	0.01	1.48	0.14
1984	Random	0.09	-0.01	0.01	1.45	0.15
1985	Random	0.09	-0.01	0.01	1.46	0.14
1986	Random	0.09	-0.01	0.01	1.44	0.15
1987	Random	0.07	-0.01	0.01	1.14	0.26
1988	Random	0.09	-0.01	0.01	1.47	0.14
1989	Random	0.04	-0.01	0.01	0.70	0.49
1990	Random	0.09	-0.01	0.01	1.39	0.16
1991	Random	0.10	-0.01	0.01	1.53	0.13
1992	Clustered	0.15	-0.01	0.01	2.24	0.03
1993	Random	0.00	-0.01	0.01	0.13	0.90
1994	Random	0.02	-0.01	0.01	0.47	0.64
1995	Random	0.02	-0.01	0.01	0.47	0.64
1996	Random	0.02	-0.01	0.01	0.50	0.62
1997	Random	0.02	-0.01	0.01	0.47	0.64
1998	Random	-0.04	-0.01	0.01	-0.40	0.69
1999	Random	-0.01	-0.01	0.01	0.05	0.96
2000	Random	-0.01	-0.01	0.01	0.02	0.99
2001	Random	-0.01	-0.01	0.01	0.00	1.00
2002	Random	-0.01	-0.01	0.01	0.03	0.98
2003	Random	-0.01	-0.01	0.01	0.08	0.94
2004	Random	-0.01	-0.01	0.01	0.00	1.00
2005	Random	-0.01	-0.01	0.01	0.04	0.97
2006	Random	-0.02	-0.01	0.01	-0.03	0.97
2007	Random	-0.01	-0.01	0.01	0.00	1.00
2008	Random	-0.01	-0.01	0.01	0.03	0.98
2009	Random	-0.01	-0.01	0.01	0.06	0.95
2010	Random	-0.01	-0.01	0.01	0.10	0.92
2011	Random	-0.02	-0.01	0.01	0.00	1.00
2012	Random	-0.02	-0.01	0.01	-0.04	0.97
2013	Random	-0.02	-0.01	0.01	-0.04	0.97
2014	Random	-0.02	-0.01	0.01	-0.07	0.94
2015	Random	-0.02	-0.01	0.01	-0.05	0.96

Appendix F Correlation between yield and rice biophysical

F.1 Correlation between yield and rice biophysical variables as a function of growth stage

Area	Rice variable	Correlation	Stage					
			Seeding	Tillering	Panicle	Flowering	Harvesting	Overall
Overall area	Stem density	r	0.28	0.03	-0.32	-0.29	0.1	0.03
		sig.	(0.2)	(0.88)	(0.15)	(0.19)	(0.65)	(0.8)
	Height	r	NA	**0.37***	0.07	-0.19	-0.1	0.03
		sig.		**(0.09)**	(0.77)	(0.4)	(0.66)	(0.78)
	LAI	r	NA	0.13	0.28	-0.00	-0.09	0.02
		sig.		(0.59)	(0.21)	(0.99)	(0.69)	0.83
	Chlorophyll content	r	NA	-0.23	-0.2	0.07	0.03	-0.09
		sig.		(0.31)	(0.34)	(0.77)	(0.88)	(0.4)
	Wet total Biomass	r	NA	NA	0.95	0.16	0.01	0.06
		sig.			(0.2)	(0.49)	(0.99)	(0.7)
	Wet Stem biomass	r	NA	NA	0.95	0.07	-0.09	-0.02
		sig.			(0.2)	(0.77)	(0.69)	(0.9)
	Wet grain biomass	r	NA	NA	0.95	**0.45****	0.30	**0.27***
		sig.			(0.21)	**(0.04)**	(0.17)	**(0.07**
	Dry total biomass	r	NA	NA	0.88	0.22	0.15	0.13
		sig.			(0.32)	(0.34)	(0.5)	(0.4)
	Dry stem biomass	r	NA	NA	0.83	0.03	0.04	0.02
		sig.			(0.38)	(0.92)	(0.87)	(0.92)
	Dry grain biomass	r	NA	NA	0.94	**0.43****	0.28	0.21
		sig.			(0.22)	**(0.05)**	0.21	0.16
Irrigated area	Stem density	r	**0.45***	0.23	-0.39	**-0.46***	0.2	0.08
		sig.	**(0.08)**	(0.39)	(0.16)	**(0.08)**	(0.46)	(0.47)
	Height	r	NA	0.14	-0.1	-0.14	-0.3	-0.04
		sig.		(0.59)	(0.7)	(0.62)	(0.26)	(0.78)
	LAI	r	NA	0.17	0.57*	0.09	0.18	0.16
		sig.		(0.59)	(0.02)	(0.75)	(0.51)	(0.21)
	Chlorophyll content	r	NA	-0.22	0.11	0.33	0.08	-0.02
		sig.		(0.42)	(0.68)	(0.21)	(0.77)	(0.89)
	Wet total biomass	r	NA	NA	0.95	0.32	0.24	0.23
		sig.			(0.2)	(0.25)	(0.37)	(0.19)
	Wet stem biomass	r	NA	NA	0.95	0.25	0.17	0.18
		sig.			(0.2)	(0.37)	(0.54)	(0.32)
	Wet grain biomass	r	NA	NA	0.95	**0.47***	0.37	**0.31***
		sig.			(0.21)	**(0.08)**	(0.15)	**(0.08)**
	Dry total biomass	r	NA	NA	0.88	0.34	0.28	0.22
		sig.			(0.32)	(0.21)	(0.29)	(0.2)
	Dry stem biomass	r	NA	NA	0.83	0.25	0.22	0.20
		sig.			(0.38)	(0.37)	(0.41)	(0.27)
	Dry grain biomass	r	NA	NA	0.94	0.37	0.32	0.21
		sig.			(0.22)	(0.17)	(0.23)	(0.24)
Non-irrigated area	Stem density	r	-0.24	-0.51	-0.13	0.12	-0.39	-0.14
		sig.	(0.65)	(0.3)	0.81	(0.82)	(0.45)	(0.46)
	Height	r	NA	**0.74***	0.35	-0.37	**0.81****	0.19
		sig.		**(0.09)**	(0.5)	(0.47)	**(0.05)**	(0.38)
	LAI	r	NA	0.08	-0.25	-0.27	-0.71	-0.29
		sig.		(0.91)	(0.64)	(0.61)	(0.12)	(0.18)

Area	Rice variable	Correlation	Stage					
			Seeding	Tillering	Panicle	Flowering	Harvesting	Overall
	Chlorophyll content	r sig.	NA	-0.38 (0.46)	-0.8 (0.6)	-0.58 (0.22)	-0.09 (0.86)	**-0.36*** **(0.08)**
	Chlorophyll content	r sig.	NA	-0.38 (0.46)	-0.8 (0.6)	-0.58 (0.22)	-0.09 (0.86)	**-0.36*** **(0.08)**
	Wet total biomass	r sig.	NA	NA	NA	-0.44 (0.38)	**-0.97**** **(0.00)**	**-0.58**** **(0.05)**
	Wet stem biomass	r sig.	NA	NA	NA	-0.57 (0.24)	**-0.95**** **(0.00)**	**-0.69**** **(0.01)**
	Wet grain biomass	r sig.	NA	NA	NA	0.38 (0.46)	-0.13 (0.81)	0.13 (0.69)
	Dry total biomass	r sig.	NA	NA	NA	-0.23 (0.66)	**-0.97**** **(0.00)**	-0.32 (0.31)
	Dry stem biomass	r sig.	NA	NA	NA	-0.63 (0.18)	**-0.93**** **(0.00)**	**-0.69**** **(0.01)**
	Dry grain biomass	r sig.	NA	NA	NA	0.57 (0.24)	0.05 (0.92)	0.23 (0.48)

Where *, ** value significant at the 0.05 and 0.01 probability level (2-tailed)
NA No measurement

F.2 Correlation between yield and rice biophysical variables as a function of rice variety in irrigated areas.

Rice variable	Correlation	HomMali 105	Phitsanulok2	RD41	RD47	RD49	RD57	RD61
Stem density	r sig.	.[c]	0.22 (0.54)	0.02 (0.93)	-0.06 (0.87)	0.37 (0.17)	.[c]	.[c]
Height	r sig.	.[c]	0.05 (0.91)	0.12 (0.57)	-0.31 (0.46)	-0.26 (0.41)	.[c]	.[c]
LAI	r sig.	.[c]	0.45 (0.32)	0.22 (0.32)	0.02 (0.96)	-0.44 (0.18)	.[c]	.[c]
Chlorophyll content	r sig.	.[c]	0.21 (0.63)	-0.11 (0.61)	-0.17 (0.69)	**-0.52*** **(0.08)**	.[c]	.[c]
Wet total biomass	r sig.	.[c]	0.29 (0.71)	**0.64**** **(0.02)**	-0.54 (0.46)	0.19 (0.72)	.[c]	.[c]
Wet stem biomass	r sig.	.[c]	0.26 (0.74)	**0.65**** **(0.02)**	-0.52 (0.48)	0.17 0.75)	.[c]	.[c]
Wet grain biomass	r sig.	.[c]	0.4 (0.6)	**0.54*** **(0.06)**	-0.29 (0.72)	0.16 (0.76)	.[c]	.[c]
Dry total biomass	r sig.	.[c]	0.36 (0.64)	**0.63**** **(0.02)**	-0.39 (0.61)	0.25 (0.63)	.[c]	.[c]
Dry stem biomass	r sig.	.[c]	0.37 (0.64)	**0.7**** **(0.01)**	-0.52 (0.48)	0.3 (0.56)	.[c]	.[c]
Dry grain biomass	r sig.	.[c]	0.19 (0.81)	**0.5*** **(0.08)**	-0.22 (0.79)	-0.06 (0.92)	.[c]	.[c]

Where *, ** value significant at the 0.05 and 0.01 probability level (2-tailed)
NA No measurement

F.3 Correlation coefficient between yields with rice biophysical variables in non-irrigated areas for different rice varieties.

Rice variable	Correlation	Phitsanulok2	RD13	RD31	RD49
Stem density	r	0.56*	.[c]	.[c]	0.04
	sig.	(0.09)			(0.91)
Height	r	0.43	.[c]	.[c]	0.21
	sig.	(0.29)			(0.61)
LAI	r	0.16	.[c]	.[c]	0.28
	sig.	(0.70)			(0.50)
Chlorophyll content	r	0.37	.[c]	.[c]	-0.51
	sig.	(0.37)			(0.2)
Wet total biomass	r	0.2	.[c]	.[c]	**-0.97****
	sig.	(0.8)			**(0.03)**
Wet stem biomass	r	0.01	.[c]	.[c]	-0.88
	sig.	0.99			(0.13)
Wet grain biomass	r	0.46	.[c]	.[c]	0.03
	sig.	(0.54)			(0.97)
Dry total biomass	r	0.26	.[c]	.[c]	-0.82
	sig.	(0.74)			(0.19)
Dry stem biomass	r	-0.11	.[c]	.[c]	-0.79
	sig.	(0.89)			(0.21)
Dry grain biomass	r	0.46	.[c]	.[c]	0.16
	sig.	(0.54)			(0.84)

Where *, ** value significant at the 0.05 and 0.01 probability level (2-tailed)
NA No measurement

F.4 Correlation of RD41 overall and in each growth stage.

Rice variable	Correlation	Seeding	Tillering	Panicle	Flowering	Harvesting	Overall
Stem Density	r	0.05	0.4	0.11	**-0.86***	0.15	**-0.79****
	sig.	(0.93)	(0.43)	(0.84)	**(0.03)**	(0.77)	**(0.00)**
Height	r	NA	0.47	0.04	0.36	0.21	**0.67****
	sig.		(0.35)	(0.93)	(0.48)	(0.69)	**(0.00)**
LAI	r	NA	0.27	0.74	0.50	0.66	0.22
	sig.		(0.66)	(0.09)	(0.31)	(0.15)	(0.32)
Chlorophyll content	r	NA	-0.72	-0.06	0.49	-0.04	**0.64****
	sig.		(0.11)	(0.91)	(0.32)	(0.93)	**(0.00)**
Wet total biomass	r	NA	NA	**1.00****	0.62	**0.87****	**0.67***
	sig.				(0.26)	**0.02**	**(0.01)**
Wet stem biomass	r	NA	NA	**1.00****	0.62	**0.85****	**0.69****
	sig.				(0.27)	**(0.03)**	**(0.01)**
Wet grain biomass	r	NA	NA	**1.00****	0.63	**0.83****	**0.57****
	sig.				(0.26)	**(0.04)**	**(0.04)**
Dry total biomass	r	NA	NA	**1.00****	0.67	**0.94****	**0.62****
	sig.				(0.22)	**(0.00)**	**(0.02)**
Dry stem biomass	r	NA	NA	**1.00****	0.68	**0.89****	**0.67****
	sig.				(0.21)	**(0.02)**	**(0.01)**
Dry grain biomass	r	NA	NA	**1.00****	0.65	**0.87***	**0.52***
	sig.				(0.24)	**(0.03)**	**(0.07)**

Where *, ** value significant at the 0.05 and 0.01 probability level (2-tailed)
NA No measurement

Appendix G Histogram of backscatter coefficient

G.1 Phichit province

Stage	Orbit direction and polarisation			
	Ascending and VV	**Ascending and VH**	**Descending and VV**	**Descending and VH**
Seeding	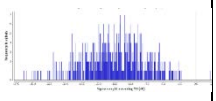 Mean -12.45, Max 3.38, Min -26.38,	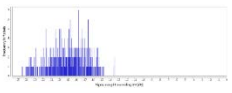 Mean -19.11, Max -13.38, Min -24.45	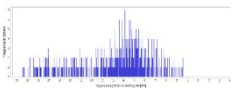 Mean -10.83, , Max -4.35, Min -19.45	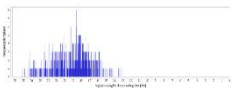 Mean -19.15, Max -12.99, Min -25.03,
Tillering	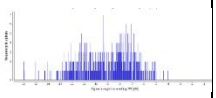 Mean -9.06, Max -3.97, Min -16.01	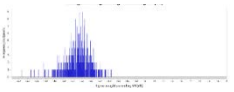 Mean -16.44, Max -12.68, Min -22.63	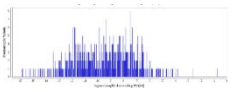 Mean -9.47, Max -0.69, Min -15.82	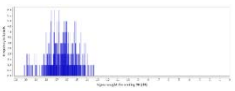 Mean -16.45, Max -13.3, Min -20.11
Panicle	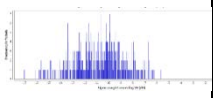 Mean -10.68, Max -5.6, Min -17.01	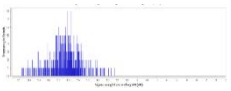 Mean -16.27, Max -11.27, Min -20.65	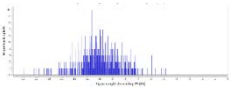 Mean -9.96, Max -4.84, Min -15.96	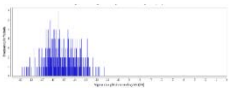 Mean -15.16, Max -11.23, Min -18.8
Flowering	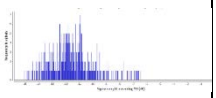 Mean -11.61, Max -6.45, Min -15.07	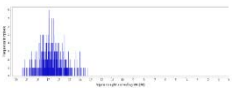 Mean -16.57, Max -13.19, Min -19.36	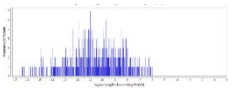 Mean -10.51, Max -5.92, Min -16.41	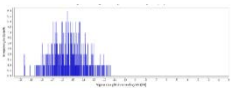 Mean -15.35, Max -11.36, Min -19.65
Harvesting	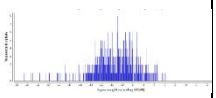 Mean -10.55, Max -5.9, Min -19.27	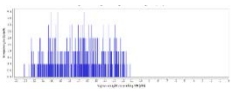 Mean -16.91, Max -11.1, Min -23.07	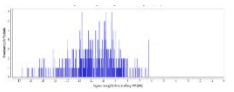 Mean -10.77, Max -6.22, Min -16.71	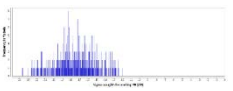 Mean -17.44, Max -11.96, Min -23.64

G.2 Ang Thong province

Stage	Orbit direction and polarisation			
	Ascending and VV	**Ascending and VH**	**Descending and VV**	**Descending and VH**
Seeding	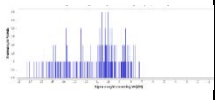 Mean -11.19, Max -6.78, Min -17.23	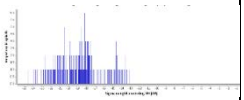 Mean -18.7, Max -13.06, Min -24.56	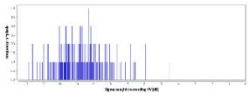 Mean -9.8, Max -4.51, Min -12.81	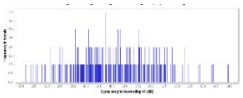 Mean -18.43, Max -14, Min -21.8
Tillering	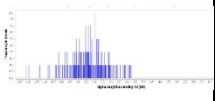 Mean -8.31, Max -5.74, Min -12.13	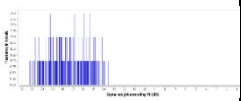 Mean -17.56, Max -13.53, Min -21.18	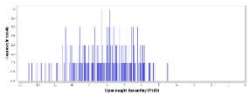 Mean -8.12, Max -4.48, Min -12.48	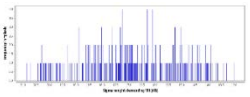 Mean -16.85, Max -12.99, Min -20.85
Panicle	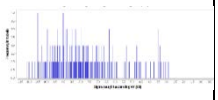 Mean -7.8, Max -2.87, Min -11.11	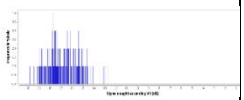 Mean -16.83, Max -12.7, Min -19.8	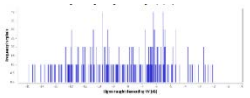 Mean -8.36, Max -2.07, Min -14.92	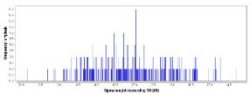 Mean -17.04, Max -14.29, Min -19.83
Flowering	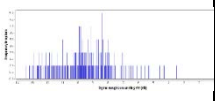 Mean -9.56, Max -3.45, Min -13.37	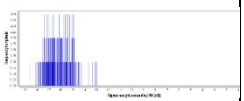 Mean -16.11, Max -12.89, Min -18.55	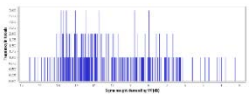 Mean -10.2, Max -3.22, Min -14.56	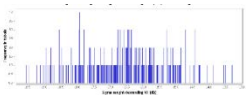 Mean -16.61, Max -13.28, Min -19.54
Harvesting	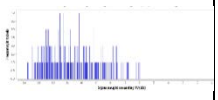 Mean -10.67, Max -5.94, Min -13.74	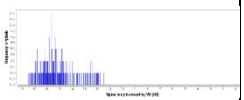 Mean -15.1, Max -11.42, Min -17.43	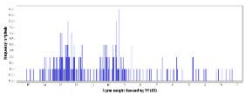 Mean -10.57, Max -2.27, Min -15.05	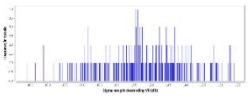 Mean -15.22, Max -12.59, Min -18.6

G.3 Pathum Thani province

Stage	Orbit direction and polarisation			
	Ascending and VV	**Ascending and VH**	**Descending and VV**	**Descending and VH**
Seeding	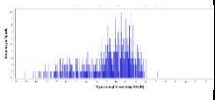 Mean -11.72, Max -6.71, Min -20.05	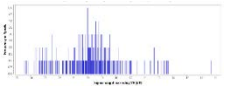 Mean -19.93, Max -11.27, Min -24.45	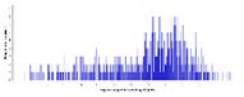 Mean -10.13, Max -5.09, Min -24.45	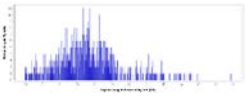 Mean -19.3, Max -11.08, Min -23
Tillering	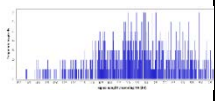 Mean -8.48, Max -4.03, Min -14.59	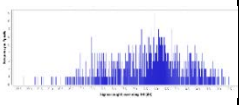 Mean -16.28, Max -12.46, Min -22.26	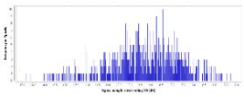 Mean -9.32, Max -5.22, Min -14.83	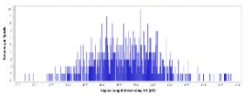 Mean -15.3, Max -12.17, Min -18.27
Panicle	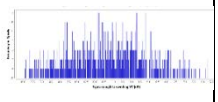 Mean -11.26, Max -5.69, Min -15.87	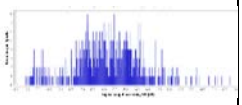 Mean -15.8, Max -10.22, Min -19.54	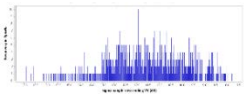 Mean -9.32, Max -5.22, Min -14.83	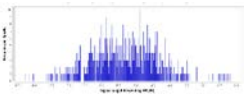 Mean -16.35, Max -14.25, Min -20.2
Flowering	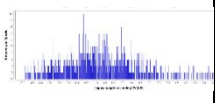 Mean -10.69, Max -4.48, Min -14.86	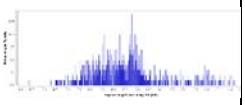 Mean -15.4, Max -10.79, Min -19.65	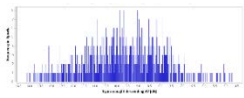 Mean -9.67, Max -4.69, Min -14.11	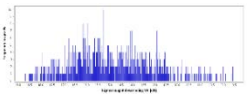 Mean -14.82, Max -9.54, Min -18.67
Harvesting	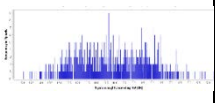 Mean -10.18, Max -4.64, Min -14.91	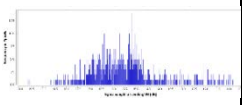 Mean -15.72, Max -11.2, Min -22.19	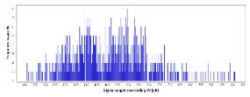 Mean -9.85, Max -3.85, Min -13.82	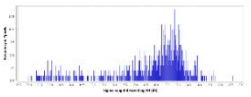 Mean -16.32, Max -12.36, Min -22.03

Appendix H Sentinel-2 and Sentinel-1 specifications

H.1 Sentinel-2 wavelength

Satellite product	Revisit time (days)	Swath width (km)	Bands
Sentinel-2	10 days with one satellite and 5 days with two satellites	290	Band 1 – Coastal/Aerosol (60 m) Band 2 – Blue (10 m) Band 3 – Green (10 m) Band 4 – Red (10 m) Band 5 – Vegetation red edge (20 m) Band 6 – Vegetation red edge (20 m) Band 7 – Vegetation red edge (20 m) Band 8 – Near infrared (10 m) Band 8A – Narrow near infrared (20 m) Band 9 – Water vapour (60 m) Band 10 - Short wavelength infrared - Cirrus (60 m) Band 11 – Short wavelength infrared (20 m) Band 12 - Short wavelength infrared (20 m)

H.2 Sentinel-1 characteristic of each sub-swath

Beam ID	IW1	IW2	IW3
Spatial resolution (range x azimuth) m	2.7 x 22.5	3.1 x 22.7	3.5 x 22.6
Pixel spacing (range x azimuth) m	2.3 x 14.1	2.3 x 14.1	2.3 x 14.1
Incidence angle at min orbit altitude (°)	32.9	38.3	43.1
Range look bandwidth MHz	56.5	48.3	42.8
Azimuth look bandwidth Hz	315	301	301
Range hamming weighting coefficient	0.75	0.75	0.75
Azimuth hamming weighting coefficient	0.70	0.75	0.75

H.3 Sentinel-1 main properties on IW mode

Product ID	IW_SLC
Pixel value	Complex
Coordinate system	Slant range
Bits per pixel	16I and 16Q
Polarisation options	Single (HH or VV) or dual (HH+HV or VV+VH)
Ground range coverage (km)	251.8
Equivalent number of looks (ENL)	1
Radiometric correction	3
Absolute location accuracy m (NRT)	7
Number of looks (range x azimuth)	1x1

Appendix I Photo of sample field during the study period

Sample unit 1

Seeding

Tillering

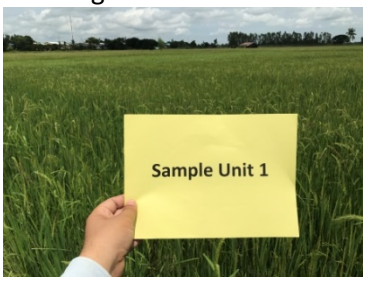

Panicle

Flowering

Harvesting

Sample unit 2

Seeding

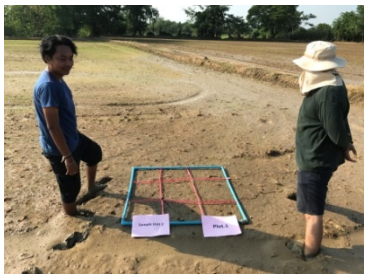

Tillering

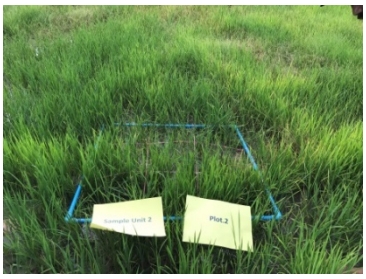

Panicle

Flowering

Harvesting

Appendix I

Sample unit 3

Seeding

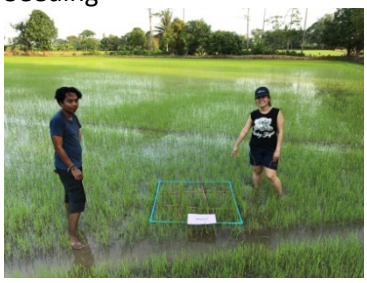

Tillering

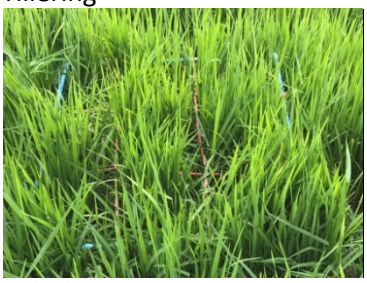

Panicle

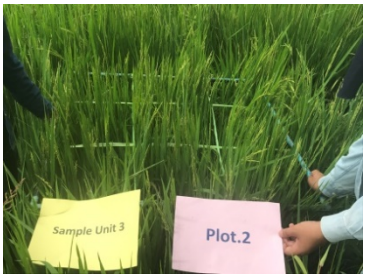

Flowering

Harvesting

Sample unit 5

Seeding

Tillering

Panicle

Flowering

Harvesting

Sample unit 7

Seeding

Tillering

Panicle

Flowering

Harvesting

Sample unit 9

Seeding

Tillering

Panicle

Flowering

Harvesting

Appendix I

Sample unit 10

Seeding

Tillering

Panicle

Flowering

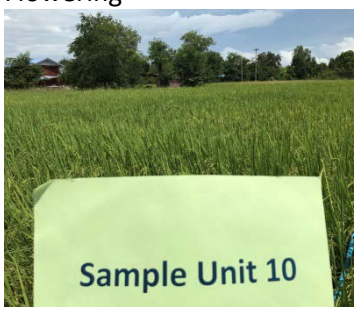

Harvesting

Sample unit 11

Seeding

Tillering

Panicle

Flowering

Harvesting

Sample unit 12

Seeding

Tillering

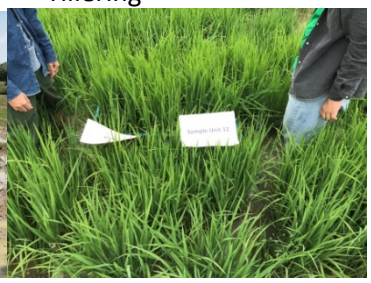

Panicle

Flowering

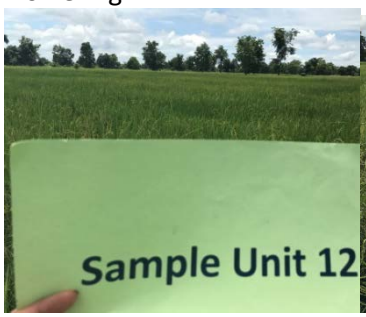

Harvesting

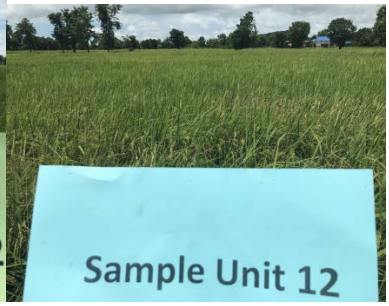

Sample unit 13

Seeding

Tillering

Panicle

Flowering

Harvesting

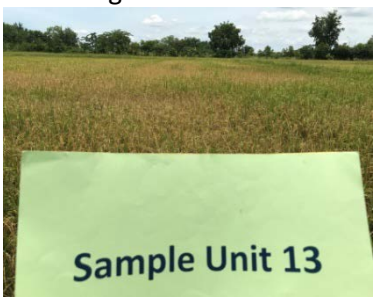

Appendix I

Sample unit 14

Seeding

Tillering

Panicle

Flowering

Harvesting

Sample unit 15

Seeding

Tillering

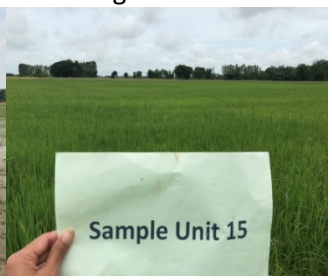

Panicle

Flowering

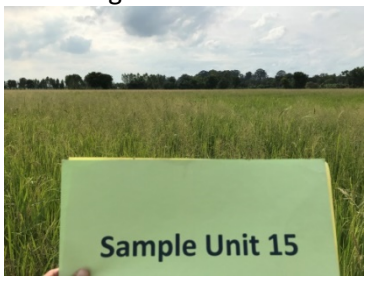

Harvesting

Sample unit 17

Seeding

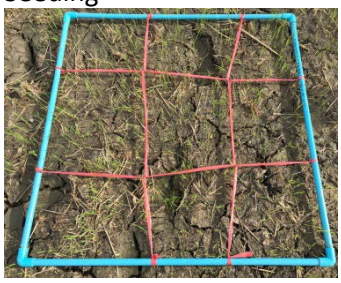

Tillering

Panicle

Flowering

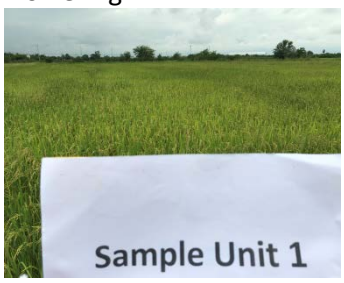

Harvesting

Sample unit 18

Seeding

Tillering

Panicle

Flowering

Harvesting

Appendix I

Sample unit 19

Seeding

Tillering

Panicle

Flowering

Harvesting

Sample unit 20

Seeding

Tillering

Panicle

Flowering

Harvesting

Sample unit 21

Seeding

Tillering

Panicle

Flowering

Harvesting

Sample unit 23

Seeding

Tillering

Panicle

Flowering

Harvesting

Sample unit 24

Seeding

Tillering

Panicle

Flowering

Harvesting

Sample unit 25

Seeding

Tillering

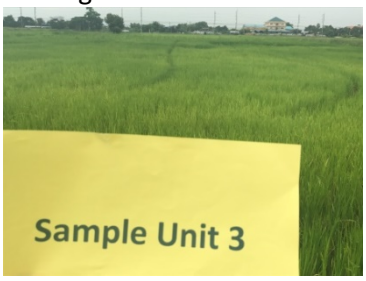

Panicle

Flowering

Harvesting

Sample unit 26

Seeding

Tillering

Panicle

Flowering

Harvesting

Sample unit 27

Seeding

Tillering

Panicle

Flowering

Harvesting

Appendix J Average of satellite values during growing season

J.1 Average of VI values during growing season

VI	Average and standard deviation (S.D.) of VI values									
	Seeding	S.D.	Tillering	S.D.	Panicle	S.D.	Flowering	S.D.	Harvesting	S.D.
Overall area										
NDVI	0.03	0.09	0.47	0.18	0.61	0.05	0.27	0.16	0.20	0.11
EVI	0.12	0.12	0.57	0.16	0.60	0.10	0.36	0.21	0.19	0.10
Phichit										
Irrigated areas										
NDVI	-0.01	0.01	0.47	0.23	0.63	0.04	0.42	0.15	0.20	0.16
EVI	0.07	0.09	0.51	0.24	0.59	0.12	0.50	0.14	0.13	0.05
Non-irrigated areas										
NDVI	-0.02	0.13	0.63	0.09	0.62	0.06	0.24	0.15	0.19	0.06
EVI	0.07	0.18	0.61	0.12	0.63	0.11	0.55	0.21	0.15	0.08
Ang Thong										
NDVI	0.03	0.03	0.34	0.11	0.63	0.05	0.17	0.05	0.12	0.07
EVI	0.14	0.06	0.61	0.08	0.60	0.10	0.16	0.04	0.22	0.13
Pathum Thani										
NDVI	0.13	0.02	0.41	0.13	0.57	0.04	0.23	0.17	0.30	0.07
EVI	0.22	0.05	0.54	0.18	0.55	0.07	0.20	0.07	0.28	0.10

J.2 Average of backscatter values during growing season

Backscatter	Average and standard deviation (S.D.) of backscatter values									
	Seeding	S.D.	Tillering	S.D.	Panicle	S.D.	Flowering	S.D.	Harvesting	S.D.
Overall area										
AscVV	-13.14	4.02	-8.76	2.15	-9.80	3.07	-10.82	2.54	-9.91	3.14
AscVH	-19.85	2.20	-17.17	1.66	-16.53	1.86	-16.08	1.38	-16.36	2.62
AscVV/VH	0.66	0.19	0.52	0.14	0.59	0.16	0.67	0.13	0.61	0.17
DescVV	-11.09	3.13	-9.69	2.19	-9.65	2.74	-9.90	2.82	-10.26	2.30
DescVH	-19.70	2.01	-16.65	1.37	-16.20	1.51	-15.45	1.64	-16.95	2.34
DescVV/VH	0.56	0.12	0.58	0.13	0.60	0.17	0.64	0.16	0.61	0.14
Phichit										
Irrigated area										
AscVV	-11.67	5.34	-7.66	2.00	-10.51	2.01	-11.56	3.34	-10.80	1.55

Backscatter	Average and standard deviation (S.D.) of backscatter values									
	Seeding	S.D.	Tillering	S.D.	Panicle	S.D.	Flowering	S.D.	Harvesting	S.D.
Phichit- Irrigated area (Cont.)										
AscVH	-18.85	2.60	-16.87	1.47	-16.72	1.62	-16.44	1.28	-16.27	3.19
AscVV/VH	0.61	0.27	0.46	0.13	0.63	0.08	0.70	0.17	0.67	0.06
DescVV	-10.59	3.78	-9.68	1.79	-10.29	2.22	-11.89	2.58	-11.52	2.59
DescVH	-19.11	2.73	-16.98	1.48	-15.93	0.52	-16.22	1.06	-18.35	2.52
DescVV/VH	0.55	0.12	0.57	0.11	0.64	0.13	0.73	0.13	0.63	0.12
Non-irrigated area										
AscVV	-15.53	3.01	-10.22	1.63	-10.74	2.92	-12.08	0.46	-9.38	4.26
AscVH	-19.43	1.43	-16.50	0.71	-16.21	1.46	-17.19	0.63	-17.78	2.29
AscVV/VH	0.80	0.13	0.62	0.08	0.66	0.14	0.70	0.03	0.52	0.19
DescVV	-11.88	3.49	-10.91	2.53	-9.88	1.31	-9.99	1.59	-9.83	0.93
DescVH	-19.98	1.90	-16.57	1.06	-14.63	1.61	-14.57	1.50	-16.73	2.52
DescVV/VH	0.59	0.14	0.65	0.11	0.68	0.09	0.69	0.09	0.59	0.07
Ang Thong										
AscVV	-11.52	2.90	-8.17	0.52	-6.51	2.16	-9.69	1.46	-11.24	1.57
AscVH	1-.92	1.67	-18.30	1.79	-17.45	0.68	-15.76	0.49	-15.26	0.94
AscVV/VH	0.57	0.10	0.45	0.02	0.38	0.13	0.62	0.10	0.74	0.12
DescVV	-9.60	1.46	-8.20	1.03	-6.59	2.74	-9.55	3.02	-10.94	3.04
DescVH	-18.50	0.96	-17.72	1.06	-17.46	0.64	-16.86	1.33	-15.43	0.54
DescVV/VH	0.52	0.07	0.46	0.03	0.38	0.16	0.56	0.16	0.71	0.21
Pathum Thani										
AscVV	-13.65	3.78	-8.91	3.19	-11.12	3.36	-9.57	3.28	-8.13	3.98
AscVH	-21.49	2.52	-17.20	2.36	-15.77	3.13	-14.66	1.59	-15.86	3.29
AscVV/VH	0.63	0.14	0.53	0.21	0.70	0.11	0.64	0.18	0.51	0.21
DescVV	-12.23	3.21	-9.72	2.66	-11.65	2.47	-7.74	3.05	-8.60	1.57
DescVH	-21.26	1.07	-15.28	0.78	-17.15	0.10	-14.16	1.22	-17.03	2.59
DescVV/VH	0.57	0.14	0.63	0.16	0.68	0.13	0.55	0.22	0.51	0.07

Appendix K Rice yield and rice production in 2017 in 3 representative provinces

Province/Amphoe	Rice harvested area (hectare)	Rice yield (ton/ha)	Rice production (tonnes)
Phichit	**232,536**	**3.77**	**876,596**
Muang Phichit	23,669	3.98	94,084
Taphan Hin	25,984	4.09	106,373
Bang Mun Nak	22,600	3.88	87,716
Pho Thale	26,821	4.09	109,632
Pho Prathap Chang	19,274	3.84	74,083
Sam Ngam	21,524	3.74	80,445
Wang Sai Phun	17,983	3.42	61,478
Thap Khlo	24,612	3.48	85,525
Sak Lek	6,919	3.08	21,277
Bueng Na Rang	13,718	3.97	54,444
Dong Charoen	14,745	3.39	49,947
Wachirabarami	14,688	3.51	51,592
Ang Thong	**55,421**	**4.16**	**230,547**
Muang Ang Thong	3,916	4.12	16,131
Chaiyo	2,885	3.84	11,089
Pa Mok	593	3.80	2,252
Pho Thong	13,508	4.13	55,719
Wiset Chai Chan	15,342	4.12	63,190
Samko	7,798	4.24	33,093
Sawaeng Ha	11,379	4.31	49,073
Pathum Thani	**49,657**	**4.49**	**223,167**
Muang Pathum Thani	3,099	4.31	13,363
Khlong Luang	8,066	4.58	36,903
Thanyaburi	1,484	4.51	6,687
Lat Lum Kaeo	11,548	4.63	53,408
Lam Luk Ka	11,846	4.50	53,307
Sam Khok	2,892	4.47	12,924
Nong Suea	10,722	4.34	46,575

Appendix L Correlation between satellite and rice biophysical variables

L.1 Correlation between vegetation indices and rice biophysical variables in overall areas, irrigated areas, and non-irrigated areas across growth stages.

Irrigated system	Stage	Rice biophysical variables	Statistical	Vegetation indices	
				NDVI	EVI
Overall	Seeding	Rice age	Pearson (sig. 2-tailed)	-0.11 0.61	0.23 0.30
		Stem density	Pearson (sig. 2-tailed)	-0.22 0.33	-0.33 0.14
		Water depth	Pearson (sig. 2-tailed)	-0.04 0.85	0.16 0.48
		Height	Pearson (sig. 2-tailed)	.[c]	.[c]
		Absolut height	Pearson (sig. 2-tailed)	.[c]	.[c]
		LAI	Pearson (sig. 2-tailed)	.[c]	.[c]
		Chlorophyll	Pearson (sig. 2-tailed)	.[c]	.[c]
		Wet total biomass	Pearson (sig. 2-tailed)	.[c]	.[c]
		Wet stem biomass	Pearson (sig. 2-tailed)	.[c]	.[c]
		Wet grain biomass	Pearson (sig. 2-tailed)	.[c]	.[c]
		Dry total biomass	Pearson (sig. 2-tailed)	.[c]	.[c]
		Dry stem biomass	Pearson (sig. 2-tailed)	.[c]	.[c]
		Dry grain biomass	Pearson (sig. 2-tailed)	.[c]	.[c]
	Tillering	Rice age	Pearson (sig. 2-tailed)	-0.11 0.63	-0.06 0.78
		Stem density	Pearson (sig. 2-tailed)	0.03 0.88	0.11 0.62
		Water depth	Pearson (sig. 2-tailed)	-0.12 0.59	0.13 0.58

Irrigated system	Stage	Rice biophysical variables	Statistical	Vegetation indices	
				NDVI	EVI
Overall (Cont.)	Tillering	Height	Pearson (sig. 2-tailed)	0.15 0.50	0.35 0.11
		Absolut height	Pearson (sig. 2-tailed)	0.21 0.34	0.31 0.16
		LAI	Pearson (sig. 2-tailed)	0.05 0.85	0.02 0.93
		Chlorophyll	Pearson (sig. 2-tailed)	0.13 0.55	-0.06 0.79
		Wet total biomass	Pearson (sig. 2-tailed)	.[c]	.[c]
		Wet stem biomass	Pearson (sig. 2-tailed)	.[c]	.[c]
		Wet grain biomass	Pearson (sig. 2-tailed)	.[c]	.[c]
		Dry total biomass	Pearson (sig. 2-tailed)	.[c]	.[c]
		Dry stem biomass	Pearson (sig. 2-tailed)	.[c]	.[c]
		Dry grain biomass	Pearson (sig. 2-tailed)	.[c]	.[c]
	Panicle	Rice age	Pearson (sig. 2-tailed)	0.13 0.57	**-0.45*** **0.04**
		Stem density	Pearson (sig. 2-tailed)	-0.33 0.14	-0.06 0.80
		Water depth	Pearson (sig. 2-tailed)	-0.30 0.18	-0.07 0.77
		Height	Pearson (sig. 2-tailed)	0.23 0.30	-0.39 0.08
		Absolut height	Pearson (sig. 2-tailed)	0.28 0.21	-0.31 0.17
		LAI	Pearson (sig. 2-tailed)	-0.19 0.41	0.03 0.88
		Chlorophyll	Pearson (sig. 2-tailed)	-0.11 0.63	-0.04 0.86
		Wet total biomass	Pearson (sig. 2-tailed)	-0.58 0.61	0.92 0.26
		Wet stem biomass	Pearson (sig. 2-tailed)	-0.57 0.61	0.92 0.26
		Wet grain biomass	Pearson (sig. 2-tailed)	-0.59 0.6	0.93 0.25
		Dry total biomass	Pearson (sig. 2-tailed)	-0.72 0.49	0.98 0.14
		Dry stem biomass	Pearson (sig. 2-tailed)	-0.78 0.43	0.99 0.08

Irrigated system	Stage	Rice biophysical variables	Statistical	Vegetation indices	
				NDVI	EVI
Overall (Cont.)	Panicle	Dry grain biomass	Pearson (sig. 2-tailed)	-0.60 0.59	0.93 0.24
	Flowering	Rice age	Pearson (sig. 2-tailed)	0.10 0.69	0.20 0.38
		Stem density	Pearson (sig. 2-tailed)	0.04 0.88	0.23 0.31
		Water depth	Pearson (sig. 2-tailed)	**-0.62**** **0.01**	**-0.59**** **0.01**
		Height	Pearson (sig. 2-tailed)	**-0.52*** **0.03**	0.05 0.83
		Absolut height	Pearson (sig. 2-tailed)	-0.26 0.30	0.30 0.19
		LAI	Pearson (sig. 2-tailed)	-0.07 0.80	0.03 0.91
		Chlorophyll	Pearson (sig. 2-tailed)	-0.09 0.73	-0.07 0.76
		Wet total biomass	Pearson (sig. 2-tailed)	0.02 0.95	-0.25 0.30
		Wet stem biomass	Pearson (sig. 2-tailed)	-0.08 0.77	-0.30 0.20
		Wet grain biomass	Pearson (sig. 2-tailed)	0.35 0.17	0.07 0.78
		Dry total biomass	Pearson (sig. 2-tailed)	0.22 0.40	-0.12 0.62
		Dry stem biomass	Pearson (sig. 2-tailed)	0.05 0.86	-0.23 0.32
		Dry grain biomass	Pearson (sig. 2-tailed)	0.39 0.13	0.13 0.59
	Harvesting	Rice age	Pearson (sig. 2-tailed)	0.34 0.12	0.27 0.23
		Stem density	Pearson (sig. 2-tailed)	**-0.57**** **0.01**	0.05 0.83
		Water depth	Pearson (sig. 2-tailed)	0.42 0.05	**0.47*** **0.03**
		Height	Pearson (sig. 2-tailed)	0.21 0.35	0.25 0.25
		Absolute height	Pearson (sig. 2-tailed)	0.06 0.8	0.08 0.72
		LAI	Pearson (sig. 2-tailed)	0.25 0.26	0.07 0.75
		Chlorophyll	Pearson (sig. 2-tailed)	0.05 0.82	-0.36 0.10
		Wet total biomass	Pearson (sig. 2-tailed)	0.30 0.17	**0.45*** **0.04**

Irrigated system	Stage	Rice biophysical variables	Statistical	Vegetation indices	
				NDVI	EVI
Overall (Cont.)	Harvesting	Wet stem biomass	Pearson (sig. 2-tailed)	0.34 0.12	**0.45*** **0.03**
		Wet grain biomass	Pearson (sig. 2-tailed)	0.10 0.68	0.28 0.20
		Dry total biomass	Pearson (sig. 2-tailed)	0.28 0.21	**0.43*** **0.05**
		Dry stem biomass	Pearson (sig. 2-tailed)	0.35 0.11	**0.46*** **0.03**
		Dry grain biomass	Pearson (sig. 2-tailed)	0.13 0.58	0.31 0.15
	Overall growth stage	Rice age	Pearson (sig. 2-tailed)	**0.27**** **0.01**	0.11 0.24
		Stem density	Pearson (sig. 2-tailed)	0.03 0.78	0.16 0.09
		Water depth	Pearson (sig. 2-tailed)	0.10 0.30	0.17 0.07
		Height	Pearson (sig. 2-tailed)	**-0.40**** **0.00**	**-0.48**** **0.00**
		Absolute height	Pearson (sig. 2-tailed)	**-0.39**** **0.00**	**-0.49**** **0.00**
		LAI	Pearson (sig. 2-tailed)	-0.21 0.07	**-0.25*** **0.02**
		Chlorophyll	Pearson (sig. 2-tailed)	0.08 0.50	-0.02 0.87
		Wet total biomass	Pearson (sig. 2-tailed)	-0.19 0.22	-0.20 0.19
		Wet stem biomass	Pearson (sig. 2-tailed)	-0.15 0.35	-0.16 0.29
		Wet grain biomass	Pearson (sig. 2-tailed)	-0.23 0.14	-0.24 0.11
		Dry total biomass	Pearson (sig. 2-tailed)	-0.20 0.20	-0.24 0.12
		Dry stem biomass	Pearson (sig. 2-tailed)	-0.11 0.51	-0.16 0.31
		Dry grain biomass	Pearson (sig. 2-tailed)	-0.25 0.11	-0.27 0.08

L.2 Correlation between vegetation indices and rice yield in overall areas, irrigated areas, and non-irrigated areas across growth stages.

Irrigated system	Stage	Statistical	Vegetation indices	
			NDVI	EVI
Overall	Seeding	Pearson (sig. 2-tailed)	-0.20 0.39	**0.57**** **0.01**
	Tillering	Pearson (sig. 2-tailed)	-0.06 0.78	0.06 0.78
	Panicle	Pearson (sig. 2-tailed)	0.37 0.11	-0.03 0.89
	Flowering	Pearson (sig. 2-tailed)	-0.35 0.12	-0.19 0.40
	Harvesting	Pearson (sig. 2-tailed)	-0.12 0.60	0.00 0.99
	Overall growth stage	Pearson (sig. 2-tailed)	-0.08 0.41	0.02 0.88
Irrigated	Seeding	Pearson (sig. 2-tailed)	-0.01 0.98	0.40 0.14
	Tillering	Pearson (sig. 2-tailed)	-0.19 0.48	-0.10 0.70
	Panicle	Pearson (sig. 2-tailed)	0.21 0.48	0.02 0.94
	Flowering	Pearson (sig. 2-tailed)	-0.23 0.38	-0.21 0.43
	Harvesting	Pearson (sig. 2-tailed)	-0.12 0.67	0.07 0.81
	Overall growth stage	Pearson (sig. 2-tailed)	-0.09 0.46	-0.03 0.81
Non- irrigated	Seeding	Pearson (sig. 2-tailed)	-0.56 0.25	0.79 0.06
	Tillering	Pearson (sig. 2-tailed)	0.72 0.11	**0.84*** **0.04**
	Panicle	Pearson (sig. 2-tailed)	0.67 0.15	-0.09 0.87
	Flowering	Pearson (sig. 2-tailed)	-0.85 0.07	-0.44 0.46
	Harvesting	Pearson (sig. 2-tailed)	-0.18 0.73	-0.31 0.55
	Overall growth stage	Pearson (sig. 2-tailed)	-0.61 0.75	0.12 0.53

L.3 Correlation between vegetation indices and rice yield in overall area, irrigated areas and non-irrigated areas across growth stages specific growth stage.

Irrigated system	Stage	Statistical	Vegetation indices	
			NDVI	EVI
Phitsanulok2	Seeding	Pearson (sig. 2-tailed)	0.73 0.27	0.45 0.56
	Tillering	Pearson (sig. 2-tailed)	-0.09 0.91	**0.95*** **0.05**
	Panicle	Pearson (sig. 2-tailed)	0.03 0.97	-0.36 0.64
	Flowering	Pearson (sig. 2-tailed)	**-1****	0.18 0.82
	Harvesting	Pearson (sig. 2-tailed)	0.11 0.89	-0.47 0.53
	Overall growth	Pearson (sig. 2-tailed)	.[c]	.[c]
RD41	Seeding	Pearson (sig. 2-tailed)	0.33 0.53	**0.86*** **0.03**
	Tillering	Pearson (sig. 2-tailed)	-0.26 0.62	0.18 0.74
	Panicle	Pearson (sig. 2-tailed)	-0.33 0.53	0.18 0.74
	Flowering	Pearson (sig. 2-tailed)	-0.01 0.99	-0.52 0.29
	Harvesting	Pearson (sig. 2-tailed)	-0.01 0.99	0.49 0.32
	Overall growth	Pearson (sig. 2-tailed)	-0.04 0.83	0.07 0.71
RD49	Seeding	Pearson (sig. 2-tailed)	-0.75 0.14	-0.46 0.43
	Tillering	Pearson (sig. 2-tailed)	-0.06 0.92	0.38 0.53
	Panicle	Pearson (sig. 2-tailed)	0.88 0.05	-0.21 0.74
	Flowering	Pearson (sig. 2-tailed)	0.51 0.39	0.20 0.74
	Harvesting	Pearson (sig. 2-tailed)	-0.44 0.46	0.04 0.95
	Overall growth	Pearson (sig. 2-tailed)	-0.06 0.77	0.02 0.94

Where *, ** value significant at the 0.05 and 0.01 probability level (2-tailed)

NA No measurement

Appendix M Descriptive statistical table based on Sentinel-2 and Sentinel-1

M.1 Descriptive statistical table based on Sentinel-2

M.1.1 Descriptive statistical table based on Sentinel-2: EVI (seeding stage)

Descriptive Statistics[a]			
	Mean	Std. Deviation	N
Yield	4.9169	.73107	21
EVI	.1130	.11939	21
a. Stage = Seeding			

Correlations[a]			
		Yield	EVI
Pearson Correlation	Yield	1.000	.567
	EVI	.567	1.000
Sig. (1-tailed)	Yield	.	.004
	EVI	.004	.
N	Yield	21	21
	EVI	21	21
a. Stage = Seeding			

Variables Entered/Removed[a,b]			
Model	Variables Entered	Variables Removed	Method
1	EVI[c]	.	Enter
a. Stage = Seeding			
b. Dependent Variable: Yield			
c. All requested variables entered.			

Model Summary[a]									
					Change Statistics				
Model	R	R Square	Adjusted R Square	Std. Error of the Estimate	R Square Change	F Change	df1	df2	Sig. F Change
1	.567[b]	.321	.285	.61808	.321	8.981	1	19	.007
a. Stage = Seeding									
b. Predictors: (Constant), EVI									

ANOVA[a,b]						
Model		Sum of Squares	df	Mean Square	F	Sig.
1	Regression	3.431	1	3.431	8.981	.007[c]
	Residual	7.258	19	.382		
	Total	10.689	20			
a. Stage = Seeding						
b. Dependent Variable: Yield						
c. Predictors: (Constant), EVI						

Coefficients[a,b]											
Model		Unstandardized Coefficients		Standardized Coefficients	t	Sig.	95.0% Confidence Interval for B		Correlations		
		B	Std. Error	Beta			Lower Bound	Upper Bound	Zero-order	Partial	Part
1	(Constant)	4.525	.188		24.083	.000	4.132	4.918			
	EVI	3.469	1.158	.567	2.997	.007	1.046	5.892	.567	.567	.567
a. Stage = Seeding											
b. Dependent Variable: Yield											

M.1.2 Descriptive statistical table based on Sentinel-2: NDVI (panicle stage)

Descriptive Statistics[a]			
	Mean	Std. Deviation	N
Yield	4.8844	.73429	20
NDVI	.6141	.04976	20
a. Stage = Panicle			

Correlations[a]			
		Yield	NDVI
Pearson Correlation	Yield	1.000	.373
	NDVI	.373	1.000
Sig. (1-tailed)	Yield	.	.053
	NDVI	.053	.
N	Yield	20	20
	NDVI	20	20
a. Stage= Panicle			

Variables Entered/Removed[a,b]			
Model	Variables Entered	Variables Removed	Method
1	NDVI[c]	.	Enter
a. Stage= Panicle			
b. Dependent Variable: Yield			
c. All requested variables entered.			

Model Summary[a]									
					Change Statistics				
Model	R	R Square	Adjusted R Square	Std. Error of the Estimate	R Square Change	F Change	df1	df2	Sig. F Change
1	.373[b]	.139	.091	.70011	.139	2.900	1	18	.106
a. Stage = Panicle									
b. Predictors: (Constant), NDVI									

ANOVA[a,b]						
Model		Sum of Squares	df	Mean Square	F	Sig.
1	Regression	1.422	1	1.422	2.900	.106[c]
	Residual	8.823	18	.490		
	Total	10.244	19			
a. Stage= Panicle						
b. Dependent Variable: Yield						
c. Predictors: (Constant), NDVI						

Coefficients[a,b]											
		Unstandardized Coefficients		Standardized Coefficients			95.0% Confidence Interval for B		Correlations		
Model		B	Std. Error	Beta	t	Sig.	Lower Bound	Upper Bound	Zero-order	Partial	Part
1	(Constant)	1.508	1.989		.758	.458	-2.670	5.686			
	NDVI_	5.497	3.228	.373	1.703	.106	-1.285	12.279	.373	.373	.373
a. Stage= Panicle											
b. Dependent Variable: Yield											

M.2 Descriptive statistical table based on Sentinel-1

Descriptive Statistics[a]			
	Mean	Std. Deviation	N
Yield	4.8436	.79087	22
AscVV/VH	.6100	.17449	22
a. Stage = Harvesting			

Correlations[a]			
		Yield	AscVV/VH
Pearson Correlation	Yield	1.000	.540
	AscVV/VH	.540	1.000
Sig. (1-tailed)	Yield	.	.005
	AscVV/VH	.005	.
N	Yield	22	22
	AscVV/VH	22	22
a. Stage = Harvesting			

Variables Entered/Removed[a,b]			
Model	Variables Entered	Variables Removed	Method
1	AscVV/VH	.	Stepwise (Criteria: Probability-of-F-to-enter <= .050, Probability-of-F-to-remove >= .100).
a. Stage= Harvesting			
b. Dependent Variable: Yield			

Model Summary[a]									
					Change Statistics				
Model	R	R Square	Adjusted R Square	Std. Error of the Estimate	R Square Change	F Change	df1	df2	Sig. F Change
1	.540[b]	.291	.256	.68218	.291	8.225	1	20	.010
a. Stage= Harvesting									
b. Predictors: (Constant), AscVV/VH									

Appendix M

ANOVA[a,b]						
Model		Sum of Squares	df	Mean Square	F	Sig.
1	Regression	3.828	1	3.828	8.225	.010[c]
	Residual	9.307	20	.465		
	Total	13.135	21			
a. Stage= Harvesting						
b. Dependent Variable: Yield						
c. Predictors: (Constant), AscVV/VH						

Coefficients[a,b]								
		Unstandardized Coefficients		Standardized Coefficients			95.0% Confidence Interval for B	
Model		B	Std. Error	Beta	t	Sig.	Lower Bound	Upper Bound
1	(Constant)	3.351	.540		6.201	.000	2.224	4.478
	AscVV/VH	2.447	.853	.540	2.868	.010	.667	4.226
a. Stage= Harvesting								
b. Dependent Variable: Yield								

Coefficient Correlations[a,b]			
Model			AscVV/VH
1	Correlations	AscVV/VH	1.000
	Covariances	AscVV/VH	.728
a. Stage= Harvesting			
b. Dependent Variable: Yield			

Glossary of Terms

Polarisation	Process of confining the vibrations of the magnetic, or electric field, vector of light or other radiation to one plane
Sigma Nought	Scattering coefficient or the conventional measure of the strength of radar signals reflects by a distributed scatter, usually expressed in decibel (dB). It is normalised dimensionless number, compares the strength observed to expect from an area of one square meter. In general, the value of sigma nought varies with incidence angle, wavelength, and polarisation
Vertical Transmit-Horizontal Receive Polarisation (VH)	A mode of radar where the microwave of the electric field is oriented in the vertical plane for transmission signal and where the horizontally polarised electric field of backscatter energy is received by radar antenna
Vertical Transmit-Vertical Receive Polarisation (VV)	A mode of radar polarisation where the microwave of the electric field is oriented in the vertical plane for both signal transmission and reception by radar antenna

List of References

A. Martinez-Agirre, J. Álvarez-Mozos, H. Lievens, N. E. C. V. and R. G. (2017). Influence of surface roughness sample size for C-band SAR backscatter applications on agricultural soils. *IEEE Geoscience and Remote Sensing Letters*, *14*(12), 2300–2304. https://doi.org/10.1109/LGRS.2017.2762434

A. Martinez-Agirre, J. Álvarez-Mozos, H. L. and N. E. C. V. (2017). Influence of surface roughness measurement scale on radar backscattering in different agricultural soils. *EEE Transactions on Geoscience and Remote Sensing*, *55*(10), 5925–5936. https://doi.org/10.1109/TGRS.2017.2717043

Abbas, S., & Mayo, Z. A. (2021). Impact of temperature and rainfall on rice production in Punjab, Pakistan. In *Environment, Development and Sustainability* (Vol. 23, Issue 2, pp. 1706–1728). https://doi.org/10.1007/s10668-020-00647-8

Abdulwaheed, A., Opadotun, O. O., & Amusat, M. A. (2017). Rice self-sufficiency: A review of government policies on rice production. *International Journal of Scientific & Engineering Research*, *8*(2), 1289–1302. https://doi.org/10.14299/ijser.2017.02.011

Aboelghar, M., Arafat, S., Abo Yousef, M., El-Shirbeny, M., Naeem, S., Massoud, A., & Saleh, N. (2011). Using SPOT data and leaf area index for rice yield estimation in Egyptian Nile delta. *The Egyptian Journal of Remote Sensing and Space Science*, *14*(2), 81–89. https://doi.org/10.1016/j.ejrs.2011.09.002

Aboelghar, M., Arafat, S., Saleh, A., Naeem, S., Shirbeny, M., & Belal, A. (2010). Retrieving leaf area index from SPOT4 satellite data. *Egyptian Journal of Remote Sensing and Space Science*, *13*(2), 121–127. https://doi.org/10.1016/j.ejrs.2010.06.001

Acevedo-Siaca, L. G., Coe, R., Quick, W. P., & Long, S. P. (2021). Variation between rice accessions in photosynthetic induction in flag leaves and underlying mechanisms. *Journal of Experimental Botany*, *72*(4), 1282–1294.

ADB. (2012). *Guidelines for climate proofing investment in agriculture, rural development, and food security*.

Adeluyi, O., Harris, A., Verrelst, J., Foster, T., & Clay, G. D. (2021). Estimating the phenological dynamics of irrigated rice leaf area index using the combination of PROSAIL and Gaussian

Process Regression. *International Journal of Applied Earth Observation and Geoinformation*, *102*(July), 102454. https://doi.org/10.1016/j.jag.2021.102454

Agustan, Mubekti, & Sumargana, L. (2015). The utilization of ALOS-2 data to identify the potential area for paddy field. *ACRS 2015 - 36th Asian Conference on Remote Sensing: Fostering Resilient Growth in Asia, Proceedings*.

Ahmad, T., Sahoo, P. M., Singh, M., & Biswas, A. (2021). *Crop Cutting Experiment techniques for determination of yield rates of field crops*.

Ahuja, I., de Vos, R. C., Bones, A. M., & Hall, R. D. (2010). Plant molecular stress responses face climate change. *Trends in Plant Science*, *15*(12), 664–674. https://doi.org/10.1016/j.tplants.2010.08.002

Ajith, K., Geethalakshmi, V., Ragunath, K. P., Pazhanivelan, S., & Dheebakaran, G. (2017). Rice yield prediction using MODIS - NDVI (MOD13Q1) and land based observations. *International Journal of Current Microbiology and Applied Sciences*, *6*(12), 2277–2293. https://doi.org/10.20546/ijcmas.2017.612.263

Ali, A. M., Savin, I., Poddubskiy, A., Abouelghar, M., Saleh, N., Abutaleb, K., ... & Dokukin, P. (2021). Integrated method for rice cultivation monitoring using Sentinel-2 data and Leaf Area Index. *The Egyptian Journal of Remote Sensing and Space Science*, *24*(3), 431–441.

Ali, A. M., Savin, I., Poddubskiy, A., Abouelghar, M., Saleh, N., Abutaleb, K., El-Shirbeny, M., & Dokukin, P. (2020). Integrated method for rice cultivation monitoring using Sentinel-2 data and Leaf Area Index. *Egyptian Journal of Remote Sensing and Space Science*, *xxxx*, 0–10. https://doi.org/10.1016/j.ejrs.2020.06.007

Alipour Abookheili, F., & Mobasser, H. R. (2021). Effect of planting density on growth characteristics and grain yield increase in successive cultivations of two rice cultivars. In *Agrosystems, Geosciences and Environment* (Vol. 4, Issue 4). https://doi.org/10.1002/agg2.20213

Allen, P. G., & Fildes, R. (2001). Econometric forecasting. In *International Series in Operations Research & Management Science* (Vol. 30). Springer US.

Amanullah, & Inamullah. (2016). Dry Matter Partitioning and Harvest Index Differ in Rice Genotypes with Variable Rates of Phosphorus and Zinc Nutrition. *Rice Science*, *23*(2), 78–87. https://doi.org/10.1016/j.rsci.2015.09.006

Ambika, A. K., & Mishra, V. (2019). Observational evidence of irrigation influence on vegetation health and land surface temperature in India. *Geophysical Research Letters*, *46*(22), 13441–13451.

Amien, I., Redjekiningrum, P., Kartiwa, B., & Estiningtyas, W. (1999). Simulated rice yields as affected by interannual climate variability and possible climate change in Java. *Climate Research*, *12*(2–3), 145–152.

Anisuzzaman, M., Kader, M., Ali, M., Haque, M., & Halder, T. (2016). Development of high yielding rice varieties for favorable ecosystem with 40% higher yield than the present variety: A review paper. *Middle East Journal of Scientific Research*, *24*, 3644–3653.

Anselin, L. (1995). Local Indicators of Spatial Association—LISA. In *Geographical Analysis* (Vol. 27, Issue 2, pp. 93–115). https://doi.org/10.1111/j.1538-4632.1995.tb00338.x

Arii, M., Yamada, H., Kojima, S., & Ohki, M. (2019). Review of the comprehensive SAR approach to identify scattering mechanisms of radar backscatter from vegetated terrain. *Electronics (Switzerland)*, *8*(10), 1098. https://doi.org/10.3390/electronics8101098

Arnell, N. W. (1999). Climate change and global water resources. *Global Environmental Change*, *9*, S31–S49. https://doi.org/10.1016/S0959-Get

Asada, H., Matsumoto, J., & Rahman, R. (2005). Impact of recent severe floods on rice production in Bangladesh. *Climate Research*, *78*(12), 783–793. https://doi.org/10.3354/cr00785

Aschbacher, J., Pongsrihadulchai, A., Karnchanasutham, S., Rodprom, C., Paudyal, D. R., & Le Toan, T. (1995). Assessment of ERS-1 SAR data for rice crop mapping and monitoring. *International Geoscience and Remote Sensing Symposium, IGARSS'95. Quantitative Remote Sensing for Science and Applications*, *3*, 2183–2185.

Aschonitis, V. G., Papamichail, D. M., Lithourgidis, A., & Fano, E. A. (2014). Estimation of leaf area index and foliage area index of rice using an indirect gravimetric method. *Communications in Soil Science and Plant Analysis*, *45*(13), 1726–1740. https://doi.org/10.1080/00103624.2014.907917

ASEAN Information Center. (2021). *Estimated rice production in ASEAN 2021*. http://www.aseanthai.net/english/mobile_detail.php?cid=14&nid=4030

Ata-Ul-Karim, S. T., Cao, Q., Zhu, Y., Tang, L., Rehmani, M. I. A., & Cao, W. (2016). Non-destructive assessment of plant nitrogen parameters using leaf chlorophyll measurements in rice.

Frontiers in Plant Science, *7*, 1829. https://doi.org/10.3389/fpls.2016.01829

Awad, M. M. (2019). Toward precision in crop yield estimation using remote sensing and optimization techniques. *Agriculture (Switzerland)*, *9*(3), 54. https://doi.org/10.3390/agriculture9030054

Badshah, M. A., Naimei, T., Zou, Y., Ibrahim, M., & Wang, K. (2014). Yield and tillering response of super hybrid rice Liangyoupeijiu to tillage and establishment methods. *The Crop Journal*, *2*(1), 79–86. https://doi.org/10.1016/j.cj.2013.11.004

Bakare, O. S., Ewert, F., Ablede, K. A., Mossi, I. M., Kamissoko, N., Rodenburg, J., Segda, Z., Dogbe, W., Senthilkumar, K., Saito, K., Becker, M., Gbakatchetche, H., Dieng, I., Niang, A., Tanaka, A., Gaiser, T., Bam, R. K., Keita, S., Akakpo, C., … Cissé, M. (2017). Variability and determinants of yields in rice production systems of West Africa. *Field Crops Research*, *207*, 1–12. https://doi.org/10.1016/j.fcr.2017.02.014

Baloch, A. W., Soomro, A. M., Javed, M. A., Ahmed, M., Bughio, H. R., Bughio, M. S., & Mastoi, N. N. (2001). Optimum plant density for high yield in rice (Oryza sativa L.). *Asian Journal of Plant Sciences*, *1*(1), 25–27. https://doi.org/10.3923/ajps.2002.25.27

Baloch, A. W., Soomro, A. M., Javed, M. A., Ahmed, M., Bughio, H. R., Bughio, M. S., & Mastoi, N. N., Bozorgi, H. R., Faraji, A., Danesh, R. K., Keshavarz, A., Azarpour, E., Tarighi, F., Alipour Abookheili, F., & Mobasser, H. R. (2011). Effect of plant density on yield and yield components of rice. *Agrosystems, Geosciences and Environment*, *12*(4), 25–27. https://doi.org/10.1002/agg2.20213

Bamler, R., & Hartl, P. (1998). Synthetic aperture radar interferometry. *Inverse Problems*, *14*(4). https://doi.org/10.1088/0266-5611/14/4/001

Banerjee, L. (2010). Effects of flood on agricultural productivity in Bangladesh. *Oxford Development Studies*, *38*(3), 339–356.

Bao, N., Li, W., Gu, X., & Liu, Y. (2019). Biomass estimation for semiarid vegetation and mine rehabilitation using worldview-3 and sentinel-1 SAR imagery. *Remote Sensing*, *11*(23), 2855. https://doi.org/10.3390/rs11232855

Barclay, H. J., & Goodman, D. (2000). Conversion of total to projected leaf area index in conifers. *Canadian Journal of Botany*, *78*(4), 447–454. https://doi.org/10.1139/b00-020

Baret, F., Jacquemoud, S., Guyot, G., & Leprieur, C. (1992). Modeled analysis of the biophysical

nature of spectral shifts and comparison with information content of broad bands. *Remote Sensing of Environment*, *41*(2–3), 133–142. https://doi.org/10.1016/0034-4257(92)90073-S

Baret, F., & Guyot, G. (1991). Potentials and limits of vegetation indices for LAI and APAR assessment. *Remote Sensing of Environment*, *35*(2–3), 161–173. https://doi.org/10.1016/0034-4257(91)90009-U

Barker, R. and H. (1979). Rainfed lowland rice as a research priority – An economists view. *In Rainfed Lowland Rice Selected Papers from the 1978-International Rice Research Conference*, 3–50.

Bauer, M., & Quinton, J. (2019). Soil erosion and flood mitigation in cz and uk – comparision, discussion and lesson learned. *International Multidisciplinary Scientific GeoConference Surveying Geology and Mining Ecology Management, SGEM*, *19*(3.2), 403–410. https://doi.org/10.5593/sgem2019/3.2/S13.053

Bayanudin, A. A., & Jatmiko, R. H. (2016). Orthorectification of Sentinel-1 SAR (synthetic aperture radar) data in some parts of south-eastern Sulawesi using Sentinel-1 toolbox. *IOP Conference Series: Earth and Environmental Science*, *47*(1), 012007. https://doi.org/10.1088/1755-1315/47/1/012007

Bazzi, H., Baghdadi, N., El Hajj, M., Zribi, M., Minh, D. H. T., Ndikumana, E., Courault, D., & Belhouchette, H. (2019). Mapping paddy rice using Sentinel-1 SAR time series in Camargue, France. In *Remote Sensing* (Vol. 11, Issue 7, p. 887). https://doi.org/10.3390/RS11070887

Belder, P., Bouman, B. A. M., Cabangon, R., Guoan, L., Quilang, E. J. P., Yuanhua, L., Spiertz, J. H. J., & Tuong, T. P. (2004). Effect of water-saving irrigation on rice yield and water use in typical lowland conditions in Asia. *Agricultural Water Management*, *65*(3), 193–210. https://doi.org/10.1016/j.agwat.2003.09.002

Bemal, S., Singh, D., & Singh, S. (2009). Seasonal climatic variability impact on rice productivity in Haryana. *Journal of Agrometeorology*, *11*(SPECIAL ISSUE), 64–66.

Bera, A. K., & Kelley, T. G. (1990). Adoption of high yielding rice varieties in Bangladesh: an econometric analysis. *Journal of Development Economics*, *33*(2), 263–285.

Beretta, C., Stoessel, F., Baier, U., & Hellweg, S. (2013). Quantifying food losses and the potential for reduction in Switzerland. *Waste Management*, *33*(3), 764–773. https://doi.org/10.1016/j.wasman.2012.11.007

Berga, H., & Tamb, N. T. (2012). Use of pesticides and attitude to pest management strategies among rice and rice-fish farmers in the mekong delta, Vietnam. *International Journal of Pest Management*, *58*(2), 153–164. https://doi.org/10.1080/09670874.2012.672776

Bharti, V., & Singh, C. (2015). Evaluation of error in TRMM 3B42V7 precipitation estimates over the Himalayan region. *Journal of Geophysical Research: Atmospheres*, *120*(24), 12458–12473. https://doi.org/10.1002/2015JD023779.Received

Bhattacharya, T. (2013). Effect of climate change on rice yield at Kharagpur, West Bengal. *IOSR Journal of Agriculture and Veterinary Science*, *4*(2), 06–12. https://doi.org/10.9790/2380-0420612

Bhutada, P., Kohirepatli, V., & Chavan, A. (2016). Remote Sensing and GIS use for yield forecasting and in Crop Cutting Experiment. *Remote Sensing*, *21*(18), 3487–3508.

Bindlish, R., & Barros, A. P. (2001). Parameterization of vegetation backscatter in radar-based, soil moisture estimation. *Remote Sensing of Environment*, *76*(1), 130–137. https://doi.org/10.1016/S0034-4257(00)00200-5

Biswal, A., Srikanth, P., Murthy, C. S., & Rao, P. V. N. (2019). Spatialisation of rice growth and yield model using optical and SAR derived biophysical parameters. *International Archives of the Photogrammetry, Remote Sensing and Spatial Information Sciences - ISPRS Archives*, *42*(3/W6), 181–185. https://doi.org/10.5194/isprs-archives-XLII-3-W6-181-2019

Biswas, R., Bhattacharyya, B., & Banerjee, S. (2017). Predicting Rice Yield From Weather Variable Through Detrended Production Index. *Contemporary Research in India*, *7*(3), 462–466. https://www.researchgate.net/publication/337707523_PREDICTING_RICE_YIELD_FROM_WEATHER_VARIABLE_THROUGH_DETRENDED_PRODUCTION_INDEX

Bolton, D. K., & Friedl, M. A. (2013). Forecasting crop yield using remotely sensed vegetation indices and crop phenology metrics. *Agricultural and Forest Meteorology*, *173*, 74–84. https://doi.org/10.1016/j.agrformet.2013.01.007

Boonjung, H., & Fukai, S. (1996). Effects of soil water deficit at different growth stages on rice growth and yield under upland conditions. 2. Phenology, biomass production and yield. *Field Crops Research*, *48*(1), 47–55. https://doi.org/10.1016/0378-4290(96)00039-1

Boonwichai, S., Shrestha, S., Babel, M. S., Weesakul, S., & Datta, A. (2018). Climate change impacts on irrigation water requirement, crop water productivity and rice yield in the Songkhram River Basin, Thailand. *Journal of Cleaner Production*, *198*, 1157–1164.

https://doi.org/10.1016/j.jclepro.2018.07.146

Boschetti, M., Busetto, L., Manfron, G., Laborte, A., Asilo, S., Pazhanivelan, S., & Nelson, A. (2017). PhenoRice: A method for automatic extraction of spatio-temporal information on rice crops using satellite data time series. *Remote Sensing of Environment*, *194*, 347–365. https://doi.org/10.1016/j.rse.2017.03.029

Boschetti, M., Stroppiana, D., Brivio, P. A., & Bocchi, S. (2009). Multi-year monitoring of rice crop phenology through time series analysis of MODIS images. *International Journal of Remote Sensing*, *30*(18), 4643–4662. https://doi.org/10.1080/01431160802632249

Boschetti, M., Nutini, F., Manfron, G., Brivio, P. A., & Nelson, A. (2014). Comparative analysis of normalised difference spectral indices derived from MODIS for detecting surface water in flooded rice cropping systems. *PLoS ONE*, *9*(2), e88741. https://doi.org/10.1371/journal.pone.0088741

Botlaguduru, V. S. V., & Kommalapati, R. R. (2020). Meteorological detrending of long-term (2003-2017) ozone and precursor concentrations at three sites in the Houston Ship Channel Region. *Journal of the Air and Waste Management Association*, *70*(1), 93–107. https://doi.org/10.1080/10962247.2019.1694088

Bouman, B. A. M., & Tuong, T. P. (2001). Field water mangement to save water and increase its productivity in irrigated lowland rice. *Agricultural Water Management*, *49*(1), 11–30. https://doi.org/10.1016/S0378-3774(00)00128-1

Bouvet, A., Le Toan, T., & Dao, N. L. (2014). Estimation of agricultural and biophysical parameters of rice fields in Vietnam using X-band dual-polarization SAR. *International Geoscience and Remote Sensing Symposium (IGARSS)*, 1504–1507. https://doi.org/10.1109/IGARSS.2014.6946723

Bro-Jørgensen, J., Brown, M. E., & Pettorelli, N. (2008). Using the satellite-derived NDVI to assess ecological responses to environmental change. *Oecologia*, *158*(1), 177–182. https://doi.org/10.1016/j.tree.2005.05.011

Bronge, L. B., & AB, S. (2004). Satellite remote sensing for estimating leaf area index, FPAR and primary production. *Swedish Nuclear Fuel and Waste Management Co.*, 52.

Burgess, A. J., Retkute, R., Herman, T., & Murchie, E. H. (2017). Exploring relationships between canopy architecture, light distribution, and photosynthesis in contrasting rice genotypes using 3D canopy reconstruction. In *Frontiers in Plant Science* (Vol. 8, p. 734).

https://doi.org/10.3389/fpls.2017.00734

Burgos, N. R., Norman, R. J., Gealy, D. R., & Black, H. (2006). Competitive N uptake between rice and weedy rice. *Field Crops Research*, *99*(2–3), 96–105. https://doi.org/10.1016/j.fcr.2006.03.009

Campos-Taberner, M., García-Haro, F. J., Busetto, L., Ranghetti, L., Martínez, B., Gilabert, M. A., Camps-Valls, G., Camacho, F., & Boschetti, M. (2018). A critical comparison of remote sensing Leaf Area Index estimates over rice-cultivated areas: From Sentinel-2 and Landsat-7/8 to MODIS, GEOV1 and EUMETSAT polar system. *Remote Sensing*, *10*(5). https://doi.org/10.3390/rs10050763

Campos-Taberner, M., García-Haro, F. J., Camps-Valls, G., Grau-Muedra, G., Nutini, F., Busetto, L., Katsantonis, D., Stavrakoudis, D., Minakou, C., Gatti, L., Barbieri, M., Holecz, F., Stroppiana, D., & Boschetti, M. (2017). Exploitation of SAR and optical sentinel data to detect rice crop and estimate seasonal dynamics of leaf area index. *Remote Sensing*, *9*(3), 248. https://doi.org/10.3390/rs9030248

Campos-Taberner, M., García-Haro, F. J., Camps-Valls, G., Grau-Muedra, G., Nutini, F., Crema, A., & Boschetti, M. (2016). Multitemporal and multiresolution leaf area index retrieval for operational local rice crop monitoring. In *Remote Sensing of Environment* (Vol. 187, pp. 102–118). https://doi.org/10.1016/j.rse.2016.10.009

CEOS. (2013). *CEOS acquisition strategy for GEOGLAM phase1* (Issue November).

CEOS. (2018). A Layman's interpretation guide to L-band and C-band Synthetic Aperture Radar data. In *Nippon Ronen Igakkai Zasshi. Japanese Journal of Geriatrics*. https://doi.org/10.3143/geriatrics.55.contents1

Chakraborty, D., Ladha, J. K., Rana, D. S., Jat, M. L., Gathala, M. K., Yadav, S., Rao, A. N., Ramesha, M. S., & Raman, A. (2017). A global analysis of alternative tillage and crop establishment practices for economically and environmentally efficient rice production. *Scientific Reports*, *7*(1), 1–11. https://doi.org/10.1038/s41598-017-09742-9

Chang, K. W., Shen, Y., & Lo, J. C. (2005). Predicting rice yield using canopy reflectance measured at booting stage. *Agronomy Journal*, *97*(3), 872–878. https://doi.org/10.2134/agronj2004.0162

Chang, S., Chang, T., Song, Q., Zhu, X. G., & Deng, Q. (2016). Photosynthetic and agronomic traits of an elite hybrid rice Y-Liang-You 900 with a record-high yield. *Field Crops Research*, *187*,

49–57. https://doi.org/10.1016/j.fcr.2015.10.011

Chang, T. G., Zhao, H., Wang, N., Song, Q. F., Xiao, Y., Qu, M., & Zhu, X. G. (2019). A three-dimensional canopy photosynthesis model in rice with a complete description of the canopy architecture, leaf physiology, and mechanical properties. *Journal of Experimental Botany*, *70*(9), 2479–2490. https://doi.org/10.1093/jxb/ery430

Chaowiwat, W. (2016). Impact of climate change assessment on agriculture water demand in Thailand. *Naresuan University Engineering Journal*, *11*(1), 35–42. https://doi.org/10.51248/.v40i4.306

Chaturvedi, I. (2005). Effect of nitrogen fertilizers on growth, yield and quality of hybrid rice (Oryza Sativa). *Journal of Central European Agriculture*, *6*(4), 611–618. https://doi.org/10.1016/j.vetmic.2008.09.083

Chen, C., Baethgen, W. E., & Robertson, A. (2013). Contributions of individual variation in temperature, solar radiation and precipitation to crop yield in the North China Plain, 1961–2003. *Climate Change*, *116*(3), 767–788.

Chen, J., Chen, C., Tian, Y., Zhang, X., Dong, W., Zhang, B., ... & Peng, C. (2017). Differences in the impacts of nighttime warming on crop growth of rice-based cropping systems under field conditions. *European Journal of Agronomy*, *82*, 80–92. https://doi.org/10.1016/j.eja.2016.10.006

Chen, J. M., & Black, T. A. (1992). Defining leaf area index for non-flat leaves. *Plant, Cell & Environment*, *15*(4), 421–429.

Chen, J. M. (1996). Evaluation of vegetation indices and a modified simple ratio for boreal applications. *Canadian Journal of Remote Sensing*, *22*(3), 229–242.

Chen, Jiana, Zhang, R., Cao, F., Yin, X., Zou, Y., Huang, M., & Abou-Elwafa, S. F. (2020). Evaluation of late-season short- and long-duration rice cultivars for potential yield under mechanical transplanting conditions. *Agronomy*, *10*(9), 1307. https://doi.org/10.3390/agronomy10091307

Chen, Jinsong, Lin, H., Huang, C., & Fang, C. (2009). The relationship between the leaf area index (LAI) of rice and the C-band SAR vertical/horizontal (VV/HH) polarization ratio. *International Journal of Remote Sensing*, *30*(8), 2149–2154. https://doi.org/10.1080/01431160802609700

Chen, Jinsong, Lin, H., Liu, A., Shao, Y., & Yang, L. (2007). A semi-empirical backscattering model

for estimation of leaf area index (LAI) of rice in southern China. *International Geoscience and Remote Sensing Symposium (IGARSS)*, 3667–3680. https://doi.org/10.1109/IGARSS.2007.4423641

Chen, S., Chen, X., & Xu, J. (2016). Assessing the impacts of temperature variations on rice yield in China. *Climatic Change*, *138*(1–2), 191–205. https://doi.org/10.1007/s10584-016-1707-0

Chen, X. L., Zhao, H. M., Li, P. X., & Yin, Z. Y. (2006). Remote sensing image-based analysis of the relationship between urban heat island and land use/cover changes. *Remote Sensing of Environment*, *104*(2), 133–146. https://doi.org/10.1016/j.rse.2005.11.016

Cheng, T., Song, R., Li, D., Zhou, K., Zheng, H., Yao, X., ... & Zhu, Y. (2017). Spectroscopic estimation of biomass in canopy components of paddy rice using dry matter and chlorophyll indices. *Remote Sensing*, *9*(4), 319. https://doi.org/10.3390/rs9040319

Cheng, S. H., Cao, L. Y., Zhuang, J. Y., Chen, S. G., Zhan, X. D., Fan, Y. Y., Zhu, D. F., & Min, S. K. (2007). Super hybrid rice breeding in China: achievements and prospects. *Journal of Integrative Plant Biology*, *49*(6), 805–810. https://doi.org/10.1111/j.1744-7909.2007.00514.x

Chhogyel, N., & Bajgai, Y. (2015). Modern rice varieties adoption to raise productivity: A case study of two districts in Bhutan. *SAARC Journal of Agriculture*, *13*(2), 34–49. https://doi.org/10.3329/sja.v13i2.26567

Choudhury, A. H., Jones, J. R., Choudhury, R. L., & Spaulding, A. D. (2015). Association of rainfall and detrended crop yield based on piecewise regression for agricultural insurance. *Journal of Economics and Economic Education Research*, *16*(2), 31–44.

Choudhury, B. U., Singh, A. K., Bouman, B. A. M., & Prasad, J. (2007). System of Rice Intensification and Irrigated Transplanted Rice : Effect on Crop Water Productivity. *Journal of the Indian Society of Soil Science*, *55*(4), 464–470.

Choudhury, I., & Chakraborty, M. (2006). SAR signature investigation of rice crop using RADARSAT data. *International Journal of Remote Sensing*, *27*(3), 519–534. https://doi.org/10.1080/01431160500239172

Chowdhury, I. U. A., & Khan, M. A. E. (2015). The impact of climate change on rice yield in Bangladesh: A time series analysis. *Russian Journal of Agricultural and Socio-Economic Sciences*, *40*(4), 12–28.

Chowhan, S., Haider, M. R., Hasan, A. F. M. F., Hoque, M. I., Kamruzzaman, M., & Gupta, R. (2017). Comparative on farm performance of five modern rice varieties with two local cultivars. *Journal of Bioscience and Agriculture Research*, *13*(1), 1074–1086. https://doi.org/10.18801/jbar.130117.131

Chun, J. A., Li, S., Wang, Q., Lee, W. S., Lee, E. J., Horstmann, N., Park, H., Veasna, T., Vanndy, L., Pros, K., & Vang, S. (2016). Assessing rice productivity and adaptation strategies for Southeast Asia under climate change through multi-scale crop modeling. *Agricultural Systems*, *143*, 14–21. https://doi.org/10.1016/j.agsy.2015.12.001

Chung, N. T., Jintrawet, A., & Promburom, P. (2015). Impacts of seasonal climate variability on rice production in the central highlands of Vietnam. *Agriculture and Agricultural Science Procedia*, *5*, 83–88. https://doi.org/10.1016/j.aaspro.2015.08.012

Clauss, K., Ottinger, M., Leinenkugel, P., & Kuenzer, C. (2018). Estimating rice production in the Mekong Delta, Vietnam, utilizing time series of Sentinel-1 SAR data. *International Journal of Applied Earth Observation and Geoinformation*, *73*, 574–585. https://doi.org/10.1016/j.jag.2018.07.022

Clevers, J. G. P. W., & Van Leeuwen, H. J. C. (1996). Combined use of optical and microwave remote sensing data for crop growth monitoring. *Remote Sensing of Environment*, *56*(1), 42–51.

Collinson, S., Ellis, R., Summerfield, R., & Roberts, E. (1992). Durations of the photoperiod-sensitive and photoperiod-insensitive phases of development to flowering in four cultivars of rice (Oryza sativa L.). *Annals of Botany*, *70*(4), 339–346.

Cooper, N. T. W., Siebenmorgen, T. J., Counce, P. A., & Meullenet, J. F. (2006). Explaining rice milling quality variation using historical weather data analysis. *Cereal Chemistry*, *83*(4), 447–450. https://doi.org/10.1094/CC-83-0447

Croft, H., Chen, J. M., & Zhang, Y. (2014). The applicability of empirical vegetation indices for determining leaf chlorophyll content over different leaf and canopy structures. *Ecological Complexity*, *17*, 119–130. https://doi.org/10.1016/j.ecocom.2013.11.005

Curnel, Y., de Wit, A. J. W., Duveiller, G., & Defourny, P. (2011). Potential performances of remotely sensed LAI assimilation in WOFOST model based on an OSS Experiment. *Agricultural and Forest Meteorology*, *151*(12), 1843–1855. https://doi.org/10.1016/j.agrformet.2011.08.002

Curran, P. J., Dungan, J. L., Macler, B. A., & Plummer, S. E. (1991). The effect of a red leaf pigment on the relationship between red edge and chlorophyll concentration. *Remote Sensing of Environment*, *35*(1), 69–76.

Dangi, K., Singh, S. K., Malviya, D. K., Gautam, A., Kanapuriya, N., & Kumar, B. (2017). Effect of rice varieties on growth, yield and economics at varying levels of nitrogen under direct seeded upland condition Rewa Region. *International Journal of Current Microbiology and Applied Sciences*, *6*, 2313–2318. https://doi.org/10.20546/ijcmas.2017.609.283

Dao, P. D., & Liou, Y. A. (2015). Object-based flood mapping and affected rice field estimation with Landsat 8 OLI and MODIS data. *Remote Sensing*, *7*(5), 5077–5097. https://doi.org/10.3390/rs70505077

Darvishzadeh, R., Matkan, A. A., & Dashti Ahangar, A. (2012). Inversion of a radiative transfer model for estimation of rice canopy chlorophyll content using a lookup-table approach. *IEEE Journal of Selected Topics in Applied Earth Observations and Remote Sensing*, *5*(4), 1222–1230. https://doi.org/10.1109/JSTARS.2012.2186118

Dasari, K., & Anjaneyulu, L. (2017). Importance of Speckle filter window size and its impact on Speckle reduction in SAR images. *International Journal of Advances in Microwave Technology*, *2*(2), 98–102.

Dash, J., & Curran, P. J. (2004). The MERIS terrestrial chlorophyll index. *International Journal of Remote Sensing*, *25*(23), 5403–5413. https://doi.org/https://doi.org/10.1080/0143116042000274015

Dash, J., & Curran, P. J. (2007). Relationship between the MERIS vegetation indices and crop yield for the state of South Dakota, USA. *Proc. Envisat Symposium*.

DDPM. (2020). *25 provinces declare drought disaster*. https://reliefweb.int/report/thailand/25-provinces-declare-drought-disaster

De Datta, S. K. (1981). *Principles and practices of rice production*. Wiley, New York. http://books.irri.org/0471097608_content.pdf

De los Reyes, B. G., Myers, S. J., & McGrath, J. M. (2003). Differential induction of glyoxylate cycle enzymes by stress as a marker for seedling vigor in sugar beet (Beta vulgaris). *Molecular Genetics and Genomics*, *269*(5), 692–698.

Dente, L., Satalino, G., Mattia, F., & Rinaldi, M. (2008). Assimilation of leaf area index derived from

ASAR and MERIS data into CERES-Wheat model to map wheat yield. *Remote Sensing of Environment*, *112*(4), 1395–1407. https://doi.org/10.1016/j.rse.2007.05.023

Dharmarathna, W. R. S. S., Herath, S., & Weerakoon, S. B. (2014). Changing the planting date as a climate change adaptation strategy for rice production in Kurunegala district, Sri Lanka. *Sustainability Science*, *9*(1), 103–111. https://doi.org/10.1007/s11625-012-0192-2

Ding, Y., Zhao, K., Zheng, X., & Jiang, T. (2014). Temporal dynamics of spatial heterogeneity over cropland quantified by time-series NDVI, near infrared and red reflectance of Landsat 8 OLI imagery. *International Journal of Applied Earth Observation and Geoinformation*, *30*, 139–145.

Ding, Y., Wang, W., Zhuang, Q., & Luo, Y. (2020). Adaptation of paddy rice in China to climate change: The effects of shifting sowing date on yield and irrigation water requirement. *Agricultural Water Management*, *228*, 105890. https://doi.org/10.1016/j.agwat.2019.105890

Domiri, D. D. (2017). The method for detecting biological parameter of rice growth and early planting of paddy crop by using multi temporal remote sensing data. *Earth and Environmental Science*, *54*(1), 012002. https://doi.org/10.1088/1742-6596/755/1/011001

Dong, W., Chen, J., Wang, L., Tian, Y., Zhang, B., Lai, Y., ... & Guo, J. (2014). Impacts of nighttime post-anthesis warming on rice productivity and grain quality in East China. *The Crop Journal*, *2*(1), 63–69. https://doi.org/10.1016/j.cj.2013.11.002

Dong, T. Y., Dong, W. J., Guo, Y., Chou, J. M., Yang, S. L., Tian, D., & Yan, D. D. (2018). Future temperature changes over the critical Belt and Road region based on CMIP5 models. *Advances in Climate Change Research*, *9*(1), 57–65. https://doi.org/10.1016/j.accre.2018.01.003

Doraiswamy, P. C., Moulin, S., Cook, P. W., & Stern, A. (2003). Crop yield assessment from remote sensing. *Photogrammetric Engineering & Remote Sensing*, *69*(6), 665–674. https://doi.org/10.14358/pers.69.6.665

Dou, F., Soriano, J., Tabien, R. E., & Chen, K. (2016). Soil texture and cultivar fffects on rice (Oryza sativa, L.) grain yield, yield components and water productivity in three water regimes. In *PLoS ONE* (Vol. 11, Issue 3, p. e0150549). https://doi.org/10.1371/journal.pone.0150549

Du, H. W., Wang, Y., Zhuang, D. F., & Jiang, X. S. (2017). Temporal and spatial distribution characteristics in the natural plague foci of Chinese Mongolian gerbils based on spatial

autocorrelation. *Infectious Diseases of Poverty*, *6*(4), 84–93. https://doi.org/10.21832/9781788926959-013

E Schaedler, C., UM Taborda, C., AP Goulart, F., M Chiapinotto, D., & Pinho, P. J. (2020). Rice root growth and development in competition with weedy rice. *Planta Daninha*, *38*, 1–7.

Egamberdiyeva, D. (2007). The effect of plant growth promoting bacteria on growth and nutrient uptake of maize in two different soils. *Applied Soil Ecology*, *36*(2–3), 184–189. https://doi.org/10.1016/j.apsoil.2007.02.005

Ehammer, A., Fritsch, S., Conrad, C., Lamers, J., & Dech, S. (2010). Statistical derivation of fPAR and LAI for irrigated cotton and rice in arid Uzbekistan by combining multi-temporal RapidEye data and ground measurements. *Remote Sensing for Agriculture, Ecosystems, and Hydrology XII*, *7824*, 66–75. https://doi.org/10.1117/12.864796

Elliott, J., Deryng, D., Müller, C., Frieler, K., Konzmann, M., Gerten, D., Glotter, M., Flörke, M., Wada, Y., Best, N., Eisner, S., Fekete, B. M., Folberth, C., Foster, I., Gosling, S. N., Haddeland, I., Khabarov, N., Ludwig, F., Masaki, Y., … Wisser, D. (2014). Constraints and potentials of future irrigation water availability on agricultural production under climate change. *Proceedings of the National Academy of Sciences of the United States of America*, *111*(9), 3239–3244. https://doi.org/10.1073/pnas.1222474110

Enríquez-de-Salamanca, Á., Díaz-Sierra, R., Martín-Aranda, R. M., & Santos, M. J. (2017). Environmental impacts of climate change adaptation. *Environmental Impact Assessment Review*, *64*, 87–96. https://doi.org/10.1016/j.eiar.2017.03.005

Ermanto, A., Suryanto, A., & Hariyono, D. (2021). Efforts to improve productivity of paddy (oryza sativa L.) var. inpari 30 by settings of planting and different cropping patterns. *PLANTROPICA: Journal of Agricultural Science*, *6*(2), 163–173. https://doi.org/10.21776/ub.jpt.2021.006.2.9

Erten, E., Lopez-Sanchez, J. M., Yuzugullu, O., & Hajnsek, I. (2016). Retrieval of agricultural crop height from space: A comparison of SAR techniques. *Remote Sensing of Environment*, *187*, 130–144. https://doi.org/10.1016/j.rse.2016.10.007

Evenson, R. E., & Gollin, D. (2003). Assessing the impact of the Green Revolution, 1960 to 2000. *Science*, *300*(5620), 758–762. https://doi.org/10.1126/science.1078710

Fang, S., Cammarano, D., Zhou, G., Tan, K., & Ren, S. (2015). Effects of increased day and night temperature with supplemental infrared heating on winter wheat growth in North China.

European Journal of Agronomy, *64*, 67–77. https://doi.org/10.1016/j.eja.2014.12.012

Fang, H., Li, W., Wei, S., & Jiang, C. (2014). Seasonal variation of leaf area index (LAI) over paddy rice fields in NE China: Intercomparison of destructive sampling, LAI-2200, digital hemispherical photography (DHP), and AccuPAR methods. *Agricultural and Forest Meteorology*, *198*, 126–141. https://doi.org/10.1016/j.agrformet.2014.08.005

FAO. (n.d.). *Experience of Crop Cutting Experiments in Thailand*. http://www.fao.org/fileadmin/templates/rap/files/Project/Expert_Meeting__17Feb2014_/P3-3_Experience_of_Crop_Cutting_Experiments_in_Thailand.pdf

FAO. (1982). *Estimation of crop areas and yields in agricultural statistics*.

FAO. (2000). *Bridging the rice yield gap in the Asia-Pacific Region*.

FAO. (2018). *FAO rice market monitor*. *XXI*(1), 1–36.

FAOSTAT. (2010). *Statistical database of the Food and Agricultural Organization of the United Nations*.

Farooq, M., Siddique, K. H. M., Rehman, H., Aziz, T., Lee, D. J., & Wahid, A. (2011). Rice direct seeding: Experiences, challenges and opportunities. *Soil and Tillage Research*, *111*(2), 87–98. https://doi.org/10.1016/j.still.2010.10.008

Feizolahpour, Farid & H. Afshar, Mehdi & Düzenli, Eren & Besharat, Sina & Yilmaz, M. (2019). *Evaluating different vegetation indices for assessing crop growth condition derived from UAV images*. *July*.

Felkner, J., Tazhibayeva, K., & Townsend, R. (2009). Impact of climate change on rice production in Thailand. *The American Economic Review*, *99*(2), 205–210. https://doi.org/10.1257/aer.99.2.205.IMPACT

Fen, L. L., Mohd, R. I., Zulkarami, B., Mohammad, S., & Islam, M. R. (2015). Physiological and molecular characterization of drought responses and screening of drought tolerant rice varieties. *Bioscience Journal*, *31*(3), 709–718. https://doi.org/10.14393/BJ-v31n3a2015-23461

Fermont, A., & Benson, T. (2011). Estimating yield of food crops grown by smallholder farmers. *International Food Policy Research Institute*, *1*, 68.

Fernandez-Beltran, R., Baidar, T., Kang, J., & Pla, F. (2021). Rice-yield prediction with multi-

temporal sentinel-2 data and 3D CNN: A case study in Nepal. In *Remote Sensing* (Vol. 13, Issue 7, p. 1391). https://doi.org/10.3390/rs13071391

Fischer, G., & van Velthuizen, H. (2016). *National Agro-economic Zoning for Major Crops in Thailand (NAEZ) Project TCP/THA/3403)–NAEZ Model Implementation and Results*. http://www.fao.org/3/a-i7077e.pdf

Fishman, R. (2016). More uneven distributions overturn benefits of higher precipitation for crop yields. *Environmental Research Letters*, *11*(2), 024004.

Frolking, S., Qiu, J., Boles, S., Xiao, X., Liu, J., Zhuang, Y., ... & Qin, X. (2002). Combining remote sensing and ground census data to develop new maps of the distribution of rice agriculture in China. *Global Biogeochemical Cycles*, *16*(4), 38–1. https://doi.org/10.1029/2001GB001425

Fuster, B., Sánchez-Zapero, J., Camacho, F., García-Santos, V., Verger, A., Lacaze, R., Weiss, M., Baret, F., & Smets, B. (2020). Quality assessment of PROBA-V LAI, fAPAR and fCOVER collection 300 m products of copernicus global land service. In *Remote Sensing* (Vol. 12, Issue 6, p. 1017). https://doi.org/10.3390/rs12061017

Gale, E. L., & Saunders, M. A. (2013). The 2011 Thailand flood: Climate causes and return periods. In *Weather* (Vol. 68, Issue 9, pp. 233–237). https://doi.org/10.1002/wea.2133

Gallego, F. J., Kussul, N., Skakun, S., Kravchenko, O., Shelestov, A., & Kussul, O. (2014). Efficiency assessment of using satellite data for crop area estimation in Ukraine. *International Journal of Applied Earth Observation and Geoinformation*, *29*, 22–30. https://doi.org/10.1016/j.jag.2013.12.013

Gao, S., Niu, Z., Huang, N., & Hou, X. (2013). Estimating the Leaf Area Index, height and biomass of maize using HJ-1 and RADARSAT-2. *International Journal of Applied Earth Observation and Geoinformation*, *24*(1), 1–8. https://doi.org/10.1016/j.jag.2013.02.002

Gebhardt, S., Huth, J., Nguyen, L. D., Roth, A., & Kuenzer, C. (2012). A comparison of TerraSAR-X Quadpol backscattering with RapidEye multispectral vegetation indices over rice fields in the Mekong Delta, Vietnam. *International Journal of Remote Sensing*, *33*(24), 7644–7661. https://doi.org/10.1080/01431161.2012.702233

Geng, G., Wu, J., Wang, Q., Lei, T., He, B., Li, X., ... & Liu, D. (2016). Agricultural drought hazard analysis during 1980-2008: A global perspective. *International Journal of Climatology*, *36*(1), 389–399. https://doi.org/10.1002/joc.4356

Getis, A., & Ord, J. K. (2010). The analysis of spatial association by use of distance statistics. In *Perspectives on spatial data analysis*. Springer.

Ghadirnezhad, R., & Fallah, A. (2014). Temperature effect on yield and yield components of different rice cultivars in flowering stage. *International Journal of Agronomy*, *2014*. https://doi.org/10.1155/2014/846707

Gim, H.J., Ho, C.H., Jeong, S., Kim, J., Feng, S. and Hayes, M. . (2020). Improved mapping and change detection of the start of the crop growing season in the US Corn Belt from long-term AVHRR NDVI. *Agricultural and Forest Meteorology*, *294*, 108143.

Gistemp Team. (2020). *GISS surface temperature analysis (GISTEMP), version 4*. NASA Goddard Institute for Space Studies.

Gitelson, A. A., Viña, A., Ciganda, V., Rundquist, D. C., & Arkebauer, T. J. (2005). Remote estimation of canopy chlorophyll content in crops. *Geophysical Research Letters*, *32*(8). https://doi.org/10.1029/2005GL022688

Gnyp, M. L., Miao, Y., Yuan, F., Ustin, S. L., Yu, K., Yao, Y., Huang, S., & Bareth, G. (2014). Hyperspectral canopy sensing of paddy rice aboveground biomass at different growth stages. *Field Crops Research*, *155*, 42–55. https://doi.org/10.1016/j.fcr.2013.09.023

Gong, Y., Yang, K., Lin, Z., Fang, S., Wu, X., Zhu, R., & Peng, Y. (2021). Remote estimation of leaf area index (LAI) with unmanned aerial vehicle (UAV) imaging for different rice cultivars throughout the entire growing season. *Plant Methods*, *17*(1), 1–16. https://doi.org/10.1186/s13007-021-00789-4

Graf, B., Gutierrez, A. P., Rakotobe, O., Zahner, P., & Delucchi, V. (1990). A simulation model for the dynamics of rice growth and development: Part II-The competition with weeds for nitrogen and light. *Agricultural Systems*, *32*(4), 367–392. https://doi.org/10.1016/0308-521X(90)90100-5

Guan, X., Huang, C., Liu, G., Meng, X., & Liu, Q. (2016). Mapping rice cropping systems in Vietnam using an NDVI-based time-series similarity measurement based on DTW distance. *Remote Sensing*, *8*(1), 19.

Guissard, V., Lucau-Danila, C., & Defourny, P. (2006). Crop specific LAI retrieval using optical and radar satellite data for regional crop growth monitoring and modelling. *Remote Sensing for Agriculture, Ecosystems, and Hydrology VII*, *5976*(October 2005), 59760S. https://doi.org/10.1117/12.627495

Gumma, M. K., Nelson, A., & Yamano, T. (2019). Mapping drought-induced changes in rice area in India. *International Journal of Remote Sensing*, *40*(21), 8146–8173.

Guo, X., Li, K., Shao, Y., Wang, Z., Li, H., Yang, Z., Liu, L., & Wang, S. (2018). Inversion of rice biophysical parameters using simulated compact polarimetric SAR C-band data. *Sensors*, *18*(7), 2271. https://doi.org/10.3390/s18072271

Gurung, B., Panwar, S., Singh, K. N., Banerjee, R., Gurung, S. R., & Rathore, A. (2017). Wheat yield forecast using detrended yield over a sub-humid climatic environment in five districts of Uttar Pradesh, India. *Indian Journal of Agricultural Sciences*, *87*(1), 87–91.

Gusso, A., Formaggio, A. R., Rizzi, R., Adami, M., & Rudorff, B. F. T. (2012). Soybean crop area estimation by Modis/Evi data. *Pesquisa Agropecuaria Brasileira*, *47*, 425–435. https://doi.org/10.1590/S0100-204X2012000300015

Haboudane, D., Miller, J. R., Pattey, E., Zarco-Tejada, P. J., & Strachan, I. B. (2004). Hyperspectral vegetation indices and novel algorithms for predicting green LAI of crop canopies: Modeling and validation in the context of precision agriculture. *Remote Sensing of Environment*, *90*(3), 337–352. https://doi.org/10.1016/j.rse.2003.12.013

Halsnas, K., & Trarup, S. (2009). Development and climate change: A mainstreaming approach for assessing economic, social, and environmental impacts of adaptation measures. *Environmental Management*, *43*(5), 765–778. https://doi.org/10.1007/s00267-009-9273-0

Halwart, M., & Gupta, M. V. (2004). *Culture of fish in rice fields* (WorldFish Center (ed.); Issue January 2004). FAO.

Hansen, J., Sato, M., Ruedy, R., Lo, K., Lea, D. W., & Medina-Elizade, M. (2006). Global temperature change. *Proceedings of the National Academy of Sciences of the United States of America*, *103*(39), 14288–14293. https://doi.org/10.1073/pnas.0606291103

Hardke, J. T. (2013). *Arkansas rice production handbook*. University of Arkansas Division of Agriculture Cooperative Extension Service MP192.

Harrell, D. L., Tubaña, B. S., Walker, T. W., & Phillips, S. B. (2011). Estimating rice grain yield potential using normalized difference vegetation index. *Agronomy Journal*, *103*(6), 1717–1723. https://doi.org/10.2134/agronj2011.0202

He, L., JIANG, Z. W., CHEN, Z. X., REN, J. Q., & Bin, L. I. U. (2017). Assimilation of temporal-spatial leaf area index into the CERES-Wheat model with ensemble Kalman filter and uncertainty

assessment for improving winter wheat yield estimation. *Journal of Integrative Agriculture*, *16*(10), 2283–2299. https://doi.org/10.1016/S2095-3119(16)61351-5

He, Z., Li, S., Wang, Y., Dai, L., & Lin, S. (2018). Monitoring rice phenology based on backscattering characteristics of multi-temporal RADARSAT-2 datasets. *Remote Sensing*, *10*(2), 340.

He, J., Ma, B., & Tian, J. (2022). Water production function and optimal irrigation schedule for rice (Oryza sativa L.) cultivation with drip irrigation under plastic film-mulched. *Scientific Reports*, *12*(1), 17243. https://doi.org/10.1038/s41598-022-20652-3

Heong, K. L., Cheng, J., & Escalada, M. M. (2015). Social impacts of plathopper outbreaks in Thailand. *Rice Planthoppers: Ecology, Management, Socio Economics and Policy*, *January*, 191–207. https://doi.org/10.1007/978-94-017-9535-7

Hirooka, Y., Homma, K., Maki, M., & Sekiguchi, K. (2015). Applicability of synthetic aperture radar (SAR) to evaluate leaf area index (LAI) and its growth rate of rice in farmers' fields in Lao PDR. *Field Crops Research*, *176*, 119–122. https://doi.org/10.1016/j.fcr.2015.02.022

Hmimina, G., Dufrêne, E., Pontailler, J. Y., Delpierre, N., Aubinet, M., Caquet, B., ... & Gross, P. (2013). Evaluation of the potential of MODIS satellite data to predict vegetation phenology in different biomes: an investigation using ground-based NDVI measurements. *Remote Sensing of Environment*, *132*, 145–158. https://doi.org/10.1016/j.rse.2013.01.010

Hoang, K. H., Bernier, M., Duchesne, S., & Tran, M. Y. (2013). Classification of cultivated rice fields in northern Vietnam using polarimetric RADARSAT-2 data. *Geoscience and Remote Sensing Symposium (IGARSS)*, *IEEE*, 2681–2684.

Holzman, M. E., Carmona, F., Rivas, R., & Niclòs, R. (2018). Early assessment of crop yield from remotely sensed water stress and solar radiation data. *ISPRS Journal of Photogrammetry and Remote Sensing*, *145*, 297–308. https://doi.org/10.1016/j.isprsjprs.2018.03.014

Horie, T., Kropff, M. J., Centeno, H. G., Nakagawa, H., Nakano, J., Kim, H. Y., & Ohnishi, M. (1995). Effect of anticipated change in global environment on rice yields in Japan. *Climate Change and Rice*, 291–302. https://doi.org/10.1007/978-3-642-85193-3_27

Horie, Takeshi. (2019). Global warming and rice production in Asia: Modeling, impact prediction and adaptation. *Proceedings of the Japan Academy Series B: Physical and Biological Sciences*, *95*(6), 211–245. https://doi.org/10.2183/pjab.95.016

Horvatic, D., Stanley, H. E., & Podobnik, B. (2011). Detrended cross-correlation analysis for non-

stationary time series with periodic trends. *EPL (Europhysics Letters)*, *94*(1), 18007. https://doi.org/10.1209/0295-5075/94/18007

Hosseini, M., McNairn, H., Merzouki, A., & Pacheco, A. (2015). Estimation of Leaf Area Index (LAI) in corn and soybeans using multi-polarization C- and L-band radar data. *Remote Sensing of Environment*, *170*, 77–89. https://doi.org/10.1016/j.rse.2015.09.002

Huang, M., Yin, X., Jiang, L., Zou, Y., & Deng, G. (2015). Raising potential yield of short-duration rice cultivars is possible by increasing harvest index. *Biotechnology, Agronomy and Society and Environment*, *19*(2), 153–159.

Huang, C., Yang, W., Duan, L., Jiang, N., Chen, G., Xiong, L., & Liu, Q. (2013). Rice panicle length measuring system based on dual-camera imaging. *Computers and Electronics in Agriculture*, *98*, 158–165. https://doi.org/10.1016/j.compag.2013.08.006

Huang, Jianxi, Tian, L., Liang, S., Ma, H., Becker-Reshef, I., Huang, Y., Su, W., Zhang, X., Zhu, D., & Wu, W. (2015). Improving winter wheat yield estimation by assimilation of the leaf area index from Landsat TM and MODIS data into the WOFOST model. *Agricultural and Forest Meteorology*, *204*, 106–121. https://doi.org/10.1016/j.agrformet.2015.02.001

Huang, Jikun, Hu, R., Rozelle, S., & Pray, C. (2005). Plant science: Insect-resistant GM rice in farmers' fields: Assessing productivity and health effects in China. *Science*, *308*(5722), 688–690. https://doi.org/10.1126/science.1108972

Huang, Jin, Islam, A. R. M. T., Zhang, F., & Hu, Z. (2017). Spatiotemporal analysis the precipitation extremes affecting rice yield in Jiangsu province, southeast China. *International Journal of Biometeorology*, *61*(10), 1863–1872. https://doi.org/10.1007/s00484-017-1372-7

Huang, Jingfeng, Wang, X., Li, X., Tian, H., & Pan, Z. (2013). Remotely sensed rice yield prediction using multi-temporal NDVI data derived from NOAA's-AVHRR. *PLoS ONE*, *8*(8), e70816. https://doi.org/10.1371/journal.pone.0070816

Huete, A. R., Liu, H. Q., Batchily, K. V., & Van Leeuwen, W. J. D. A. (1997). A comparison of vegetation indices over a global set of TM images for EOS-MODIS. *Remote Sensing of Environment*, *59*(3), 440–451.

Huete, A., Didan, K., Miura, H., Rodriguez, E. P., Gao, X., & Ferreira, L. F. (2002). Overview of the radiometric and biopyhsical performance of the MODIS vegetation indices. *Remote Sensing of Environment*, *83*(1–2), 195–213. https://ac-els-cdn-com.sire.ub.edu/S0034425702000962/1-s2.0-S0034425702000962-

main.pdf?_tid=420e9dda-1821-11e8-b53d-00000aacb35d&acdnat=1519339356_ef83dc686b96e75a110fbad8d8dc950a

Huete, A. R. (1988). A soil-adjusted vegetation index (SAVI). *Remote Sensing of Environment*, *25*(3), 295–309. https://doi.org/10.1016/0034-4257(88)90106-X

IFAD. (2016). *Climate change impacts in the Asia / Pacific Region*. https://doi.org/https://doi.org/10.4225/08/5924877f7776a

IFPRI. (2017). *Climate change: Impact on agriculture and costs of adaptation*. http://irri.org/news/hot-topics/rice-and-climate-change

Inoue, Y., & Sakaiya, E. (2013). Relationship between X-band backscattering coefficients from high-resolution satellite SAR and biophysical variables in paddy rice. *Remote Sensing Letters*, *4*(3), 288–295. https://doi.org/10.1080/2150704X.2012.725482

Inoue, Y., Sakaiya, E., & Wang, C. (2014a). Capability of C-band backscattering coefficients from high-resolution satellite SAR sensors to assess biophysical variables in paddy rice. *Remote Sensing of Environment*, *140*, 257–266. https://doi.org/10.1016/j.rse.2013.09.001

Inoue, Y., Sakaiya, E., & Wang, C. (2014b). Potential of X-band images from high-resolution satellite SAR sensors to assess growth and yield in paddy rice. *Remote Sensing*, *6*(7), 5995–6019. https://doi.org/10.3390/rs6075995

IPCC. (2007). *AR4 climate chagne 2007: The physical sicence basis - global climate projections*. https://doi.org/10.1109/ICEPT.2010.5582830

IPCC. (2014). Climate change 2014: Synthesis report. contribution of working groups I, II and III to the fifth assessment report of the Intergovernmental Panel on Climate Change. In *Core Writing Team, R.K. Pachauri and L.A. Meyer*. https://doi.org/10.1017/CBO9781107415324.004

IRRI. (2017). *How to manage pests and diseases*. http://www.knowledgebank.irri.org/step-by-step-production/growth/pests-and-diseases?tmpl=component-category&print=1

Ishfaq, M., Akbar, N., Anjum, S. A., & ANWAR-IJL-HAQ, M. (2020). Growth, yield and water productivity of dry direct seeded rice and transplanted aromatic rice under different irrigation management regimes. *Journal of Integrative Agriculture*, *19*(11), 2656–2673. https://doi.org/10.1016/S2095-3119(19)62876-5

Islam, M. S., & Morison, J. I. L. (1992). Influence of solar radiation and temperature on irrigated rice grain yield in Bangladesh. *Field Crops Research*, *30*(1–2), 13–28.

Jafari, R., Lewis, M. M., & Ostendorf, B. (2007). Evaluation of vegetation indices for assessing vegetation cover in southern arid lands in South Australia. *The Rangeland Journal*, *29*(1), 39–49.

Ji, Z., Pan, Y., Zhu, X., Wang, J., & Li, Q. (2021). Prediction of crop yield using phenological information extracted from remote sensing vegetation index. *Sensors*, *21*(4), 1406. https://doi.org/10.3390/s21041406

Jia, M., Tong, L., Zhang, Y., & Chen, Y. (2014). Rice biomass estimation using radar backscattering data at S-band. *IEEE Journal of Selected Topics in Applied Earth Observations and Remote Sensing*, *7*(2), 469–479. https://doi.org/10.1109/JSTARS.2013.2282641

Jiang, L., Deng, X., & Seto, K. C. (2013). The impact of urban expansion on agricultural land use intensity in China. *Land Use Policy*, *35*, 33–39. https://doi.org/10.1016/j.landusepol.2013.04.011

Jin, X., Kumar, L., Li, Z., Feng, H., Xu, X., Yang, G., & Wang, J. (2018). A review of data assimilation of remote sensing and crop models. *European Journal of Agronomy*, *92*, 141–152. https://doi.org/10.1016/j.eja.2017.11.002

Jing-feng, H., Shu-chuan, T., Abou-Ismail, O., & Ren-chao, W. (2002). Rice yield estimation using remote sensing and simulation model. *Journal of Zhejinag University: Science*, *3*(4), 461–466. https://doi.org/10.1007/BF02839491

Johnson, L. K., Bloom, J. D., Dunning, R. D., Gunter, C. C., Boyette, M. D., & Creamer, N. G. (2019). Farmer harvest decisions and vegetable loss in primary production. *Agricultural Systems*, *176*, 102672. https://doi.org/10.1016/j.agsy.2019.102672

Jonckheere, I., Fleck, S., Nackaerts, K., Muys, B., Coppin, P., Weiss, M., & Baret, F. (2004). Review of methods for in situ leaf area index determination Part I. Theories, sensors and hemispherical photography. *Agricultural and Forest Meteorology*, *121*(1–2), 19–35. https://doi.org/10.1016/j.agrformet.2003.08.027

Jones, J. W., Hoogenboom, G., Porter, C. H., Boote, K. J., Batchelor, W. D., Hunt, L. A., ... & Ritchie, J. T. (2003). The DSSAT cropping system model. *European Journal of Agronomy*, *18*(3–4), 235–265. https://doi.org/10.1016/S1161-0301(02)00107-7

Kakumanu, K. R., Kotapati, G. R., Nagothu, U. S., Kuppanan, P., & Kallam, S. R. (2019). Adaptation to climate change and variability: A case of direct seeded rice in Andhra Pradesh, India. *Journal of Water and Climate Change*, *10*(2), 419–430. https://doi.org/10.2166/wcc.2018.141

Kamthonkiat, D., Honda, K., Turral, H., Tripathi, N. K., & Wuwongse, V. (2005). Discrimination of irrigated and rainfed rice in a tropical agricultural system using SPOT VEGETATION NDVI and rainfall data. *International Journal of Remote Sensing*, *26*(12), 2527–2547. https://doi.org/10.1080/01431160500104335

Kandiannan, K., Karthikeyan, R., Krishnan, R., Kailasam, C., & Balasubramanian, T. N. (2002). A crop-weather model for prediction of rice (oryza sativa l.) Yield using an empirical-statistical technique. *Journal of Agronomy and Crop Science*, *188*(1), 59–62. https://doi.org/10.1046/j.1439-037x.2002.00533.x

Kang, Y., Khan, S., & Ma, X. (2009). Climate change impacts on crop yield, crop water productivity and food security - A review. *Progress in Natural Science*, *19*(12), 1665–1674. https://doi.org/10.1016/j.pnsc.2009.08.001

Kasampalis, D., Alexandridis, T., Deva, C., Challinor, A., Moshou, D., & Zalidis, G. (2018). Contribution of remote sensing on crop models: A review. *Journal of Imaging*, *4*(4), 52. https://doi.org/10.3390/jimaging4040052

Kasetsart University. (2000). The Chao Phraya Delta : Rainfed Agriculture, Thailand's Rice Bowl. *International Conference*, *1*(December).

Khan, M., Mia, M., & Hossain, M. (2012). Impacts of Flood on Crop Production in Haor Areas of Two Upazillas in Kishoregonj. *Journal of Environmental Science and Natural Resources*, *5*(1), 193–198. https://doi.org/10.3329/jesnr.v5i1.11581

Kiguchi, M., Takata, K., Hanasaki, N., Archevarahuprok, B., Champathong, A., Ikoma, E., ... & Oki, T. (2020). A review of climate-change impact and adaptation studies for the water sector in Thailand. *Environmental Research Letters*, *16*(2), 023004.

Kim, M. K., & Pang, A. (2009). Climate change impact on rice yield and production risk. *Journal of Rural Development/Nongchon-Gyeongje*, *32*(1071-2016–86914), 17–29. https://doi.org/10.22004/ag.econ.90682

Kim, Y. H., Hong, S. Y., & Lee, H. (2008). Radar backscattering measurements of paddy rice field using Multifrequency (L , C and X) and full polarization. *IGARSS 2008-2008 IEEE*

International Geoscience and Remote Sensing Symposium, *4*, IV–553.

Kim, M., Ko, J., Jeong, S., Yeom, J. min, & Kim, H. ok. (2017). Monitoring canopy growth and grain yield of paddy rice in South Korea by using the GRAMI model and high spatial resolution imagery. *GIScience and Remote Sensing*, *54*(4), 534–551. https://doi.org/10.1080/15481603.2017.1291783

Kim, Y., Jackson, T., Bindlish, R., Lee, H., & Hong, S. (2011). Radar vegetation index for estimating the vegetation water content of rice and soybean. *IEEE Geoscience and Remote Sensing Letters*, *9*(4), 564–568. https://doi.org/10.1109/LGRS.2011.2174772

Knyazikhin, Y. (1999). *MODIS leaf area index (LAI) and fraction of photosynthetically active radiation absorbed by vegetation (FPAR) product (MOD 15) algorithm theoretical basis document*.

Kobayashi, S., & Ide, H. (2022). Rice crop monitoring using Sentinel-1 SAR data: A Case study in Saku, Japan. In *Remote Sensing* (Vol. 14, Issue 14). https://doi.org/10.3390/rs14143254

Komori, D., Nakamura, S., Kiguchi, M., Nishijima, A., Yamazaki, D., Suzuki, S., ... & Oki, T. (2012). Characteristics of the 2011 Chao Phraya River flood in central Thailand. *Hydrological Research Letters*, *6*, 41–46. https://doi.org/10.3178/hrl.6.41

Kondhia, A., Tabien, R. E., & Ibrahim, A. (2015). Evaluation and selection of high biomass rice (Oryza sativa L.) for drought tolerance. *American Journal of Plant Sciences*, *6*(12), 1962.

Koppe, W., Gnyp, M. L., Hütt, C., Yao, Y., Miao, Y., Chen, X., & Bareth, G. (2012). Rice monitoring with multi-temporal and dual-polarimetric terrasar-X data. *International Journal of Applied Earth Observation and Geoinformation*, *21*(1), 568–576. https://doi.org/10.1016/j.jag.2012.07.016

Kotsuki, S., & Tanaka, K. (2015). SACRA-a method for the estimation of global high-resolution crop calendars from a satellite-sensed NDVI. *Hydrology and Earth System Sciences*, *19*(11), 4441–4461. https://doi.org/10.5194/hess-19-4441-2015

Krishnan, P., Ramakrishnan, B., Reddy, K. R., & Reddy, V. R. (2011). High-Temperature Effects on Rice Growth , Yield , and Grain Quality. In *Advances in Agronomy* (1st ed., Vol. 111). Elsevier Inc. https://doi.org/10.1016/B978-0-12-387689-8.00004-7

Kuenzer, C., & Knauer, K. (2013). Remote sensing of rice crop areas. *International Journal of Remote Sensing*, *34*(6), 2101–2139. https://doi.org/10.1080/01431161.2012.738946

Kuhlgert, S., Austic, G., Zegarac, R., Osei-Bonsu, I., Hoh, D., Chilvers, M. I., Roth, M. G., Bi, K., TerAvest, D., Weebadde, P., & Kramer, D. M. (2016). MultispeQ Beta: A tool for large-scale plant phenotyping connected to the open PhotosynQ network. *Royal Society Open Science*, *3*(10), 160592. https://doi.org/10.1098/rsos.160592

Kukal, M. S., & Irmak, S. (2018). Climate-driven crop yield and yield variability and climate change impacts on the U.S. Great Plains agricultural production. *Scientific Reports*, *8*(1), 1–18. https://doi.org/10.1038/s41598-018-21848-2

Kumar, A., Dixit, S., Ram, T., Yadaw, R. B., Mishra, K. K., & Mandal, N. P. (2014). Breeding high-yielding drought-tolerant rice: genetic variations and conventional and molecular approaches. *Journal of Experimental Botany*, *65*(21), 6265–6278.

Kumar, C. P. (2016). Impact of climate change on groundwater resources. *Handbook of Research on Climate Change Impact on Health and Environmental Sustainability*, 196–221. https://doi.org/10.4018/978-1-5225-0803-8.ch052

Kumar, R., Choudhary, J. S., Mishra, J. S., Mondal, S., Poonia, S., Monobrullah, M., Hans, H., Verma, M., Kumar, U., Bhatt, B. P., Malik, R. K., Kumar, V., & McDonald, A. (2022). Outburst of pest populations in rice-based cropping systems under conservation agricultural practices in the middle Indo-Gangetic Plains of South Asia. In *Scientific Reports* (Vol. 12, Issue 1). https://doi.org/10.1038/s41598-022-07760-w

Kumar, S., Kour, S., Gupta, M., Kachroo, D., & Singh, H. (2017). Influence of rice varieties and fertility levels on performance of rice and soil nutrient status under aerobic conditions. *Journal of Applied and Natural Science*, *9*(2), 1164–1169. https://doi.org/10.31018/jans.v9i2.1341

Kumar, V., Kumari, M., & Saha, S. K. (2013). Leaf area index estimation of lowland rice using semi-empirical backscattering model. *Journal of Applied Remote Sensing*, *7*(1), 073474. https://doi.org/10.1117/1.jrs.7.073474

Lam-Dao, N., Hoang-Phi, P., Huth, J., & Cao-Van, P. (2011). Estimation of the rice yield in the Mekong Delta using SAR dual polarisation data. *32nd Asian Conference on Remote Sensing 2011, ACRS 2011*, *2*(October), 1047–1052.

Landsberg, J. J., Prince, S. D., Jarvis, P. G., McMurtrie, R. E., Luxmoore, R., & Medlyn, B. E. (1997). Energy conversion and use in forests: An analysis of forest production in terms of radiation utilisation efficiency (ε). *The Use of Remote Sensing in the Modeling of Forest Productivity*,

50, 273–298.

Lang, Y. Z., Yang, X. D., Wang, M. E., & Zhu, Q. S. (2012). Effects of lodging at different filling stages on rice yield and grain quality. *Rice Science*, *19*(4), 315–319.

Lanning, S. B., Siebenmorgen, T. J., Counce, P. A., Ambardekar, A. A., & Mauromoustakos, A. (2011). Extreme nighttime air temperatures in 2010 impact rice chalkiness and milling quality. *Field Crops Research*, *124*(1), 132–136.

Latif, M. A., Ali, M. Y., Islam, M. R., Badshah, M. A., & Hasan, M. S. (2009). Evaluation of management principles and performance of the System of Rice Intensification (SRI) in Bangladesh. *Field Crops Research*, *114*(2), 255–262. https://doi.org/10.1016/j.fcr.2009.08.006

Latif, M. A., Islam, M. R., Ali, M. Y., & Saleque, M. A. (2005). Validation of the system of rice intensification (SRI) in Bangladesh. *Field Crops Research*, *93*(2–3), 281–292. https://doi.org/10.1016/j.fcr.2004.10.005

Laukkonen, J., Blanco, P. K., Lenhart, J., Keiner, M., Cavric, B., & Kinuthia-Njenga, C. (2009). Combining climate change adaptation and mitigation measures at the local level. *Habitat International*, *33*(3), 287–292. https://doi.org/10.1016/j.habitatint.2008.10.003

Launay, M., & Guerif, M. (2005). Assimilating remote sensing data into a crop model to improve predictive performance for spatial applications. *Agriculture, Ecosystems and Environment*, *111*(1–4), 321–339. https://doi.org/10.1016/j.agee.2005.06.005

Laux, P., Jäckel, G., Tingem, R. M., & Kunstmann, H. (2010). Impact of climate change on agricultural productivity under rainfed conditions in Cameroon-A method to improve attainable crop yields by planting date adaptations. *Agricultural and Forest Meteorology*, *150*(9), 1258–1271. https://doi.org/10.1016/j.agrformet.2010.05.008

Lawler, J. J. (2009). Climate change adaptation strategies for resource management and conservation planning. *Annals of the New York Academy of Sciences*, *1162*, 79–98. https://doi.org/10.1111/j.1749-6632.2009.04147.x

Laza, M. R. C., Peng, S., Akita, S., & Saka, H. (2004). Effect of panicle size on grain yield of IRRI-released Indica rice cultivars in the wet season. *Plant Production Science*, *7*(3), 271–276. https://doi.org/10.1626/pps.7.271

Leblanc, S. G., & Chen, J. M. (2001). A practical scheme for correcting multiple scattering effects

on optical LAI measurements. *Agricultural and Forest Meteorology*, *110*(2), 125–139. https://doi.org/10.1016/S0168-1923(01)00284-2

Lee, J. S. (1980). Digital image enhancement and noise filtering by use of local statistics. *IEEE Transactions on Pattern Analysis and Machine Intelligence*, *2*, 165–168.

Lemoine, L., & Delignieres, D. (2009). Detrended windowed (lag one) autocorrelation : A new method for distinguishing between event-based and emergent timing. *Quarterly Journal of Experimental Psychology*, *62*(3), 585–604. https://doi.org/10.1080/17470210802131896

Lencucha, R., Pal, N. E., Appau, A., Thow, A. M., & Drope, J. (2020). Government policy and agricultural production: A scoping review to inform research and policy on healthy agricultural commodities. *Globalization and Health*, *16*(1), 1–15. https://doi.org/10.1186/s12992-020-0542-2

Leonenko, G., Los, S. O., & North, P. R. J. (2013). Retrieval of leaf area index from MODIS surface reflectance by model inversion using different minimization criteria. *Remote Sensing of Environment*, *139*, 257–270. https://doi.org/10.1016/j.rse.2013.07.012

Leung, H., Zhu, Y., Revilla-Molina, I., Fan, J. X., Chen, H., Pangga, I., Vera Cruz, C., & Mew, T. W. (2003). Using genetic diversity to achieve sustainable rice disease management. *Plant Disease*, *87*(10), 1156–1169. https://doi.org/10.1094/PDIS.2003.87.10.1156

Li, T., Angeles, O., Marcaida III, M., Manalo, E., Manalili, M. P., Radanielson, A., & Mohanty, S. (2017). From ORYZA2000 to ORYZA (v3): An improved simulation model for rice in drought and nitrogen-deficient environments. *Agricultural and Forest Meteorology*, *237*, 246–256. https://doi.org/10.1016/j.agrformet.2017.02.025

Li, Z., Wang, J., Xu, X., Zhao, C., Jin, X., Yang, G., & Feng, H. (2015). Assimilation of two variables derived from hyperspectral data into the DSSAT-CERES model for grain yield and quality estimation. *Remote Sensing*, *7*(9), 12400–12418. https://doi.org/10.3390/rs70912400

LI, B., TI, C., & YAN, X. (2020). Estimating rice paddy areas in China using multi-temporal cloud-free normalized difference vegetation index (NDVI) imagery based on change detection. *Pedosphere*, *30*(6), 734–746. https://doi.org/10.1016/S1002-0160(17)60405-3

Li, L., Friedl, M. A., Xin, Q., Gray, J., Pan, Y., & Frolking, S. (2014). Mapping crop cycles in China using MODIS-EVI time series. *Remote Sensing*, *6*(3), 2473–2493. https://doi.org/10.3390/rs6032473

Li, P., Zhang, X., Wang, W., Zheng, H., Yao, X., Tian, Y., Zhu, Y., Cao, W., Chen, Q., & Cheng, T. (2020). Estimating aboveground and organ biomass of plant canopies across the entire season of rice growth with terrestrial laser scanning. *International Journal of Applied Earth Observation and Geoinformation*, *91*(April), 102132. https://doi.org/10.1016/j.jag.2020.102132

Li, R., Li, M., Ashraf, U., Liu, S., & Zhang, J. (2019). Exploring the relationships between yield and yield-related traits for rice varieties released in china from 1978 to 2017. *Frontiers in Plant Science*, *10*(May). https://doi.org/10.3389/fpls.2019.00543

Li, S., Ni, P., Cui, G., He, P., Liu, H., Li, L., & Liang, Z. (2016). Estimation of rice biophysical parameters using multitemporal RADARSAT-2 images. *IOP Conference Series: Earth and Environmental Science*, *34*(1), 012019. https://doi.org/10.1088/1755-1315/34/1/012019

Li, Songyang, Yuan, F., Ata-UI-Karim, S. T., Zheng, H., Cheng, T., Liu, X., Tian, Y., Zhu, Y., Cao, W., & Cao, Q. (2019). Combining color indices and textures of UAV-based digital imagery for rice LAI estimation. *Remote Sensing*, *11*(15), 1763. https://doi.org/10.3390/rs11151763

Li, Y., Wang, H., & Li, X. B. (2015). Fractional vegetation cover estimation based on an improved selective endmember spectral mixture model. *PLoS ONE*, *10*(4), e0124608. https://doi.org/10.1371/journal.pone.0124608

Liao, J., Hu, Y., Zhang, H., Liu, L., Liu, Z., Tan, Z., & Wang, G. (2018). A rice mapping method based on time-series Landsat data for the extraction of growth period characteristics. *Sustainability (Switzerland)*, *10*(7), 2570. https://doi.org/10.3390/su10072570

Liu, H., Hussain, S., Zheng, M., Peng, S., Huang, J., Cui, K., & Nie, L. (2014). Dry direct-seeded rice as an alternative to transplanted-flooded rice in Central China. *Agronomy for Sustainable Development*, *35*(1), 285–294. https://doi.org/10.1007/s13593-014-0239-0

LIU, C. an, CHEN, Z. xin, SHAO, Y., CHEN, J. song, Hasi, T., & PAN, H. zhu. (2019). Research advances of SAR remote sensing for agriculture applications: A review. *Journal of Integrative Agriculture*, *18*(3), 506–525. https://doi.org/10.1016/S2095-3119(18)62016-7

Liu, D., You, J., Xie, Q., Huang, Y., & Tong, H. (2018). Spatial and temporal characteristics of drought and flood in Quanzhou based on standardized precipitation index (SPI) in recent 55 years. *Journal of Geoscience and Environment Protection*, *06*(08), 25–37. https://doi.org/10.4236/gep.2018.68003

Liu, J., & van Iersel, M. W. (2021). Photosynthetic physiology of blue, green, and red light: Light

intensity effects and underlying mechanisms. In *Frontiers in Plant Science* (Vol. 328). https://doi.org/10.3389/fpls.2021.619987

Liu, K. Lou, Ishaq, M., Rehmani, A., Liu, K., Li, Y., Hu, H., Zhou, L., Xiao, X., & Yu, P. (2015). Estimating Rice Yield Based on Normalized Difference Vegetation Index at Heading Stage of Different Nitrogen Application... View project A district level study with HEC,Pakistan View project Estimating Rice Yield Based on Normalized Difference Vegetation . *Journal of Environmental and Agricultural Sciences*, *2*(13). https://www.researchgate.net/publication/272785841

Liu, Q., Li, K., Shao, Y., Yang, Z., Brisco, B., & Liu, L. (2017). An improved scheme for rice phenology estimation based on time-series multispectral HJ-1A/B and polarimetric RADARSAT-2 data. *Remote Sensing of Environment*, *195*, 184–201. https://doi.org/10.1016/j.rse.2017.04.016

LIU, X. jun, CAO, Q., YUAN, Z. feng, LIU, X., WANG, X. ling, TIAN, Y. chao, CAO, W. xing, & ZHU, Y. (2018). Leaf area index based nitrogen diagnosis in irrigated lowland rice. *Journal of Integrative Agriculture*, *17*(1), 111–121. https://doi.org/10.1016/S2095-3119(17)61714-3

Lobell, D. B., Schlenker, W., & Costa-Roberts, J. (2011). Climate trends and global crop production since 1980. *Science*, *333*(6042), 616–620. https://doi.org/10.1126/science.1204531

Lobell, D. B., & Field, C. B. (2007). Global scale climate-crop yield relationships and the impacts of recent warming. *Environmental Research Letters*, *2*(1). https://doi.org/10.1088/1748-9326/2/1/014002

Longtau, S. R. (2003). Multi-agency partnerships in West African agriculture: A review and description of rice production systems in Nigeria. *Ecosystems Development Organisationsystems Development Organisation*, 1–50.

Loo, Y. Y., Billa, L., & Singh, A. (2015). Effect of climate change on seasonal monsoon in Asia and its impact on the variability of monsoon rainfall in Southeast Asia. *Geoscience Frontiers*, *6*(6), 817–823. https://doi.org/10.1016/j.gsf.2014.02.009

Lopez-Sanchez, J. M., Vicente-Guijalba, F., Erten, E., Campos-Taberner, M., & Garcia-Haro, F. J. (2017). Retrieval of vegetation height in rice fields using polarimetric SAR interferometry with TanDEM-X data. *Remote Sensing of Environment*, *192*, 30–44. https://doi.org/10.1016/j.rse.2017.02.004

Lopresti, M. F., Di Bella, C. M., & Degioanni, A. J. (2015). Relationship between MODIS-NDVI data and wheat yield: A case study in Northern Buenos Aires province, Argentina. *Information*

Processing in Agriculture, *2*(2), 73–84. https://doi.org/10.1016/j.inpa.2015.06.001

Lu, J., Carbone, G. J., & Gao, P. (2017). Detrending crop yield data for spatial visualization of drought impacts in the United States, 1895–2014. *Agricultural and Forest Meteorology*, *237–238*, 196–208. https://doi.org/10.1016/j.agrformet.2017.02.001

Lusch, D. P. (1999). *Introduction to microwave remote sensing* (Michigan State University (ed.)).

M.J. Kropff, K.G. Cassman, and H. H. V. L. (1994). Quantitative understanding of the irrigation ecosystem and yield potential. *Hybrid Rice Technology: New Developments and Future Prospects*, 97–113.

Maas, S. J. (1992). GRAMI: A crop growth model that can use remotely sensed information. *Agricultural Research Service (USA)*.

Machwitz, M., Giustarini, L., Bossung, C., Frantz, D., Schlerf, M., Lilienthal, H., ... & Udelhoven, T. (2014). Enhanced biomass prediction by assimilating satellite data into a crop growth model. *Environmental Modelling & Software*, *62*, 437–453. https://doi.org/10.1016/j.envsoft.2014.08.010

Maftukhah, R., Suli, A. S., Annisa, H. N., & Nugroho, B. D. A. (2019). Leaf area index development of local rice varieties as a response to different irrigation management. *IOP Conference Series: Earth and Environmental Science*, *355*(1), 012006. https://doi.org/10.1088/1755-1315/355/1/012006

Mahmood, N., Ahmad, B., Hassan, S., & Bakhsh, K. (2012). Impact of temperature ADN precipitation on rice productivity in rice-wheat cropping system of Punjab province. *Journal of Animal and Plant Sciences*, *22*, 993–997.

Main-Knorn, M., Pflug, B., Louis, J., Debaecker, V., Müller-Wilm, U., & Gascon, F. (2017). Sen2Cor for Sentinel-2. *Image and Signal Processing for Remote Sensing XXIII*, *1042704*(May), 3. https://doi.org/10.1117/12.2278218

Mainuddin, M., Kirby, M., & Hoanh, C. T. (2012). Water productivity responses and adaptation to climate change in the lower Mekong basin. *Water International*, *37*(1), 53–74. https://doi.org/10.1080/02508060.2012.645192

Maki, M., & Homma, K. (2014). Empirical regression models for estimating multiyear leaf area index of rice from several vegetation indices at the field scale. *Remote Sensing*, *6*(6), 4764–4779. https://doi.org/10.3390/rs6064764

Maki, M., Sekiguchi, K., Homma, K., Hirooka, Y., & Oki, K. (2017). Estimation of rice yield by SIMRIW-RS, a model that integrates remote sensing data into a crop growth model. *Journal of Agricultural Meteorology*, *73*(1), 2–8. https://doi.org/10.2480/agrmet.D-14-00023

Malhi, Y., Franklin, J., Seddon, N., Solan, M., Turner, M. G., Field, C. B., & Knowlton, N. (2020). Climate change and ecosystems: Threats, opportunities and solutions. *Philosophical Transactions of the Royal Society B*, *375*(1794), 20190104. https://doi.org/10.1098/rstb.2019.0104

Mandal, D., Kumar, V., Ratha, D., Lopez-Sanchez, J. M., Bhattacharya, A., McNairn, H., Rao, Y. S., & Ramana, K. V. (2020). Assessment of rice growth conditions in a semi-arid region of India using the Generalized Radar Vegetation Index derived from RADARSAT-2 polarimetric SAR data. *Remote Sensing of Environment*, *237*(November 2019), 111561. https://doi.org/10.1016/j.rse.2019.111561

Marghany, M. (2020). Principles of synthetic aperture radar. *Advanced Remote Sensing Technology for Tsunami Modelling and Forecasting*, 223–239. https://doi.org/10.1201/9781351175548-18

Marshall, M., & Thenkabail, P. (2015). Developing in situ non-destructive estimates of crop biomass to address issues of scale in remote sensing. *Remote Sensing*, *7*(1), 808–835. https://doi.org/10.3390/rs70100808

Masud, M. M., Azam, M. N., Mohiuddin, M., Banna, H., Akhtar, R., Alam, A. S. A. F., & Begum, H. (2017). Adaptation barriers and strategies towards climate change: Challenges in the agricultural sector. *Journal of Cleaner Production*, *156*, 698–706. https://doi.org/10.1016/j.jclepro.2017.04.060

Mathur, M. (2015). Spatial autocorrelation analysis in plant population: An overview. *Journal of Applied and Natural Science*, *7*(1), 501–513. https://doi.org/10.31018/jans.v7i1.639

Mc Nairn, H., & Brisco, B. (2004). The application of C-band polarimetric SAR for agriculture: A review. *Canadian Journal of Remote Sensing*, *30*(3), 525–542. https://doi.org/10.5589/m03-069

Mills, T. C. (2011). *The foundations of modern time series analysis*. Springer.

Minh, H. V. T., Avtar, R., Mohan, G., Misra, P., & Kurasaki, M. (2019). Monitoring and mapping of rice cropping pattern in flooding area in the Vietnamese Mekong delta using Sentinel-1A data: A case of an Giang province. *ISPRS International Journal of Geo-Information*, *8*(5), 211.

https://doi.org/10.3390/ijgi8050211

Ministry of Agriculture and Cooperatives. (2014). *Manual of agricultural zoning*. http://www.oic.go.th/FILEWEB/CABINFOCENTER3/DRAWER073/GENERAL/DATA0000/00000109.PDF

Misra, G., Cawkwell, F., & Wingler, A. (2020). Status of phenological research using Sentinel-2 data: A review. *Remote Sensing*, *12*(17), 2760.

Moldenhauer, K. E. W. C., & Slaton, N. (2001). Rice growth and development. *Rice Production Handbook*, *192*, 7–14.

Molle, F., Chompadist, C., & Bremard, T. (2021). Intensification of rice cultivation in the floodplain of the Chao Phraya delta. *Southeast Asian Studies*, *10*(1), 141–168. https://doi.org/10.20495/seas.10.1_141

Monaco, F., Sali, G., Hassen, M. Ben, Facchi, A., Romani, M., & Valè, G. (2016). Water management options for rice cultivation in a temperate area: A multi-objective model to explore economic and water saving results. *Water (Switzerland)*, *8*(8), 336. https://doi.org/10.3390/w8080336

Mondal, S., Jeganathan, C., Sinha, N. K., Rajan, H., Roy, T., & Kumar, P. (2014). Extracting seasonal cropping patterns using multi-temporal vegetation indices from IRS LISS-III data in Muzaffarpur District of Bihar, India. *Egyptian Journal of Remote Sensing and Space Science*, *17*(2), 123–134. https://doi.org/10.1016/j.ejrs.2014.09.002

Moormann, F. R., & Breemen, N. V. (1978). Rice: soil, water, land. In *Los Banos*. IRRI.

Moradpour, S., Amiri, E., Delkhosh, B., Mobaser, H. R., & Haghverdiyan, M. (2011). Effect of planting date and plant density on yield and yield components of rice. *Ecology, Environment and Conservation*, *17*(2), 251–256.

Morecroft, M. D., Duffield, S., Harley, M., Pearce-Higgins, J. W., Stevens, N., Watts, O., & Whitaker, J. (2019). Measuring the success of climate change adaptation and mitigation in terrestrial ecosystems. *Science*, *366*(6471), eaaw9256. https://doi.org/10.1126/science.aaw9256

Mosleh, M. K., & Hassan, Q. K. (2014). Development of a remote sensing-based “Boro” rice mapping system. In *Remote Sensing* (Vol. 6, Issue 3, pp. 1938–1953). https://doi.org/10.3390/rs6031938

Mosleh, M. K., Hassan, Q. K., & Chowdhury, E. H. (2016). Development of a remote sensing-based rice yield forecasting model. *Spanish Journal of Agricultural Research*, *14*(3), e0907. https://doi.org/10.5424/sjar/2016143-8347

Moulin, S., Bondeau, A., & Delecolle, R. (1998). Combining agricultural crop models and satellite observations: From field to regional scales. *International Journal of Remote Sensing*, *19*(6), 1021–1036. https://doi.org/10.1080/014311698215586

Mullan, D., Matthews, T., Vandaele, K., Barr, I. D., Swindles, G. T., Meneely, J., ... & Murphy, C. (2019). Climate impacts on soil erosion and muddy flooding at 1.5 versus 2°C warming. *Land Degradation & Development*, *30*(1), 94–108.

Murgai, R., Ali, M., & Byerlee, D. (2001). Productivity growth and sustainability in post-Green Revolution agriculture: the case of the Indian and Pakistan Punjabs. *The World Bank Research Observer*, *16*(2), 199–218. https://doi.org/10.1093/wbro/16.2.199

Mutert, E., & Fairhurst, T. H. (2002). Developments in rice production in Southeast Asia. *Better Crops International*, *15*, 12–17.

Myhre, G., Alterskjær, K., Stjern, C. W., Hodnebrog, Marelle, L., Samset, B. H., Sillmann, J., Schaller, N., Fischer, E., Schulz, M., & Stohl, A. (2019). Frequency of extreme precipitation increases extensively with event rareness under global warming. In *Scientific Reports* (Vol. 9, Issue 1). https://doi.org/10.1038/s41598-019-52277-4

Nagai, T., & Makino, A. (2009). Differences between rice and wheat in temperature responses of photosynthesis and plant growth. *Plant and Cell Physiology*, *50*(4), 744–755. https://doi.org/10.1093/pcp/pcp029

Nawata, E., Nagata, Y., Sasaki, A., IWAMA, K., & SAKURATANI, T. (2005). Mapping of climatic data in Northeast Thailand: Rainfall. *Tropics*, *14*(2), 191–201. https://doi.org/10.3759/tropics.14.191

Naylor, R. L., Battisti, D. S., Vimont, D. J., Falcon, W. P., & Burke, M. B. (2007). Assessing risks of climate variability and climate change for Indonesian rice agriculture. *Proceedings of the National Academy of Sciences of the United States of America*, *104*(19), 7752–7757. https://doi.org/10.1073/pnas.0701825104

Ndikumana, E., Minh, D. H. T., Nguyen, H. T. D., Baghdadi, N., Courault, D., Hossard, L., & Moussawi, I. El. (2018). Estimation of rice height and biomass using multitemporal SAR Sentinel-1 for Camargue, Southern France. *Remote Sensing*, *10*(9), 0–18.

https://doi.org/10.3390/rs10091394

Nelson, A., Setiyono, T., Rala, A., Quicho, E., Raviz, J., Abonete, P., ... & Thongbai, P. (2014). Towards an operational SAR-based rice monitoring system in Asia: Examples from 13 demonstration sites across Asia in the RIICE project. *Remote Sensing*, *6*(11), 10773–10812. https://doi.org/10.3390/rs61110773

Ngoen-Klan, R., Deelee, R., & Amornsak, W. (2019). Preliminary survey of the brown planthopper, Nilaparvata lugens (Stål) (Hemiptera: Delphacidae) on different varieties of rice and its natural enemies in Central Thailand. *Agriculture and Natural Resources*, *53*(4), 410–422. https://doi.org/10.34044/j.anres.2019.53.4.12

Nguy-Robertson, A. L., Peng, Y., Gitelson, A. A., Arkebauer, T. J., Pimstein, A., Herrmann, I., Karnieli, A., Rundquist, D. C., & Bonfil, D. J. (2014). Estimating green LAI in four crops: Potential of determining optimal spectral bands for a universal algorithm. *Agricultural and Forest Meteorology*, *192*, 140–148. https://doi.org/10.1016/j.agrformet.2014.03.004

Nguyen, T. T. H., De Bie, C. A. J. M., Ali, A., Smaling, E. M. A., & Chu, T. H. (2012). Mapping the irrigated rice cropping patterns of the Mekong delta, Vietnam, through hyper-temporal spot NDVI image analysis. *International Journal of Remote Sensing*, *33*(2), 415–434. https://doi.org/10.1080/01431161.2010.532826

Nguyen, L. D., Phung, H. P., Huth, J., & Phung, C. Van. (2012). Estimation of the rice yield in the Mekong Delta using dual polarisation TerraSAR-X data. *VNU Journal of Science: Earth and Environmental Sciences*, *28*(1).

Nicknejad, Y., Zarghami, R., Nasiri, M., Pirdashti, H., Tari, D. B., & Fallah, H. (2009). Investigation of physiological indices of different rice (Oryza sativa L.) varieties in relation to source and sink limitation. In *Asian Journal of Plant Sciences* (Vol. 8, Issue 5, pp. 385–389). https://doi.org/10.3923/ajps.2009.385.389

Nikolaou, G., Neocleous, D., Christou, A., Kitta, E., & Katsoulas, N. (2020). Implementing sustainable irrigation in water-scarce regions under the impact of climate change. *Agronomy*, *10*(8), 1120.

Niles, M. T., Lubell, M., & Brown, M. (2015). How limiting factors drive agricultural adaptation to climate change. *Agriculture, Ecosystems and Environment*, *200*, 178–185. https://doi.org/10.1016/j.agee.2014.11.010

Nishad, A., Mishra, A. N., Chaudhari, R., Aryan, R. K., & Katiyar, P. (2018). Effect of temperature on

growth and yield of rice (Oryza sativa L.) cultivars. *IJCS*, *6*(5), 1381–1383.

Nonvide, G. M. A. (2017). Effect of Adoption of Irrigation on Rice Yield in the Municipality of Malanville, Benin. In *African Development Review* (Vol. 29, pp. 109–120). https://doi.org/10.1111/1467-8268.12266

Norman, J. M., & Jarvis, P. G. (1974). Photosynthesis in Sitka spruce (Picea sitchensis (Bong.) Carr.) III. Measurements of canopy structure and interception of radiation. *Journal of Applied Ecology*, 375–398. https://doi.org/10.2307/2402028

Noureldin, N. A., Aboelghar, M. A., Saudy, H. S., & Ali, A. M. (2013). Rice yield forecasting models using satellite imagery in Egypt. *Egyptian Journal of Remote Sensing and Space Science*, *16*(1), 125–131. https://doi.org/10.1016/j.ejrs.2013.04.005

Nuarsa, I. I. W., Si, M., & Nuarsa, I. W. (2011). Relationship between rice spectral and rice yield ssing Modis data. *Journal of Agricultural Science*, *3*. https://doi.org/10.5539/jas.v3n2p80

Nuarsa, I. W., Nishio, F., & Hongo, C. (2011). Rice yield estimation using Landsat ETM+ data and field observation. *Journal of Agricultural Science*, *4*(3), 45. https://doi.org/10.5539/jas.v4n3p45

Nuarsa, I. W., Nishio, F., Nishio, F., Hongo, C., & Hongo, C. (2011). Relationship between rice spectral and rice yield using Modis data. *Journal of Agricultural Science*, *3*(2), 80. https://doi.org/10.5539/jas.v3n2p80

Nwite, J., Essien, B., Keke, C., Igwe, C., & Wakatsuki, T. (2016). Effect of different land preparation methods for sawah system development on soil productivity improvement and rice grain yield in inland valleys of southeastern Nigeria. *Advances in Research*, *6*(2), 1–17. https://doi.org/10.9734/air/2016/20792

OAE. (2014a). *Agricultural information*.

OAE. (2014b). Agricultural statistics of Thailand 2014. In *OAE*.

OAE. (2014c). *Definition: Agricultural statistic data*.

OAE. (2017a). *Agricultural Statistics of Thailand 2017*. http://www.oae.go.th/assets/portals/1/files/yearbook60.pdf

OAE. (2017b). *Major rice: Cultivated areas, harvested areas, production, and yield between 2014-2016*. http://aginfo.oae.go.th/ewtnews/majorrice.html

OAE. (2018a). *Irrigation for wet season rice in 2018*.

OAE. (2018b). *Rice exports 2018*. http://impexp.oae.go.th/service/export.php?S_YEAR=2561&E_YEAR=2561&PRODUCT_GROUP=5250&wf_search=&WF_SEARCH=Y

OAE. (2018c). *Wet season rice seperated with irrigation system*. https://www.oae.go.th/assets/portals/1/fileups/prcaidata/files/Irrigation61.pdf

OAE. (2020a). *Agricultural commodity 2020*.

OAE. (2020b). *Thailand foreign agricultural trade statistic 2020*.

Ohe, M., Okita, N., & Daimon, H. (2010). Effects of deep-flooding irrigation on growth, canopy structure and panicle weight yield under different planting patterns in rice. *Plant Production Science*, *13*(2), 193–198. https://doi.org/10.1626/pps.13.193

Okamura, M., Arai-Sanoh, Y., Yoshida, H., Mukouyama, T., Adachi, S., Yabe, S., Nakagawa, H., Tsutsumi, K., Taniguchi, Y., Kobayashi, N., & Kondo, M. (2018). Characterization of high-yielding rice cultivars with different grain-filling properties to clarify limiting factors for improving grain yield. *Field Crops Research*, *219*, 139–147. https://doi.org/10.1016/j.fcr.2018.01.035

Oladele, S. O., Adeyemo, A. J., & Awodun, M. A. (2019). Influence of rice husk biochar and inorganic fertilizer on soil nutrients availability and rain-fed rice yield in two contrasting soils. *Geoderma*, *336*, 1–11.

Olioso, A., Ollivier, C., Martin, N., Simioni, G., Guillevic, P. C., Marloie, O., Carriere, S., Davi, H., Olioso, A., Ollivier, C., Martin, N., Simioni, G., Weiss, M., Olioso, A., Ollivier, C., N, M. S., Simioni, G., Weiss, M., Marloie, O., … Huard, F. (2019). Monitoring vegetation fraction cover of French Mediterranean forests for evapotranspiration and water stress mapping. *ESA Living Planet Symposium*.

Oyoshi, K., Tomiyama, N., Okumura, T., & Sobue, S. (2013). Asia Rice Crop Estimation and Monitoring (Asia-RiCE) for GEOGLAM. *AGU Fall Meeting Abstracts*.

Ozdogan, M., Yang, Y., Allez, G., & Cervantes, C. (2010). Remote sensing of irrigated agriculture: Opportunities and challenges. *Remote Sensing*, *2*(9), 2274–2304. https://doi.org/10.3390/rs2092274

Padilla, F. L. M., Maas, S. J., González-Dugo, M. P., Mansilla, F., Rajan, N., Gavilán, P., & Domínguez, J. (2012). Monitoring regional wheat yield in Southern Spain using the GRAMI model and satellite imagery. *Field Crops Research*, *130*, 145–154.

Pan, Y., Li, L., Zhang, J., Liang, S., Zhu, X., & Sulla-Menashe, D. (2012). Winter wheat area estimation from MODIS-EVI time series data using the Crop Proportion Phenology Index. *Remote Sensing of Environment*, *119*, 232–242. https://doi.org/10.1016/j.rse.2011.10.011

Pan, Z., Huang, J., Zhou, Q., Wang, L., Cheng, Y., Zhang, H., ... & Liu, J. (2015). Mapping crop phenology using NDVI time-series derived from HJ-1 A/B data. *International Journal of Applied Earth Observation and Geoinformation*, *34*, 188–197.

Pan, L., Xia, H., Yang, J., Niu, W., Wang, R., Song, H., Guo, Y., & Qin, Y. (2021). Mapping cropping intensity in Huaihe basin using phenology algorithm, all Sentinel-2 and Landsat images in Google Earth Engine. *International Journal of Applied Earth Observation and Geoinformation*, *102*, 102376. https://doi.org/10.1016/j.jag.2021.102376

Panda, S. S., Ames, D. P., & Panigrahi, S. (2010). Application of vegetation indices for agricultural crop yield prediction using neural network techniques. *Remote Sensing*, *2*(3), 673–696. https://doi.org/10.3390/rs2030673

Pandey, S., Byerlee, D., Dawe, D., Dobermann, A., Mohanty, S., Rozelle, S., & Hardy, B. (2010). Rice in the global economy. In I. R. R. Institute (Ed.), *Journal of Gender, Agriculture and Food Security*.

Pandey, S. (2002). *Direct seeding: Research strategies and opportunities.* (Int. Rice Res. Inst.. (ed.)).

Park, S., Im, J., Park, S., Yoo, C., Han, H., & Rhee, J. (2018). Classification and mapping of paddy rice by combining Landsat and SAR time series data. *Remote Sensing*, *10*(3), 447. https://doi.org/10.3390/rs10030447

Patel, N. R., Chopra, P., & Dadhwal, V. K. (2007). Analyzing spatial patterns of meteorological drought using standardized precipitation index. *Meteorological Applications: A Journal of Forecasting, Practical Applications, Training Techniques and Modelling*, *14*(4), 329–336. https://doi.org/10.1002/met

Paul, G. C., Saha, S., & Hembram, T. K. (2020). Application of phenology-based algorithm and linear regression model for estimating rice cultivated areas and yield using remote sensing data in Bansloi River Basin, Eastern India. *Remote Sensing Applications: Society and*

Environment, *19*, 100367.

Pazhanivelan, S., Kannan, P., Christy Nirmala Mary, P., Subramanian, E., Jeyaraman, S., Nelson, A., Setiyono, T., Holecz, F., Barbieri, M., & Yadav, M. (2015). Rice crop monitoring and yield estimation through COSMO Skymed and TerraSAR-X: A SAR-based experience in India. *International Archives of the Photogrammetry, Remote Sensing and Spatial Information Sciences*, *40*(7), 85–92. https://doi.org/10.5194/isprsarchives-XL-7-W3-85-2015

Peng, S., Tang, Q., & Zou, Y. (2009). Current status and challenges of rice production in China. *Plant Production Science*, *12*(1), 3–8. https://doi.org/10.1626/pps.12.3

Peng, D., Huang, J., Li, C., Liu, L., Huang, W., Wang, F., & Yang, X. (2014). Modelling paddy rice yield using MODIS data. *Agricultural and Forest Meteorology*, *184*, 107–116. https://doi.org/10.1016/j.agrformet.2013.09.006

Peng, D., Huete, A. R., Huang, J., Wang, F., & Sun, H. (2011). Detection and estimation of mixed paddy rice cropping patterns with MODIS data. *International Journal of Applied Earth Observation and Geoinformation*, *13*(1), 13–23. https://doi.org/10.1016/j.jag.2010.06.001

Peng, S., Huang, J., Sheehy, J. E., Laza, R. C., Visperas, R. M., Zhong, X., Centeno, G. S., Khush, G. S., & Cassman, K. G. (2004). Rice yields decline with higher night temperature from global warming. *Proceedings of the National Academy of Sciences*, *101*(27), 9971–9975. https://doi.org/10.1073/pnas.0403720101

Peng, X., Han, W., Ao, J., & Wang, Y. (2021). Assimilation of lai derived from UAV multispectral data into the safy model to estimate maize yield. *Remote Sensing*, *13*(6), 1–17. https://doi.org/10.3390/rs13061094

Peters, A. J., Walter-Shea, E. A., Ji, L., Viña, A., Hayes, M., & Svoboda, M. D. (2002). Drought monitoring with NDVI-based standardized vegetation index. *Photogrammetric Engineering and Remote Sensing*, *68*(1), 71–75.

Phan, A. T. T., Rikimaru, A., Higuchi, Y., & Takahashi, K. (2017). Fundamental study for estimating rice-plant stem number using laser scanner measurements. *Journal of Applied Remote Sensing*, *11*(3), 036012. https://doi.org/10.1117/1.jrs.11.036012

Phan, H., Toan, T. Le, & Bouvet, A. (2021). Understanding dense time series of sentinel-1 backscatter from rice fields: Case study in a province of the mekong delta, Vietnam. *Remote Sensing*, *13*(5), 1–23. https://doi.org/10.3390/rs13050921

Phan, T. H. (2018). *Rice monitoring using radar remote sensing*. Université Paul Sabatier-Toulouse III.

Phung, H.-P., Nguyen, L.-D., Thong, N.-H., Thuy, L.-T., & Apan, A. A. (2020). Monitoring rice growth status in the Mekong Delta, Vietnam using multitemporal Sentinel-1 data. *Journal of Applied Remote Sensing*, *14*(1), 014518. https://doi.org/10.1117/1.jrs.14.014518

Pichierri, M., Hajnsek, I., Zwieback, S., & Rabus, B. (2018). On the potential of Polarimetric SAR Interferometry to characterize the biomass, moisture and structure of agricultural crops at L-, C-and X-Bands. *Remote Sensing of Environment*, *204*, 596–616.

Pitchapa Jular. (2017). The 2011 Thailand Floods in The Lower Chao Phraya River Basin in Bangkok Metropolis The 2011 Thailand Floods in The Lower Chao Phraya River Basin in Bangkok Metropolis. *Global Water Partnership*.

Piyapakorn.p. (n.d.). *Soil in Thailand*.

Polthanee, A., & Promkhambut, A. (2014). Impact of climate change on rice-based cropping system and farmer's adaptation strategies in Northeast Thailand. *Asian Journal of Crop Science*, *6*(3), 262–272. https://doi.org/10.3923/ajcs.2014

Pourgholam-Amiji, M., Liaghat, A., Khoshravesh, M., & Azamathulla, H. M. (2021). Improving rice water productivity using alternative irrigation (case study: North of Iran). *Water Science and Technology: Water Supply*, *21*(3), 1216–1227. https://doi.org/10.2166/ws.2020.371

Pradhan, S. (2001). Crop area estimation using GIS, remote sensing and area frame sampling. *International Journal of Applied Earth Observation and Geoinformation*, *3*(1), 86–92. https://doi.org/10.1016/S0303-2434(01)85025-X

Preston, B. L., Suppiah, R., Macadam, I., & Bathols, J. (2006). *Climate change in the Asia / Pacific region A consultancy report prepared for the climate change and development roundtable*.

Pushpavesa, S., Somrith, B., & Petpisit, V. (1986). Breeding for drought and submergence-prone rainfed lowland rice in Thailand. *Progress in Rainfed Lowland Rice.*, 167–175.

Qingquan, Y. (2002). The system of rice intensification and its sse with hybrid rice varieties in CHINA hybrid varieties for SRI. *Seedling*, *8*(12), 25–35.

Quero, G., Bonnecarrère, V., Fernández, S., Silva, P., Simondi, S., & Borsani, O. (2019). Light-use efficiency and energy partitioning in rice is cultivar dependent. *Photosynthesis Research*,

140(1), 51–63. https://doi.org/10.1007/s11120-018-0605-x

Quicho, E., Setiyono, T., Romuga, G. C., Maunahan, A., Garcia, C., Raviz, J., Rala, A., Holecz, F., Collivignarelli, F., & Gatti, L. (2015). *Monitoring rice crop yield using Sentinel-1A Sar data*.

Rahman, A., Khan, K., Y Krakauer, N., Roytman, L., & Kogan, F. (2012). Use of remote sensing data for estimation of Aman rice yield. *International Journal of Agriculture and Forestry*, *2*(1), 101–107. https://doi.org/10.5923/j.ijaf.20120201.16

Rahman, M. A., Kang, S. C., Nagabhatla, N., & Macnee, R. (2017). Impacts of temperature and rainfall variation on rice productivity in major ecosystems of Bangladesh. *Agriculture and Food Security*, *6*(1), 1–11. https://doi.org/10.1186/s40066-017-0089-5

Rajavel, M., Khare, P., Prasad, J. R., Singh, K. K., Puranik, H. V, & Das, G. K. (2018). *Development of Rice Yield Forecast in Mid-season Using Weather Indices based Agrometeorological Model in Chhattisgarh*. *44*(1).

Ramadhani, F., Pullanagari, R., Kereszturi, G., & Procter, J. (2020). Automatic mapping of rice growth stages using the integration of sentinel-2, mod13q1, and sentinel-1. *Remote Sensing*, *12*(21), 3613. https://doi.org/10.3390/rs12213613

Ramesh, K., Chandrasekaran, B., Balasubramanian, T. N., Bangarusamy, U., Sivasamy, R., & Sankaran, N. (2002). Chlorophyll dynamics in rice (Oryza sativa) before and after flowering based on SPAD (chlorophyll) meter monitoring and its relation with grain yield. *Journal of Agronomy and Crop Science*, *188*(2), 102–105. https://doi.org/10.1046/j.1439-037X.2002.00532.x

Rang, Z. W., Jagadish, S. V. K., Zhou, Q. M., Craufurd, P. Q., & Heuer, S. (2011). Effect of high temperature and water stress on pollen germination and spikelet fertility in rice. *Environmental and Experimental Botany*, *70*(1), 58–65. https://doi.org/10.1016/j.envexpbot.2010.08.009

Ranjan, A. K., & Parida, B. R. (2021). Predicting paddy yield at spatial scale using optical and Synthetic Aperture Radar (SAR) based satellite data in conjunction with field-based Crop Cutting Experiment (CCE) data. *International Journal of Remote Sensing*, *42*(6), 2046–2071.

Rann, V., Anusontpornperm, S., Thanachit, S., & Sreewongchai, T. (2016). Response of KDML105 and RD41 rice varieties grown on a Typic Natrustalf to granulated pig manure and chemical fertilizers. *Agriculture and Natural Resources*, *50*(2), 104–113. https://doi.org/10.1016/j.anres.2015.12.001

Rathnayaka, R. M. N. N., Iqbal, Y. B., & Rifnas, L. M. (2018). Influence of urea and nano-nitrogen fertilizers on the growth and yield of rice (Oryza sativa L .) cultivar ' Bg 250 .' *Influence of Urea and Nano-Nitrogen Fertilizers on the Growth and Yield of Rice (Oryza Sativa L.) Cultivar 'Bg 250,' 5*(2), 1–7.

Ray, D. K., Mueller, N. D., West, P. C., & Foley, J. A. (2013). Yield trends are insufficient to double global crop production by 2050. *PLoS ONE*, *8*(6), e66428. https://doi.org/10.1371/journal.pone.0066428

Redfern, S. K., Azzu, N., & Binamira, J. S. (2012). Rice in Southeast Asia: Facing risks and vulnerabilities to respond to climate change. *Build Resilience Adapt Change Agri Sector*, *23*(295), 1–14. http://www.fao.org/fileadmin/templates/agphome/documents/faooecd/oecd_proceedings.pdf#page=302

Rehmani, M. I. A., Ding, C., Li, G., Ata-Ul-Karim, S. T., Hadifa, A., Bashir, M. A., Hashem, M., Alamri, S., Al-Zubair, F., & Ding, Y. (2021). Vulnerability of rice production to temperature extremes during rice reproductive stage in Yangtze River Valley, China. *Journal of King Saud University - Science*, *33*(8), 101599. https://doi.org/10.1016/j.jksus.2021.101599

Remote Sensing Applications Consultants Ltd (RSAC). (2021). *Spectral signatures of water, vegetation and soil*. http://www.rsacl.co.uk/images/base2.jpg

Reser, J. P., & Swim, J. K. (2011). Adapting to and coping with the threat and impacts of climate change. *American Psychologist*, *66*(4), 277. https://doi.org/10.1037/a0023412

Rianto, D. F., Guntoro, D., & Santosa, E. (2019). Weed growth and lowland rice production as affected by planting patterns and rice varieties. *Journal of Tropical Crop Science*, *6*(01), 67–75. https://doi.org/10.29244/jtcs.6.01.67-75

Rice Department. (2016a). *Rice Categories in Different Rice Ecosystem*. Rice Knowledge Bank. https://www.ricethailand.go.th/rkb3/title-index.php-file=content.php&id=1.htm

Rice Department. (2016b). *Rice Knowledge Bank*. https://webold.ricethailand.go.th/rkb3/Varieties.htm

Rice Department. (2017). *Rice knowledge bank*. www.ricethailand.go.th/Rkb/varieties

Richards, J. A. (2013). *Remote sensing digital image analysis: An introduction* (Fifth Edit). Springer Heidelberg New York Dordrecht London. https://doi.org/10.1007/978-3-642-30062-2

RID. (2013). *No Title*. http://www.rid.go.th/2009/_data/docs/56/Conclusion55.pdf

Robert A. Schowengerdt. (2007). Spectral transforms. In R. A. Schowengerdt (Ed.), *Remote Sensing* (Third edit, pp. 183–228). Academic Press. https://doi.org/doi.org/10.1016/B978-012369407-2/50008-5

Roberts, L. (2011). Population is growing —fast ... *Science*, *333*(6042), 540–543.

Rockström, J., Karlberg, L., Wani, S. P., Barron, J., Hatibu, N., Oweis, T., Bruggeman, A., Farahani, J., & Qiang, Z. (2010). Managing water in rainfed agriculture-the need for a paradigm shift. *Agricultural Water Management*, *97*(4), 543–550. https://doi.org/10.1016/j.agwat.2009.09.009

Rosentrater, K. A., & Evers, A. D. (2017). Kent's technology of cereals: An introduction for students of food science and agriculture. In A. D. E. Kurt A. Rosentrater (Ed.), *Woodhead Publishing* (Fifth edit). Woodhead Publishing.

Rotairo, L., Durante, A. C., Lapitan, P., & Rao, L. N. (2019). *Use of remote sensing to estimate paddy area and production: A handbook*. https://www.adb.org/publications/remote-sensing-paddy-area-production-handbook

Rouse, J. W., Haas, R. H., Schell, J. A., Deering, D. W., & Harlan, J. C. (1973). *Monitoring the vernal advancement and retrogradation (green wave effect) of natural vegetation*. https://ntrs.nasa.gov/search.jsp?R=19750020419

Rouse Jr, J., Haas, R. H., Schell, J. A., & Deering, D. W. (1974). Monitoring vegetation systems in the great plains with ERTS. *Third Earth Resources Technology Satellite (ERTS) Symposium*, 309–317. https://doi.org/citeulike-article-id:12009708

Roy, K. S., Bhattacharyya, P., Neogi, S., Rao, K. S., & Adhya, T. K. (2012). Combined effect of elevated CO2 and temperature on dry matter production, net assimilation rate, C and N allocations in tropical rice (Oryza sativa L.). *Field Crops Research*, *139*, 71–79.

Royal Irrigation Department. (2007). *Report of irrigation project information*. https://www.rid.go.th/main/_data/docs/stat50.pdf

S. Lek, Y. S. P. (2008). Artificial neural networks. In B. D. F. Sven Erik Jørgensen (Ed.), *Encyclopedia of Ecology*. Academic Press.

Sabaruddin, Z., Toshiaki, M., Shingo, T., & Youji, N. (2002). Effect of high temperature at ripening

stage on the reserve accumulation in seed in some rice cultivars. *Plant Production Science*, *5*(2), 160–168. https://doi.org/10.1626/pps.5.160

Sakamoto, T., Yokozawa, M., Toritani, H., Shibayama, M., Ishitsuka, N., & Ohno, H. (2005). A crop phenology detection method using time-series MODIS data. *Remote Sensing of Environment*, *96*(3–4), 366–374. https://doi.org/10.1016/j.rse.2005.03.008

Salassi, M. E., Deliberto, M. A., Linscombe, S. D., Wilson, C. E., Walker, T. W., McCauley, G. N., & Blouin, D. C. (2013). Impact of harvest lodging on rough rice milling yield and market price. In *Agronomy Journal* (Vol. 105, Issue 6, pp. 1860–1867). https://doi.org/10.2134/agronj2013.0238

Samanta, S., Banerjee, S., Mukherjee, A., Patra, P. K., & Chakraborty, P. (2019). Deriving PAR use efficiency of wet season rice from bright sunshine hour data and canopy characteristics. *Mausam*, *70*(2), 347–356.

Sanchez, P. A. (2019). Soil management in rice cultivation. In *Properties and Management of Soils in the Tropics*. Cambridge University Press. https://doi.org/10.1017/9781316809785.019

Santos, M. P. dos, Zanon Junior, A., Cuadra, S. V., Steinmetz, S., Castro, J. R. de, & Heinemann, A. B. (2017). Yield and morphophysiological indices of irrigated rice genotypes in contrasting ecosystems. *Pesquisa Agropecuária Tropical*, *47*, 253–264. https://doi.org/10.1590/1983-40632016v4745955

Sarker, M. A. R., Alam, K., & Gow, J. (2012). Exploring the relationship between climate change and rice yield in Bangladesh: An analysis of time series data. *Agricultural Systems*, *112*, 11–16. https://doi.org/10.1016/j.agsy.2012.06.004

Saseendran, S. A., Singh, K. K., Rathore, L. S., Rao, G. S. L. H. V. P., Mendiratta, N., Lakshmi Narayan, K., & Singh, S. V. (1998). Evaluation of the CERES-Rice version 3.0 model for the climate conditions of the state of Kerala, India. *Meteorological Applications*, *5*(4), 385–392. https://doi.org/10.1017/S1350482798000954

Saseendran, S. A., Singh, K. K., Rathore, L. S., Singh, S. V., & Sinha, S. K. (2000). Effects of climate change on rice production in the tropical humid climate of Kerala, India. *Climatic Change*, *44*(4), 495–514. https://doi.org/10.1023/A:1005542414134

Sattar, A., Kumar, M., Vijayakumar, P., & Khan, S. A. (2017). Crop weather relation in kharif rice for North-west Alluvial Plain Zone of Bihar. *Journal of Agrometeorology*, *19*(1), 71–74.

Satyanarayana, A., Thiyagarajan, T. M., & Uphoff, N. (2007). Opportunities for water saving with higher yield from the system of rice intensification. *Irrigation Science*, *25*(2), 99–115. https://doi.org/10.1007/s00271-006-0038-8

Saud, S., Wang, D., Fahad, S., Alharby, H. F., Bamagoos, A. A., Mjrashi, A., Alabdallah, N. M., AlZahrani, S. S., AbdElgawad, H., Adnan, M., Sayyed, R. Z., Ali, S., & Hassan, S. (2022). Comprehensive Impacts of Climate Change on Rice Production and Adaptive Strategies in China. *Frontiers in Microbiology*, *13*(June), 1–12. https://doi.org/10.3389/fmicb.2022.926059

Schubert, A. (2019). *Guide to Sentinel-1 geocoding*.

Scrucca, L. (2005). Clustering multivariate spatial data based on local measures of spatial autocorrelation: an application to the labour market of Umbria. *Quaderni Del Dipartimento Di Economia, Finanza e …*, *20*(1), 11. http://www.ec.unipg.it/DEFS/uploads/spatcluster.pdf

Setiyono, T. D., Holecz, F., Khan, N. I., Barbieri, M., Quicho, E., Collivignarelli, F. & Romuga, G. C. (2017). Synthetic Aperture Radar (SAR)-based paddy rice monitoring system: Development and application in key rice producing areas in Tropical Asia. *IOP Conference Series: Earth and Environmental Science*, *54*(1), 012015. https://doi.org/10.1088/1755-1315/54/1/012015

Setiyono, T. D., Quicho, E. D., Holecz, F. H., Khan, N. I., Romuga, G., Maunahan, A., Garcia, C., Rala, A., Raviz, J., Collivignarelli, F., Gatti, L., Barbieri, M., Phuong, D. M., Minh, V. Q., Vo, Q. T., Intrman, A., Rakwatin, P., Sothy, M., Veasna, T., … Mabalay, M. R. O. (2019). Rice yield estimation using synthetic aperture radar (SAR) and the ORYZA crop growth model: development and application of the system in South and South-east Asian countries. *International Journal of Remote Sensing*, *40*(21), 8093–8124. https://doi.org/10.1080/01431161.2018.1547457

Setiyono, T., Quicho, E., Gatti, L., Campos-Taberner, M., Busetto, L., Collivignarelli, F., García-Haro, F., Boschetti, M., Khan, N., & Holecz, F. (2018). Spatial rice yield estimation based on MODIS and Sentinel-1 SAR data and ORYZA crop growth model. *Remote Sensing*, *10*(2), 293. https://doi.org/10.3390/rs10020293

Seyed Raoufi, R., Soufizadeh, S., Amiri Larijani, B., AghaAlikhani, M., & Kambouzia, J. (2018). Simulation of growth and yield of various irrigated rice (Oryza sativa L.) genotypes by AquaCrop under different seedling ages. *Natural Resource Modeling*, *31*(2), e12162. https://doi.org/10.1111/nrm.12162

Shah, F., Huang, J., Cui, K., & Nie, L. (2011). Impact of high-temperature stress on rice plant and its traits related to tolerance. *The Journal of Agricultural Science*, *149*(5), 545–556. https://doi.org/10.1017/S0021859611000360

Shalaby, A., & Tateishi, R. (2007). Remote sensing and GIS for mapping and monitoring land cover and land-use changes in the Northwestern coastal zone of Egypt. *Applied Geography*, *27*(1), 28–41. https://doi.org/10.1016/j.apgeog.2006.09.004

Shammi, S. A., & Meng, Q. (2021). Use time series NDVI and EVI to develop dynamic crop growth metrics for yield modeling. *Ecological Indicators*, *121*, 107124. https://doi.org/10.1016/j.ecolind.2020.107124

Shao, Y., Fan, X., Liu, H., Xiao, J., Ross, S., Brisco, B. & Staples, G. (2001). Rice monitoring and production estimation using multitemporal RADARSAT. *Remote Sensing of Environment*, *76*(3), 310–325. https://doi.org/10.1016/S0034-4257(00)00212-1

Sharma, B. R., Rao, K. V., Vittal, K. P. R., Ramakrishna, Y. S., & Amarasinghe, U. (2010). Estimating the potential of rainfed agriculture in India: Prospects for water productivity improvements. *Agricultural Water Management*, *97*(1), 23–30. https://doi.org/10.1016/j.agwat.2009.08.002

Sheehy, J. E., & Mitchell, P. L. (2015). Calculating maximum theoretical yield in rice. *Field Crops Research*, *182*, 68–75. https://doi.org/10.1016/j.fcr.2015.05.013

Shi, H., & Jiang, Z. (2016). The efficiency of composite weather index insurance in hedging rice yield risk: Evidence from China. *Agricultural Economics*, *47*(3), 319–328. https://doi.org/10.1111/agec.12232

Shihua, L., Jiangtao, X., Ping, N., Jing, Z., & Hongshu, W. (2014). Monitoring paddy rice phenology using time series modis data over Jiangxi province, China. *International Journal of Agricultural and Biological Engineering*, *7*(6), 28–36. https://doi.org/10.3965/j.ijabe.20140706.005

Shiu, Y. S., & Chuang, Y. C. (2019). Yield estimation of paddy rice based on satellite imagery: comparison of global and local regression models. *Remote Sensing*, *11*(2), 111. https://doi.org/10.3390/rs11020111

Shrestha, S., Asch, F., Dusserre, J., Ramanantsoanirina, A., & Brueck, H. (2012). Climate effects on yield components as affected by genotypic responses to variable environmental conditions in upland rice systems at different altitudes. *Field Crops Research*, *134*, 216–228. https://doi.org/10.1016/j.fcr.2012.06.011

Singh, P. K., Singh, K. K., Baxla, A. K., Kumar, B., Bhan, S. C., & Rathore, L. S. (2014). Crop yield prediction using CERES-Rice vs 4.5 model for the climate variability of different agroclimatic zone of south and north-west plane zone of Bihar (India). *Mausam*, *65*(4), 529–552.

Singh, V., & Qin, X. (2020). Study of rainfall variabilities in Southeast Asia using long-term gridded rainfall and its substantiation through global climate indices. *Journal of Hydrology*, *585*, 124320.

Singh, R. P., Roy, S., & Kogan, F. (2003). Vegetation and temperature condition indices from NOAA AVHRR data for drought monitoring over India. *International Journal of Remote Sensing*, *24*(22), 4393–4402. https://doi.org/10.1080/0143116031000084323

Sinha, S. K., & Talati, J. (2007). Productivity impacts of the system of rice intensification (SRI): A case study in West Bengal, India. *Agricultural Water Management*, *87*(1), 55–60. https://doi.org/10.1016/j.agwat.2006.06.009

Siopongco, J., Ingram, K., Pablico, P., & Moody, K. (1994). Crop and soil responses to post-emergence tillage and weed control in lowland rice. *Experimental Agriculture*, *30*(1), 95–103.

Sjöström, M., Ardö, J., Arneth, A., Boulain, N., Cappelaere, B., Eklundh, L., de Grandcourt, A., Kutsch, W. L., Merbold, L., Nouvellon, Y., Scholes, R. J., Schubert, P., Seaquist, J., & Veenendaal, E. M. (2011). Exploring the potential of MODIS EVI for modeling gross primary production across African ecosystems. *Remote Sensing of Environment*, *115*(4), 1081–1089. https://doi.org/10.1016/j.rse.2010.12.013

Slattery, R. A., VanLoocke, A., Bernacchi, C. J., Zhu, X. G., & Ort, D. R. (2017). Photosynthesis, light use efficiency, and yield of reduced-chlorophyll soybean mutants in field conditions. *Frontiers in Plant Science*, *8*, 549.

Sola, I., García-Martín, A., Sandonís-Pozo, L., Álvarez-Mozos, J., Pérez-Cabello, F., González-Audícana, M., & Llovería, R. M. (2018). Assessment of atmospheric correction methods for Sentinel-2 images in Mediterranean landscapes. *International Journal of Applied Earth Observation and Geoinformation*, *73*, 63–76.

Son, N. T., Chen, C. F., Chen, C. R., Duc, H. N., & Chang, L. Y. (2013). A phenology-based classification of time-series MODIS data for rice crop monitoring in Mekong Delta, Vietnam. *Remote Sensing*, *6*(1), 135–156. https://doi.org/10.3390/rs6010135

Son, N. T., Chen, C. F., Chen, C. R., Toscano, P., Cheng, Y. S., Guo, H. Y., & Syu, C. H. (2021). A phenological object-based approach for rice crop classification using time-series Sentinel-1

Synthetic Aperture Radar (SAR) data in Taiwan. *International Journal of Remote Sensing*, *42*(7), 2722–2739.

Son, N. T., Chen, C. F., Chen, C. R., & Chang, L. Y. (2013). Satellite-based investigation of flood-affected rice cultivation areas in Chao Phraya River Delta, Thailand. *ISPRS Journal of Photogrammetry and Remote Sensing*, *86*, 77–88. https://doi.org/10.1016/j.isprsjprs.2013.09.008

Son, N. T., Chen, C. F., Chen, C. R., Chang, L. Y., & Chiang, S. H. (2016). Rice yield estimation through assimilating satellite data into a crop simumlation model. *International Archives of the Photogrammetry, Remote Sensing and Spatial Information Sciences*, *8*. https://doi.org/10.5194/isprsarchives-XLI-B8-993-2016

Son, N. T., Chen, C. F., Chen, C. R., Chang, L. Y., Duc, H. N., & Nguyen, L. D. (2013). Prediction of rice crop yield using MODIS EVI-LAI data in the Mekong Delta, Vietnam. *International Journal of Remote Sensing*, *34*(20), 7275–7292. https://doi.org/10.1080/01431161.2013.818258

Son, N. T., Chen, C. F., Chen, C. R., Minh, V. Q., & Trung, N. H. (2014). A comparative analysis of multitemporal MODIS EVI and NDVI data for large-scale rice yield estimation. *Agricultural and Forest Meteorology*, *197*, 52–64. https://doi.org/10.1016/j.agrformet.2014.06.007

Son, N. T., Chen, C. F., & Cru, C. R. (2012). Mapping major cropping patterns in Southeast Asia From Modis data using wavelet transform and artificial neural networks. *ISPRS - International Archives of the Photogrammetry, Remote Sensing and Spatial Information Sciences*, *39-B3*. https://doi.org/10.5194/isprsarchives-XXXIX-B3-421-2012

Soria-Ruiz, J., Fernandez-Ordonez, Y., McNairm, H., & Bugden-Storie, J. (2007). Corn monitoring and crop yield using optical and RADARSAT-2 images. *International Geoscience and Remote Sensing Symposium (IGARSS)*, *January 2016*, 3655–3658. https://doi.org/10.1109/IGARSS.2007.4423638

Steele-Dunne, S. C., McNairn, H., Monsivais-Huertero, A., Judge, J., Liu, P. W., & Papathanassiou, K. (2017). Radar Remote Sensing of Agricultural Canopies: A Review. *IEEE Journal of Selected Topics in Applied Earth Observations and Remote Sensing*, *10*(5), 2249–2273. https://doi.org/10.1109/JSTARS.2016.2639043

Stroppiana, D., Boschetti, M., Azar, R., Barbieri, M., Collivignarelli, F., Gatti, L., Fontanelli, G., Busetto, L., & Holecz, F. (2019). In-season early mapping of rice area and flooding dynamics from optical and SAR satellite data. *European Journal of Remote Sensing*, *52*(1), 206–220.

https://doi.org/10.1080/22797254.2019.1581583

Stroppiana, Daniela, Boschetti, M., Confalonieri, R., Bocchi, S., & Brivio, P. A. (2006). Evaluation of LAI-2000 for leaf area index monitoring in paddy rice. *Field Crops Research*, *99*(2–3), 167–170. https://doi.org/10.1016/j.fcr.2006.04.002

Stuecker, M. F., Tigchelaar, M., & Kantar, M. B. (2018). Climate variability impacts on rice production in the Philippines. *PLoS ONE*, *13*(8), e0201426. https://doi.org/10.1371/journal.pone.0201426

Sudarmanian, N. S., & Pazhanivelan, S. (2019). Detection of SAR signature for rice crop using SENTINEL 1A data. *Bull. Env. Pharmacol. Life Sci*, *8*(June), 32–39.

Sujariya, S., Jongrungklang, N., Jongdee, B., Inthavong, T., Budhaboon, C., & Fukai, S. (2020). Rainfall variability and its effects on growing period and grain yield for rainfed lowland rice under transplanting system in Northeast Thailand. *Plant Production Science*, *23*(1), 48–59. https://doi.org/10.1080/1343943X.2019.1698970

Sun, T., Fang, H., Liu, W., & Ye, Y. (2017). Impact of water background on canopy reflectance anisotropy of a paddy rice field from multi-angle measurements. *Agricultural and Forest Meteorology*, *233*, 143–152. https://doi.org/10.1016/j.agrformet.2016.11.010

Suwanmontri, P., Kamoshita, A., & Fukai, S. (2021). Recent changes in rice production in rainfedlowland and irrigated ecosystems in Thailand. *Plant Production Science*, *24*(1), 15–28.

Suwanmontri, P., Kamoshita, A., & Fukai, S. (2020). Recent changes in rice production in rainfed lowland and irrigated ecosystems in Thailand. *Plant Production Science*, *24*(1), 15–28. https://doi.org/10.1080/1343943X.2020.1787182

Takai, T., Matsuura, S., Nishio, T., Ohsumi, A., Shiraiwa, T., & Horie, T. (2006). Rice yield potential is closely related to crop growth rate during late reproductive period. *Field Crops Research*, *96*(2–3), 328–335. https://doi.org/10.1016/j.fcr.2005.08.001

Tang, L., Zhu, Y., Hannaway, D., Meng, Y., Liu, L., Chen, L., & Cao, W. (2009). RiceGrow: A rice growth and productivity model. *NJAS - Wageningen Journal of Life Sciences*, *57*(1), 83–92. https://doi.org/10.1016/j.njas.2009.12.003

Taniyama, S. (2002). Water resources and rice paddy cultivation in the Asian monsoon region. *International Review for Environmental Strategies*, *3*(2), 248–263. http://search.ebscohost.com/login.aspx?direct=true&AuthType=ip,shib&db=buh&AN=1531

7179&site=ehost-live

Tian, H., Wu, M., Wang, L., & Niu, Z. (2018). Mapping early, middle and late rice extent using Sentinel-1A and Landsat-8 data in the poyang lake plain, China. *Sensors*, *18*(1), 185. https://doi.org/10.3390/s18010185

Tilman, D. (1998). The greening of the green revolution. *Nature*, *396*(6708), 211–212.

Tingting, L., & Chuang, L. (2010). Study on extraction of crop information using time-series MODIS data in the Chao Phraya Basin of Thailand. *Advances in Space Research*, *45*(6), 775–784. https://doi.org/10.1016/j.asr.2009.11.013

Titapiwatanakun, B. (2012). *The rice situation in Thailand* (Issue January). http://www.adb.org/sites/default/files/project-document/73082/43430-012-reg-tacr-03.pdf

TMD. (2015). *The climate of Thailand*. https://www.tmd.go.th/en/archive/thailand_climate.pdf

Todaka, D., Shinozaki, K., & Yamaguchi-Shinozaki, K. (2015). Recent advances in the dissection of drought-stress regulatory networks and strategies for development of drought-tolerant transgenic rice plants. In *Frontiers in Plant Science* (Vol. 6, Issue FEB). https://doi.org/10.3389/fpls.2015.00084

Torbick, N., Salas, W. A., Hagen, S., & Xiao, X. (2011). Monitoring rice agriculture in the Sacramento Valley, USA With multitemporal PALSAR and MODIS imagery. *IEEE Journal of Selected Topics in Applied Earth Observations and Remote Sensing*, *4*(2), 451–457. https://doi.org/10.1109/JSTARS.2010.2091493

Tsiligirides, T. A. (1998). Remote sensing as a tool for agricultural statistics: a case study of area frame sampling methodology in Hellas. *Computers and Electronics in Agriculture*, *20*(1), 45–77. https://doi.org/10.1016/S0168-1699(98)00011-8

Tubaña, B., Harrell, D., Walker, T., Teboh, J., Lofton, J., Kanke, Y., & Phillips, S. (2011). Relationships of spectral vegetation indices with rice biomass and grain yield at different sensor view angles. *Agronomy Journal*, *103*(5), 1405–1413.

Tucker, C. J. (1979). Red and photographic infrared linear combinations for monitoring vegetation. *Remote Sensing of Environment*, *8*(2), 127–150.

United Nations. (2017). *World population projected to reach 9.8 billion in 2050 and 11.2 billion in 2100*.

Upboff, N. (2008). The system of rice intensification (Sri) as a system of agricultural innovation. *Jurnal Ilmu Tanah Dan Lingkungan*, *10*(1), 27–40. https://doi.org/10.29244/jitl.10.1.27-40

Uwe, M.-W., Jerome, L., Rudolf, R., Ferran, G., & Marc, N. (2013). Sentinel-2 level 2a prototype processor : Architecture , algorithms and first results. *Proceedings of the ESA Living Planet Symposium, Edinburgh, UK*, 9–13.

Uzzaman, T., Sikder, R. K., Asif, M. I., Mehraj, H., & Uddin, A. J. (2015). Growth and yield trial of sixteen rice varieties under System of Rice Intensification. *Scientia Agriculturae*, *11*(2), 81–89. https://doi.org/10.15192/pscp.sa.2015.11.2.8189

V, H., B, A., P, L. D., C, L. J., & A, L. (2021). Growing season weather impacts on rice phenology development in the central zone of Kerala. *Journal of Pharmacognosy and Phytochemistry*, *10*(1), 2406–2410. https://doi.org/10.22271/phyto.2021.v10.i1ah.13719

van der Meer, F. D., Bakker, W. H., Scholte, K., Skidmore, A. K., de Jong, S. M., Clevers, J. G. P. W., & Epema, G. F. (2000). Vegetation indices, above ground biomass estimates and the red edge from MERIS. *In ISPRS 2000 Congress: Geoinformation for All: Amsterdam, the Netherlands*, 1580–1587. https://www.isprs.org/publications/archives.aspx

van Oort, P. A. J., Balde, A., Diagne, M., Dingkuhn, M., Manneh, B., Muller, B., Sow, A., & Stuerz, S. (2016). Intensification of an irrigated rice system in Senegal: Crop rotations, climate risks, sowing dates and varietal adaptation options. *European Journal of Agronomy*, *80*, 168–181. https://doi.org/10.1016/j.eja.2016.06.012

Vedenov, D., & Sanchez, L. (2011). Weather Derivatives as Risk Management Tool in Ecuador : A Case Study of Rice Production. *Agricultural Economics Association*.

Vergara, B., & Chang, T. (1985). The flowering response of the rice plant to photoperiod: A review of the literature. In *International Rice Research Institute (IRRI)*. http://books.google.com/books?hl=en&lr=&id=TCtF5INb-f0C&oi=fnd&pg=PP2&dq=The+flowering+response+of+the+rice+plant+to+photoperiod,+a+review+of+the+literature&ots=xEPmkEXa37&sig=4e3dZ2p1D3hdi9c18qRZCZKB_lg

Vergara, B. S., & Chang, T. T. (1985). *The flowering response of the rice plant to photoperiod: A review of the literature*.

Vergara, B. S., Tanaka, A., Lilis, R., & Puranabhavung, S. (1966). Relationship between growth duration and grain yield of rice plants. *Soil Science and Plant Nutrition*, *12*(1), 31–39. https://doi.org/10.1080/00380768.1966.10431180

Verma, A. K., Nandan, R., & Verma, A. (2019). Knowledge based classifier based on backscattering coefficient for monitoring the crop growth analysis using multi-temporal images of space-borne synthetic aperture radar (SAR) sensors. *International Archives of the Photogrammetry, Remote Sensing and Spatial Information Sciences - ISPRS Archives*, *42*, 643–647. https://doi.org/10.5194/isprs-archives-XLII-3-W6-643-2019

Vermeer, M., & Rahmstorf, S. (2009). Global sea level linked to global temperature. *Proceedings of the National Academy of Sciences of the United States of America*, *106*(51), 21527–21532. https://doi.org/10.1073/pnas.0907765106

Verrelst, J., Rivera, J. P., Veroustraete, F., Muñoz-Marí, J., Clevers, J. G. P. W., Camps-Valls, G., & Moreno, J. (2015). Experimental Sentinel-2 LAI estimation using parametric, non-parametric and physical retrieval methods - A comparison. *ISPRS Journal of Photogrammetry and Remote Sensing*, *108*, 260–272. https://doi.org/10.1016/j.isprsjprs.2015.04.013

Vicari, M. B., Pisek, J., & Disney, M. (2019). New estimates of leaf angle distribution from terrestrial LiDAR: Comparison with measured and modelled estimates from nine broadleaf tree species. *Agricultural and Forest Meteorology*, *264*, 322–333.

Wali, E., Tasumi, M., & Moriyama, M. (2020). Combination of linear regression lines to understand the response of sentinel-1 dual polarization SAR data with crop phenology-case study in Miyazaki, Japan. In *Remote Sensing* (Vol. 12, Issue 1). https://doi.org/10.3390/rs12010189

Wang, F. M., Huang, J. F., Tang, Y. L., & Wang, X. Z. (2007). New vegetation index and its application in estimating leaf area index of rice. *Rice Science*, *14*(3), 195–203.

Wang, C., Wu, J., Zhang, Y., Pan, G., Qi, J., & Salas, W. A. (2009). Characterizing L-band scattering of paddy rice in southeast china with radiative transfer model and multitemporal ALOS/PALSAR imagery. *IEEE Transactions on Geoscience and Remote Sensing*, *47*(4), 988–998. https://doi.org/10.1109/TGRS.2008.2008309

Wang, D., Laza, M. R. C., Cassman, K. G., Huang, J., Nie, L., Ling, X., Centeno, G. S., Cui, K., Wang, F., Li, Y., & Peng, S. (2016). Temperature explains the yield difference of double-season rice between tropical and subtropical environments. *Field Crops Research*, *198*, 303–311. https://doi.org/10.1016/j.fcr.2016.05.008

Wang, F., Wang, F., Zhang, Y., Hu, J., Huang, J., & Xie, J. (2019). Rice yield estimation using parcel-level relative spectral variables from UAV-based hyperspectral imagery. *Frontiers in Plant Science*, *10*, 453. https://doi.org/10.3389/fpls.2019.00453

Wang, L., Chang, Q., Li, F., Yan, L., Huang, Y., Wang, Q., & Luo, L. (2019). Effects of growth stage development on paddy rice leaf area index prediction models. *Remote Sensing*, *11*(3), 361. https://doi.org/10.3390/rs11030361

Wang, L., Chang, Q., Yang, J., Zhang, X., & Li, F. (2018). Estimation of paddy rice leaf area index using machine learning methods based on hyperspectral data from multi-year experiments. In *PLoS ONE* (Vol. 13, Issue 12). https://doi.org/10.1371/journal.pone.0207624

Wang, W., Yu, Z., Zhang, W., Shao, Q., Zhang, Y., Luo, Y., Jiao, X., & Xu, J. (2014). Responses of rice yield, irrigation water requirement and water use efficiency to climate change in China: Historical simulation and future projections. *Agricultural Water Management*, *146*, 249–261. https://doi.org/10.1016/j.agwat.2014.08.019

Wang, Y., Xue, Y., & Li, J. (2005). Towards molecular breeding and improvement of rice in China. *Trends in Plant Science*, *10*(12), 610–614. https://doi.org/10.1016/j.tplants.2005.10.008

Wei, X., & Huang, X. (2019). Origin, taxonomy, and phylogenetics of rice. In Jinsong Bao (Ed.), *Rice* (4th ed.). AACC International Press. https://doi.org/https://doi.org/10.1016/B978-0-12-811508-4.00001-0

Weiss, J. (2009). *The economics of climate change in Southeast Asia: A regional review*. https://www.adb.org/sites/default/files/publication/29657/economics-climate-change-se-asia.pdf

Wen, Y. W. J., Ponnusamy, R. R., & Kang, H. M. (2019). Application of weather index-based insurance for paddy yield: The case of Malaysia. *International Journal of ADVANCED AND APPLIED SCIENCES*, *6*(6), 51–59. https://doi.org/10.21833/ijaas.2019.06.008

Weng, Q. (2011). *Advances in envionmental remote sensing-sensors, algorithms, and applications*. CRC Press Taylor & Francis Group.

Whaley, J. M., Sparkes, D. L., Foulkes, M. J., Spink, J. H., Semere, T., & Scott, R. K. (2000). The physiological response of winter wheat to reductions in plant density. *Annals of Applied Biology*, *137*(2), 165–177.

Wiboonpongse, A., & Chaovanapoonphol, Y. (2001). Rice marketing system in Thailand. *International Symposium Agribusiness Management towards Strengthening Agricultural Development on Trade: III Agribusiness Research on Marketing and Trade*, 295–305.

Wiegand, C. L., Richardson, A. J., Escobar, D. E., & Gerbermann, A. H. (1991). Vegetation indices in

crop assessments. *Remote Sensing of Environment*, *35*(2–3), 105–119. https://doi.org/10.1016/0034-4257(91)90004-P

Wigley, T. M., & Raper, S. C. B. (1987). Thermal expansion of sea water associated with global warming. *Nature*, *330*(6144), 127–131.

Williams, J. R., Jones, C. A., Kiniry, J. R., & Spanel, D. A. (1989). The EPIC crop growth model. *Transactions of the ASAE*, *32*(2), 497–511. https://doi.org/10.13031/2013.31032

Winterbottom, R., Reij, C., Garrity, D., Glover, J., Hellums, D., McGahuey, M., & Scherr, S. (2013). Improving land and water management. *World Resources Institute*. http://www.wri.org/sites/default/files/improving_land_and_water_management_0.pdf

Wiseman, G., McNairn, H., Homayouni, S., & Shang, J. (2014). RADARSAT-2 polarimetric SAR response to crop biomass for agricultural production monitoring. *IEEE Journal of Selected Topics in Applied Earth Observations and Remote Sensing*, *7*(11), 4461–4471.

Wu, J., Han, Z., Xu, Y., Zhou, B., & Gao, X. (2020). Changes in extreme climate events in China under 1.5 C–4 C global warming targets: Projections using an ensemble of regional climate model simulations. *Journal of Geophysical Research: Atmospheres*, *125*(2), e2019JD031057.

Wu, X., Washaya, P., Liu, L., Li, K., Shao, Y., Meng, L., & Hu, B. (2020). Rice yield estimation based on spaceborne SAR: A review from 1988 to 2018. *IEEE Access*, *8*, 157462–157469. https://doi.org/10.1109/ACCESS.2020.3020182

Xiao, W., Xu, S., & He, T. (2021). Mapping paddy rice with Sentinel-1/2 and phenology-, object-based algorithm—A implementation in Hangjiahu plain in China using GEE platform. *Remote Sensing*, *13*(5), 990.

Xiao, X., Boles, S., Frolking, S., Salas, W., Moore, I., Li, C., He, L., & Zhao, R. (2002). Observation of flooding and rice transplanting of paddy rice fields at the site to landscape scales in China using VEGETATION sensor data. *International Journal of Remote Sensing*, *23*(15), 3009–3022. https://doi.org/10.1080/01431160110107734

Xiao, Xiangming, Boles, S., Frolking, S., Li, C., Babu, J. Y., Salas, W., & Moore, B. (2006). Mapping paddy rice agriculture in South and Southeast Asia using multi-temporal MODIS images. *Remote Sensing of Environment*, *100*(1), 95–113. https://doi.org/10.1016/j.rse.2005.10.004

Xu, D., An, D., & Guo, X. (2020). The impact of non-photosynthetic vegetation on LAI estimation by NDVI in mixed grassland. In *Remote Sensing* (Vol. 12, Issue 12, p. 1979).

https://doi.org/10.3390/rs12121979

Xu, L., Li, X., Wang, X., Xiong, D., & Wang, F. (2019). Comparing the grain yields of direct-seeded and transplanted rice: A meta-analysis. In *Agronomy* (Vol. 9, Issue 11, p. 767). https://doi.org/10.3390/agronomy9110767

Xu, X., Gu, X., Song, X., Li, C., & Huang, W. (2010). Assessing rice chlorophyll content with vegetation indices from hyperspectral data. *International Conference on Computer and Computing Technologies in Agriculture*, 296–303. https://doi.org/10.1007/978-3-642-18333-1_35

Xu, Y., Chu, C., & Yao, S. (2021). The impact of high-temperature stress on rice: Challenges and solutions. *Crop Journal*, *9*(5), 963–976. https://doi.org/10.1016/j.cj.2021.02.011

Xue, J., & Su, B. (2017). Significant remote sensing vegetation indices: A review of developments and applications. *Journal of Sensors*. https://doi.org/10.1155/2017/1353691

Yagci, A. L., Di, L., Deng, M., Han, W., & Peng, C. (2011). Vegetation index based technique for global agricultural drought monitoring. *Proceedings of 5th International Conference on Recent Advances in Space Technologies-RAST2011*, 137–141. https://doi.org/10.1109/RAST.2011.5966808

Yamano, T., Arouna, A., Labarta, R. A., Huelgas, Z. M., & Mohanty, S. (2016). Adoption and impacts of international rice research technologies. *Global Food Security*, *8*, 1–8. https://doi.org/10.1016/j.gfs.2016.01.002

Yamauchi, K. (2014). Climate change impacts on agriculture and irrigation in the Lower Mekong Basin. *Paddy and Water Environment*, *12*(2), 227–240. https://doi.org/10.1007/s10333-013-0388-9

Yan, H., Liu, F., Qin, Y., Niu, Z., Doughty, R., & Xiao, X. (2019). Tracking the spatio-temporal change of cropping intensity in China during 2000-2015. *Environmental Research Letters*, *14*(3), 035008. https://doi.org/10.1088/1748-9326/aaf9c7

Yan, K., Park, T., Yan, G., Liu, Z., Yang, B., Chen, C., Nemani, R. R., Knyazikhin, Y., & Myneni, R. B. (2016). Evaluation of MODIS LAI/FPAR product collection 6. Part 2: Validation and intercomparison. *Remote Sensing*, *8*(6), 460. https://doi.org/10.3390/rs8060460

Yang, C., Yang, L., Yang, Y., & Ouyang, Z. (2004). Rice root growth and nutrient uptake as influenced by organic manure in continuously and alternately flooded paddy soils.

Agricultural Water Management, *70*(1), 67–81. https://doi.org/10.1016/j.agwat.2004.05.003

Yang, Zhi, Shao, Y., Li, K., Liu, Q., Liu, L., & Brisco, B. (2017). An improved scheme for rice phenology estimation based on time-series multispectral HJ-1A/B and polarimetric RADARSAT-2 data. *Remote Sensing of Environment*, *195*, 184–201. https://doi.org/10.1016/j.rse.2017.04.016

Yang, Zhiyuan, Zhang, Z., Zhang, T., Fahad, S., Cui, K., Nie, L., Peng, S., & Huang, J. (2017). The effect of season-long temperature increases on rice cultivars grown in the central and southern regions of China. *Frontiers in Plant Science*, *8*, 1908. https://doi.org/10.3389/fpls.2017.01908

Ye, Q., Yang, X., Dai, S., Chen, G., Li, Y., & Zhang, C. (2015). Effects of climate change on suitable rice cropping areas, cropping systems and crop water requirements in southern China. *Agricultural Water Management*, *159*, 35–44. https://doi.org/10.1016/j.agwat.2015.05.022

Ye, T., Nie, J., Wang, J., Shi, P., & Wang, Z. (2015). Performance of detrending models of crop yield risk assessment: Evaluation on real and hypothetical yield data. *Stochastic Environmental Research and Risk Assessment*, *29*(1), 109–117. https://doi.org/10.1007/s00477-014-0871-x

Ye, T., Zong, S., Kleidon, A., Yuan, W., Wang, Y., & Shi, P. (2019). Impacts of climate warming, cultivar shifts, and phenological dates on rice growth period length in China after correction for seasonal shift effects. *Climatic Change*, *155*(1), 127–143. https://doi.org/10.1007/s10584-019-02450-5

Ye, Y., Liang, X., Chen, Y., Liu, J., Gu, J., Guo, R., & Li, L. (2013). Alternate wetting and drying irrigation and controlled-release nitrogen fertilizer in late-season rice. Effects on dry matter accumulation, yield, water and nitrogen use. *Field Crops Research*, *144*, 212–224. https://doi.org/10.1016/j.fcr.2012.12.003

Yenda, S., Das, S., Swain, S., Sahu, G. S., Baliarsingh, A., Jagadev, P. N., & Sarkar, S. (2018). Predicting the effect of weather parameters on yield performance of tomato genotypes under late rabi planting condition. *The Pharma Innovation Journal*, *7*(3), 439–446.

Yeom, J. M., Jeong, S., Deo, R. C., & Ko, J. (2021). Mapping rice area and yield in northeastern asia by incorporating a crop model with dense vegetation index profiles from a geostationary satellite. *GIScience and Remote Sensing*, *58*(1), 1–27. https://doi.org/10.1080/15481603.2020.1853352

Yuan, S., Peng, S., & Li, T. (2017). Evaluation and application of the ORYZA rice model under

different crop managements with high-yielding rice cultivars in central China. *Field Crops Research*, *212*, 115–125. https://doi.org/10.1016/j.fcr.2017.07.010

Yuliawan, T., & Handoko, I. (2016). The effect of temperature rise to rice crop yield in Indonesia uses Shierary Rice model with geographical information system (GIS) feature. *Procedia Environmental Sciences*, *33*, 214–220. https://doi.org/10.1016/j.proenv.2016.03.072

Yuzugullu, O., Erten, E., & Hajnsek, I. (2015). Rice growth monitoring by means of X-band co-polar SAR: Feature clustering and BBCH scale. *IEEE Geoscience and Remote Sensing Letters*, *12*(6), 1218–1222.

Yuzugullu, O., Erten, E., & Hajnsek, I. (2016). Estimation of rice crop height from X-and C-band PolSAR by metamodel-based optimization. *IEEE Journal of Selected Topics in Applied Earth Observations and Remote Sensing*, *10*(1), 194–204. https://doi.org/10.1109/JSTARS.2016.2575362

Zhang, X., Friedl, M. A., Schaaf, C. B., Strahler, A. H., Hodges, J. C., Gao, F., ... & Huete, A. (2003). Monitoring vegetation phenology using MODIS. *Remote Sensing of Environment*, *84*(3), 471–475. https://doi.org/10.1016/S0034-4257(02)00135-9

Zhang, G., Xiao, X., Dong, J., Kou, W., Jin, C., Qin, Y., Zhou, Y., Wang, J., Menarguez, M. A., & Biradar, C. (2015). Mapping paddy rice planting areas through time series analysis of MODIS land surface temperature and vegetation index data. *ISPRS Journal of Photogrammetry and Remote Sensing*, *106*, 157–171. https://doi.org/10.1016/j.isprsjprs.2015.05.011

Zhang, K., Ge, X., Shen, P., Li, W., Liu, X., Cao, Q., Zhu, Y., Cao, W., & Tian, Y. (2019). Predicting rice grain yield based on dynamic changes in vegetation indexes during early to mid-growth stages. *Remote Sensing*, *11*(4), 387. https://doi.org/10.3390/rs11040387

Zhang, M., Lin, H., Wang, G., Sun, H., & Fu, J. (2018). Mapping paddy rice using a convolutional neural network (CNN) with Landsat 8 datasets in the Dongting Lake Area, China. *Remote Sensing*, *10*(11), 1840. https://doi.org/10.3390/rs10111840

Zhang, S., & Tao, F. (2013). Modeling the response of rice phenology to climate change and variability in different climatic zones: Comparisons of five models. *European Journal of Agronomy*, *45*, 165–176. https://doi.org/10.1016/j.eja.2012.10.005

Zhang, Xin, Wu, B., Ponce-Campos, G. E., Zhang, M., Chang, S., & Tian, F. (2018). Mapping up-to-date paddy rice extent at 10 M resolution in China through the integration of optical and synthetic aperture radar images. *Remote Sensing*, *10*(8), 1–26.

https://doi.org/10.3390/rs10081200

Zhang, Xiying, Chen, S., Sun, H., Pei, D., & Wang, Y. (2008). Dry matter, harvest index, grain yield and water use efficiency as affected by water supply in winter wheat. *Irrigation Science*, *27*(1), 1–10. https://doi.org/10.1007/s00271-008-0131-2

Zhang, Y., Huang, H., Chen, X., Wu, J., & Wang, C. (2009). Mapping paddy rice biomass using ALOS/PALSAR imagery. *2008 International Workshop on Education Technology and Training and 2008 International Workshop on Geoscience and Remote Sensing, ETT and GRS 2008*, *2*, 207–210. https://doi.org/10.1109/ETTandGRS.2008.195

Zhang, Yuan, Liu, X., Su, S., & Wang, C. (2014). Retrieving canopy height and density of paddy rice from Radarsat-2 images with a canopy scattering model. *International Journal of Applied Earth Observation and Geoinformation*, *28*, 170–180. https://doi.org/10.1016/j.jag.2013.12.005

Zhang, Yuan, Yang, B., Liu, X., & Wang, C. (2017). Estimation of rice grain yield from dual-polarization Radarsat-2 SAR data by integrating a rice canopy scattering model and a genetic algorithm. *International Journal of Applied Earth Observation and Geoinformation*, *57*, 75–85. https://doi.org/10.1016/j.jag.2016.12.014

Zhao, B., & Cui, T. J. (2013). Scattering characteristics of targets above a rough surface in SAR images. *International Journal of Antennas and Propagation*. https://doi.org/10.1155/2013/653438

Zhao, H., & Pei, Z. (2013). Crop growth monitoring by integration of time series remote sensing imagery and the WOFOST model. *2013 2nd International Conference on Agro-Geoinformatics: Information for Sustainable Agriculture, Agro-Geoinformatics 2013*, *ii*, 568–571. https://doi.org/10.1109/Argo-Geoinformatics.2013.6621940

Zhao, J., Xu, C., Huang, L., Zhang, D., & Liang, D. (2016). Characterisation of spatial patterns of regional paddy rice with time series remotely sensed data. *Paddy and Water Environment*, *14*(4), 439–449. https://doi.org/10.1007/s10333-015-0513-z

Zhao, R., Li, Y., & Ma, M. (2021). Mapping paddy rice with satellite remote sensing: A review. *Sustainability (Switzerland)*, *13*(2), 503. https://doi.org/10.3390/su13020503

Zhao, Y., Weng, Z., Chen, H., & Yang, J. (2020). Analysis of the evolution of drought, flood, and drought-flood abrupt alternation events under climate change using the daily SWAP index. *Water*, *12*(7), 1969. https://doi.org/10.3390/w12071969

Zheng, S., Ye, C., Lu, J., Liufu, J., Lin, L., Dong, Z., ... & Zhuang, C. (2021). Improving the rice photosynthetic efficiency and yield by editing OsHXK1 via CRISPR/Cas9 system. *International Journal of Molecular Sciences*, *22*(17), 9554.

Zheng, G., & Moskal, L. M. (2009). Retrieving Leaf Area Index (LAI) Using Remote Sensing: Theories, Methods and Sensors. *Sensors*, *9*(4), 2719–2745. https://doi.org/10.3390/s90402719

Zheng, H., Cheng, T., Yao, X., Deng, X., Tian, Y., Cao, W., & Zhu, Y. (2016a). Detection of rice phenology through time series analysis of ground-based spectral index data. *Field Crops Research*, *198*, 131–139. https://doi.org/10.1016/j.fcr.2016.08.027

Zheng, H., Cheng, T., Yao, X., Deng, X., Tian, Y., Cao, W., & Zhu, Y. (2016b). Detection of rice phenology through time series analysis of ground-based spectral index data. *Field Crops Research*, *198*, 131–139. https://doi.org/10.1016/j.fcr.2016.08.027

Zhong, X., Peng, S., Sheehy, J. E., Visperas, R. M., & Liu, H. (2002). Relationship between tillering and leaf area index: Quantifying critical leaf area index for tillering in rice. *Journal of Agricultural Science*, *138*(3), 269–279. https://doi.org/10.1017/S0021859601001903

Zhou, G., Liu, X., & Liu, M. (2019). Assimilating remote sensing phenological information into the WOFOST model for rice growth simulation. *Remote Sensing*, *11*(3), 268.

Zhou, G., Liu, X., Zhao, S., Liu, M., & Wu, L. (2017). Estimating FAPAR of rice growth period using radiation transfer model coupled with the WOFOST model for analyzing heavy metal stress. *Remote Sensing*, *9*(5). https://doi.org/10.3390/rs9050424

Zhou, Y.-F., Sun, Y.-M., & Chen, Y.-Q. (2021). *Identification and characterization of high-yielding, short-duration rice genotypes for tropical Asia* (pp. 1–19). https://doi.org/10.1007/978-1-0716-1645-1_1

Zhu, L., Xu, J. F., Huang, J. F., Wang, F. M., Liu, Z. Y., & Wang, Y. (2008). Study on hyperspectral estimation model of crop vegetation cover percentage. *Guang Pu Xue Yu Guang Pu Fen Xi= Guang Pu*, *28*(8), 1827–1831.